Gene expression patterns of the female genital tract and immunomodulation by *Lactobacillus* species

Andrea Gillian Abrahams

ABRAND006

Supervisor: Dr Lindi Masson

Co-Supervisors: Dr Arghavan Alisoltani-Dehkordi

Dr Heather Jaspan

Presented for Master of Science Degree (MSc) in Medical Virology

Division of Medical Virology

Faculty of Health Sciences

University of Cape Town

23 September 2020

Plagiarism Declaration

"This thesis/dissertation has been submitted to the Turnitin module (or equivalent similarity and originality checking software) and I confirm that my supervisor has seen my report and any concerns revealed by such have been resolved with my supervisor."

Name: Andrea Gillian Abrahams

Student number: ABRAND006

Signature: Signed by candidate

Date: 23 September 2020

Acknowledgements

First and foremost, I thank God for His grace and strength that has sustained me during this study and the completion of this thesis.

To my supervisor, Dr Lindi Masson, I cannot thank you enough for all the support and encouragement you've given me these past two years. Thank you for your understanding and kindness during every challenge I've faced. You have taught me so much in this field and I am very grateful to you.

A special thanks to my co-supervisor Dr Arghavan Alisoltani-Dehkordi for assistance in microarray data analysis training.

Thank you to Associate Professor Jo-Ann Passmore for generously providing the *Lactobacillus* isolates included in this study.

Thank you to the WISH and Groote Schuur clinic cohorts, without these participants, this research would not be possible.

Thank you to SATVI and CIDRI for the use of your ELISA and Luminex plate readers.

Thank you to Professor Carolyn Williamson for the use of the RNA extraction lab.

Thank you to the Centre for Proteomics and Genomics Research for the professional service provided.

Thank you to my parents Paul and Dawn Abrahams, my siblings Linieve, Lyle and Allison Abrahams, Uncle Clyde and Aunty Karin Ebden, for your constant love and support. You've seen the highs and lows of these past two years and supported me every step of the way.

A special thanks to Paul Abrahams, Dawn Abrahams, Ps Andrew Lamb, Kulsum Lamb, Ps Junaid Esau, Kelly-Anne Esau, Hendrisa Swanepoel, Robin Brooks, Lynn Brooks, Clyde Ebden, Karin Ebden, Vernon Daniels, Peter Daniels, Lavona Daniels, Quintin McLaren, Ingrid McLaren, Janine McLaren and Neville McLaren for all your prayers.

Thank you to my amazing friend Nina Radzey for your constant support.

Thank you to the **National Research Foundation (NRF)** who has funded my MSc. Degree.

Contents

List of Figures

List of Tables

List of units

°C: degrees Celsius

µl: microlitres

ml: millilitres

ng/µl: nanograms per microlitre

pg/ml: picograms per millilitre

rpm: revolutions per minute

CFU: colony forming units

nm: nanometers

nmole: nanomole

Abstract

Inflammation in the female genital tract (FGT) is associated with increased HIV-1 viral replication, HIV-1 transmission and HIV-1 acquisition. The optimal commensal *Lactobacillus* bacterial species is associated with reduced inflammation in the FGT and dampened immune responses to non-optimal bacteria *in vitro.* Using a transcriptomics approach, this research aimed to investigate gene expression patterns in the FGT of HIV-infected women compared to peripheral blood. Furthermore, transcriptomics was used to investigate interactions between different vaginal *Lactobacillus* species and the host to elucidate its immunomodulatory mechanisms.

Cervical cytobrushes and blood samples were collected from chronically HIV-infected South African women. Cervical and peripheral blood mononuclear cells (CMCs and PBMCs) were isolated and mRNA was extracted for microarray analysis using the Illumina HumanHT-12 v3 Expression BeadChip system. Eight *Lactobacillus* isolates, two of each *L. jensenii*, *L. mucosae*, *L. crispatus* and *L. vaginalis* species were included in this study. The effects of these lactobacilli on cytokine production by vaginal epithelial (VK2) cells stimulated with *Gardnerella vaginalis* (ATCC 14018) were tested *in vitro*, RNA was extracted and used for Affymetrix Genechip whole transcript microarray analysis.

This study found that significantly over-expressed genes in CMCs compared to PBMCs were mapped to proinflammatory signaling pathways (including Nuclear factor kappa B (NFκB), Tumor necrosis factor (TNF), Toll-like receptor (TLR) and Nucleotide-binding and oligomerization domain (NOD)-like receptor). Concurrently, a signature of reduced potential for adaptive immunity was observed in CMCs compared to PBMCs, as evidenced by underrepresentation of the T cell receptor signaling and natural killer cell mediated cytotoxicity pathways. *G. vaginalis* induced a potent proinflammatory cytokine response by VK2 cells *in vitro*. Over-expressed genes in *G. vaginalis*-stimulated VK2 cells compared to unstimulated VK2 cells were mapped to inflammatory signalling pathways. In contrast, 3/8 *Lactobacillus* isolates, including two *L. mucosae* and one *L. vaginalis* species, reduced inflammatory cytokine production by VK2 cells in response to *G. vaginalis* and were thus termed “cytokine-suppressive”. Several genes, 7/8 of which are involved in inflammation, were downregulated in VK2 cells co-cultured with lactobacilli and *G. vaginalis* in combination compared to co-culture with *G. vaginalis* only. Futhermore, when gene expression changes were investigated in cells cultured with cytokine-suppresive lactobacilli versus non-cytokine-suppressive lactobacilli, it was found that SAMD9L, DDX58, IFIT1 gene expression was downregulated exclusively in VK2 cells co-cultured with cytokine-suppressive lactobacilli and *G. vaginalis* compared to co-culture with *G. vaginalis* only.

The findings of this study have identified distinct gene expression patterns in the FGT compared to peripheral blood. Furthermore, key genes that may play a critical role in the immunomodulatory effects of vaginal lactobacilli were identified, motivating for further confirmatory research.

Abbreviations

APE1- Apurinic/apyrimidinic endonuclease 1

ART- Antiretroviral therapy

ATF4- Transcription activator 4

BHI- Brain Heart Infusion

BHIB- Brain-Heart-Infused Broth

BME- Beta-mercaptoethanol

BME- Beta-mercaptoethanol

BPE- Bovine pituitary extract

BMDMs- Bone marrow derived macrophages

BV- Bacterial vaginosis

cDNA- Complementary DNA

CLRs- C-type lectin receptors

CMC- Cervically derived mononuclear cells

COX- Cyclooxygenase

CPGR- Centre for Proteomics and Genomic Research

CTACK- Cutaneous T-cell attracting chemokine

CTLs- Cytotoxic T Lymphocytes

CVF- Cervicovaginal fluid

CVL- Cervicovaginal lavarge

DAMPS- Danger associated molecular patterns

DAVID- Database for Annotation, Visualization and Integrated Discovery

DMEM- Dulbecco's Modified Eagle's Medium

dNTPs- Deoxyribonucleoside triphosphates

EDCTP- European & Developing Countries Clinical Trials Partnership

EDTA- ethylenediaminetetraacetic acid

EETs- Epoxyeicosatrienoic acids

EGF- human recombinant epidermal growth factor

ELISA- Enzyme-linked immunosorbent assay

FCS- bovine foetal calf serum

FGT- Female genital tract

G-CSF- Granulocyte colony stimulating factor

GM-CSF- Granulocyte-macrophage colony stimulating factor

GRO-α- Growth-regulated oncogene alpha

HGF- Hepatocyte growth factor

HIV- Human immunodeficiency virus

HSV- Herpes Simplex Virus

IFN-α2- Interferon alpha 2

IFN-γ- Interferon gamma

IKK- IkB kinase

IL- Interleukin

IL-1RA- Interleukin 1 receptor antagonist

IL-2Rα- Interleukin 2 receptor alpha chain

IP-10- Interferon gamma induced protein 10

IRF- Interferon regulatory factor

KEGG- Kyoto Encyclopedia of Genes and Genomes

KSFM- Keratinocyte-Serum Free medium

LIF- Leukaemia inhibitor factor

LOX- Lipoxygenase

LPS- Lipopolysaccharide

MALDI-TOF- Matrix Assisted Laser Desorption Ionization-Time of Flight

MAP- mitogen activated protein

MCP- Monocyte chemoattractant protein

M-CSF- Macrophage colony stimulating factor

MIG- Mitogen inducible gene

MIP- Mitogen inflammatory protein

MIST- Mucosal Injury from Sexual Trauma

MRS- Man, Rogosa Sharpe

MRS- Man-Rogosa and Sharpe

MyD88- myeloid differentiation primary response88.

NFkB- Nuclear factor kappa light-chain-enhancer of activated B cells.

NHLS- National Health Laboratory service

NICD- National Institute of Communicable Diseases

NLRs- Nucleotide oligomerization domain-like receptors

NTPs- Nucleotide triphosphates

OD: optical density

PAMPS- Pathogen associated molecular patterns

PBMC- Peripheral blood mononuclear cells

PBS- Phosphate Buffered Saline

PC- Principal Component

PDGF-bb- Platelet derived growth factor

PE- Streptavidin-Phycoerythrin

PGN- Peptidoglycan

PRR- Pattern recognition receptor

RANTES- Regulated on activation, normal T cell expressed and secreted.

RNA- Ribonucleic Acid

RNAse- Ribonuclease

SCF- Stem cell factor

SDF-1α- Stromal cell-derived factor 1 alpha

ss-cDNA- single-stranded complementary DNA

STI- Sexually transmitted Infections

TdT- Terminal deoxynucleotidyl Transferase

TLRs- Toll-like receptors

TNFα- Tumor necrosis factor apha

TRIF- TIR-domain-containing adaptor protein inducing interferon

UDG- Uracil-DNA glycosylase

UPR- Unfolded protein response

VEGF- Vascular endothelial growth factor

VK2- vaginal epithelial

WISH- Women's Initiative in Sexual Health

Chapter 1: Introduction

The maintenance of health in the female genital tract (FGT) involves the microbiome, epithelial cell barrier and immune system (1). A *Lactobacillus*-dominated vaginal microbiome has long been considered optimal (2), by producing lactic acid, hydrogen peroxide and bacteriocins, and hence creating an unfavourable environment for pathogens (3–8). In contrast, bacterial vaginosis (BV) occurs when lactobacilli are replaced by a diverse population of non-optimal bacteria (9). BV is highly prevalent, with 30-40% of women in sub-Saharan Africa having this condition (10). BV is associated with increased inflammation in the FGT that subsequently increases susceptibility to Human Immunodeficiency Virus (HIV) acquisition and may reduce the efficacy of some forms of antiretroviral pre-exposure prophylaxis (11–15). In addition, BV is associated with poor reproductive health outcomes, including preterm birth, pelvic inflammatory disease (PID) and infertility (16). Induction of the inflammatory cascade plays a critical role in the onset of labour (17,18) and thus, modulation of inflammatory responses by vaginal bacteria likely has an important influence on pregnancy outcomes. The condition may present with symptoms, however most cases are asymptomatic (19,20). Therefore, it is possible for BV to be unnoticed and thus not treated, allowing persistent inflammation in the FGT, and causing these women to be particularly vulnerable to HIV infection, as well as poor reproductive health outcomes. On the other hand, *Lactobacillus* species play a critical role in regulating inflammatory responses in the FGT and women with *Lactobacillus* dominated FGTs are at low risk of HIV infection (21).

Given the prevalence of HIV in South Africa in particular (22), our knowledge of biological factors that increase acquisition risk in this population, are a necessity in combating this epidemic. Furthermore, adverse reproductive outcomes are highly prevalent in sub-Saharan Africa, with a preterm birth rate of 28.2% (23) and many children born preternaturally have lifelong health sequalae (24). Moreover, PID is associated with infertility (25). A study by Haggerty *et al*. (2016) (26) found an association between endometrial BV-associated bacteria and recurrent PID, and women who tested positive for PID were more likely to develop infertility in a United States cohort of women. Thus, an improved understanding of the biological factors that increase poor reproductive outcomes is imperative to reduce the prevalence of PID, preterm birth and infertility.

It is possible that the immunoregulatory ability of *Lactobacillus* spp. (27–29) may be harnessed to reduce susceptibility to HIV acquisition. Improving our understanding of the underlying immunomodulatory mechanisms of these commensal bacteria, will inform on biomedical intervention strategies for preventing HIV and adverse reproductive outcomes.

Using transcriptomics, the aims of this thesis were to describe microbial pattern recognition and inflammatory signalling pathways in the FGT and to determine the mechanisms underlying the anti-inflammatory effect of *Lactobacillus* spp. in the FGT.

1.1 The vaginal microbiome in optimal and non-optimal states

An optimal vaginal microbiome consists of predominantly *Lactobacillus* spp., vaginal pH lower than 4.5 and low levels of BV-associated bacteria (9). One of the primary mechanisms by which vaginal *Lactobacillus* spp. inhibit the growth of pathogenic microorganisms is via the production of lactic acid that is responsible for the low pH associated with an optimal state (3–6). In addition, *Lactobacillus* spp. inhibit the adhesion of BV-associated bacteria to the epithelium of the FGT and produce bacteriocins and hydrogen peroxide, although the role of the latter is controversial (3,7,27,30) (**Figure 1**). The *Lactobacillus* spp. *L. crispatus*, *L. iners*, *L. jensenii* and *L. gasseri* were identified as predominant vaginal lactobacilli from South African women (31). A more recent cohort study by Jespers *et al*. (2017) (32), including women from Kenya, Rawanda and South Africa, identified the same species in the vaginal microbiomes of these women. The study also found that women with an abundance of *L. crispatus*, had low levels of *L. iners* and vice versa. A recent study by Campisciano *et al*. (2018) (33) found that *L. iners* was the dominant *Lactobacillus* spp. isolated from Caucasian women with BV. *L. iners* is associated with increased risk of conversion from an optimal to a non-optimal vaginal microbiome (34) and acquisition of sexually transmitted infections (STIs) (35). In contrast, *L. crispatus* has been identified in women considered to have optimal vaginal microbiota (33). Furthermore, *L. crispatus*, *L. jensenii* and *L. gasseri* have antagonistic activity against BV-associated bacteria (36). Thus, a vaginal microbiome dominated by *Lactobacillus* spp. confers an optimal state to the host; however, the ability to maintain this state is largely influenced by the specific sp. which predominates.

An imbalance in the vaginal microbiome occurs when there is a decreased abundance of *Lactobacillus* spp., increased vaginal pH above 4.5 and the outgrowth of potentially pathogenic anaerobic microorganisms, such as *Gardnerella*, *Prevotella*, *Mobiluncus* and *Atopobium* spp. (9,33), resulting in BV. Nugent scoring by Gram stain and microscopy is the gold standard for diagnosis of BV and is used to determine whether the vaginal microbiome is optimal (predominantly lactobacilli; score: 0-3), intermediate (some lactobacilli and some Gram variable coccobacilli and *Mobiluncus*; score: 4-6) or BV (few to no lactobacilli with abundant Gram variable coccobacilli and *Mobiluncus*; 7-10) (37). BV has been described as a polymicrobial condition (38) and its exact aetiology is not fully understood. However,

Gardnerella vaginalis has been found to be a key BV-associated bacterium and it is commonly isolated from the vaginal tracts of women with BV (32,39,40). However, *G. vaginalis* is also isolated from women with intermediate vaginal microbiomes (33) and those with optimal states (41,42). Four subtypes of *G. vaginalis* have been identified, of which clade one, two and three are prevalent in women with BV and clade four is prevalent in women without BV (43). It has been suggested that *G. vaginalis* is an early colonizer of the vaginal tract involved in the progression to BV and promotes the colonization and growth of other BV-associated bacteria (44). This pathogenic property has been attributed to its ability to self-aggregate which produces a robust biofilm (45). *G. vaginalis* strains may display varying pathogenic potential in the FGT, as genes which encode biofilm components, antimicrobial resistance and virulence factors, are strain specific. Furthermore, *G. vaginalis* strains isolated from women with BV are more virulent *in vitro* compared to those isolated from women with non-optimal vaginal microbiomes (46). Therefore, *G. vaginalis* is an important BV-associated bacterium and an improved understanding of its pathogenicity in the FGT, together with the host immune response, is needed.

1.2 The innate immune response in the FGT

The interplay between the microbiome and the immune system allows for the defence against pathogens, while maintaining tolerance to commensal bacteria and allogeneic sperm (47). An intricate network of receptors, intracellular signalling mechanisms and cytokines function together to initiate host defences against pathogens (48). Cytokines are chemical messengers which regulate the innate and adaptive immune systems (49). Pro-inflammatory cytokines, such as interleukin (IL)-1α and IL-1β, IL-6, IL-8, and tumor necrosis factor alpha (TNFα), function to promote an inflammatory response via vasodilation and recruitment of immune cells to the site of infection or tissue damage (50). The pleotropic IL-1 cytokine family has pro-inflammatory, immunoregulatory and haematopoietic functions, as well as promoting the development of Th17 helper T cells (51). Both IL-1α and IL-1β initiates downstream signalling in various cell types by binding to the IL-1 receptor (IL-1R) (51), however, IL-1α also contains a nuclear localisation site enabling it to promote

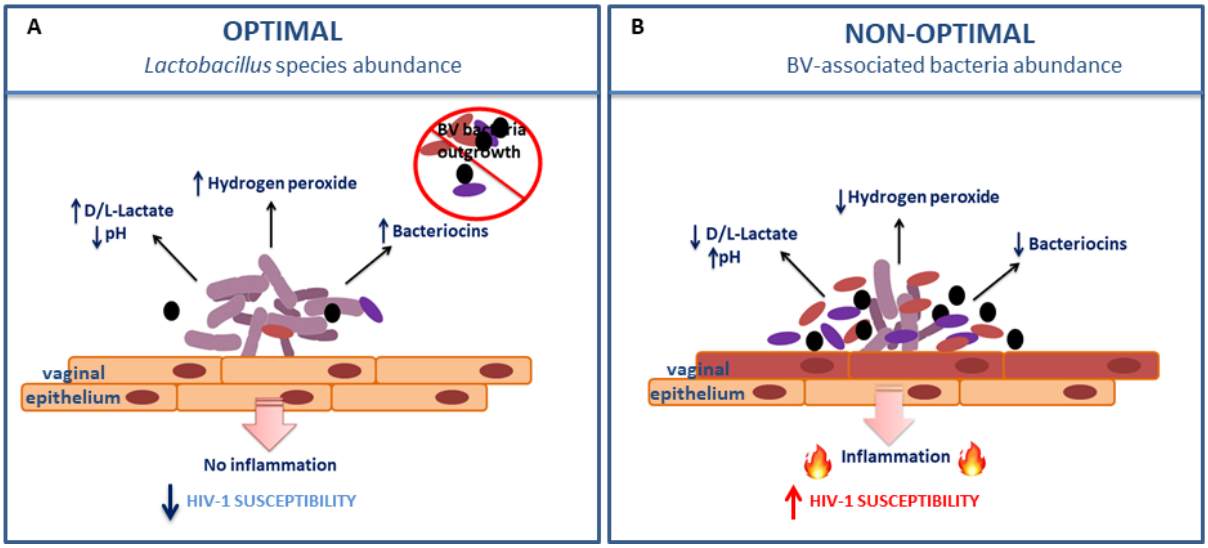

Figure 1: Implications of the vaginal microbiome in optimal and non-optimal states. A) Depicts an optimal vaginal microbiome with lactobacilli abundance, lactate production, low pH, hydrogen peroxide production and bacteriocins which inhibit the outgrowth of BV-associated bacteria. Consequently, inflammation and HIV-1 susceptibility are reduced. **B)** Depicts a non-optimal vaginal microbiome, with the outgrowth of BV-associated bacteria, reduced lactobacilli, lactate and hydrogen peroxide production, increased pH and reduced bacteriocins. Consequently, inflammation and HIV-1 susceptibility are increased. **HIV-1**: Human Immunodeficiency Virus-1.

proinflammatory gene transcription independently of the IL-1R (52). In contrast, the IL-1R antagonist (IL-1RA) is an anti-inflammatory cytokine which competes for the IL-1R, thus reducing inflammation (51,52). The IL-6 cytokine binds the IL-6 receptor and the transmembrane glycoprotein130 (gp130) to induce intracellular signalling which initiates the acute phase inflammatory response, causing the neutralization of pathogens and minimizing

tissue damage (53). The chemokine IL-8 is a potent chemoattractant and activator of neutrophils at infection sites, which combat invading pathogens (51,54). Macrophage inflammatory protein (MIP)-1α is a chemokine which functions to recruit and activate T lymphocytes and monocytes (55) . The structurally similar chemokine MIP-1β functions in neutrophil chemotaxis, as well as T cell activation and recruitment, resulting in proliferation, IL-2 secretion and IL-2 cell receptor expression (56). The chemokine MIP-3α is responsible for the chemotaxis of immature dendritic cells, memory T cells and B cells, and is involved in the formation of lymphoid mucosal tissues (57). Interferon gamma inducible protein 10 (IP-10) is a chemokine secreted by cells stimulated by interferons and lipopolysaccharides (LPS), which recruits activated T cells (58).

1.2.1 Mucosal barrier of the FGT

The mucosal barrier of the FGT provides a robust protective layer to infection. A single layer of columnar epithelial cells lines the upper FGT, while a multi-layered non-keratinized stratified squamous epithelium lines the lower FGT (49). In addition, a layer of mucus inhibits direct contact of pathogens with the epithelium and contains mucins composed of glycosylated proteins, which trap pathogens and prevent their entry (49). Intraepithelial immune cells such as T cells, macrophages, dendritic cells, natural killer cells and neutrophils are present in the epithelial layer to combat potential invading microorganisms (59).

1.2.2 Pathogen detection in the FGT

In addition to providing a physical barrier to infection, epithelial cells of the FGT play a crucial role in pathogen detection via their pattern recognition receptors (PRR). These receptors detect pathogens by recognizing conserved molecular structures, known as pathogen-associated molecular patterns (PAMPs) (60). In addition, PRRs detect danger associated molecular patterns (DAMPs) which are released by damaged tissue (61). Bacterial PAMPS include LPS, flagellin, peptidoglycan and bacterial nucleic acid structures, while viral PAMPS are double or single stranded RNA or viral DNA (62).

Toll-like receptors (TLRs) were the first class of PRRs to be identified. Ten different TLRs have been identified in humans, which recognize diverse pathogen classes (60). They are either located on the cell surface or intracellularly (63). TLR1 and 2 recognize peptidoglycan and lipoproteins of Gram-positive bacteria, whereas TLR4 recognizes LPS in the cell wall of Gram-

negative bacteria (60). Immune cells such as neutrophils, macrophages and dendritic cells, as well as dermal endothelial and mucosal epithelial cells, express TLRs, as they are involved in the first line of defence against invading pathogens (64). Fazeli *et al*. (2005) (65) detected TLR1-6 in epithelia from different regions of the FGT, however, TLR4 was not detected in vaginal and cervical epithelia. Similarly, Fichorova *et al.* (2002) (66) found that cervical and vaginal epithelial cells did not express TLR4 *in vitro*. However, Zariffard *et al*. (2005) (67) found higher expression of TLR4 and TLR2 mRNA in cells obtained from cervicovaginal lavage (CVL) samples of women with BV compared to cervical mucosal tissue. The authors thus concluded that these TLRs were expressed in the FGT, although TLR4 may have been expressed by immune cells present in the lumen and not epithelial cells.

Other classes of PRRs include C-type lectins receptors (CLRs), Retinoic acid inducible (RIG-I)-like receptors and nucleotide oligomerization domain (NOD)-like receptors (NLRs) (62). Langerhans cells, myeloid dendritic cells and macrophages isolated from endocervical tissue have been found to express CLRs (68). CLRs are widely known for the recognition of fungal microbes (69). Vaginal candidiasis is a common condition caused by the fungal spp. *Candida albicans* (70). CLRs are important in the detection of this pathogen and polymorphisms in these receptors are associated with recurrent vulvovaginal candidiasis (71,72), as well as recurrent BV (72). RIG-I receptors recognize viral RNA (73). Sathe & Reddy (2014) (74) found that these are key receptors intracellularly expressed by endocervical epithelial cells and are important for anti-viral immune responses. NLRs are intracellular proteins which function as scaffolding proteins involved in signalling cascades which trigger inflammatory pathways (75). They recognize Gram-negative and Gram-positive bacteria by detection of peptidoglycan, a major component of bacterial cell walls (75).

1.2.3 Downstream inflammatory networks

The activation of PRRs initiates intracellular signalling cascades which activate inflammatory pathways of a cell (76). The main inflammatory pathways activated by PRRs are the nuclear factor kappa light-chain-enhancer of activated B cells (NF-κB) pathway and the mitogen activated protein (MAP) kinase pathway (63).

After TLR detection of a microbial PAMP, an adaptor molecule myeloid differentiation primary response 88 (MyD88), is recruited to the TLR. MyD88 then associates with the cytoplasmic domain of the receptor and mediates signal transduction (63). Thereafter, a series of phosphorylation, ubiquitination and protein-protein interactions occur to activate downstream

signal transduction pathways. These signals result in the activation of transcription factors necessary for the regulation of genes involved in inflammation (63). The NF-κB pathway is an example of a downstream inflammatory network.

The NF-κB complex consists of p50 and p65 subunits bound to inhibitor of κB (IκBα) in its inactive state in the cytoplasm. Upon PRR activation by PAMPS, IκB kinase (IKK) is activated and phosphorylates IκBα which results in its dissociation from NF-κB, ubiquitination and degradation. The NF-κB complex is then able to translocate into the nucleus and induce specific gene expression, many of these being pro-inflammatory cytokines (77).

Similarly, the MAP kinase pathway involves sequential signalling steps which culminate to induce pro-inflammatory cytokine production. The pathway includes MAP kinases which propagate signals from the cell surface to the nucleus (78). The p38 MAP kinase pathway is associated with inflammation, being activated by extracellular stimuli including cytokines and pathogens which activate p38 via TLRs (79,80). Following this extracellular stimulus, phosphorylation of MAP kinase isoforms activates the p38 MAP kinase, resulting in production of inflammatory mediators for the recruitment and activation of leukocytes (78).

1.3 BV-associated bacteria cause inflammation in the FGT

BV and the inflammation caused by BV-associated bacteria increase risk of HIV acquisition in women, as well as HIV transmission to uninfected partners (81,82). BV has been associated with increased inflammatory mediators and immune cells in the FGT (33,83,84) and biomarkers of damage to the epithelium of the vaginal mucosa (85). In contrast, some chemokines are downregulated (83) which may suggest a tolerogenic mechanism used by pathogenic bacteria to persist in the FGT. Recent studies have found that *G. vaginalis* specifically induces pro-inflammatory cytokine production. Santos *et al*. (2018) (86) found that HeLa cells stimulated with *G. vaginalis* induced the production of TNF-α, IL-1β, IL-6 and IL-8 *in vitro*. Similarly, an *in vivo* study by Sierra *et al*. (2018) (87) found high levels of IL-6 in the cervicovaginal fluid (CVF) and increased expression of IL-1β, IL-8 and IL-10 in the cervices of pregnant mice inoculated intravaginally with *G. vaginalis* compared to the control group.

Inflammation caused by BV may increase HIV risk by increasing recruitment of HIV target cells, including CD4+ T cells, macrophages and dendritic cells, into the FGT (81). Interestingly, Campisciano *et al*. (2018) (33) found that *G. vaginalis* abundance correlated with IL-15 in a cohort of Italian Caucasian women. Studies have found that IL-15 is involved in the activation (88) and proliferation (89) of CD4+ T cells *in vitro*. Thus, increased concentrations of this

cytokine may be an important factor in the persistence of HIV target cells in FGTs with microbiomes dominated by *G. vaginalis.*

FGT inflammation also influences susceptibility to different HIV viral phenotypes, as pre-infection genital tract inflammation is associated with increased acquisition of less infectious HIV variants (90). Furthermore, following activation by inflammatory cytokines, NF-κB binds to the long terminal repeat (LTR) situated in the HIV promoter to initiate HIV replication (91). In agreement with this, Mitchell *et al*. (2011) (92) reported an association between HIV RNA shedding and pro-inflammatory IL-8 and IL-1β concentrations in CVF. Moreover, BV-associated bacteria were associated with increased HIV RNA shedding in CVF compared to *L. jensenii* abundance (93), which likely explains the increased risk of HIV transmission to uninfected partners that is associated with BV.

In addition to directly inducing a pro-inflammatory response, *G. vaginalis* produces a toxin, vaginolysin, which is cytolytic to the host cells (94). *In vitro* stimulation of vaginal keratinocytes with vaginolysin causes the release of lactate dehydrogenase, which is indicative of cellular permeabilization (95). Sierra *et al*. (2018) (87) quantified soluble e-cadherin (a molecular marker of a disrupted cervical epithelial barrier) in CVF of *G. vaginalis* colonized mice and similarly found that e-cadherin was significantly increased in *G. vaginalis* colonized mice compared to controls. As previously mentioned, damaged tissue releases DAMPs which activate PRRs to induce a pro-inflammatory response. Thus, the ability of *G. vaginalis* to disrupt the epithelial barrier is likely to exacerbate inflammation due to tissue damage, as well as allow for entry of cell-free and cell-associated HIV particles (96). It has further been reported that vaginolysin treatment of HeLa cells *in vitro* activates the p38 MAP kinase pathway and increases IL-8 production (94).

1.4 Anti-inflammatory effect of *Lactobacillus* species

In contrast to BV-associated bacteria, vaginal *Lactobacillus* spp. have been associated with decreased inflammatory mediator concentrations in the FGT and a reduced inflammatory response to bacterial (27,29,86,97) and fungal pathogens (86) *in vitro*. Hearps *et al*. (2017) (28) found that lactic acid (a metabolite produced by lactobacilli) reduced pro-inflammatory cytokine IL-8, IL-6 and TNF-α production by ectocervical, endocervical and vaginal epithelial cells in response to TLR agonists. The authors thus proposed that lactic acid plays a role in the anti-inflammatory effect of *Lactobacillus* spp. A recent study by Santos *et al.* (2018) (86) isolated *L. fermentum* and *L. plantarum* from women with optimal vaginal microbiomes. The

study found that these *Lactobacillus* spp. suppressed pro-inflammatory cytokine (TNF-α, IL-1β, IL-6, IL-8) secretion by HeLa cells stimulated with *G. vaginalis* and *Candida albicans*. Similarly, we have previously found that clinical vaginal *Lactobacillus* isolates, including *L. crispatus, L. jensenii, L. mucosae* and *L. vaginalis,* obtained from South African women, significantly supressed IL-6 and IL-8 production by ectocervical (CaSki) and vaginal epithelial (VK2) cells in response to *G. vaginalis,* although IL-1α and IL-1β were upregulated in the presence of the *Lactobacillus spp.* (29,98). Furthermore, the production of D-lactate produced in the cell culture system correlated with decreased cytokine production (98). At present, the molecular mechanisms by which *Lactobacillus* spp. may regulate inflammatory responses, and hence reduce risk of HIV acquisition, are largely unknown.

1.4.1 Effect of FGT bacteria on the expression and activation of PRRs

Microorganisms in the FGT activate TLRs to initiate an immune response via the TLR signalling cascade. It has been found that CVL from women with BV significantly increased TLR4 expression by peripheral blood mononuclear cells (PBMCs) compared to CVL from women without BV, however TLR2 remained unchanged (67). Finamore *et al*. (2014) (99) found that *Lactobacillus* spp. reduced TLR4 expression by intestinal Caco-2 cells stimulated with enteropathogenic *Escherichia coli in vitro*. More relevant to the FGT, a recent study by Tobita *et al*. (2017) (100) investigated the anti-inflammatory effect of vaginal *Lactobacillus* bacteria on human embryonic intestinal cells in the context of mother-to-child bacterial transfer and the establishment of the gut microbiome. The study reported that LPS stimulated cells had reduced TLR4 expression in the presence of *L. gasseri* and *L. crispatus in vitro.* Thus, inhibition of TLR activation and signalling by *Lactobacillus* spp. may be a plausible anti-inflammatory mechanism in the FGT. Further research is necessary, as studies using appropriate cell lines from the FGT, BV-associated bacteria and vaginal *Lactobacillus* spp. have not been done before. Horton *et al*. (2009) (101) used a microarray approach to compare gene expression of cervical mononuclear cells (CMCs) to peripheral blood mononuclear cells (PBMCs). The study found that TLRs 1, 2, 4, 5, 6 and 8 were significantly overexpressed in CMCs compared to PBMCs. Using a similar transcriptomics approach, this study aimed to investigate potential changes in TLR expression and activation of TLR signalling pathways in vaginal epithelial cells stimulated with BV-associated bacteria in the presence and absence of *Lactobacillus* spp. The role of suppression of certain TLR signalling cascades in mediating the anti-inflammatory effect of *Lactobacillus* spp. in the FGT was thus evaluated.

1.4.2 The effect of FGT bacteria on intracellular inflammatory pathways

The modulation of FGT epithelial cell inflammatory responses by *Lactobacillus* spp. has not been extensively studied. However, previous studies have proposed that *Lactobacillus* spp. act on intracellular signalling pathways involved in inflammation (28). Zalenskaya *et al*. (2015) (102) found that *P. bivia* induced the expression of seven pro-inflammatory genes (3 to 75 fold) by vaginal epithelial cells *in vitro*, while *L. gasseri* did not, thus, discriminating the transcriptome of an optimal FGT compared to a non-optimal one.

In other cell lines, such as macrophages and monocytes, *Lactobacillus* spp. have been found to interfere with the NF-κB pathway (80,103). Lee *et al*. (2008) (103) found that *L. casei* reduced IκBα degradation and cytosolic p65 in LPS-stimulated macrophages *in vitro*. Similarly, *L. johnsonii* was found to reduce the activation of NF-kB and inhibit the translocation of p65 into the nucleus of LPS-stimulated macrophages *in vitro* (104). Furthermore, lactic acid, which is one of the main metabolites produced by *Lactobacillus* bacteria (105), was found to delay LPS induced IκBα degradation in human monocytes *in vitro* (106). It has also been proposed that *Lactobacillus* spp. modulate cytokine release by monocyte-macrophages by upregulating negative regulators of the NF-κB pathway *in vitro* (107). Studies using these cell lines suggest that *Lactobacillus* spp. may act on similar intracellular pathways involved in inflammation in vaginal epithelial cells. However, the exact mechanisms by which *Lactobacillus* spp. may target this pathway are still unknown. Contrary to these findings, in non-immune cells, heat labile components of *Lactobacillus* spp. were found to enhance NF-κB activation and TNF production while reducing IL-6 and IL-8 production by urinary bladder cells stimulated with *E. coli in vitro* (108). However, research using epithelial cells of the FGT, as well as *Lactobacillus* spp. commonly isolated from the FGT, is limited and necessary to fully understand how *Lactobacillus* spp. potentially act on inflammatory pathways of epithelial cells in the FGT.

This study investigated the anti-inflammatory properties of *Lactobacillus* spp. isolated from the FGTs of South African women. *G. vaginalis* was used to stimulate vaginal epithelial cells in the presence or absence of vaginal *Lactobacillus* spp., inflammatory cytokine production was measured using Luminex and changes in gene expression evaluated using microarray. Microarray assay allows for the detection of upregulated and downregulated gene expression in a sample. mRNA is transcribed from DNA and is the intermediary molecule which transfers the genetic information obtained in the nucleus, to the cytoplasm where protein expression takes place. When a gene is expressed, many copies of mRNA, specific for the gene, are transcribed and translated to produce the corresponding protein. Therefore, by evaluating the mRNA, the relative gene expression can be assessed (109). Thus, this approach has identified

potential inflammatory signalling pathways targeted by *Lactobacillus* spp. to modulate pro-inflammatory cytokine production induced by *G. vaginalis.*

1.5 Aims and Objectives

Objective: Evaluate the underlying mechanisms of the immunomodulatory effect of *Lactobacillus* species on vaginal immune cells stimulated by *Gardnerella vaginalis.*

Specific aims:

1. To use transcriptomics to investigate whether pro-inflammatory signalling pathways are overexpressed in CMCs versus matching PBMCs isolated from South African women.
2. To investigate the effect of vaginal *Lactobacillus* isolates on pro-inflammatory cytokine production by vaginal epithelial cells stimulated with BV-associated *G. vaginalis* (ATCC® 14018™).
3. To use transcriptomics to evaluate whether lactobacilli modulate vaginal epithelial cell pro-inflammatory cytokine responses to *G. vaginalis* by influencing the expression of components of inflammatory signalling pathways, including PRRs, negative feedback regulators, anti-inflammatory cytokines and transcription factors.

Chapter 2: Materials and Methods

2.1 Comparison of gene expression in CMC and PBMC samples

2.1.1 Groote Schuur study cohort and sample collection

Matched cervical cytobrush and blood samples were collected from n=5 black, chronically HIV-infected women on antiretroviral therapy (ART), from the Gynaecology Outpatient Clinic, Groote Schuur Hospital, Cape Town, South Africa (Principal Investigator: Associate Professor Jo-Ann Passmore). The presence of clinical signs and symptoms of STIs and BV were recorded by the study nurse and plasma HIV viral load was measured for each participant using Nuclisens Easyq HIV-1 Version 1.2 (BioMerieux, Lyon, France) by the National Health Laboratory Service (NHLS).

2.1.2 CMC and PBMC sample processing

CMCs and PBMCs were isolated from the cytobrush and blood samples, respectively, by Ficoll density gradient centrifugation. Thereafter, the samples were stored in RNAlater reagent (Qiagen, Germany) at -80°C until RNA extraction. RNA was extracted from the samples using the RNeasy Plus Mini Kit (Qiagen, Germany), by Dr Lindi Masson (Division of Medical Virology, UCT, Cape Town, South Africa).

2.1.3 Gene expression analysis of CMC and PBMC samples using microarray Illumina platform

Prior to evaluation of CMC and PBMC gene expression profiles, RNA quality and quantity were assessed using a NanoDrop and Agilent RNA 6000 Pico Kits on an Agilent 2100 Bioanalyzer (Agilent Technologies, CA, USA). RNA was amplified using Illumina® TotalPrep™ RNA Amplification Kits (Ambion, Inc., TX, USA). Gene expression in the matched CMC and PBMC samples was evaluated using the microarray Illumina HumanHT-12 v3 Gene Expression BeadChip (Ambion, Inc., TX, USA), at the Baylor Centre for Immunology Research (Dallas, TX, US) by Dr Lindi Masson. The assay was performed according to the manufacturer's instructions and all samples were processed in a single batch and loaded on the same BeadChip (Ambion, Inc., TX, USA). Briefly, mRNA was reverse transcribed to synthesize first strand cDNA. The first strand-cDNA was then converted to a double-stranded DNA (dsDNA) template for transcription. The cDNA product was then purified to remove RNA and other contaminants using purification beads which would inhibit *in vitro* transcription. cDNA yield and size distribution of each sample was assessed using a NanoDrop spectrophotometer and an Aligent 2100 Bioanalyzer. *In vitro* transcription (IVT) was then

performed and multiple copies of biotinylated cRNA were amplified and labelled from the ds-cDNA templates. The cRNA was then purified to remove unincorporated nucleotide triphosphates (NTPs), salts and other contaminants. The cRNA was then quantitated. Hybridization was then performed and cRNA was normalized and dispensed onto the BeadChip. The RNA-loaded BeadChips were placed in Hyb chambers and incubated in the Illumina hybridization oven overnight at 58°C. Thereafter, the BeadChip underwent a series of wash steps according to the manufacturer's instructions. Cy3-Streptavidin was then added to the BeadChip to bind to the analytical probes hybridized to the BeadChip to allow for signal detection. Thereafter, the BeadChip was washed, dried and scanned with the iScan Reader. All downstream data analysis was then conducted as part of this dissertation.

2.2 Effect of vaginal *Lactobacillus* isolates on inflammatory responses to *G. vaginalis*

2.2.1 Women's Initiative in Sexual health (WISH) study

A total of 149 women aged 16-22 years old were enrolled in the WISH European & Developing Countries Clinical Trials Partnership (EDCTP)-funded study (Principal Investigator: Associate Professor Jo-Ann Passmore) in Masiphumelele, Cape Town (2013-2015). Several clinical samples were collected for each participant, along with demographic and behavioural data. Menstrual cups (Softcup®, Evofem Inc, San Diego, CA, USA) were used to collect cervicovaginal fluid (CVF). Lateral vaginal wall and vulvovaginal swabs were also collected. The lateral vaginal wall swabs were used to measure pH and test for the presence of STIs by PCR [by the National Institute of Communicable Diseases (NICD) STI Surveillance Laboratory, Sandringham, Johannesburg] (110). The STI tests included bacterial STIs, *Chlamydia trachomatis*, *Neisseria gonorrhoeae* and *Treponema pallidum*; protozoan, *Trichomonas vaginalis*; and viral, herpes simplex virus (HSV). Swabs were used for the diagnosis of BV (Gram-strain Nugent score of 7-10) and candidiasis (NICD Laboratory).

2.2.2 Isolation of Lactobacillus bacteria

Preceding this study, CVF samples were processed by Dr Smritee Dabee, Dr Shameem Jaumdally and Mrs Hoyam Gamieldien (Medical Virology, UCT). Phosphate buffered saline was used to dilute the CVF samples and stored in 20% glycerol at -80°C. For the isolation of *Lactobacillus* species, CVF samples were thawed and cultured in Man, Rogosa Sharpe (MRS; Sigma-Aldrich, USA) broth at 37°C, anaerobically for 48hrs. Thereafter, to obtain single colonies, the samples were streaked on MRS agar and incubated for an additional 48hrs at

37°C anaerobically. Colonies with varying morphology were then selected and cultured separately in MRS broth at 37°C, anaerobically for 72hrs. Lactobacilli were isolated by Mrs Hoyam Gamieldien and Dr Monalisa Manhanzva. A total of 115 lactobacilli were isolated from vaginal fluid samples and identified to species level by Matrix Assisted Laser Desorption Ionization-Time of Flight (MALDI-TOF) at the University of the Western Cape (UWC) and by Dr Remy Froissart (University of Montpellier, France).

2.2.3 Bacterial isolate selection

Inflammatory cytokine production by VK2 cells induced by *G. vaginalis* and these *Lactobacillus* isolates were previously evaluated (98). Chemokines MIP-3α, MIP-1α, MIP-1β, IP-10 and cytokines IL-8, IL-6, IL-1α and IL-1β were measured using Luminex. Overall, *Lactobacillus* isolates suppressed the inflammatory response of VK2 cells to *G. vaginalis* (98). A total of eight *Lactobacillus* isolates, including *L. jensenii* 3, *L. vaginalis* 3, *L. crispatus* 3, *L. mucosae* 2, *L. crispatus* 1, *L. jensenii* 2, *L. mucosae* 4, *L. vaginalis* 4 were selected for the current study based on their abilities to suppress inflammatory responses to *G. vaginalis* (ATCC 14018), clade 1 (111).

2.2.4 Bacterial culture and standardisation

Bacterial culture media was prepared according to **Appendix I.** *Lactobacillus* spp. and *G. vaginalis* frozen stocks stored in 60% glycerol were used to inoculate MRS broth (Sigma-Aldrich, USA) and Brain heart infusion broth (BHI; Sigma-Aldrich, USA), respectively.

Prior to this study, baseline CFU/ml in cultures standardised to an optical density (OD) of 0.1±0.01 for the *Lactobacillus* spp. and *G. vaginalis* were quantified by Ms Manhanzva (Medical Virology, UCT) to allow for standardisation of cultures using OD measurements. *Lactobacillus* spp. and *G. vaginalis* were inoculated from frozen stocks in 1.5ml MRS and BHI broth and incubated anaerobically for 48 hours, at 37°C. Thereafter, 1ml of each culture was sub-cultured in 14ml MRS (for lactobacilli) or BHI (for *G. vaginalis*) and incubated for 24 hours. An aliquot of 1.5ml of each culture was then centrifuged at 10 000rpm for 5 minutes, washed twice with 1ml PBS (Sigma-Aldrich, USA) and resuspended in 1ml of MRS or BHI. The OD at wavelength 600nm (OD_{600}) was measured for each culture using a spectrophotometer (Thermo Fisher Scientific Inc., USA) and standardised to an OD_{600} of 0.1±0.01 with MRS or BHI broth. For all *Lactobacillus* spp. and the *G. vaginalis* culture, serial dilutions of 1:100 in MRS or BHI were performed and 50µl of each dilution was plated onto MRS or BHI agar plates and incubated anaerobically for 48 hours at 37°C. Thereafter, the CFU/ml per plate were counted and used to calculate the baseline CFU/ml for each sample at OD_{600} 0.1±0.01, to be used for downstream standardization of samples.

Standardisation of the bacterial cultures to CFU/ml was performed by measuring the optical density at 600nm (OD_{600}) using a spectrophotometer (Thermo Fisher Scientific Inc., USA), of 1:10 dilutions of the cultures. These OD_{600} readings were then multiplied by 10 to obtain the OD_{600} of the neat cultures. Using these readings the number of bacteria in the neat cultures, baseline CFU/ml and the relative volumes needed to obtain the required CFU/ml, were calculated.

2.2.5 Human primary vaginal epithelial cell (VK2) culture

2.2.5.1 Thawing VK2 cells

Human vaginal epithelial cells [VK2/E6E7 (ATCC® CRL-2616™)] were cultured in Keratinocyte-Serum Free Medium (KSFM; GIBCO-BRL 17005042, Thermo Fisher Scientific, USA), supplemented with 0.1ng/ml human recombinant epidermal growth factor (EGF), 0.05mg/ml bovine pituitary extract (BPE), additional calcium chloride 44.1mg/L (final concentration 0.4mM) and 1% penicillin and streptomycin (pen/strep), recommended by ATCC. The frozen cell stocks were thawed by gentle agitation in a 37°C water bath, transferred to 9ml prewarmed (at 37°C) KSFM and centrifuged at 2000rpm for 7 minutes. The supernatant was then removed, and the cell pellet was resuspended in 1ml KSFM and transferred to a T25 cell culture flask containing 7.5ml prewarmed (at 37°C) KSFM and incubated at 37°C with 5% CO_2.

2.2.5.2 VK2 cell subculture

An inverted light microscope was used to monitor the confluency of the cells and the cells were subcultured at 60% confluency. To subculture, the old KSFM media was removed and the cells were washed twice with 5ml PBS (Sigma-Aldrich, USA) prewarmed at 37°C. Thereafter, the cells were lifted with prewarmed 3ml tryplE express reagent (ThermoFischer Scientific, USA) for a T25 flask or 5ml for a T75 flask and incubated at 37°C, 5% CO_2 for 5-10 minutes. Alternatively, 1ml trypsin/ethylenediaminetetraacetic acid (EDTA) (0.25%) for a T25 flask and 3ml for a T75 flask was used to detach the cells. Once the cells were detached from the culture flask the dissociation reagent was neutralised with 5ml (for a T25 flask) or 8ml (for a T75 flask) of Dulbecco's Modified Eagle's Medium/HamsF12 (DMEM:HamsF12; Sigma-Aldrich, USA) containing 10% bovine foetal calf serum (FCS) and centrifuged at 2000rpm for 7 minutes. The supernatant was then removed, and the cell pellet was resuspended in 1ml KSFM. A manual cell count was done by trypan blue staining of 15µl of the cell suspension with 15µl of trypan blue dye (Gibco, ThermoFischer, USA). This suspension was then pipetted

onto a haemocytometer and viewed using a light microscope. The cells were counted in two quadrants of the haemocytometer and the total cell count was obtained using the following formula: *(A + B) x 10^4 x 1ml*. The volume of cell suspension for the required seeding density into culture flasks, transwells or 24 well plates, was then calculated based on the ratio of cells in the 1ml suspension, to the required cell seeding density.

2.2.6 Optimization of methods for bacterial-VK2 cell coculture

Pilot assays were performed in order to assess and optimize (i) VK2 cell growth and viability under experimental conditions, (ii) cell storage media to optimize RNA yield and quality and (iii) cytokine responses under different culture conditions.

2.2.6.1 VK2 cell culture in transwells

As previous experiments characterising the anti-inflammatory effects of *Lactobacillus* isolates had been conducted in 24-well culture plates (29), culture of VK2 cells in transwell systems was first optimised. Corning transwell polyester membrane 24mm (6 well) cell culture inserts (Sigma-Aldrich CLS3450, USA) were used to culture VK2 cells. The system contains an apical and basal compartment which contain KSFM media, with the cells cultured on the polyester membrane containing 0.4µm pores to allow for the diffusion of media and cellular metabolites (manufacturer's protocol). Prior to seeding the cells, 2.6ml KSFM media was added to the apical and 1.4ml to the basal compartments of the transwell system and incubated at 37°C, 5% CO_2 for 1 hr for an initial equilibrium period which aids in cell attachment, as recommended by the manufacturer's protocol. A seeding density of 0.3 x 10^6 cells/well was used and the cells were grown for 7 days at 37°C, 5% CO2, with media changed every 2-3 days.

Following the 7-day incubation period, the cells were harvested for RNA extraction. The KSFM media was removed and the cells were washed thrice with PBS. Thereafter, 1ml and 1.5ml trypsin/EDTA was added to the apical and basal compartments, respectively and incubated at 37°C, 5% CO_2 for 5-10 minutes until the cells were detached from the membrane. An inverted light microscope was used to monitor the detachment of the cells. A total of 5ml DMEM:HamsF12 (10% FCS) was used to neutralise the trypsin/EDTA and the cell suspension was centrifuged at 2000rpm for 7 minutes. Thereafter, the supernatant was discarded, the cell pellet loosened by flicking and resuspended in 1ml KSFM. Cell counts were performed as described above. The cell suspension was then centrifuged again at 2000rpm for 7 minutes, the supernatant discarded, and the cell pellet resuspended in either 350µl RLT lysis buffer (Qiagen, USA) containing 1% 12M beta-mercaptoethanol (BME) or RNALater (Sigma-Aldrich,

USA) RNA stabilizing reagent. The samples which were resuspended in RLT buffer were vigorously vortexed for 60 seconds to ensure complete homogenization. All samples were stored at -80°C until RNA extraction.

2.2.6.2 Bacterial stimulation of VK2 cells in transwell culture systems

A total of 0.3 x 10^6 cells/well was seeded onto each transwell insert and cultured for 7 days as described above, after which bacterial stimulation of the cells was performed. The *Lactobacillus* isolates and *G. vaginalis* were cultured for 24 and 48 hours, respectively and standardised as previously described (29). *Lactobacillus* isolates and *G*. *vaginalis* cultures were standardised to 16.72 x 10^6 CFU/well in 1.5ml of media. This CFU/well was based on the culture volume of the 6-well transwell inserts proportional to the 24 well plate culture. A total of 750µl of each standardized *Lactobacillus* spp. and *G. vaginalis* was added to the wells and therefore 3x the number of CFUs used in previous 24 well experiments (29) was used for the transwell culture system.

Whereas previously, we had incubated VK2 cells with *Lactobacillus* isolates for 5 hours, followed by a 20 hours incubation with *G. vaginalis* prior to measurement of protein concentrations (29), for assessment of mRNA, a shorter incubation period was needed to ensure the detection of mRNA before its degradation. *Lactobacillus* isolates were thus co-cultured with VK2 cells at 37°C, 5% CO_2 for 3 hours. Thereafter, *G. vaginalis* was co-cultured with the lactobacilli pre-treated VK2 cells and incubated for an additional 3 hours at 37°C, 5% CO_2. Unstimulated cells and cells stimulated with *G. vaginalis* in isolation were used as controls. Thereafter, the cell supernatants were collected and centrifuged in 0.4µm Corning® Costar® SpinX tubes (ThermoFischer, USA) at 4000rpm for 10 minutes and stored at -80°C for cytokine measurement. For RNA extraction, the cells were harvested from the transwells, cell counts and viability assessed and the cells stored in RLT lysis buffer (1% BME) at -80°C until RNA extraction.

2.2.6.3 Bacterial stimulation of VK2 cells in 24 well plates

Previous data show that the VK2 cell viability is unchanged by the addition of these *Lactobacillus* isolates and *G. vaginalis* in the 24 well plates (98). Therefore, bacterial-VK2 co-culture experiments were also conducted in 24 well plates. Three independent experiments were performed to obtain three biological replicates for each condition.

The *Lactobacillus* isolates and *G. vaginalis* were cultured in triplicate independent cultures for 24 hours and 48 hours respectively, as previously described. The cultures were centrifuged at 4000rpm for 10 minutes, after which the supernatants were discarded, and the bacterial cell pellet was resuspended in KSFM without antibiotics. Thereafter, the *Lactobacillus* isolates were standardised to 4.18 x 10^6 CFU/500µl and *G. vaginalis* was standardised to 4.18 x 10^7 CFU/500µl as previously described (29).

The VK2 cells were cultured as previously described, from 3 frozen vial stocks for which 3 independent assays were performed. A total of 0.5 x 10^6 VK2 cells/well were seeded into 24 well plates and cultured to 80% confluency. VK2 cells were co-cultured with each *Lactobacillus* isolate (4.18x10^6CFU/well) in 500µl of media at 37°C, 5% CO_2 for 6 hours, in triplicate. Thereafter, *G. vaginalis* (4.18x10^7CFU/well) in 500µl of media was co-cultured with lactobacilli pre-treated VK2 cells in a final volume of 1ml media/well, for an additional 6 hours at 37°C, 5% CO_2. Cells only and *G. vaginalis*-VK2 cell co-culture controls were included in duplicate for each independent biological triplicate.

Following the 12-hour incubation, the cell supernatants were collected, centrifuged in 0.4µm SpinX tubes at 4000rpm for 10 minutes and stored at -80°C for cytokine and lactic acid detection assays. Thereafter, the cells were washed thrice with 500µl PBS. To detach the cells from the well surface, 300µl of prewarmed typlE express reagent (Gibco, ThermoFischer, USA) was added to each well and the cells were incubated at 37°C, 5% CO_2 for 10 minutes. Cell scrapers (TPP, Germany) were used to detach the remaining cells on the well surface. The tryplE express reagent was neutralised with 700µl of DMEM:Ham'sF12. An aliquot of 15µl of the cell suspension was used for cell counting by trypan blue staining as described above. The cell suspension was centrifuged at 2000rpm for 7 minutes. Thereafter, the supernatant was removed, and the cell pellet was loosened by flicking, resuspended in 350µl of RLT lysis buffer (1% BME) and vortexed vigorously to homogenize the sample. The samples were then stored at -80°C for RNA extraction.

2.2.7 RNA extraction

RNA extraction was performed using the RNeasy Plus Mini Kit (Qiagen, Germany) according to the manufacturer's instructions. Reagents were reconstituted according to the kit protocol. The samples stored in RNALater were first centrifuged at 3000xg for 5 minutes, thereafter the supernatants were discarded, the cells were resuspended in 350µl RLT lysis buffer (1% BME) and homogenized by vortexing vigorously. A total of 350µl of 70% ethanol was added to each sample in a spin column placed in a collection tube and centrifuged for 15 seconds at 10 000rpm. The flow through was then discarded and the spin column placed back into the collection tube. Thereafter, 700µl RW1 buffer was added to the spin column and centrifuged at 10 000rpm for 15 seconds, the flow through was then discarded and the spin column placed back into the collection tube. A total of 500µl of buffer RPE was used to wash the column membrane and centrifuged at 10 000rpm for 15 seconds. The flow through was then discarded. Thereafter, 500µl of RPE was added to the spin column and centrifuged for 2 minutes. The spin column was then placed into a new 1.5ml collection tube. For the final RNA elution step, a total of 30µl of RNase free water prewarmed to 42°C was added to the spin column and centrifuged for 1 minute at 10 000rpm. Using another 30µl of prewarmed RNase free water, the elution step was repeated. The total RNA volume for each sample was thus 60µl. RNA samples were stored at -80°C in 2 aliquots, a separate aliquot for RNA quality assessment.

2.2.8 Cytokine detection by Luminex assay

Cell culture supernatants were thawed at 4°C overnight prior to conducting the Luminex assay.

In order to measure the concentrations of 10 cytokines in the cell culture supernatants of VK2 cells stimulated by bacteria, a magnetic Luminex Screening Assay (Human Premixed Multi-Analyte Kit; R&D Systems, Biotechne) was performed. The cytokines measured included: interleukin-8 (IL-8), macrophage inflammatory protein-1-alpha and beta (MIP-1α and MIP-1β), interleukin-6 (IL-6), interferon-gamma-induced protein (IP-10), interleukin 1-beta (IL-1β), macrophage inflammatory protein-3-alpha (MIP-3α), interleukin-1-alpha (IL-1α), interleukin-1 receptor antagonist (IL1-RA) and monokine induced by interferon-gamma (MIG/CXCL9). These cytokines were selected based on previous studies that have demonstrated that *Lactobacillus* spp. and their metabolites reduced inflammatory responses by FGT epithelial cells *in vitro* (28,29,112). In addition, these *Lactobacillus* spp. isolated from the WISH cohort demonstrated immunomodulatory effects on VK2 cells stimulated with *G. vaginalis in vitro* (98).

All the kit reagents were at room temperature and prepared according to the manufacturer's protocol. Standard 1 (highest concentration) consisted of 100µl of each standard added to 500µl of calibrator diluent RD6-52. Using standard 1, a 3-fold dilution series was performed to prepare standards 2-6 in calibrator diluent RD6-52.

Standards and samples were then added to wells on a 96 well microplate (50µl of each) according to a plate layout. Diluent RD1-2 was used to dilute the microparticles, mixed well by vortex and 50µl was added to each well containing either standard or sample. A foil plate sealer was used to protect the plate from light and incubated at room temperature for 2 hours on a horizontal plate shaker, set to 800rpm.

Thereafter, the microplate was placed on an automated magnetic plate washer (Bio-Plex Pro™ Wash Station, Bio-Rad Laboratories, USA) which draws the microparticles to the bottom of the plate during the wash steps. The microplate was washed thrice with wash buffer.

Diluent RD2-1 was used to dilute the biotin antibody cocktail and 50µl was added to each well on the 96 well microplate. The plate was then incubated at room temperature, protected from light for 1 hour on a horizontal plate shaker set at 800rpm. Thereafter, the wash steps were repeated as described above. Streptavidin-Phycoerythrin (PE) was diluted in wash buffer and 50µl was added to each well. The plate was incubated at room temperature, protected from light for 30 minutes on a horizontal plate shaker set at 800rpm. The wash steps were then repeated, followed by resuspension of the microparticles with by adding 100µl wash buffer to each well. The plate was incubated at room temperature for 2 minutes on a horizontal plate shaker set at 800rpm. Thereafter, a Bio-Plex™ Suspension Array Reader (Bio-Rad Laboratories Inc®, USA) was used to read the microplate and cytokine concentrations were calculated using BIO-plex manager software (version 4; Bio-Rad Laboratories Inc®, USA) from standard curves using a 5-parameter logistic regression **(Appendix II).**

2.2.9 Detection of lactic acid in stimulated VK2 cell culture supernatants and pH measurement

Colorimetric assay kits (Sigma-Aldrich, USA) were used to measure the concentrations of D- and L- lactate in the VK2 cell culture supernatants following stimulation with bacterial isolates in 24 well plates. Frozen supernatants were thawed at 4°C overnight and assay kits were thawed at room temperature prior to usage. Reagents were reconstituted according to the kit protocol. Standards of 0, 2, 4, 6, 8 and 10nmole were prepared according to the kit protocol. D- and L-lactate standards were added in duplicate to the appropriate wells on 96 well plates

and brought to a final volume of 50µl with D- and L- lactate assay buffers, respectively. Sample were added to appropriate wells on each plate in duplicate (50µl of each sample).

Reaction mixes were prepared according to the kit protocol; volumes were adjusted according to the number of wells used. The D-lactate reaction mix was made up of D-lactate assay buffer, D-lactate enzyme mix and D-lactate substrate. The L-lactate reaction mix was made up of L-lactate assay buffer, L-lactate enzyme mix and L-lactate probe. D- or the L-lactate reaction mix was added to all wells on the 96 well plates (50µl/well). The plates were incubated for 30 minutes at room temperature protected from light. An ELISA plate reader (VersaMax™, Molecular Devices LLC, USA) was used to measure the absorbance at 450nm for D-lactate and 570nm for L-lactate.

Prior to generating the standard curves using GraphPad Prism V.8 (GraphPad Prism Software, USA; **Appendix III**), absorbance readings of the standard blanks were subtracted from all standards. The absorbance of the sample blank was subtracted from all sample absorbance readings as well. The standard curves were used to interpolate the D- and L-lactate amounts (nmole) using GraphPad Prism and the concentrations (ng/ml) were calculated using the equations in **Appendix IV** provided by the manufacturer's protocol.

The pH levels of the samples were measured using pH strips range 1-14 (Macherey-Nagel, Germany). Calculation of total lactic acid was done using the Henderson-Hasselbalch equation:

$$pH = pK_a + log_{10}\frac{[A^-]}{[HA]}$$

2.2.10 Microarray Affymetrix assay

The microarray Affymetrix assay was performed at the Centre for Proteomics and Genomic research (CPGR), Cape Town, South Africa. The samples were prepared for microarray using a GeneChip™ WT PLUS Reagent kit according to the manufacturer's protocol. The detailed protocol is included in **Appendix V.** Briefly, double-stranded cDNA synthesis was followed by cRNA synthesis and purification. cRNA yield of each sample was assessed by using a NanoDrop spectrophotometer. cRNA size distribution was assessed using an Agilent 2100 Bioanalyzer. The cRNA was then reverse transcribed using second-cycle primers,

synthesizing sense-strand cDNA. The cRNA template of the RNA-DNA hybrid was then hydrolysed using RNAse H, generating single stranded cDNA. The remaining sense-strand cDNA was then purified using purification beads, to remove enzymes, salts and unincorporated dNTPs. cDNA yield and size distribution of each sample was assessed using a NanoDrop spectrophotometer and an Aligent 2100 Bioanalyzer. Uracil-DNA glycosylase (UDG) and apurinic/apyrimidinic endonuclease 1 (APE1) was used to fragment the sense-strand cDNA. A DNA labelling reagent linked to biotin was used to label the fragmented cDNA by terminal deoxynucleotidyl transferase (TdT). The hybridization master mix was prepared and added to the fragmented and labelled ss-cDNA samples producing a hybridization cocktail and incubated according to the manufacturer's protocol. The hybridization cocktail was added to the GeneChip™ Cartridge Array and incubated. Thereafter, the Array was washed and stained according to the manufacturer's protocol. The GeneChip Cartridge Array was then scanned.

2.2.11 Data analysis

GraphPad Prism V.8 (GraphPad Software, USA), STATA v13.1, R Studio v1.2.5001 (RStudio, USA) and the Database for Annotation, Visualization and Integrated Discovery (DAVID Bioinformatics resources) v6.8, were used to analyse data. Prior to statistical analysis, data distribution was tested using the Shapiro-Wilk test. Parametric statistical tests were used for normally distributed data and non-parametric statistical tests were used for data which was not normally distributed.

2.2.11.1. Illumina microarray data

The Illumina microarray data analysis workflow by Du *et al*. (2010) (113), with modifications, was used to analyse the data. The data were normalized using Illumina BeadStudio by subtracting background and scaling the average signal intensity for each sample to the global average signal intensity for all 10 samples. The data were then $\log_2$-transformed and normalised by quantile normalisation, followed by quality control assessment to detect potential outlier data points, using the R Studio Bioconductor lumi package. The R Studio Bioconductor limma package was then used for differential gene expression analysis of CMCs compared to PBMCs. Differentially expressed genes were filtered according to adjusted p-values and were considered significantly expressed if adj. $p \leq 0.05$. Furthermore, the significant differentially expressed genes were filtered based on log fold change (FC) and were considered upregulated or downregulated if $logFC \geq 1.5$ or $logFC \leq -1.5$, respectively. Principal components analysis (PCA) and a heatmap displaying hierarchical clustering of differentially

expressed genes were generated using R studio mixOmics and complexHeatmap packages, respectively. All R scripts used are in **Appendix VI**. Genes were annotated using the Illumina humanHT-12 v3 annotation file (114) Gene Entrez IDs were inputted into the DAVID Bioinformatics resources v6.8 (115) and to obtain Kyoto Encyclopedia of Genes and Genomes (KEGG) biological pathways upregulated and downregulated in CMCs compared to PBMCs. DAVID Bioinformatics resources v6.8 gene enrichment pathway analysis is performed using an EASE Score, which is a Fisher Exact P-value. A P-value ≤ 0.05 is considered an enriched KEGG pathway (116,117). The Fisher's Exact test statistically tests whether the proportion of DEGs mapped to the KEGG pathway are by random chance in comparison to the proportion of genes in the human genome involved in the KEGG pathway (116,117). CIBERSORT and xCell analyses of gene expression data were used to enumerate immune cell populations in CMCs and PBMCs (118,119).

2.2.11.2. Luminex cytokine data

An unpaired two-tailed non-parametric Mann-Whitney U test was used to evaluate differences in cytokine responses of VK2 cells induced by *G*. *vaginalis* ($4.18x10^7$CFU/well) alone and in combination with each *Lactobacillus* isolate ($4.18x10^6$CFU/well) in 1ml of media. PCA plots and heatmaps displaying unsupervised hierarchical clustering of cytokine responses were generated using R Studio mixOmics and heatmap packages (script in **Appendix VII**). PCA was also used to group all inflammatory cytokines and chemokines and generate estimates representative of the overall inflammatory responses. P-values were adjusted for multiple comparisons using a false discovery rate step-down procedure (120). Statistical correlations between lactic acid production and cytokine responses were evaluated using Spearman's Rank correlation.

2.2.11.3. Affymetrix microarray data

The affymetrix microarray data analysis workflow by Klaus & Reisenauer (2018) (121), with modifications, was used to pre-process the data. The raw data CEL files were inputted into R studio, log_2-transformed using the Bioconductor oligo and Biobase packages. Quality control assessments to detect potential outliers, were done using the R Studio oligo and arrayQualityMetrix packages. Affymetrix raw data were normalized by Robust Multichip Average (RMA) normalization using the oligo package in R studio. PCA and heatmaps showing hierarchical clustering of genes were generated using R Studio ggplot and ggplot2 package. The R Studio Bioconductor limma package was used for differential gene expression analysis of VK2 cells stimulated with *G*. *vaginalis* ($4.18x10^7$CFU/well) alone and in combination with each *Lactobacillus* isolate ($4.18x10^6$CFU/well) in 1ml of media. Differentially

expressed genes were filtered according to adjusted p-value and were considered significantly expressed if adj.p≤0.05. Significantly differentially expressed genes were filtered according to logFC and genes were considered upregulated or downregulated if logFC>1.5 or logFC<-1.5, respectively. Genes were annotated using the Clariom S HumanHT annotation file (122) . Gene Entrez IDs were inputted into DAVID Bioinformatics resources v6.8 (115) and the WEB-based Gene Set analysis Toolkit (WebGestalt) (123) to obtain KEGG biological pathways upregulated and downregulated in VK2 cells stimulated with *G*. *vaginalis* alone and in combination with each *Lactobacillus* isolate. Fisher's Exact statistical test was used for enrichment analysis of KEGG pathways as described above (116,117). All R scripts used are in **Appendix VIII**.

Chapter 3: Results

3.1 Groote Schuur study cohort

Matched cervical cytobrush and blood samples were collected from five black, chronically HIV-infected women who were enrolled at the Gynaecology Outpatient Clinic, Groote Schuur Hospital, Cape Town, South Africa (Principal Investigator: Associate Professor Jo-Ann Passmore). A total of 60% (n=3) of participants were viral load (VL) suppressed (plasma VL<50 copies/ml) and 40% (n= 2) of participants had detectable viral loads, while the average blood CD4+ T cell count of the participants was 605.4 cells/ul **(Table 1).** None of the women had clinical signs or symptoms of STIs or BV. However, one participant was diagnosed with a stenosed cervix **(Table 1)**.

Table 1 Demographic and clinical characteristics of Groote Schuur cohort

Demographic characteristics	n (%)
South African	5 (100)
Black race	5 (100)
Clinical characteristics	
Chronic HIV-1+	5 (100)
ARV treatment	5 (100)
Average CD4+ count (cells/µl)	605.4
Detectable VL	2/5 (40)
BV/STI signs or symptoms	0/5 (0)
Cervical stenosis	1/5 (10)
BV: bacterial vaginosis, **STI:** sexually transmitted infection.	

3.2 Gene transcription of matched CMCs and PBMCs

Using a microarray Illumina HumanHT-12 v3 Gene Expression BeadChip platform, the potential differences in gene transcription of CMC compared to matched PBMC samples obtained from HIV-infected women, were evaluated.

The RNA quality was assessed for all samples. The samples showed some RNA degradation, however the quality of all samples was suitable for microarray analysis. RNA integrity numbers (RIN) obtained were 5.3-8.4 and 8.6-9.8, for CMC and PBMC samples, respectively **(Appendix IX).** A total of three CMC samples, NY76_CMC, NY82_CMC and NY133C_CMC had partially degraded RNA, RINs 6.4, 7.4 and 5.3, respectively **(Appendix IX).** All PBMC sample RINs were above 8, which is considered good quality RNA with minimal degradation **(Appendix IX)**. The RNA quantity of the samples was above the required input for microarray analysis **(Appendix IX).**

A total of 48668 genes were detected. Prior to normalization, although median values for all samples tended to be similar, some variation was observed, particularly for sample NY76_CMC which had the highest median intensity value **(Figure 2A).** Following quantile normalization, no outliers were detected and all median values for the samples were the same **(Figure 2B).** Further analysis was done using the normalized data. Additional quality control assessment of the normalized microarray data were then performed to further detect potential outliers, of which there were none **(Appendix X)**. CMC and PBMC samples clustered together, respectively, using hierarchical clustering based on all 48668 genes detected **(Figure 3)**.

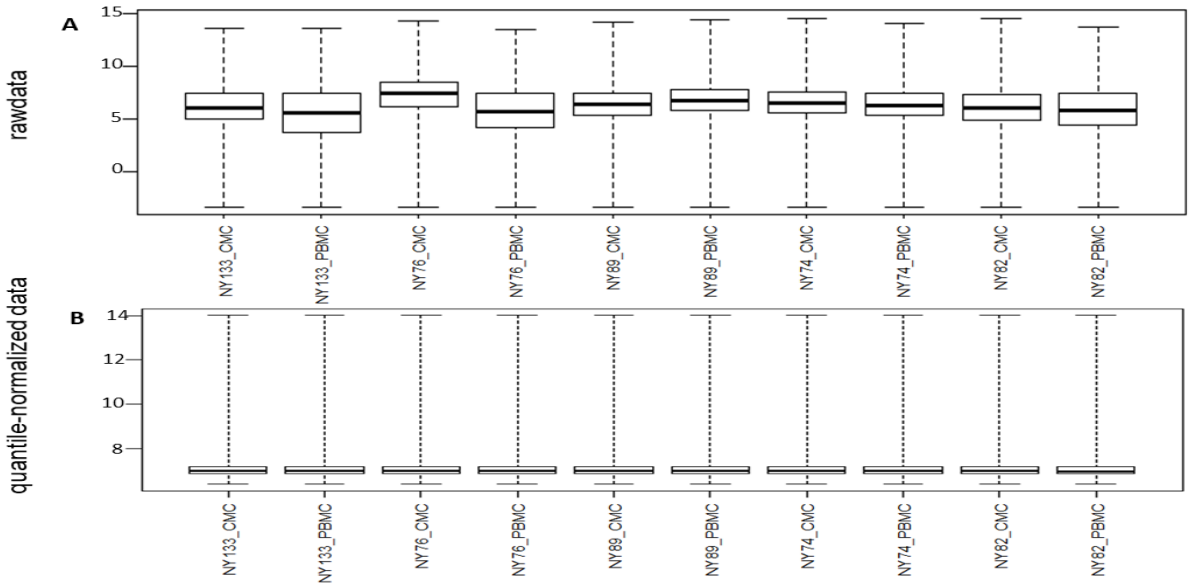

Figure 2 Quantile normalized Illumina microarray raw data of matched CMC and PBMC samples. A) Boxplots showing raw data. **B)** Boxplots showing quantile normalized raw data. Horizontal lines of boxes indicate the first quartile, median and third quartile, while the error bars indicate the minimum and maximum signal intensities, for each sample. RNA was extracted from matched CMCs and PBMCs isolated from cervical cytobrush and blood samples obtained from chronically HIV-infected women. Gene expression analysis of RNA samples were evaluated using Illumina Human HT-12 V3 Gene Expression Beadchip. Quantile normalization was performed on raw data using the lumi R package. **CMC**: cervicovaginal mononuclear cells, **PBMC**: Peripheral blood mononuclear cells.

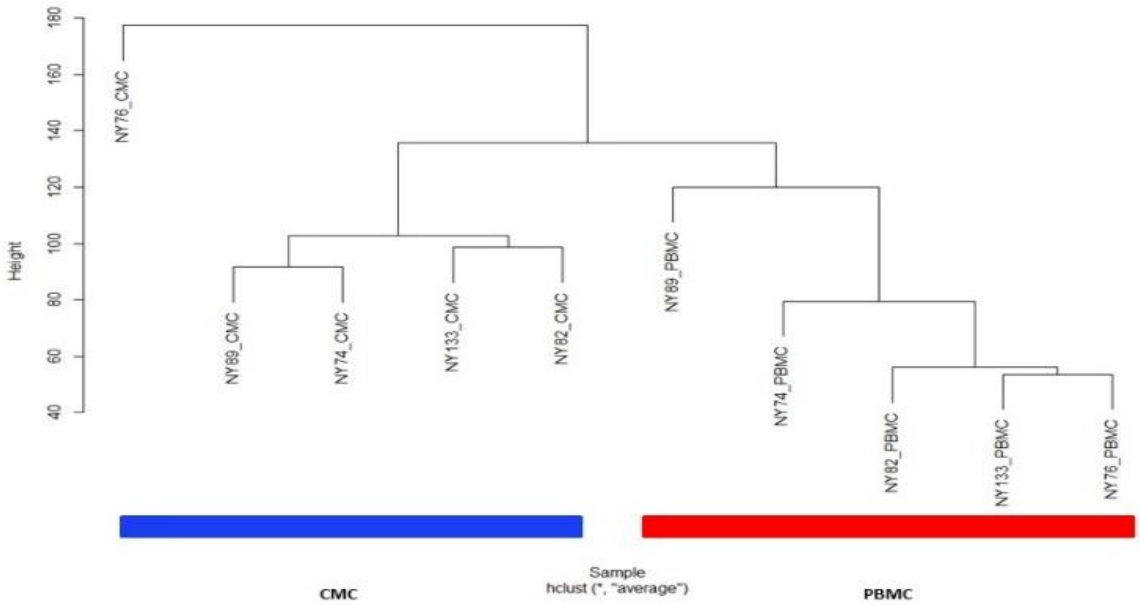

Figure 3 Relationships between samples based on 48668 genes expressed in CMC and PBMC samples. RNA was extracted from matched CMCs and PBMCs isolated from cervical cytobrush and blood samples obtained from chronically HIV-infected women. Gene expression analysis of RNA samples were evaluated using Illumina Human HT-12 V3 Gene Expression Beadchip. Quantile normalization was performed on raw data. Normalized data were preprocessed using the R Bioconductor lumi package**.** Relationships between samples based on 48668 genes was plotted using hierarchical clustering. The lengths of the vertical lines in the dendrogram indicate the degree of relatedness to the adjacent samples or clusters. Blue: CMC sample cluster, Red: PBMC sample cluster. **CMC:** cervical mononuclear cells, **PBMC**: peripheral blood mononuclear cells.

3.3 Genes differentially expressed in CMCs compared to PBMCs and downstream signalling pathways detected

The R Studio Bioconductor limma package was used to identify genes that were differentially expressed in CMCs compared to PBMCs. Although this study included a small sample size, 2867 genes were significantly differentially expressed in CMCs compared to PBMCs, adjusted (adj.) p≤0.05 **(Figure 4A)**, with 119 genes upregulated (logFC≥1.5) and 57 genes downregulated (logFC≤-1.5) in CMCs compared to PBMCs **(Figure 4B, Appendix XI).** Downstream pathway analysis, using DAVID Bioinformatics resources v6.8 revealed that five genes that were upregulated in CMCs compared to PBMCs mapped to the NF-κB signalling pathway (IL-1β, TNF-R1, IκBα, IL-8 and COX2; **Figures 5A and 6**), four mapped to the TLR signalling pathway (IκBα, OPN, IL-1β and IL-8; **Figures 5A and 7)** and five mapped to the TNF signalling pathway (TNF-R1, IκBα, IL-1β, NF-κB iα and Ptgs2; **Figures 5A and 8)**. A total of 7 genes encoding large (S15e, L17e, S3, S29e, S15Ae, L19e, S14e) and 8 genes encoding short ribosomal subunits (L30e, L21e, S3Ae, S6e, S17e, S27e, S27Ae, S12e) were downregulated in CMCs compared to PBMCs **(Figures 5B and 9)**. Downregulated genes in CMCs compared to PBMCs which mapped to the sphingolipid pathway, were Fyn, PI3K, S1P1 and S1P5 **(Figures 5B and 10)**, to the T cell receptor signalling pathway, were Fyn, CD3ζ, ITK and PI3K **(Figures 5B and 11)** and to the natural killer cell mediated cytotoxicity pathway, were CD48, Perforin, CD3ζ, Fyn and PI3K **(Figures 5B and 12)**. Key genes significantly upregulated in proinflammatory pathways were IL-1β, TNF-R1 and IL-8 (adj. $p=2.6112x10^{-5}$, adj. p=0.0036, adj. p=0.0003, respectively, **Figure 13A-C**)**.** Key genes significantly downregulated in pathways were Fyn, CD3ζ and PI3K (adj. p=0.0002, adj. p=0.0002, adj. $p=2.6112x10^{-5}$, respectively, **Figure 13D-F**). Key genes were defined as those which mapped to several pathways.

Although the NF-κB, TNF, TLR and NOD-like receptor signalling pathways were overrepresented in CMCs compared to PBMCs (p=0.0018, p=0.0261, p=0.0261, p=0.0437, respectively**, Figure 5A**), significance was not upheld after adjusting for multiple comparisons due to the small sample size (adj. p=1, **Figure 5A**). Ribosome, sphingolipid, T cell receptor and natural killer cell mediated cytotoxicity signalling pathways were underrepresented in CMCs compared to PBMCs ($p=1.8071x10^{-15}$, p=0.0243, p=0.0154, p=0.254, respectively, **Figure 5B**), with the ribosome pathway remaining significant after adjusting for multiple comparisons (adj. $p=2.0095x10^{-12}$, **Figure 5B**).

CIBERSORT and xCell analyses of the gene expression data were used to evaluate the predicted absolute abundance of cell populations in CMC and PBMC samples (**Appendix XII**). Overall, the CIBERSORT predicted abundance of the majority of immune cell types was

greater in CMCs compared to PBMCs (**Appendix XII, Figure 52A**). However, predicted absolute abundance of monocytes, CD8+ T cells, CD4+ naïve T cells, activated natural killer cells (p=0.0079) and resting mast cells (p=0.0159) were significantly underrepresented in CMCs compared to PBMCs (**Appendix XII**, **Figure 52A**). While neutrophils were significantly overrepresented in CMCs compared to PBMCs (p=0.0079). However, all significant p-values were not upheld after adjusting for multiple comparisons.

Similarly, xCell predicted abundance of CD4+ T cells, CD4+ memory T cells, CD4+ naïve T cells, CD8+ T cells, CD8+ effector T cells (Tem), and CD8+ naïve T cells were significantly underrepresented in CMCs compared to PBMCs (adj. p=0.0364, adj. p=0.0492, adj. p=0.0342, adj. p= 0.0336, adj. p=0.0346, adj. p= 0.0336, respectively, **Appendix XII, Figure 52B**). xCell predicted mast cell and CD4+ central memory (Tcm) T cell abundance was also significantly underrepresented in CMCs compared to PBMCs (p=0.0141 and p=0.0271), however, not significantly after adjusting for multiple comparisons. In contrast, xCell predicted abundances of epithelial cells and keratinocytes were significantly overrepresented in CMCs compared to PBMCs (adj. p=0.0063 and adj. p=0.01575, respectively, **Appendix XII, Figure 52B**). In addition, xCell predicted abundance of platelets, lymphoid progenitor cells (CLP), conventional dendritic cells (cDC) and Th1 cells was significantly underrepresented in CMCs compared to PBMCs (p=0.0114, p=0.0114, p=0.0322, p=0.0343, respectively), while natural killer T (NKT) cells and activated dendritic (aDC) cells were overrepresented in CMCs compared to PBMCs (p=0.0184 and p=0.0215, respectively, **Appendix XII, Figure 52B**), however not significantly after adjusting for multiple comparisons.

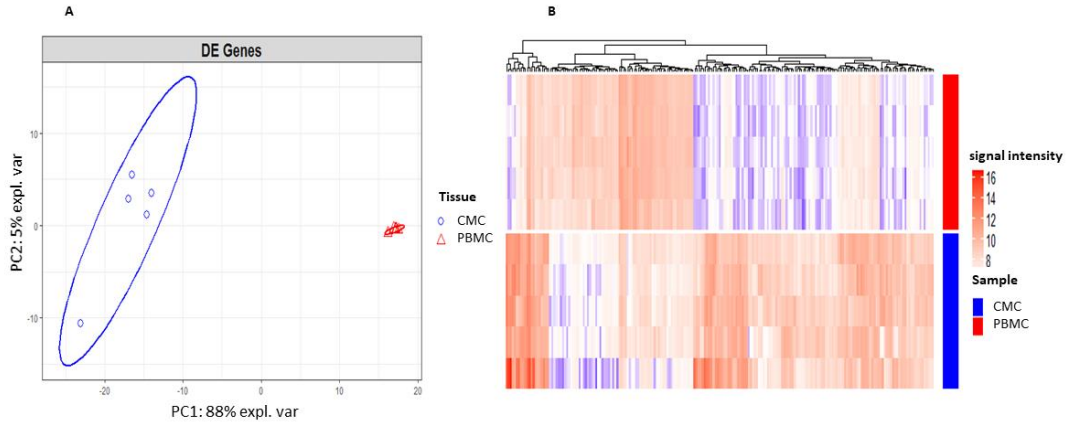

Figure 4 Differential gene expression in CMCs compared to PBMCs. A) Principal component analysis (PCA) clustering of samples based on differential gene expression. **B)** Unsupervised hierarchical clustering of groups based on differential gene expression. RNA was extracted from 5 CMC and 5 matched PBMC samples isolated from cervical cytobrush and blood samples obtained from chronically HIV-infected women. Gene expression was evaluated using the microarray Illumina HumanHT-12 v3 Gene Expression BeadChip platform. Gene expression data were normalized by quantile normalization. Differential gene expression analysis was performed using R Bioconductor limma package. Genes were considered differentially expressed if adj. p≤0.05 and up- or downregulated if log fold change (FC) ≥ 1.5 or ≤ -1.5, respectively. The dendogram above the heatmap indicates the degree of relatedness between the genes expressed. The horizontal "branches" have arbitrary lengths and the length of the vertical "branches" indicate the degrees of similarity between the gene expression profiles. Purple, through white, to red indicates low to high gene expression. **CMC***:* cervical mononuclear cells, **PBMC***:* peripheral blood mononuclear cells, **PC1**: principal component 1, **PC2**: principal component 2.

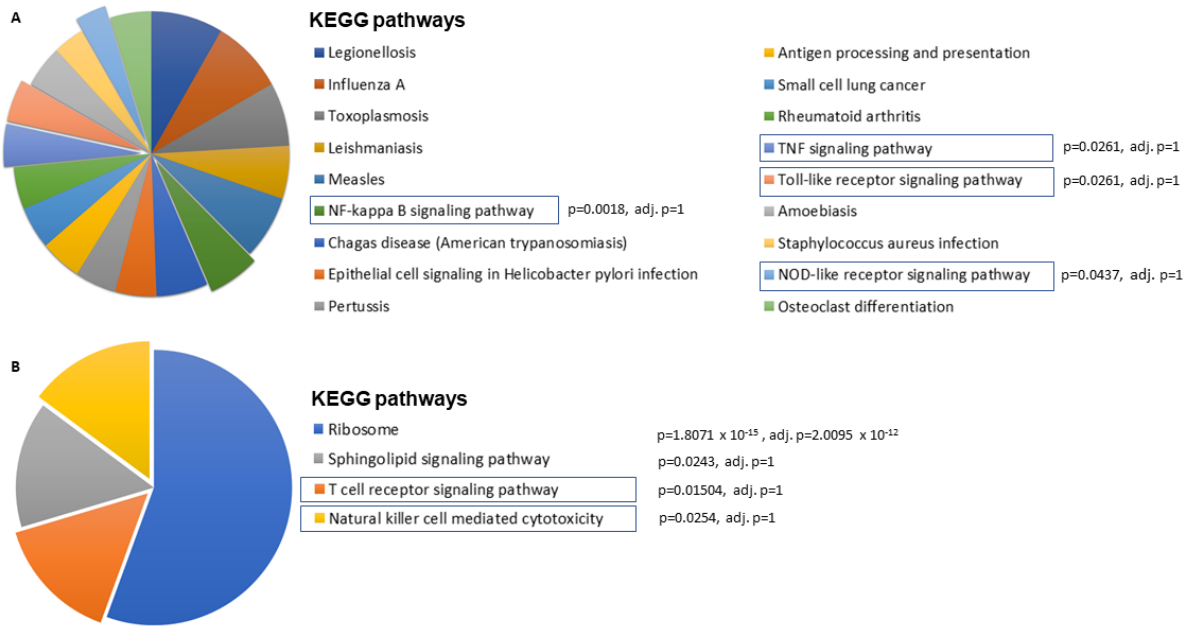

Figure 5 Signaling pathways upregulated (A) and downregulated (B) in CMCs compared to PBMCs. The pie chart shows the proportion of differentially expressed genes in CMC compared to PBMC samples for each signaling pathway, key proinflammatory signaling pathways are boxed. RNA was extracted from 5 CMC and 5 matched PBMC samples isolated from cervical cytobrush and blood samples obtained from chronically HIV-1 infected women. Gene expression was evaluated using a microarray Illumina HumanHT-12 v3 Gene Expression BeadChip platform. Gene expression data were normalized by quantile normalization. Differential gene expression analysis was performed using the R Bioconductor limma package. Genes were considered differentially expressed if adj. p≤0.05, and up- or downregulated if log fold change (FC) ≥ 1.5 or ≤ -1.5, respectively. Differentially expressed probeset IDs were annotated using the Illumina humanHT-12 v3 annotation file. Upregulated gene Entrez identity numbers were inputted to DAVID Bioinformatics resources v6.8 to obtain biological KEGG pathways upregulated. **CMC**: cervical mononuclear cells, **PBMC**: peripheral blood mononuclear cells. **TNF**: tumor necrosis factor, **NF-Kappa-B**: nuclear factor kappa-light-chain-enhancer of activated B cells, **NOD-like**: nucleotide-binding oligomerization domain-like.

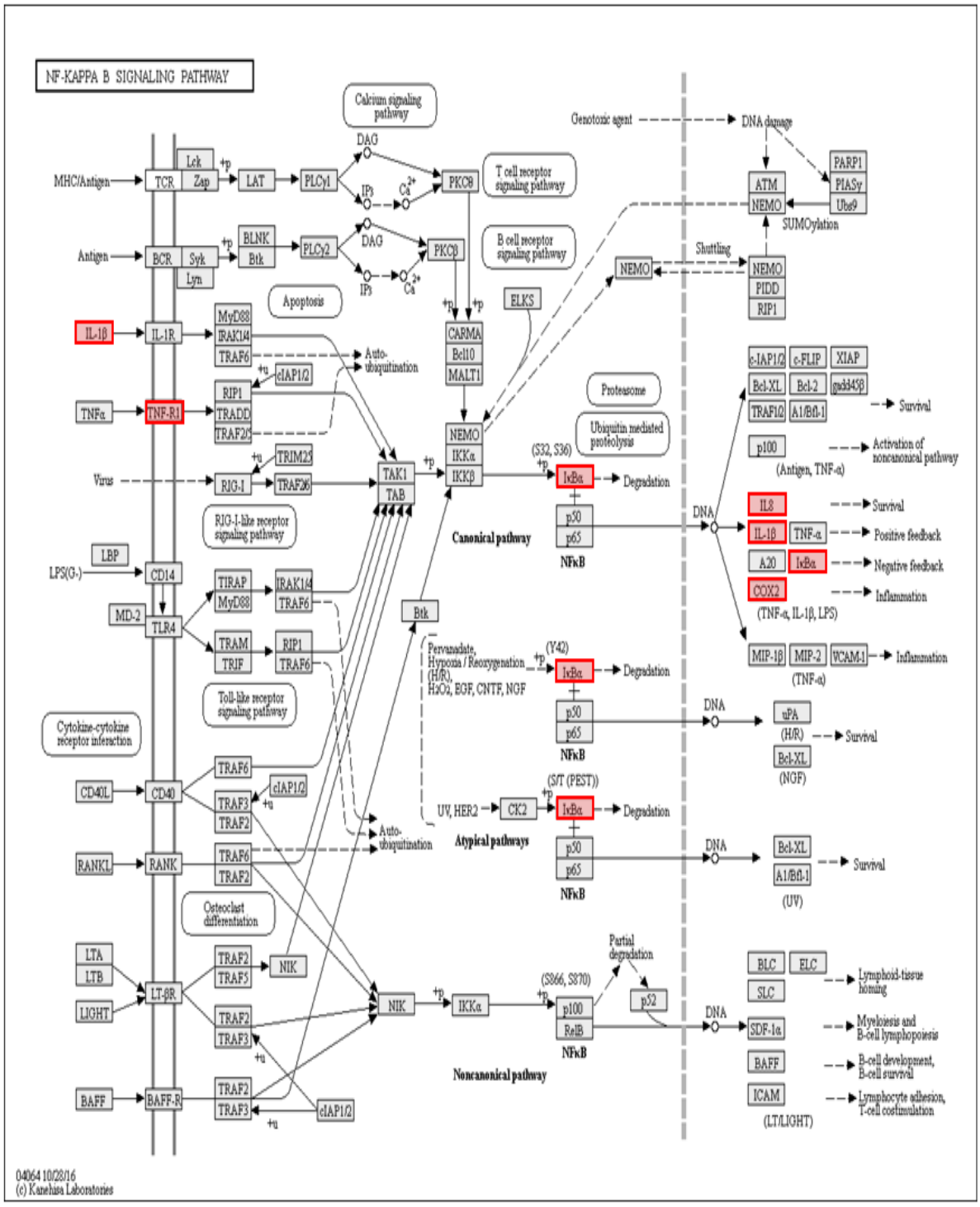

Figure 6 Upregulated genes in the NF-Kappa B signaling pathway in CMCs compared to PBMCs. KEGG pro-inflammatory signaling pathway, adapted from DAVID Bioinformatics resources v6.8 is shown. Red boxes indicate upregulated mediators in CMCs compared to PBMCs. RNA was extracted from 5 CMC and 5 matched PBMC samples, isolated from cervical cytobrush and blood samples obtained from chronically HIV-1 infected women. Gene expression was evaluated using a microarray Illumina HumanHT-12 v3 Gene Expression BeadChip platform. Gene expression data were normalized by quantile normalization. Differential gene expression analysis was performed using R Bioconductor limma package. Genes were considered differentially expressed if adj. p≤0.05 and up- or downregulated if log fold change (FC) ≥ 1.5 or ≤ -1.5, respectively. Differentially expressed probeset IDs were annotated using the Illumina humanHT-12 v3 annotation file. Upregulated gene Entrez identity numbers were inputted to DAVID Bioinformatics resources v6.8 to obtain biological KEGG pathways upregulated. **CMC:** cervical mononuclear cells, **PBMC**: peripheral blood mononuclear cells, **IL-1β**: Interleukin-1 Beta, **TNF-R1**: tumor necrosis factor receptor 1, **IκBα**: nuclear factor of kappa light polypeptide gene enhancer in B-cells inhibitor alpha, **IL-8**: Interleukin-8, **COX2**: cyclooxygenase-2.

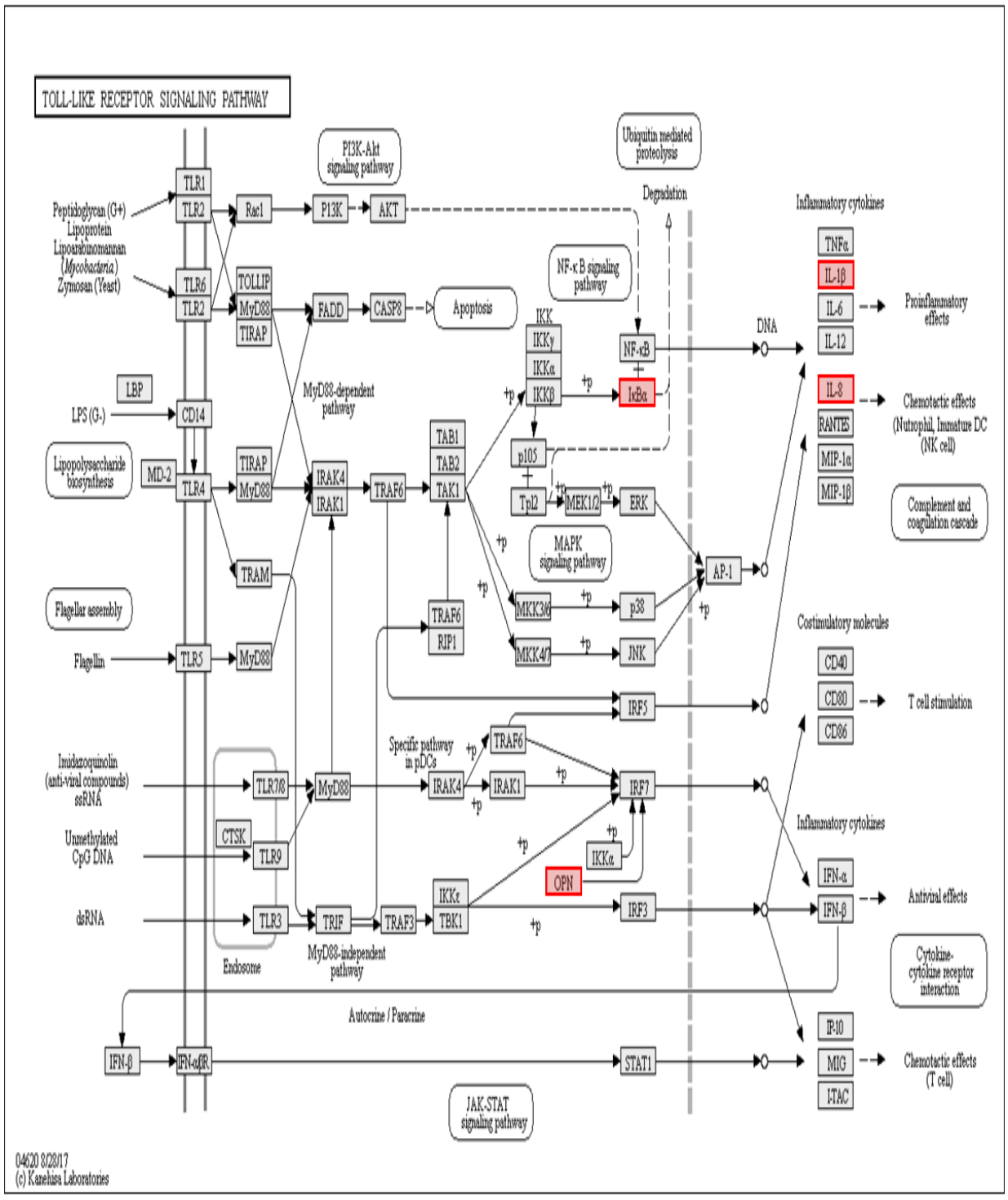

Figure 7 Upregulated genes in the Toll-like receptor signaling pathway in CMCs compared to PBMCs. The KEGG pro-inflammatory signaling pathway, adapted from DAVID Bioinformatics resources v6.8 is shown. Red boxes indicate upregulated mediators in CMCs compared to PBMCs. RNA was extracted from 5 CMC and 5 matched PBMC samples, isolated from cervical cytobrush and blood samples obtained from chronically HIV-1 infected women. Gene expression was evaluated using a microarray Illumina HumanHT-12 v3 Gene Expression BeadChip platform. Gene expression data were normalized by quantile normalization. Differential gene expression analysis was performed using R Bioconductor limma package. Genes were considered differentially expressed if adj. p≤0.05 and up- or downregulated if log fold change (FC) ≥ 1.5 or ≤ -1.5, respectively. Differentially expressed probeset IDs were annotated using the Illumina humanHT-12 v3 annotation file. Upregulated gene Entrez identity numbers were inputted to DAVID Bioinformatics resources v6.8 to obtain biological KEGG pathways upregulated. **CMC:** cervical mononuclear cells, **PBMC**: peripheral blood mononuclear cells, **IL-1β**: Interleukin-1 Beta, **IκBα**: nuclear factor of kappa light polypeptide gene enhancer in B-cells inhibitor alpha, **OPN**: osteopontin.

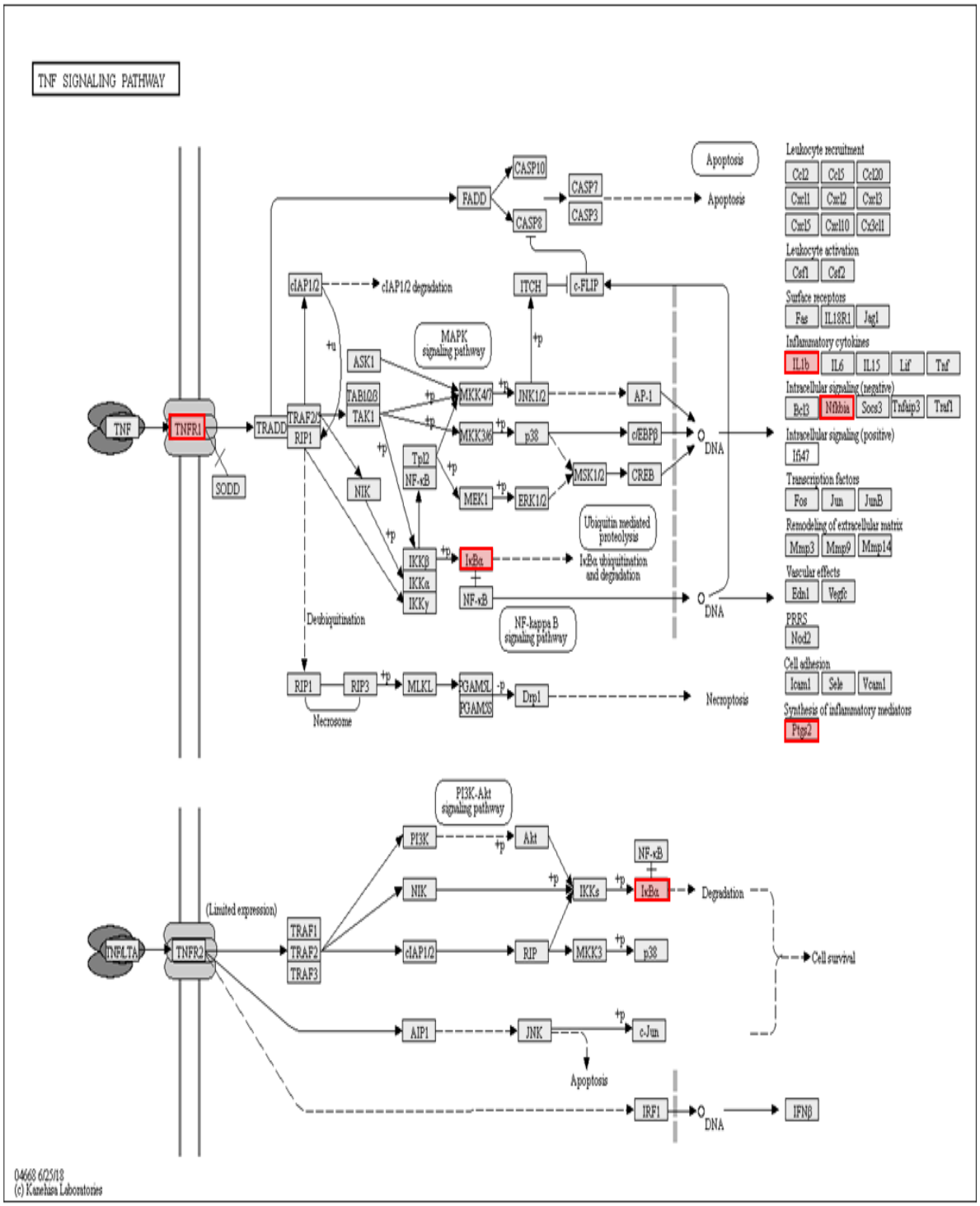

Figure 8 Upregulated genes in the TNF signaling pathway in CMCs compared to PBMCs. The KEGG pro-inflammatory signaling pathway, adapted from DAVID Bioinformatics resources v6.8 is shown. Red boxes indicate upregulated mediators in CMCs compared to PBMCs. RNA was extracted from 5 CMC and 5 matched PBMC samples, isolated from cervical cytobrush and blood samples obtained from chronically HIV-1 infected women. Gene expression was evaluated using a microarray Illumina HumanHT-12 v3 Gene Expression BeadChip platform. Gene expression data were normalized by quantile normalization. Differential gene expression analysis was performed using R Bioconductor limma package. Genes were considered differentially expressed if, adj. p≤0.05 and up- or downregulated if log fold change (FC) ≥ 1.5 or ≤ -1.5, respectively. Differentially expressed probeset IDs were annotated using the Illumina humanHT-12 v3 annotation file. Upregulated gene Entrez identity numbers were inputted to DAVID Bioinformatics resoources v6.8 to obtain biological KEGG pathways upregulated. **CMC:** cervical mononuclear cells, **PBMC**: peripheral blood mononuclear cells, **IL-1β**: Interleukin-1 Beta, **IκBα**: nuclear factor of kappa light polypeptide gene enhancer in B-cells inhibitor alpha, **TNFR1**: tumor necrosis factor receptor-1, **Nfkbia**: NFkB inhibitor alpha, **Ptgs2**: prostaglandin-endoperoxide synthase 2.

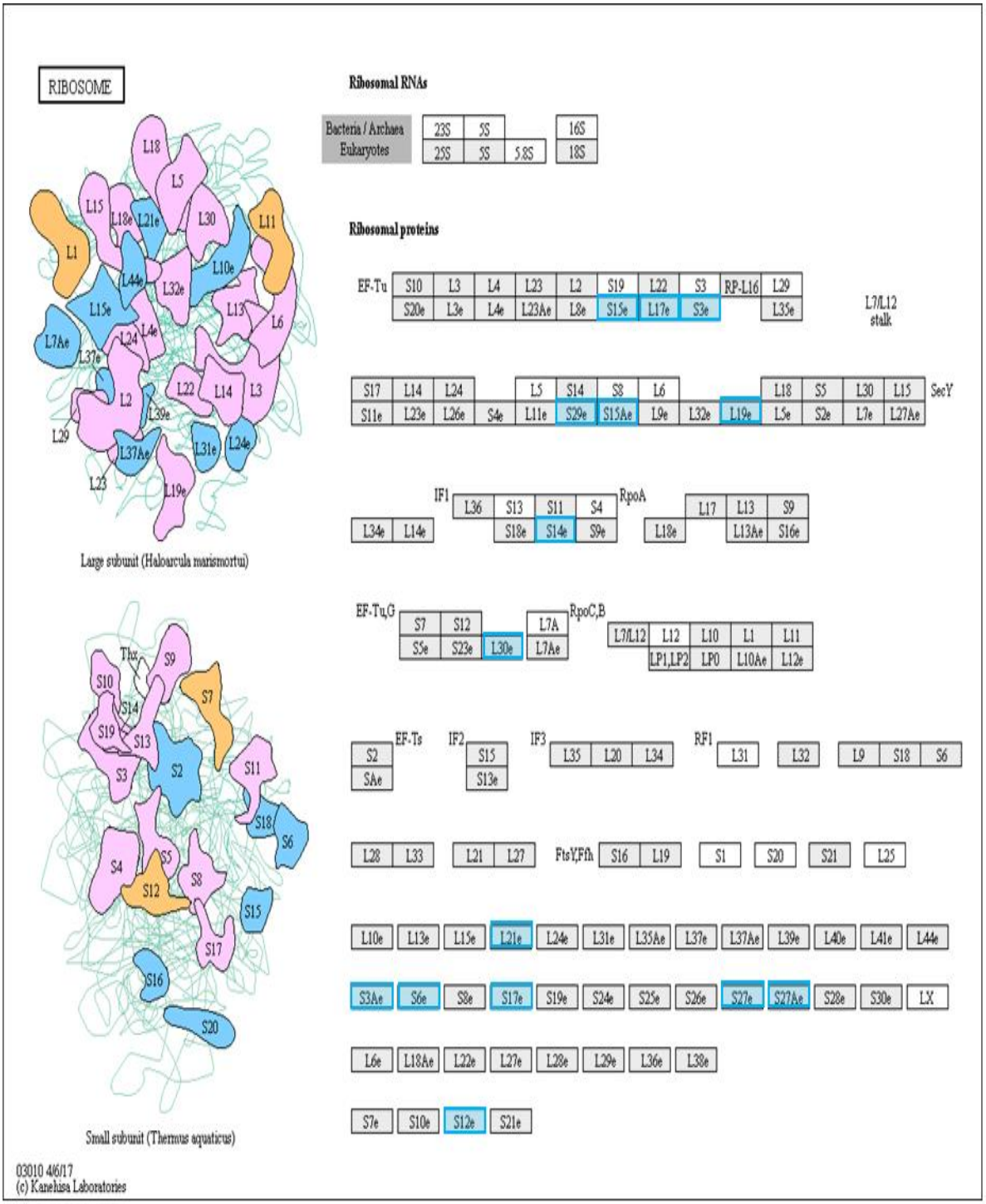

Figure 9 Ribosomal subunits downregulated in CMCs compared to PBMCs. KEGG large and short ribosomal subunits, adapted from DAVID Bioinformatics resources v6.8, are shown. Blue boxes indicate downregulated mediators in CMCs compared to PBMCs. RNA was extracted from 5 CMC and 5 matched PBMC samples, isolated from cervical cytobrush and blood samples obtained from chronically HIV-1 infected women. Gene expression was evaluated using a microarray Illumina HumanHT-12 v3 Gene Expression BeadChip platform. Gene expression data were normalized by quantile normalization. Differential gene expression analysis was performed using R Bioconductor limma package. Genes were considered differentially expressed if adj. p≤0.05 and up- or downregulated if log fold change (FC) ≥ 1.5 or ≤ -1.5, respectively. Differentially expressed probeset IDs were annotated using the Illumina humanHT-12 v3 annotation file. Upregulated gene Entrez identity numbers were inputted to DAVID Bioinformatics resources v6.8 to obtain biological KEGG pathways upregulated. **CMC:** cervical mononuclear cells, **PBMC**: peripheral blood mononuclear cells.

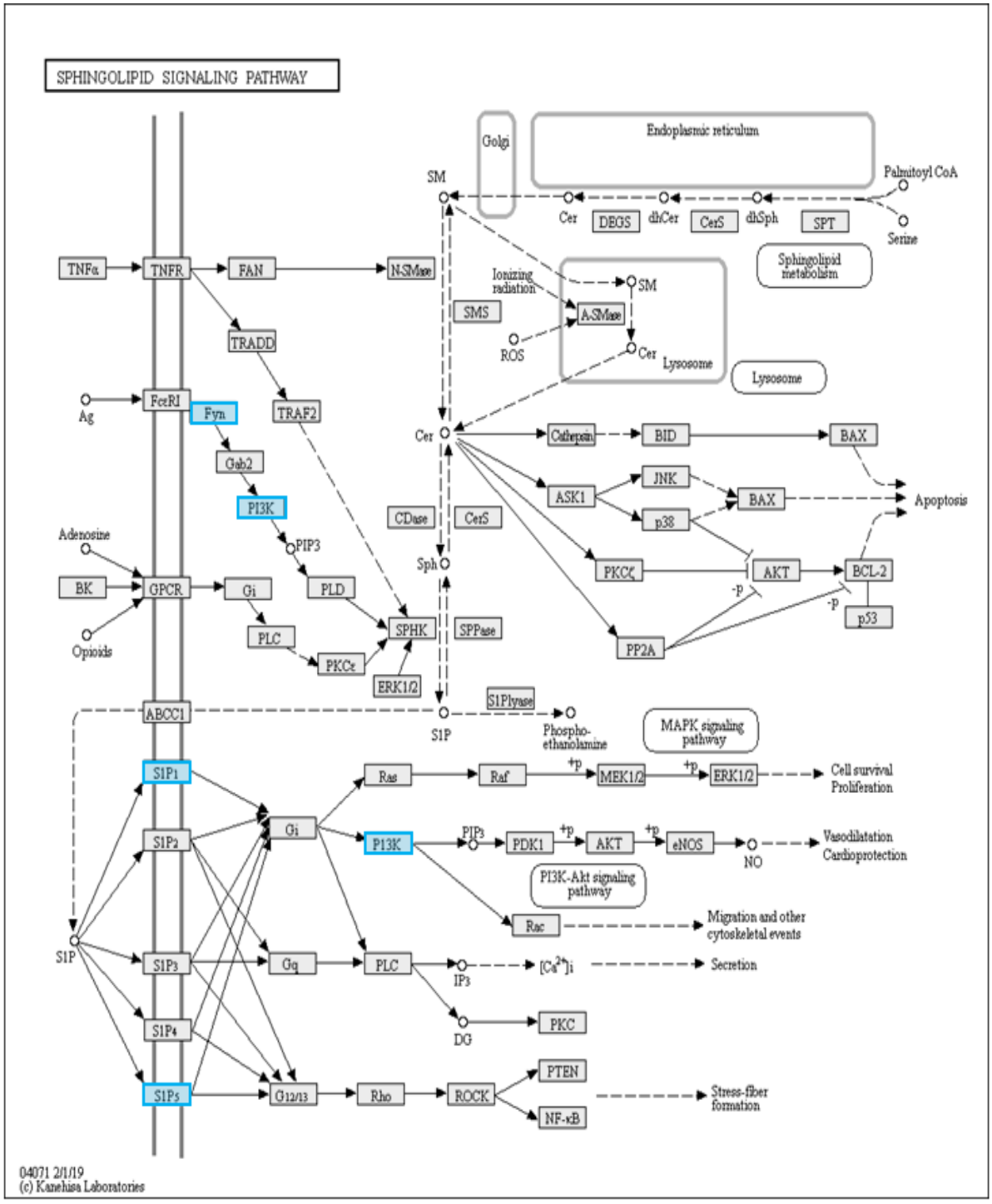

Figure 10 Downregulated genes in the Sphingolipid signalling pathway in CMCs compared to PBMCs. The KEGG sphingolipid signaling pathway, adapted from DAVID Bioinformatics resources v6.8 is shown. Blue boxes indicate downregulated mediators in CMCs compared to PBMCs. RNA was extracted from 5 CMC and 5 matched PBMC samples, isolated from cervical cytobrush and blood samples obtained from chronically HIV-1 infected women. Gene expression was evaluated using a microarray Illumina HumanHT-12 v3 Gene Expression BeadChip platform. Gene expression data were normalized by quantile normalization. Differential gene expression analysis was performed using R Bioconductor limma package. Genes were considered differentially expressed if adj. p≤0.05 and up- or downregulated if log fold change (FC) ≥ 1.5 or ≤ -1.5, respectively. Differentially expressed probeset IDs were annotated using the Illumina humanHT-12 v3 annotation file. Upregulated gene Entrez identity numbers were inputted to DAVID Bioinformatics resources v6.8 to obtain biological KEGG pathways upregulated. **CMC:** cervical mononuclear cells, **PBMC**: peripheral blood mononuclear cells, **Fyn**: proto-oncogene tyrosine-protein kinase Fyn, **PI3K**: phosphoinositide 3-kinase, **S1P1**: sphinogosine-1-phosphate 1 receptor, **S1P5**: sphingosine-1-phospate 5 receptor.

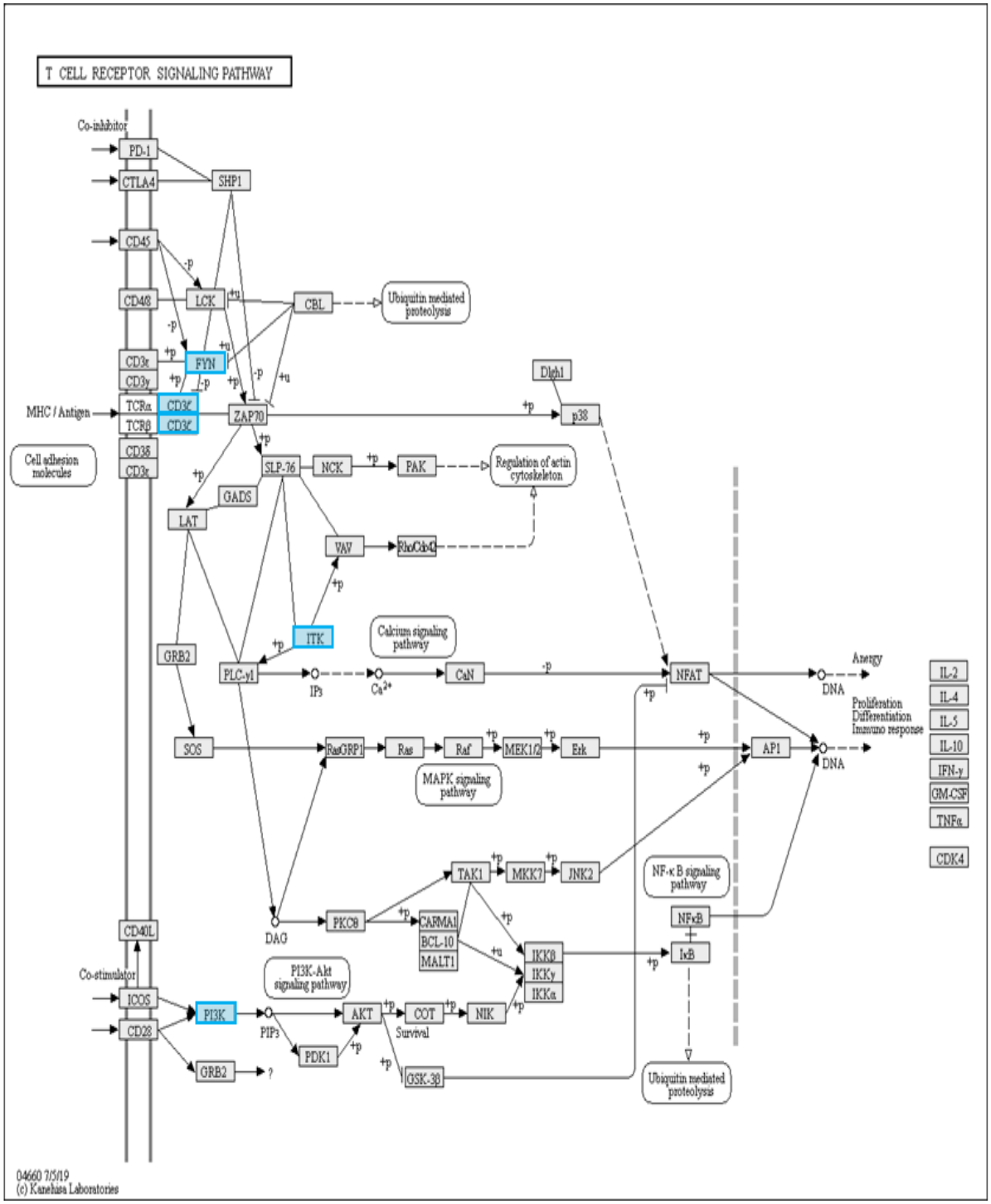

Figure 11 Downregulated genes in the T cell receptor signalling pathway in CMCs compared to PBMCs. The KEGG sphingolipid signaling pathway, adapted from DAVID Bioinformatics resources v6.8, is shown, blue boxes indicate downregulated mediators in CMCs compared to PBMCs. RNA was extracted from 5 CMC and 5 matched PBMC samples, isolated from cervical cytobrush and blood samples obtained from chronically HIV-1 infected women. Gene expression was evaluated using a microarray Illumina HumanHT-12 v3 Gene Expression BeadChip platform. Gene expression data were normalized by quantile normalization. Differential gene expression analysis was performed using R Bioconductor limma package. Genes were considered differentially expressed if adj. p≤0.05 and up- or downregulated if log fold change (FC) ≥ 1.5 or ≤ -1.5, respectively. Differentially expressed probeset IDs were annotated using the Illumina humanHT-12 v3 annotation file. Upregulated gene Entrez identity numbers were inputted to DAVID Bioinformatics resources v6.8 to obtain biological KEGG pathways upregulated. **CMC:** cervical mononuclear cells, **PBMC**: peripheral blood mononuclear cells, **Fyn**: proto-oncogene tyrosine-protein kinase Fyn, **CD3ζ**: CD3 zeta chain of $CD4^+$ and $CD8^+$ T cells, **PI3K**: phosphoinositide 3-kinase.

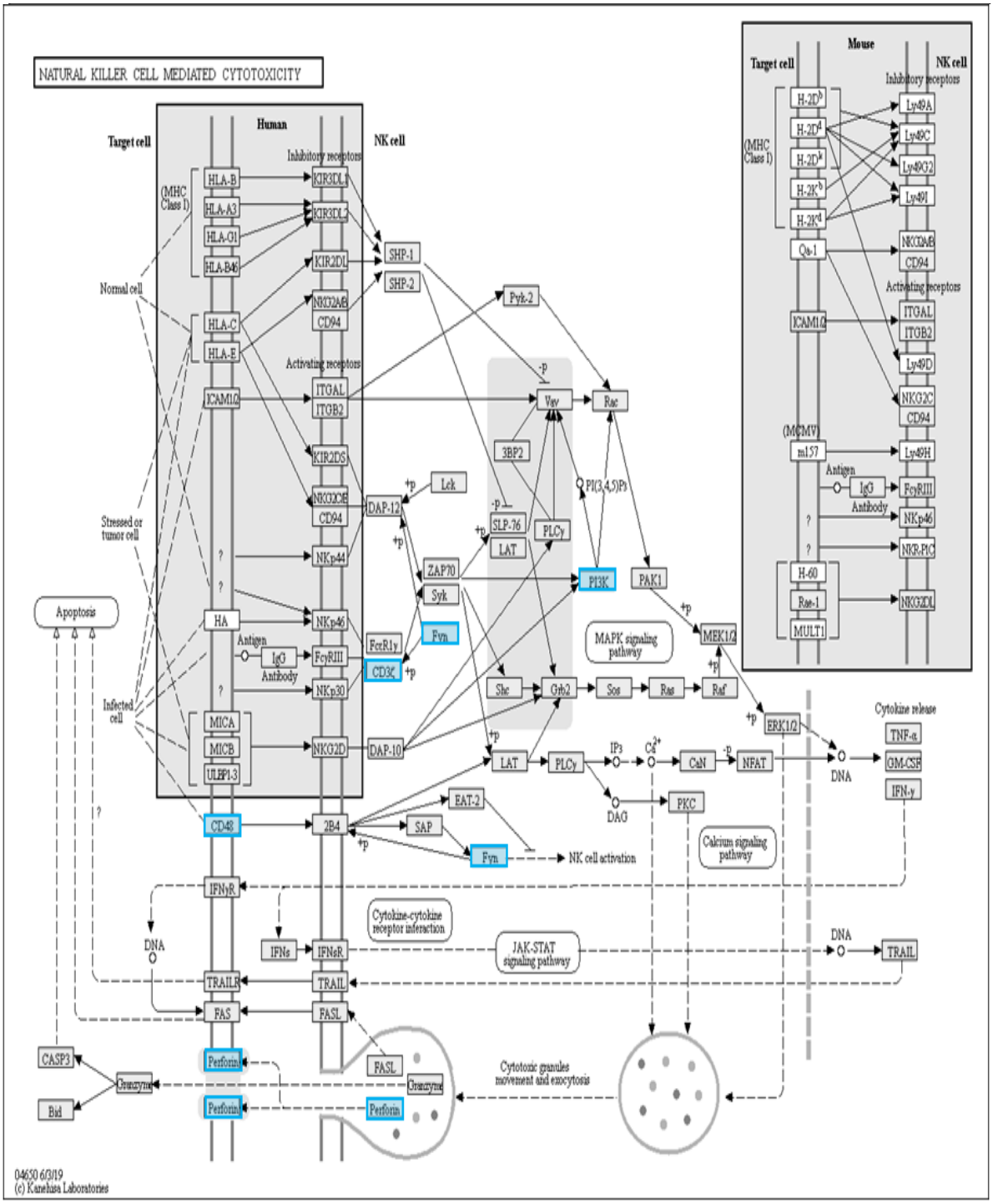

Figure 12 Downregulated genes in the Natural killer cell mediated cytotoxicity pathway in CMCs compared to PBMCs. The KEGG pro-inflammatory signaling pathway, adapted from DAVID Bioinformatics resources v6.8, is shown. Blue boxes indicate downregulated mediators in CMCs compared to PBMCs. RNA was extracted from 5 CMC and 5 matched PBMC samples, isolated from cervical cytobrush and blood samples obtained from chronically HIV-1 infected women. Gene expression was evaluated using a microarray Illumina HumanHT-12 v3 Gene Expression BeadChip platform. Gene expression data were normalized by quantile normalization. Differential gene expression analysis was performed using R Bioconductor limma package. Genes were considered differentially expressed if adj. p≤0.05 and up- or downregulated if log fold change (FC) ≥ 1.5 or ≤ -1.5, respectively. Differentially expressed probeset IDs were annotated using the Illumina humanHT-12 v3 annotation file. Upregulated gene Entrez identity numbers were inputted to DAVID Bioinformatics resources v6.8 to obtain biological KEGG pathways upregulated. **CMC:** cervical mononuclear cells, **PBMC**: peripheral blood mononuclear cells. **Fyn**: proto-oncogene tyrosine-protein kinase Fyn, **PI3K**: phosphoinositide 3-kinase, **CD3ζ**: CD3 zeta chain of $CD4^+$ and $CD8^+$ T cells, **CD48**: signaling lymphocyte activation marker 2.

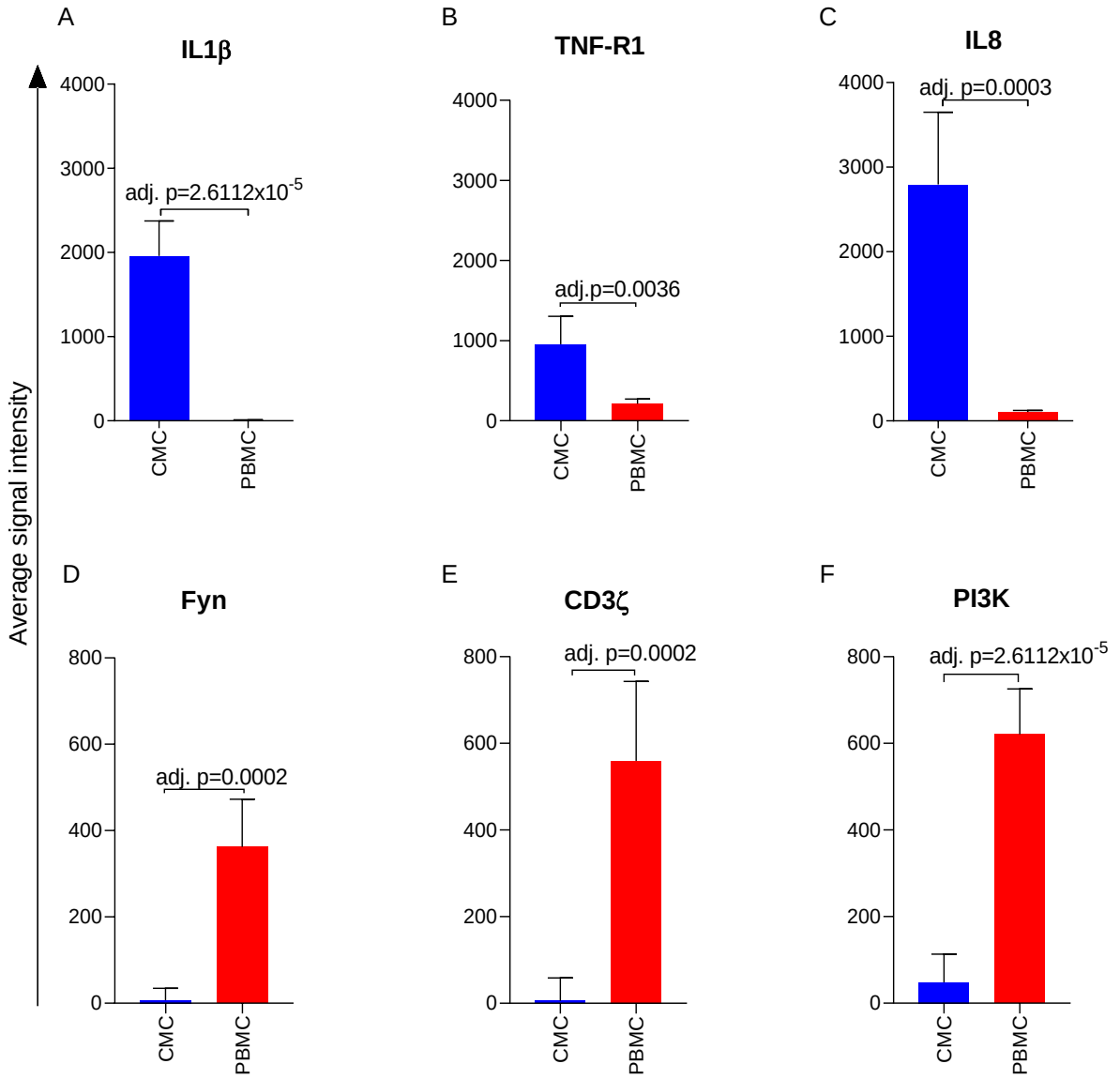

Figure 13 Key upregulated and downregulated genes common to inflammatory signalling pathways. Raw average signal intensity data for key genes involved in pro-inflammatory signalling pathways that were **A-C)** upregulated and **D-F)** downregulated in CMCs compared to PBMCs are shown. RNA was extracted from 5 CMC and 5 matched PBMC samples, isolated from cervical cytobrush and blood samples obtained from chronically HIV-1 infected women. Gene expression was evaluated using a microarray Illumina HumanHT-12 v3 Gene Expression BeadChip platform. Gene expression data were normalized by quantile normalization. Differential gene expression analysis was performed using R Bioconductor limma package. Genes were considered differentially expressed if adj. p≤0.05 and up- or downregulated if log fold change (FC) ≥ 1.5 or ≤ -1.5, respectively. Differentially expressed probeset IDs were annotated using the Illumina humanHT-12 v3 annotation file. Upregulated gene Entrez identity numbers were inputted to DAVID Bioinformatics resources to obtain biological KEGG pathways upregulated in CMCs compared to PBMCs. **CMC**: cervical mononuclear cells, **PBMC**: peripheral blood mononuclear cells, **IL1β**: Interleukin 1 Beta, **TNF-R1**: tumor necrosis factor receptor 1, **IL8**: Interleukin 8, **Fyn**: proto-oncogene tyrosine-protein kinase Fyn, **CD3ζ**: CD3 zeta chain of $CD4^+$ and $CD8^+$ T cells, **PI3K**: phosphoinositide 3-kinase.

3.4. WISH study cohort and *Lactobacillus* selection

The WISH study enrolled 149 women in Masiphumelele, Cape Town, South Africa between 2013 and 2015 (110). Lateral wall and vulvovaginal swabs were collected to test for STIs, Nugent scoring and candidiasis diagnosis, as mentioned above. Cervicovaginal fluid was also collected, from which 115 *Lactobacillus* species and strains were isolated. Eight *Lactobacillus* isolates of varying species were selected for the current study **(Table 2)** based on their previously determined *in vitro* inflammatory profiles, (**Figure 14**) (98)**.**

Table 2 Characteristics of WISH participants from whom the *Lactobacillus* species were isolated.

Bacterial Isolate	Participant age (years)	Nugent score	BV status	STI status	Swab pH	SC pH
Lactobacillus jensenii 3 (LJ3)	18	10	Pos	Neg	5.3	5.6
Lactobacillus vaginalis 3 (LV3)	18	0	Neg	NG	4.7	3.6
Lactobacillus crispatus 3 (LC3)	17	0	Neg	Neg	4.4	4.1
Lactobacillus mucosae 2 (LM2)	22	8	Pos	HSV-2	4.4	4.8
Lactobacillus crispatus 1 (LC1)	19	2	Neg	Neg	4.1	4.7
Lactobacillus jensenii 2 (LJ2)	17	1	Neg	CT,NG,TV	4.1	3.6
Lactobacillus mucosae 4 (LM4)	21	8	Pos	Neg	5.3	5
Lactobacillus vaginalis 4 (LV4)	18	9	Pos	CT	5	4.7

BV: bacterial vaginosis, **STI**: sexually transmitted infection, **SC**: softcup, **CT**: *Chlamydia trachomatis*, **NG**: *Neisseria gonorrhoeae*, **TV**: *Trichomoniasis vaginalis,* **HSV-2:** Herpes simplex virus-2, **Neg**: negative, **Pos**: positive.

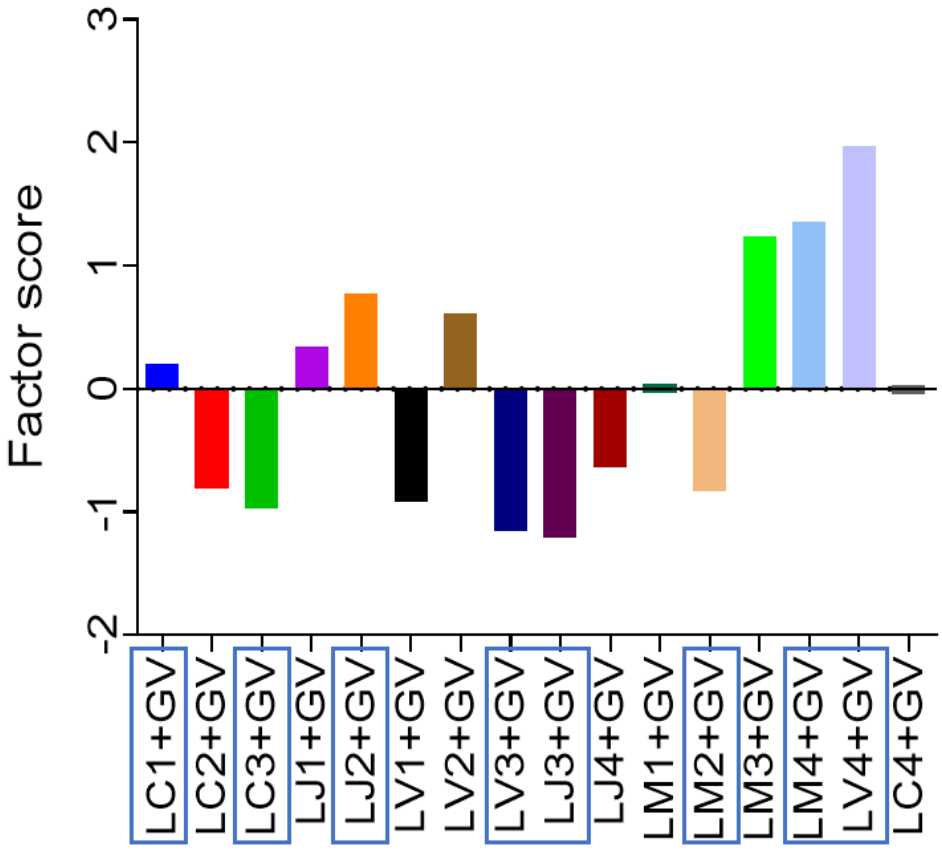

Figure 14 Previously quantified overall inflammatory responses of VK2 cells to *G. vaginalis* and *Lactobacillus* isolate co-culture. VK2 cells were seeded into 24 well plates (1 x 10^5 cells/well) and cultured to confluence. Monolayers were pre-treated with *Lactobacillus* isolates (4.18 x 10^6 CFU/well) in 500µl of media for 5 hrs at 37°C, 5% CO_2, followed by a stimulation with *G. vaginalis* (1 x 10^7 CFU/well) in 500µl for a total culture volume of 1ml, for an additional 20hrs incubation. Cell supernatants were harvested and tested for chemokine and cytokine production by Luminex assay. Raw cytokine data were $\log_{10}$ transformed and factor analysis was used to generate a factor score (including MIP-3α, MIP-1α, MIP-1β, IP-10, IL-8, IL-6, IL-1α and IL-1β) for each isolate. Blue boxes indicate isolates selected for this study. **LC**: *L. crispatus*, **LJ**: *L. jensenii*, **LV**: *L. vaginalis*, **LM**: *L. mucosae*, **GV**: *Gardnerella vaginalis.*

3.5 Quality of RNA extracted from VK2 cells stored in RLT lysis buffer compared to RNALater

To evaluate the optimal cell storage solution and the transwell cell culture system, VK2 cells were cultured in transwell inserts and harvested to assess RNA yield and quality after RNA extraction.

An average of 7.46 x 10^5 live cells was harvested from the transwell inserts **(Figure 15A)**. The RNA yield was varied among the samples **(Figure 15B)**. The samples stored in RNALater prior to RNA extraction, yielded a significantly ($p=0.0190$) lower RNA concentration (ng/µl) than the samples stored in RLT lysis buffer **(Figure 15B)**.

An acceptable RIN value is between 7-10. A total of n=9 samples passed the RNA integrity assessment, RINs: 7.9-9.8, while n=1 sample did not, with a RIN of 5.5 **(Figure 15C, Appendix XIII)**. All samples stored in RLT lysis buffer prior to RNA extraction passed the RNA integrity assessment and tended to have higher RINs (above 9) than the samples stored in RNALater **(Figure 15C, Appendix XIII)**. A total of n=7 RNA samples were "pure" based on an A260/A280 ratio of 2, while n=3 samples had A260/A280 ratios of 1.7, 1.5 and 1.9, indicating the presence of phenols, proteins or other contaminants with absorbance at 280nm **(Figure 15D)**. Notably, all the samples stored in RLT lysis buffer prior to RNA extraction, yielded "pure" RNA. In contrast, only n=1 sample had an acceptable A260/A230 ratio of 1.7, while the ratios of n=9 samples varied between 0.05 and 1.2, indicating the presence of contaminants with absorbance at 230nm **(Figure 15D).**

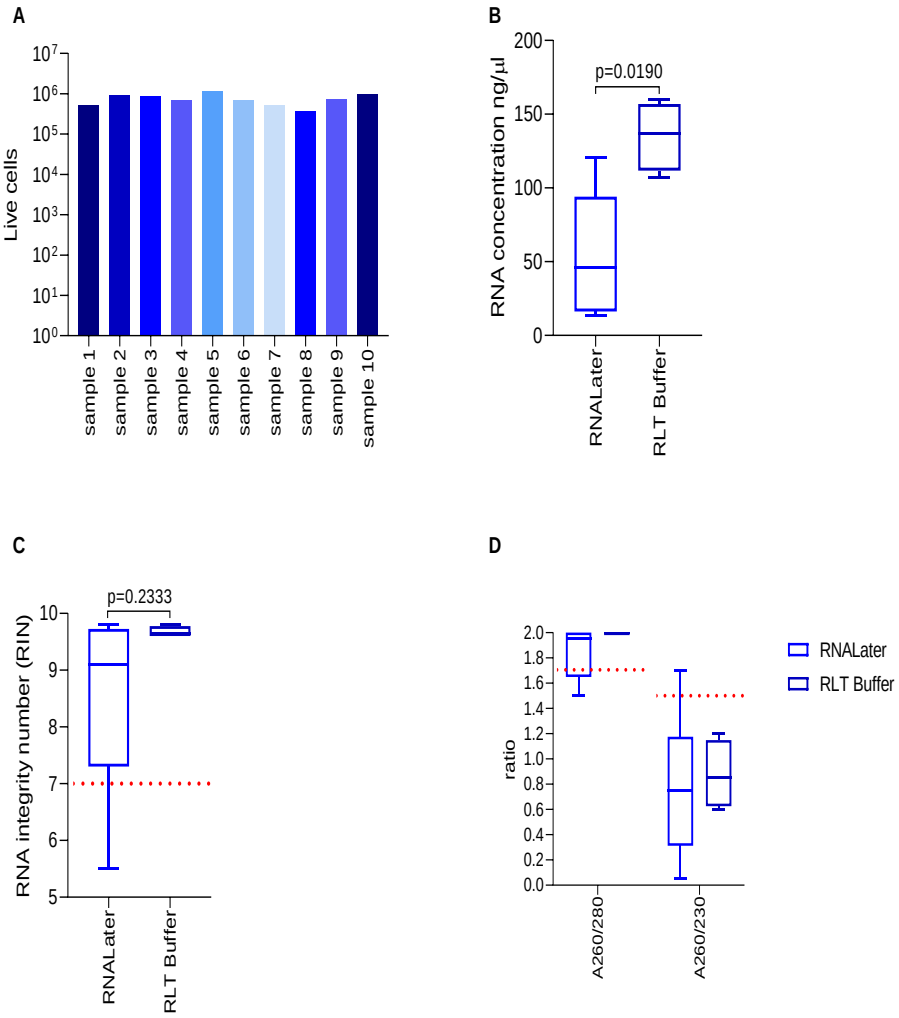

Figure 15 Quality of RNA extracted from VK2 cells cultured in transwells. A) Cell count of live VK2 cells after culture in transwell inserts for 7 days; each bar represents a separate transwell culture. **B)** RNA yield. **C-D)** RNA quality assessed by RIN, A260/A280 and A260/A230 ratios. Acceptable RINs are between 7-10. Acceptable A260/A280 and A260/A230 ratios are 1.7-2.0 and 1.5-3, respectively, red dotted lines indicate lower limits. VK2 cells were cultured in 24mm transwell inserts with 0.4µm pores, at 37°C, 5% CO_2 for 7 days, with media changed every 2-3 days. The cells were harvested and stored in either RNALater or RLT lysis buffer, at -80°C. RNA was extracted using the Qiagen RNeasy mini kit. RNA quality and quantity were assessed using an Agilent 2100 Bioanalyzer and NanoDrop 8000 spectrophotometer. Nonparametric Mann-Whitney U test was used to evaluate the difference between RNA yield of samples stored in RNALater versus RLT lysis buffer. p≤0.05 was considered significant. **RIN**: RNA integrity number.

3.6 Cytokine responses by VK2 cells stimulated with *Lactobacillus* species and *G. vaginalis* in transwells compared to stimulation in 24 well plates

The aim of the Luminex assay was to assess inflammatory responses in order to group isolates into cytokine-suppressive versus non-cytokine-suppressive lactobacilli before the microarray assay. Both isolates that induced an increase in inflammatory cytokine production and those that did not materially change cytokine production were grouped as "non-suppressive. Even though strong cytokine suppressive responses were not expected at these short incubation times (6 and 12 hours), a short incubation period was required for the detection of transcriptional changes before mRNA degradation.

As previous studies evaluating the impact of lactobacilli on inflammatory cytokine responses to *G. vaginalis* had been carried out in 24 well plate culture systems (29,98), a pilot experiment was conducted to determine whether similar responses were observed in transwell systems. VK2 cells were co-cultured with *G. vaginalis* (16.72×10^6 CFU/well) in the presence or absence of each *Lactobacillus* isolate (16.72×10^6 CFU/well) in 1.5ml of media in transwell inserts. The VK2 cell viability for all the cultures remained above 80% following co-culture with bacterial spp. **(Figure16A)**. The effect of *Lactobacillus* isolates on overall inflammatory responses varied according to species **(Figure 16B)**. The VK2 cells stimulated by *G. vaginalis* only control did not induce inflammatory responses that were markedly greater than the VK2 cells only control when assayed in transwell inserts at the bacterial concentrations mentioned above, thus the effect of the *Lactobacillus* isolates on cytokine responses in this system was unclear **(Figure 16B, Figure 17).** It is thus likely that a greater number of *G. vaginalis* CFUs appropriate for the larger surface area and volume of media, and incubation for a longer period of time are needed to stimulate a significant response in this system.

In tandem, triplicate independent assays were performed in 24 well plates using our already-optimized protocol and a longer incubation period of 12 hours. Cells only and *G. vaginalis*-VK2 cell only cultures were included as controls for each independent assay, in duplicate. In this system, similar to our previous studies, viability was generally comparable to the cells only control, except in the case of the LJ2/*G. vaginalis* coculture for which only 73% of the cells were viable **(Figure 18A)**. PCA of the cytokine data to generate component estimates showed that *G. vaginalis* significantly induced an increased overall inflammatory response by VK2 cells compared to cells only ($p=0.0022$, **Figure 18B**). LJ3, LV3, LC3, LC1 and LJ2 had higher overall inflammatory responses compared to LM2, LM4 and LV4 (**Figure 18B**).

PCA of the cytokine data showed that 63% of the variance in the cytokine data were explained by PC1 and 20% of the variance was explained by PC2 **(Figure 19A)**. Unsupervised clustering showed LM2, LM4 and LV4 to be cytokine-suppressive, clustering below *G. vaginalis*-VK2 cell

responses, while LC1, LC3, LJ3, LV3 and LJ2 were not suppressive of cytokine responses, clustering close to or above *G*. *vaginalis*-VK2 cell responses **(Figure 19B).** Based on this analysis, isolates were grouped as cytokine-suppressive or non-cytokine-suppressive of inflammatory responses to *G. vaginalis* for downstream microarray analysis.

LM2, LM4 and LV4 significantly reduced IL-6 production by VK2 cells (adj. p=0.0194, **Figure 20E**). LJ2 and LM4 showed a significant reduction in IP-10 compared to *G*. *vaginalis*-VK2 cell cultures (adj. p=0.0194, **Figure 20F**). LC1 and LJ2 significantly increased IL-1α and IL-1β responses by VK2 cells (adj. p=0.0194 and adj. p=0.0133, respectively, **Figure 20G and H**). Only LM4 significantly reduced the MIP-3α response by VK2 cells (adj. p=0.0133, **Figure 20I**). The IL-1RA response by VK2 cells remained mostly unchanged by *Lactobacillus* spp., with the exception of LJ2 which significantly increased the IL-1RA response (adj. p=0.0194, **Figure 20J**).

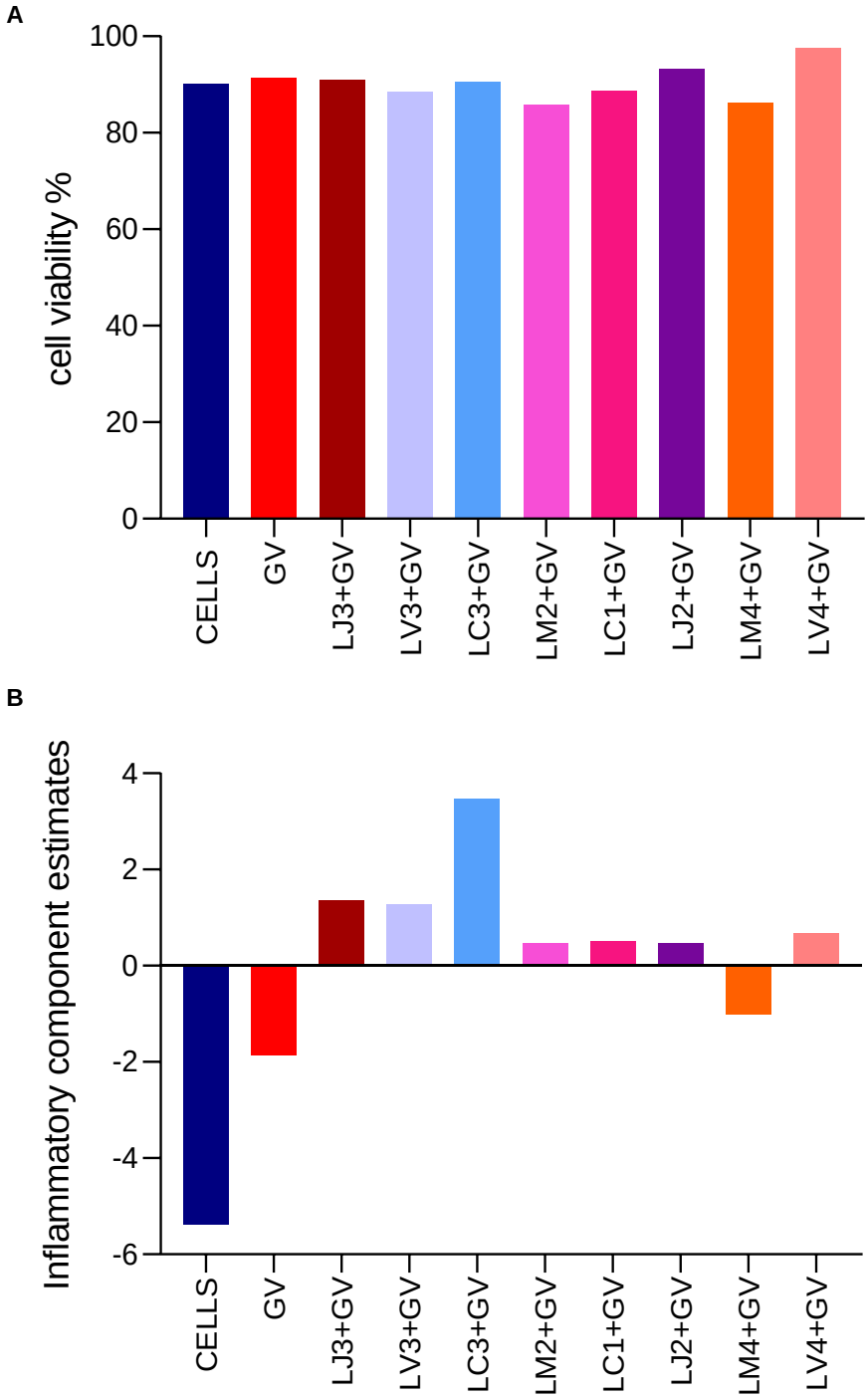

Figure 16 Overall cytokine response by VK2 cells cultured in transwells stimulated by *Lactobacillus* species and *G. vaginalis*. A) VK2 cell viability (%) after bacterial stimulation. **B)** Overall inflammatory response by VK2 cells stimulated with *G. vaginalis* in the absence or presence of *Lactobacillus* isolates. VK2 cells were seeded into transwell inserts ($0.3x10^6$ cells/well) and grown to confluence. Monolayers were stimulated with *Lactobacillus* isolates (16.72×10^6 CFU/well) and incubated for 3 hrs at 37°C, 5% CO_2. *G. vaginalis* (16.72×10^6 CFU/well) was then added to the *Lactobacillus*-VK2 cell cultures and incubated for an additional 3 hrs at 37°C, 5% CO_2. VK2 cells only and *G. vaginalis* only stimulated VK2 cells were included as controls. Cell viability was assessed by trypan blue staining. Cell culture supernatants were collected, and cytokine production assessed by Luminex assay. All cytokine and chemokine (IL-8, MIP-1α, MIP-1β, MIP-3α, IP-10, IL-6, IL-1α and IL-1β) responses were grouped onto one component (c1) to generate inflammatory estimate scores, using STATA v13.1. Bars indicate c1 scores for each isolate. **GV:** *G. vaginalis*, **LJ3:** *L. jensenii* 3, **LV3:** *L. vaginalis* 3, **LC3:** *L. crispatus* 3, **LM2:** *L. mucosae* 2, **LC1:** *L. crispatus* 1, **LJ2:** *L. jensenii* 2, **LM4:** *L. mucosae* 4. **LV4:** *L. vaginalis* 4.

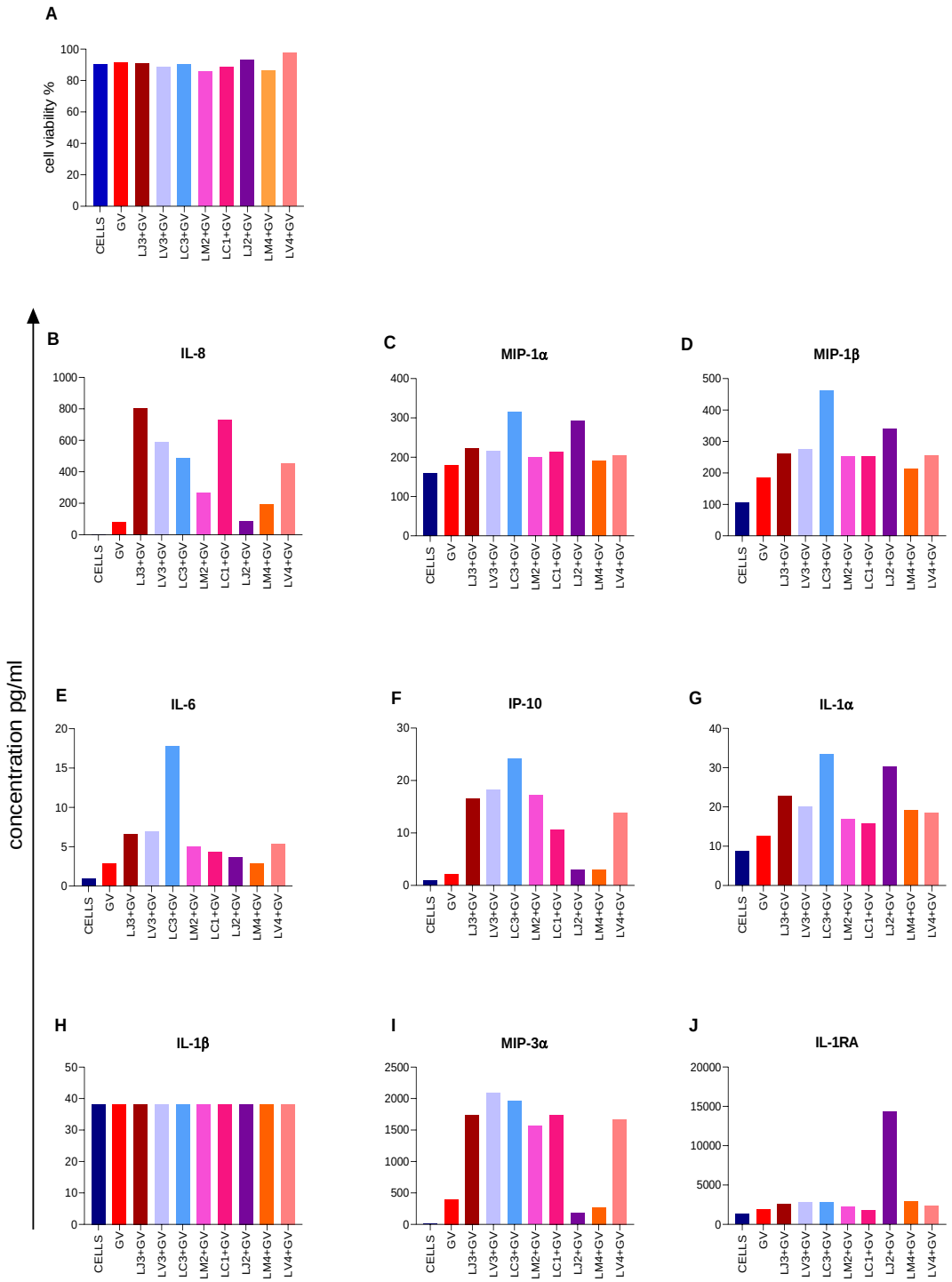

Figure 17 Cytokine responses by VK2 cells cultured in transwells stimulated by *Lactobacillus* species and *G. vaginalis*. A) VK2 cell viability (%) after bacterial stimulation. **B-J)** Cytokine production by VK2 cells stimulated by *G. vaginalis* in the absence or presence of *Lactobacillus* spp. VK2 cells were seeded into transwell inserts ($0.3x10^6$ cells/well) and grown to confluence. Monolayers were stimulated with *Lactobacillus* isolates (16.72×10^6 CFU/well) and incubated for 3 hrs at 37°C, 5% CO_2. *G. vaginalis* (16.72×10^6 CFU/well) was then added to the *Lactobacillus*-VK2 cell cultures and incubated for an additional 3 hrs at 37°C, 5% CO_2. VK2 cells only and *G. vaginalis* only stimulated VK2 cells were included as controls. Cell viability was assessed by trypan blue staining. Cell culture supernatants were collected, and cytokine production assessed by Luminex assay. **GV:** *G. vaginalis*, **LJ3:** *L. jensenii* 3, **LV3:** *L. vaginalis* 3, **LC3:** *L. crispatus* 3, **LM2:** *L. mucosae* 2, **LC1:** *L. crispatus* 1, **LJ2:** *L. jensenii* 2, **LM4:** *L. mucosae* 4. **LV4:** *L. vaginalis* 4, **IL-8**: interleukin-8, **MIP-1α**: macrophage inflammatory protein 1 alpha, **MIP-1β**: macrophage inflammatory protein 1 beta, **IL-6**: interleukin-6, **IP-10**: interferon gamma induced protein 10, **IL-1α**: interleukin 1 alpha, **IL-1β**: interleukin 1 beta, **MIP-3α**: macrophage inflammatory protein 3 alpha, **IL-1RA**: interleukin 1 receptor antagonist.

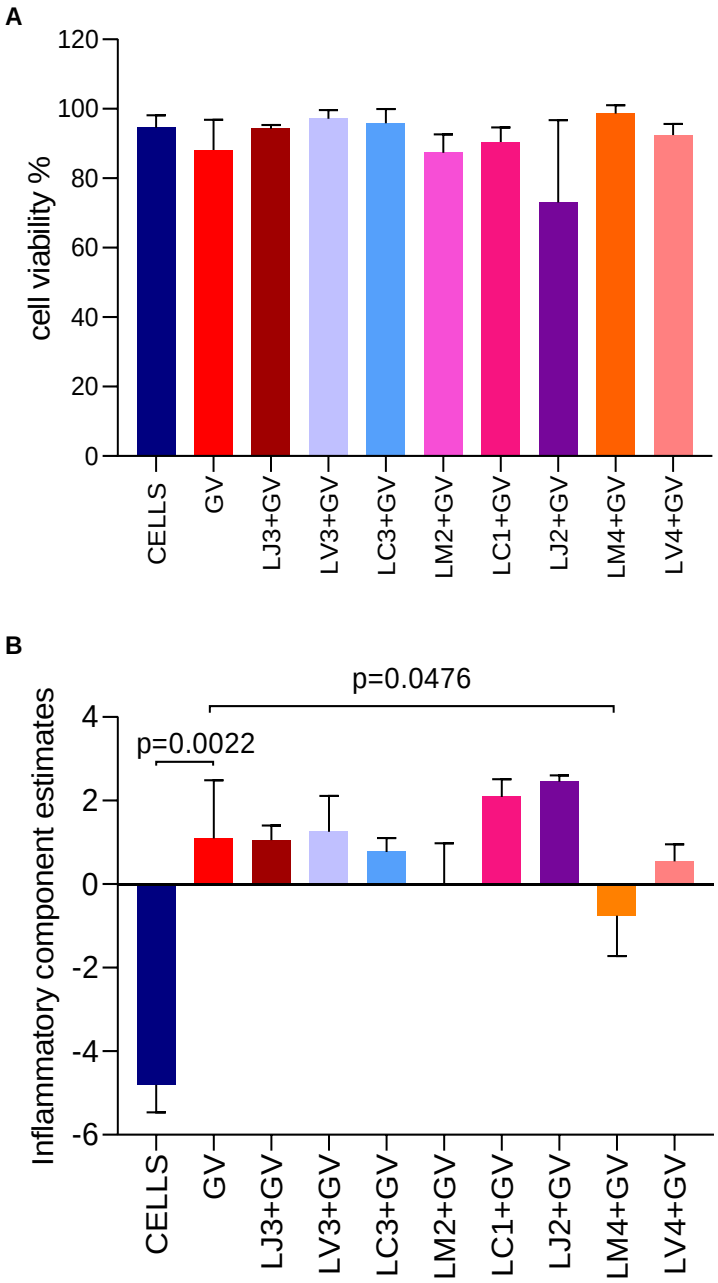

Figure 18 Overall inflammatory responses by VK2 cells cultured in 24 well plates stimulated with *Lactobacillus* isolates and *G. vaginalis*. A) VK2 cell viability (%) after bacterial stimulation. **B)** Overall inflammatory responses by VK2 cells stimulated with *G. vaginalis* in the absence or presence of *Lactobacillus* isolates. VK2 cells were seeded into 24 well plates ($0.5x10^6$ cells/well) and grown to confluence. Monolayers were stimulated with *Lactobacillus* isolates ($4.18x10^6$ CFU/well) and incubated for 6 hrs at 37°C, 5% CO_2. *G. vaginalis* ($4.18x10^7$ CFU/well) was then added to the *Lactobacillus*-VK2 cell cultures and incubated for an additional 6 hrs at 37°C, 5% CO_2. Triplicate independent assays were performed. VK2 cells only and *G. vaginalis* only stimulated VK2 cells were included as controls, in duplicate for each independent assay. Cell viability was assessed by trypan blue staining. Cell culture supernatants were collected, and cytokine production assessed by Luminex assay. All cytokine and chemokine (IL-8, MIP-1α, MIP-1β, MIP-3α, IP-10, IL-6, IL-1α, IL-1β and IL-1RA) responses were grouped onto one component (c1) to generate inflammatory estimate scores, using STATA v13.1. Bars display the mean c1 values and error bars indicate standard deviation from the mean. Nonparametric Mann Whitney U test was used to statistically test the difference in overall inflammatory response of VK2 cells induced by *G. vaginalis* compared to cells only, and overall inflammatory responses of VK2 cells co-cultured with *G. vaginalis* in the absence or presence of *Lactobacillus* isolates, $p \leq 0.05$ was considered significant. **GV:** *G. vaginalis*, **LJ3:** *L. jensenii* 3, **LV3:** *L. vaginalis* 3, **LC3:** *L. crispatus* 3, **LM2:** *L. mucosae* 2, **LC1:** *L. crispatus* 1, **LJ2:** *L. jensenii* 2, **LM4:** *L. mucosae* 4. **LV4:** *L. vaginalis* 4.

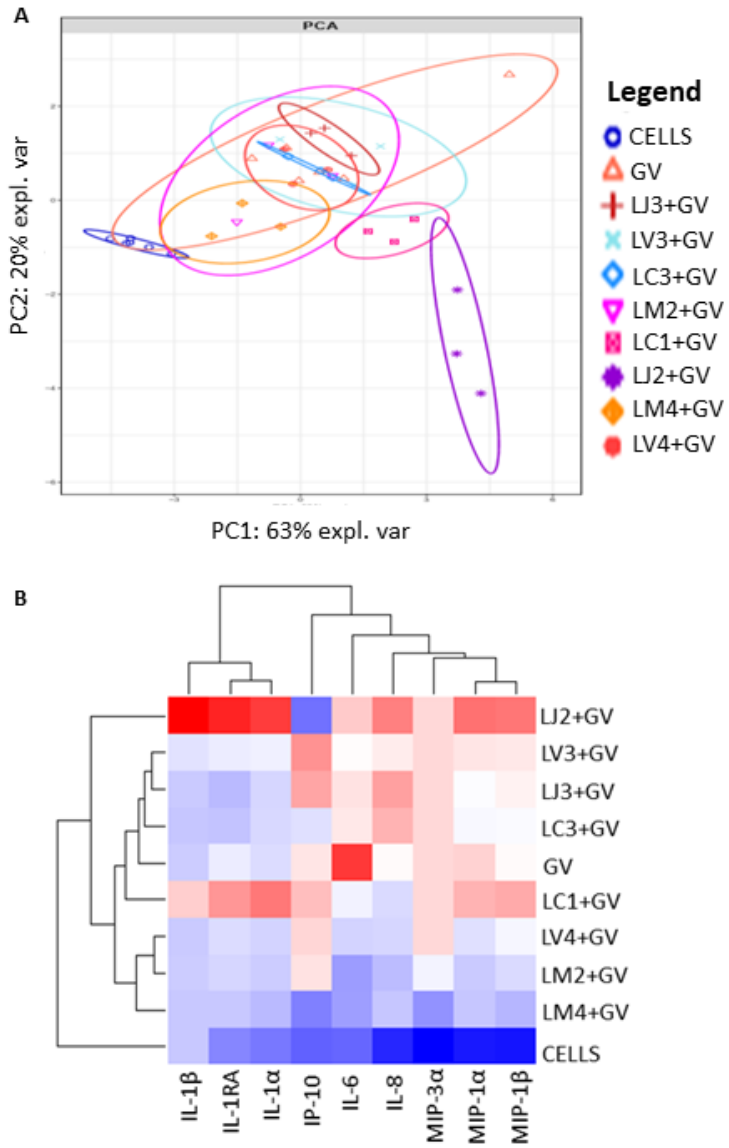

Figure 19 Principal component analysis (PCA) and heatmap showing cytokine responses of VK2 cells stimulated with *G. vaginalis* and *Lactobacillus* species. A) PCA was performed to evaluate clustering of the samples based on cytokine responses. **B)** Unsupervised hierarchical clustering was used to group the samples based on cytokine production. VK2 cells were seeded into 24 well plates ($0.5x10^6$ cells/well) and grown to confluence. Monolayers were stimulated with *Lactobacillus* isolates ($4.18x10^6$ CFU/well) and incubated for 6 hrs at 37°C, 5% CO_2. *G. vaginalis* ($4.18x10^7$ CFU/well) was then added to the *Lactobacillus*-VK2 cell cultures and incubated for an additional 6 hrs at 37°C, 5% CO_2. Triplicate independent assays were performed. VK2 cells only and *G. vaginalis* only stimulated VK2 cells were included as controls, in duplicate for each independent assay. The R Studio mixOmics package was used to conduct the PCA. R Studio was also used to perform the hierarchical clustering analysis and generate a heatmap. Data were log_{10}-transformed and matrix scaled. The averages of the replicate values are displayed. The heatmap depicts cytokine production, with low-high concentrations indicated by blue through white to red, respectively. The dendogram above the heatmap indicates the degrees of relatedness between the various cytokines measured. The horizontal "branches" have arbitrary lengths and the lengths of the vertical "branches" indicate the degrees of similarity between the cytokines. The left-hand side dendogram demonstrates relationships between the cytokine expression profiles in cells that were unstimulated, *G. vaginalis* stimulated and stimulated with *Lactobacillus* isolates and *G. vaginalis* in combination. Shorter and longer horizontal branch lengths between the isolates for this dendogram, indicate higher or lower degrees of similarity between the cytokine profiles, respectively. **GV:** *G. vaginalis*, **LJ3:** *L. jensenii* 3, **LV3:** *L. vaginalis* 3, **LC3:** *L. crispatus* 3, **LM2:** *L. mucosae* 2, **LC1:** *L. crispatus* 1, **LJ2:** *L. jensenii* 2, **LM4:** *L. mucosae* 4. **LV4:** *L. vaginalis* 4. **PC1**: principal component 1, **PC2**: principal component 2, **Expl. var**: explained variance, **IL-8**: interleukin-8, **MIP-1α**: macrophage inflammatory protein 1 alpha, **MIP-1β**: macrophage inflammatory protein 1 beta, **IL-6**: interleukin-6, **IP-10**: interferon gamma induced protein 10, **IL-1α**: interleukin 1 alpha, **IL-1β**: interleukin 1 beta, **MIP-3α**: macrophage inflammatory protein 3 alpha, **IL-1RA**: interleukin 1 receptor antagonist.

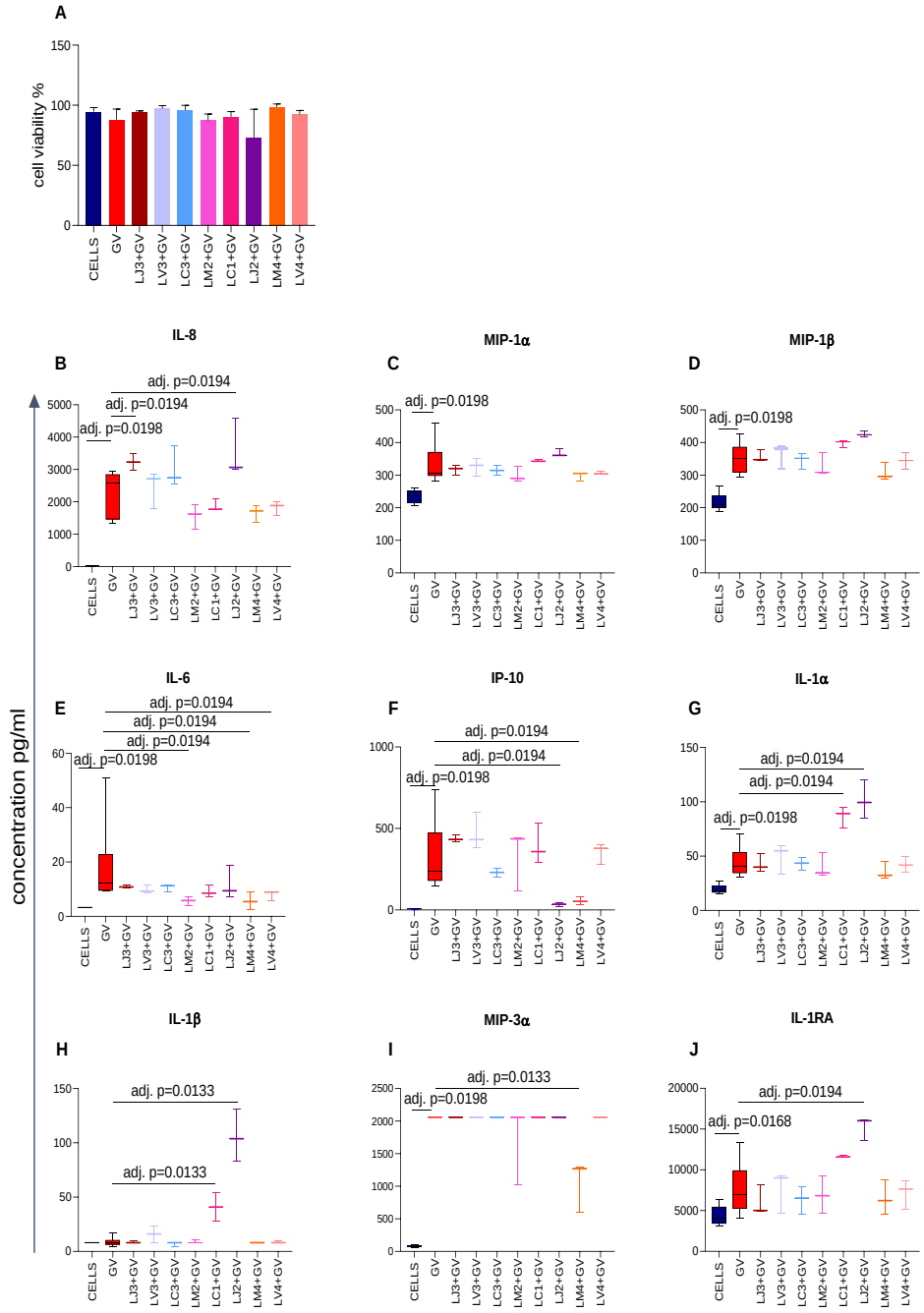

Figure 20 Cytokine responses by VK2 cells cultured in 24 well plates stimulated by *Lactobacillus* isolates and *G. vaginalis*. A) VK2 cell viability (%) after bacterial stimulation. **B-J)** Cytokine production by VK2 cells stimulated by *G. vaginalis in the* absence or presence of *Lactobacillus* spp. VK2 cells were seeded into 24 well plates ($0.5x10^6$ cells/well) and grown to confluence. Monolayers were stimulated with *Lactobacillus* isolates ($4.18x10^6$ CFU/well) and incubated for 6 hrs at 37°C, 5% CO_2. *G. vaginalis* ($4.18x10^7$ CFU/well) was then added to the *Lactobacillus*-VK2 cell cultures and incubated for an additional 6 hrs at 37°C, 5% CO_2. Triplicate independent assays were performed. VK2 cells only and *G. vaginalis* only stimulated VK2 cells were included as controls, in duplicate for each independent assay. Cell viability was assessed by trypan blue staining. Cell culture supernatants were collected, and cytokine production assessed by Luminex assay. Nonparametric Mann Whitney U test was used to statistically test the difference in cytokine responses of VK2 cells stimulated with *G. vaginalis* only and in combination with each *Lactobacillus* isolate. **GV:** *G. vaginalis*, **LJ3:** *L. jensenii* 3, **LV3:** *L. vaginalis* 3, **LC3:** *L. crispatus* 3, **LM2:** *L. mucosae* 2, **LC1:** *L. crispatus* 1, **LJ2:** *L. jensenii* 2, **LM4:** *L. mucosae* 4. **LV4:** *L. vaginalis* 4, IL-8: interleukin-8, **MIP-1α**: macrophage inflammatory protein 1 alpha, **MIP-1β**: macrophage inflammatory protein 1 beta, **IL-6**: interleukin-6, **IP-10**: interferon gamma induced protein 10, **IL-1α**: interleukin 1 alpha, **IL-1β**: interleukin 1 beta, **MIP-3α**: macrophage inflammatory protein 3 alpha, **IL-1RA**: interleukin 1 receptor antagonist.

3.7 Lactic acid production by *Lactobacillus* isolates in the VK2 cell 24 well culture system

After culture of *Lactobacillus* isolates ($4.18x10^6$CFU/well) with VK2 cells in combination with *G*. *vaginalis* ($4.18x10^7$CFU/well) in 1ml of media, all the *Lactobacillus* isolates produced D-Lactate, while LJ3, LV3 and LJ2 produced high levels **(Figure 21A)**. However, L-lactate production was low and not detected in some cultures **(Figure 21B)**. LJ3 and LC1 did not produce L lactate, while LV3, LC3, LM2, LJ2 and LV4 produced low levels and LM4 produced the highest **(Figure 21B)**. As expected, *G. vaginalis* produced very little D- and L-lactate **(Figure 21A and B)**. The sample pH measurements were between 7-9 (**Appendix XIV**), hence using the Henderson-Hasselbalch equation, the total lactic acid concentration calculated was low **(Figure 21C)**. Non-cytokine-suppressive lactobacilli produced significantly greater amounts of D-lactate than cytokine-suppressive lactobacilli (p=0.0476, **Figure 21D**), while the total lactic acid production did not differ between cytokine-suppressive and non-cytokine-suppressive lactobacilli **(Figure 21E)**.

Associations between D- and L-lactate and cytokine responses were evaluated using Spearman's rank correlation. D-lactate production was significantly positively associated with IL-8 and IL-6 responses by VK2 cells (r=0.7381, p=0.0458, **Figure 22A and E**), however, not significantly after adjusting for multiple comparisons (adj. p=0.4122, **Figure 22A and E**). L-lactate production tended to be negatively associated with MIP-1α, MIP-1β and IL-1β responses by VK2 cells (r=-0.527 and r=-0.6587, respectively), however, not significantly (p=0.1846 and p=0.0850, respectively; **Figure 23B,C and H**).

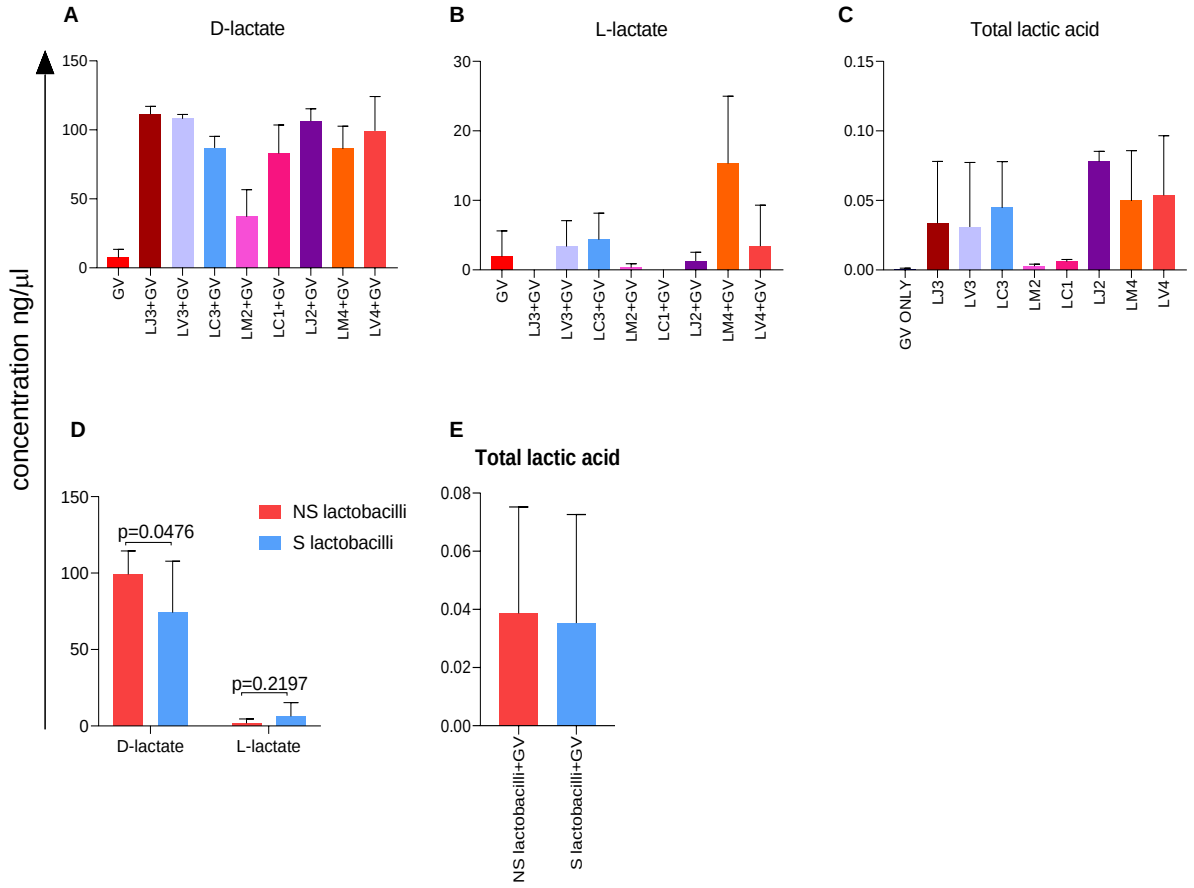

Figure 21 Lactate production by *Lactobacillus* isolates in VK2 cell cultures. A) D-Lactate and **B)** L-Lactate colorimetric detection and **C)** total lactic acid detection, in cell culture supernatants of VK2 cells stimulated with *G. vaginalis* alone and in combination with each *Lactobacillus* isolate. **D)** D- and L-lactate colorimetric detection in cell culture supernatants of VK2 cells stimulated by *G. vaginalis* and in combination with non-suppressive (NS) lactobacilli and suppressive (S) lactobacilli. VK2 cells were seeded into 24 well plates ($0.5x10^6$ cells/well) and grown to confluence. Monolayers were stimulated with each *Lactobacillus* isolate ($4.18x10^6$CFU/well) isolate and incubated for 6 hours at 37°C, 5% CO_2. Thereafter, *G. vaginalis* ($4.18x10^7$ CFU/well) was then added to the *Lactobacillus*-VK2 cell cultures and incubated for an additional 6 hrs at 37°C, 5% CO_2. Triplicate independent assays were performed. VK2 cells only and *G. vaginalis* only stimulated VK2 cells were included as controls, in duplicate for each independent assay. Cell culture supernatants were used to evaluate D- and L-lactate production using colorimetric assays, with samples assayed in duplicate. Lactate concentrations were determined by standard curves. All samples were corrected for D-and L-lactate detected in VK2 cells only cultures. Culture pH readings were measured using pH strips. Using the Henderson-Hasselbalch equation, pH values and the sum of D- and L- lactate concentrations were used to calculate the total lactic acid. Mann Whitney U test was used to statistically test the difference in lactate production between cytokine-suppressive and non-suppressive lactobacilli, p≤0.05 considered significant. **GV:** *G. vaginalis*, **LJ3:** *L. jensenii* 3, **LV3:** *L. vaginalis* 3, **LC3:** *L. crispatus* 3, **LM2:** *L. mucosae* 2, **LC1:** *L. crispatus* 1, **LJ2:** *L. jensenii* 2, **LM4:** *L. mucosae* 4. **LV4:** *L. vaginalis* 4, **NS**: non-suppressive, **S**: suppressive.

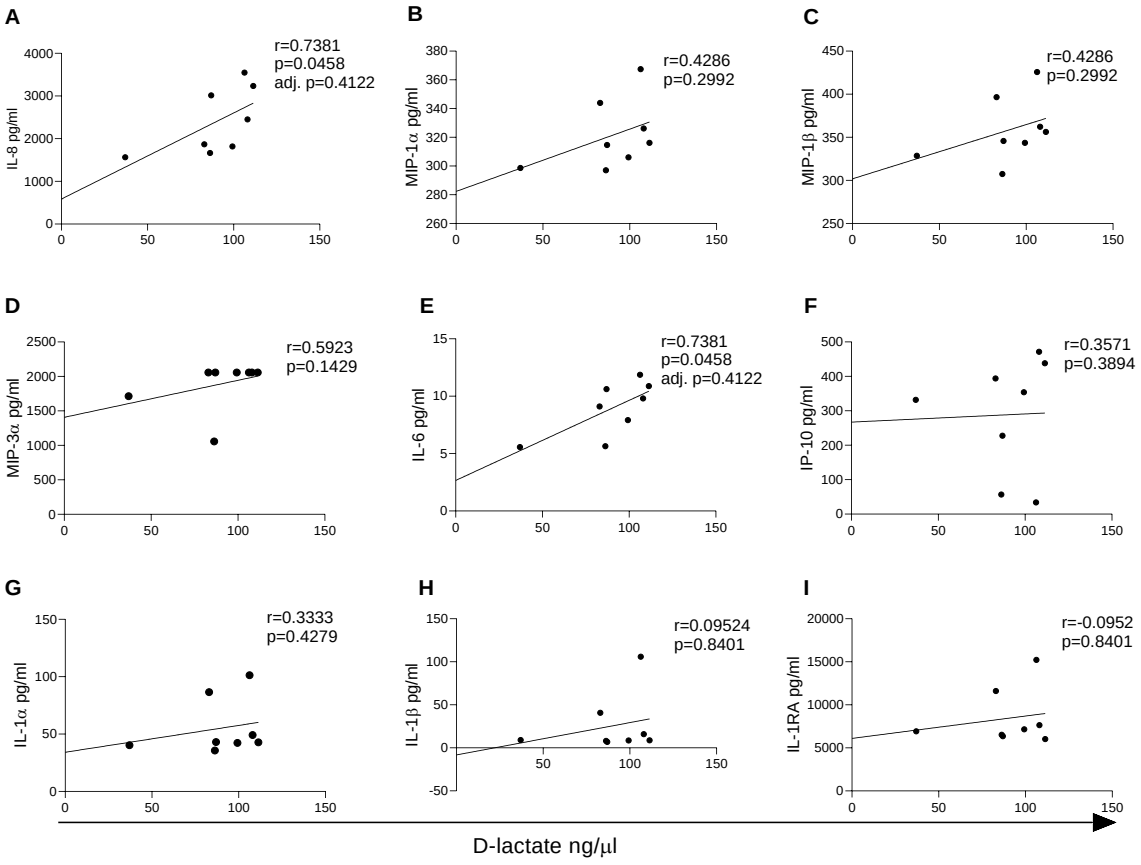

Figure 22 Correlations between D-lactate production and cytokine responses in VK2 cell cultures co-cultured with *Lactobacillus* spp. and *G. vaginalis*. A-I) Correlations between D-lactate production and cytokine responses, with the means of replicates shown. VK2 cells were seeded into 24 well plates ($0.5x10^6$ cells/well) and grown to confluence. Monolayers were stimulated with each *Lactobacillus* isolate ($4.18x10^6$CFU/well) isolate and incubated for 6 hours at 37°C, 5% CO_2. Thereafter, *G*. *vaginalis* ($4.18x10^7$ CFU/well) was then added to the *Lactobacillus*-VK2 cell cultures and incubated for an additional 6 hrs at 37°C, 5% CO_2. Triplicate independent assays were performed. VK2 cells only and *G*. *vaginalis* only stimulated VK2 cells were included as controls, in duplicate for each independent assay. Cell culture supernatants were used to evaluate D-lactate production using a colorimetric assay, with samples assayed in duplicate. D-Lactate concentrations were determined by standard curves. All samples were corrected for D-lactate detected in VK2 cells only cultures. Spearman's rank correlation was used to statistically test the correlations between D-lactate and cytokine responses, p≤0.05 considered significant. **IL-8**: interleukin-8, **MIP-1α:** macrophage inflammatory protein 1 alpha, **MIP-1β**: macrophage inflammatory protein 1 beta, **MIP-3α**: macrophage inflammatory protein 3 alpha, **IL-6**: interleukin-6, **IP-10**: interferon gamma induced protein 10, **IL-1α**: interleukin 1 alpha, **IL-1β:** interleukin 1 beta, **IL-1RA**: interleukin 1 receptor antagonist.

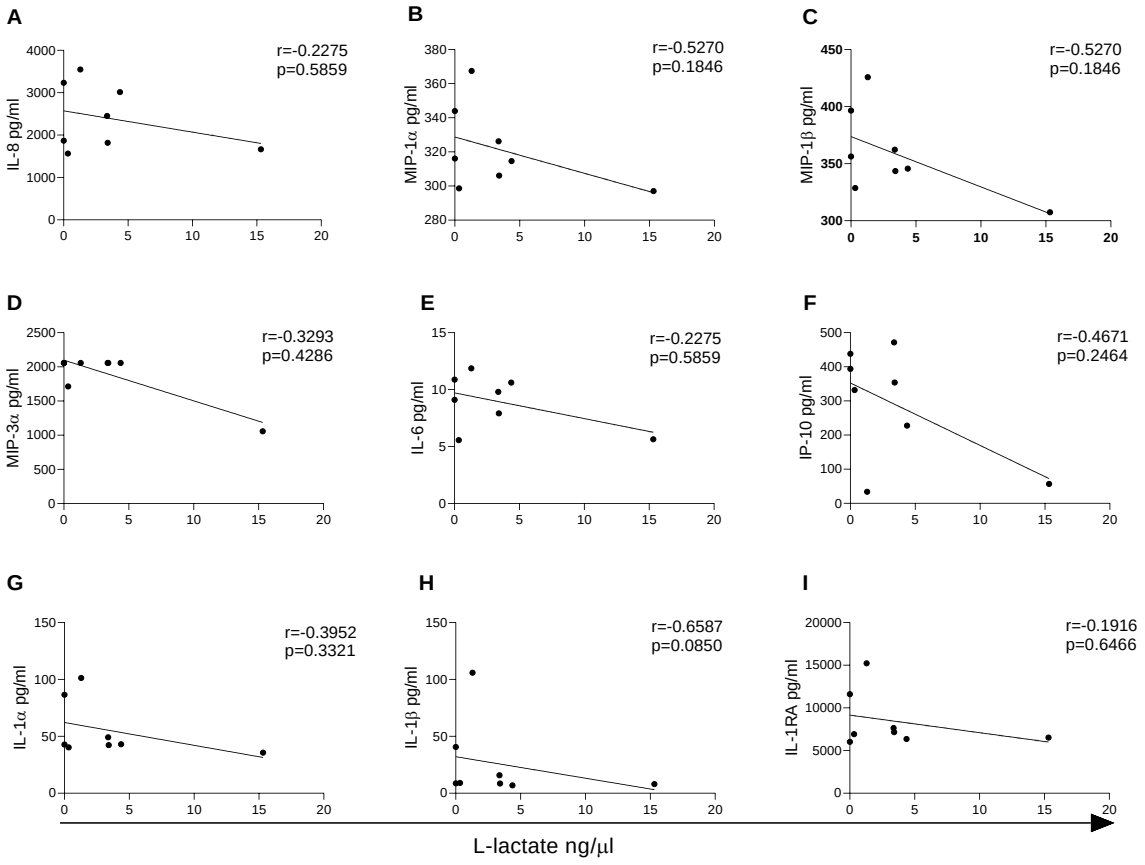

Figure 23 Correlations between L-lactate production and cytokine responses in VK2 cell cultures co-cultured with *Lactobacillus* spp. and *G. vaginalis*. A-I) Correlations between L-lactate production and cytokine responses, with the means of replicates shown. VK2 cells were seeded into 24 well plates ($0.5x10^6$ cells/well) and grown to confluence. Monolayers were stimulated with each *Lactobacillus* isolate ($4.18x10^6$CFU/well) isolate and incubated for 6 hours at 37°C, 5% CO_2. Thereafter, *G. vaginalis* ($4.18x10^7$ CFU/well) was then added to the *Lactobacillus*-VK2 cell cultures and incubated for an additional 6 hrs at 37°C, 5% CO_2. Triplicate independent assays were performed. VK2 cells only and *G. vaginalis* only stimulated VK2 cells were included as controls, in duplicate for each independent assay. Cell culture supernatants were used to evaluate L-lactate production using a colorimetric assay, with samples assayed in duplicate. L-Lactate concentrations were determined by standard curves. All samples were corrected for L-lactate detected in VK2 cells only cultures. Spearman's rank correlation was used to statistically test the correlations between L-lactate and cytokine responses, $p \leq 0.05$ considered significant. **IL-8**: interleukin-8, **MIP-1α:** macrophage inflammatory protein 1 alpha, **MIP-1β**: macrophage inflammatory protein 1 beta, **MIP-3α**: macrophage inflammatory protein 3 alpha, **IL-6**: interleukin-6, **IP-10**: interferon gamma induced protein 10, **IL-1α**: interleukin 1 alpha, **IL-1β:** interleukin 1 beta, **IL-1RA**: interleukin 1 receptor antagonist.

3.8 Quality of RNA extracted from VK2 cells stimulated with *Lactobacillus* species and *G. vaginalis* in 24 well plates

RNA was extracted from all 36 samples, including VK2 cells cultured alone, co-cultured with *G. vaginalis* (4.18 x 10^7CFU/well) and co-cultured with lactobacilli (4.18 x 10^6CFU/well) and *G. vaginalis* (4.18 x 10^7CFU/well) in combination, in 1ml of media. RNA integrity, quality and quantity were assessed using an Agilent 2100 Bioanalyzer and Nanodrop 8000 spectrophotometer.

A total of n=35 samples passed quality assessment with RINs 7.4 – 10, apart from LJ2+GV which did not (RIN: 5.2, **Figure 24A, Appendix XV**). A total of 2/3 LJ2+GV samples had acceptable RIN values (RIN: 7.4 and 8, **Figure 24A, Appendix XV**). Interestingly, LJ2+GV was the same co-culture that exhibited lower viability and induced substantially higher inflammatory responses relative to the other samples. In addition, LJ2 was isolated from a participant who tested positive for multiple STIs, including CT, NG and TV **(Table 2)**. Therefore, this sample was included in the microarray analysis. A total of n=21 samples had fully intact RNA, with RINs of 10 (**Figure 24A)**, while n=14 had partially degraded RNA, with RINs of 7.4-9.9. All samples had an acceptable A260/A280 ratios of 1.9 – 2.1, with n=33 samples “pure” with ratios of 2 **(Figure 24B)**. However, the A260/A230 ratios varied between 0.1 – 2.0 which indicated the presence of contaminants with absorbance at 230nm and additional sample clean-up procedures were thus conducted **(Figure 24B)**. The RNA quantity varied among the samples, however all of the samples yielded greater than 100ng of RNA required for microarray input **(Figure 24C)**. Based on the RNA quality results, n=30 samples were chosen for microarray analysis, which included all control and test samples in triplicate.

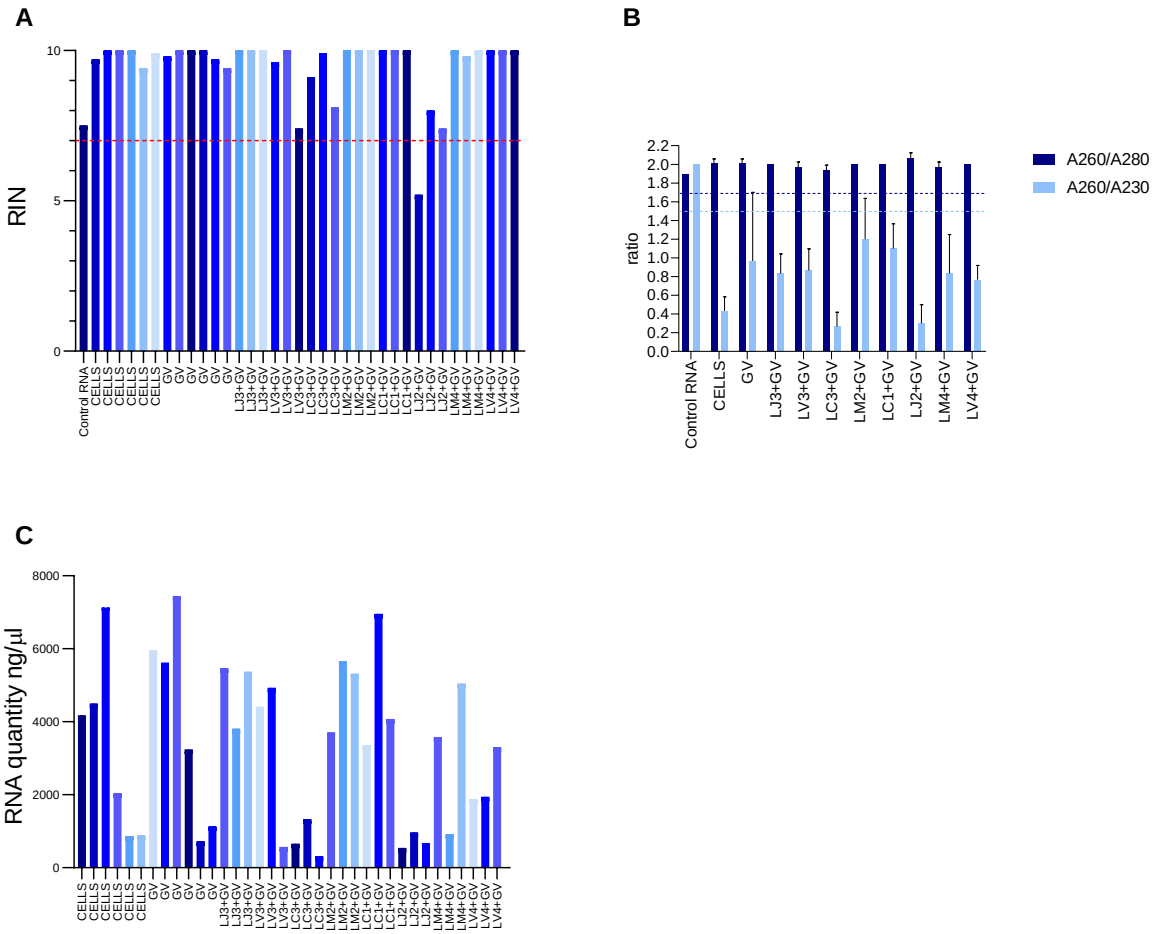

Figure 24 Quality of RNA extracted from VK2 cells stimulated with bacterial isolates. A) Bar graph showing RNA integrity numbers (RIN) for each sample. **B)** Boxplot showing A260/A280 ratios of samples. **C)** Bar graph showing RNA quantity (ng/µl) extracted from each sample. VK2 cells were seeded into 24 well plates ($0.5x10^6$ cells/well) and grown to confluence. Monolayers were stimulated with each *Lactobacillus* isolate (4.18 X 10^6CFU/500µl) and incubated for 6 hours at 37°C, 5% CO_2. Thereafter, *G. vaginalis* ($4.18x10^7$ CFU/500µl) was then added to the *Lactobacillus*-VK2 cell cultures and incubated for an additional 6 hrs at 37°C, 5% CO_2. Triplicate independent assays were performed. VK2 cells only and *G. vaginalis* only stimulated VK2 cells were included as controls, in duplicate for each independent assay. VK2 cells were harvested following the stimulation assay and stored in RLT lysis buffer at -80°C. RNA was extracted, and quality assessment was performed using an Agilent 2100 Bioanalyzer and NanoDrop 8000 spectrometer. Acceptable RINs are between 7-10. Acceptable A260/A280 and A260/A230 ratios are 1.7-2.0 and 1.5-3, respectively, dotted lines indicate lower limits. **RIN**: RNA integrity number, **GV:** *G. vaginalis*, **LJ3:** *L. jensenii* 3, **LV3:** *L. vaginalis* 3, **LC3:** *L. crispatus* 3, **LM2:** *L. mucosae* 2, **LC1:** *L. crispatus* 1, **LJ2:** *L. jensenii* 2, **LM4:** *L. mucosae* 4. **LV4:** *L. vaginalis* 4.

While bacterial stimulation in both the transwell and the 24 well plate culture systems yielded viable VK2 cells and good quality RNA of sufficient quantity, only the stimulation assay performed in the 24 well plates yielded expected cytokine responses and these samples were thus assessed by microarray analysis (**Figure 25**). The transwell culture system thus requires further optimization and, in the future, *G. vaginalis* and *Lactobacillus* isolates will be titrated for this system and different incubation periods will be investigated.

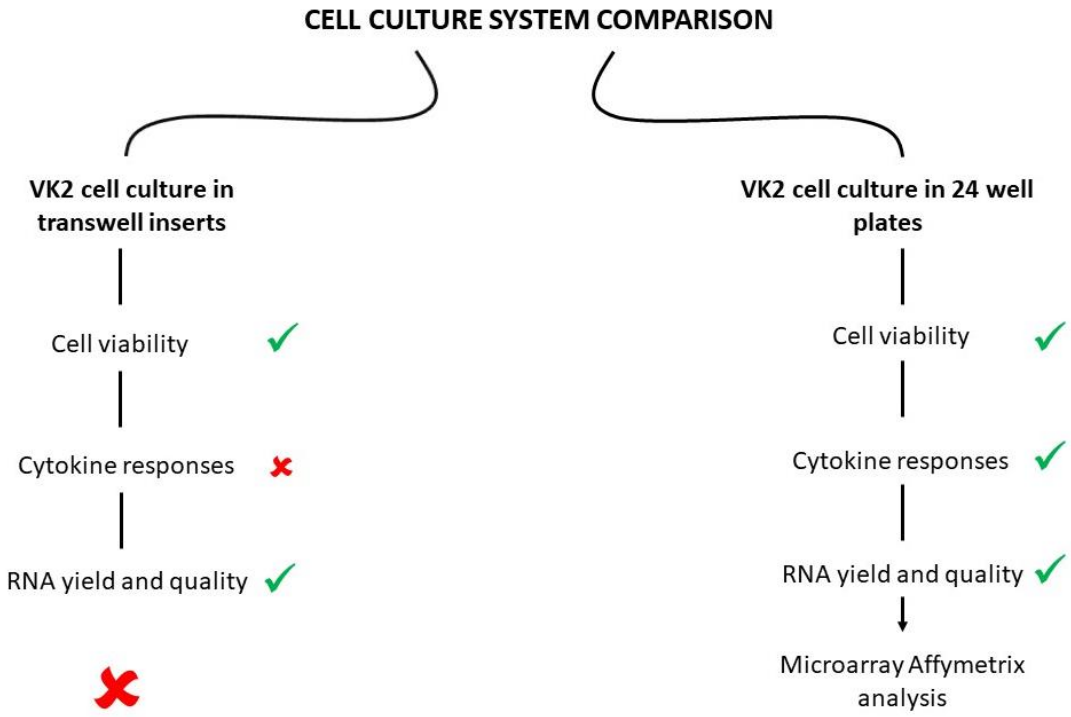

Figure 25 Comparison of transwell and 24 well VK2 cell culture systems. VK2 cells were seeded into transwells or 24 well plates and grown to confluence. Monolayers were stimulated with each *Lactobacillus* isolate and *G. vaginalis* in combination. Cytokine concentrations in the cell supernatants were measured by Luminex assay. VK2 cells were harvested and RNA extracted using the RNeasy mini kit. RNA quality and yield were assessed by an Agilent 2100 Bioanalyzer and NanoDrop 8000 spectrophotometer.

3.9 Overall gene transcription of VK2 cells stimulated by *Lactobacillus* isolates and *G. vaginalis* in combination

The Affymetrix Microarray Platform was used to evaluate the potential effect of *Lactobacillus* isolates ($4.18x10^6$CFU/well) on VK2 cell gene expression, particularly those involved in inflammatory responses induced by *G. vaginalis* ($4.18x10^7$CFU/well), in 1ml of media.

Although, 1/3 LJ2+GV samples had a RIN of 5.2, cRNA and sscDNA synthesis, and cDNA fragmentation of the microarray assay passed QC assessment using an Agilent 2100 Bioanalyzer and Nanodrop 8000 spectrophotometer (not shown). Thus, this sample was included in the microarray data analysis, as more detailed characterization of this isolate in the future would be interesting.

Following log-2 transformation and normalization by Robust MultiChip Average normalization (RMA) of gene expression raw data, no outliers were detected **(Figure 26A and B).** Furthermore, log_2-transformed raw data revealed similar median values for all samples **(Figure 26A)**, while all median values were the same after RMA normalization of raw data **(Figure 26B).** Further analysis was performed using the RMA normalized data.

A total of 27189 genes were expressed. Based on PCA clustering analysis of samples, three clusters are observed: the cells only samples; GV, LJ3+GV, LV3+GV, LC3+GV, LM2+GV, LC1+GV, LM4+GV and LV4+GV samples; and LJ2+GV samples **(Figure 27)**. PC1 explained 26.6% of the variance, while PC2 explained 13.7% of the variance in the dataset **(Figure 27)**.

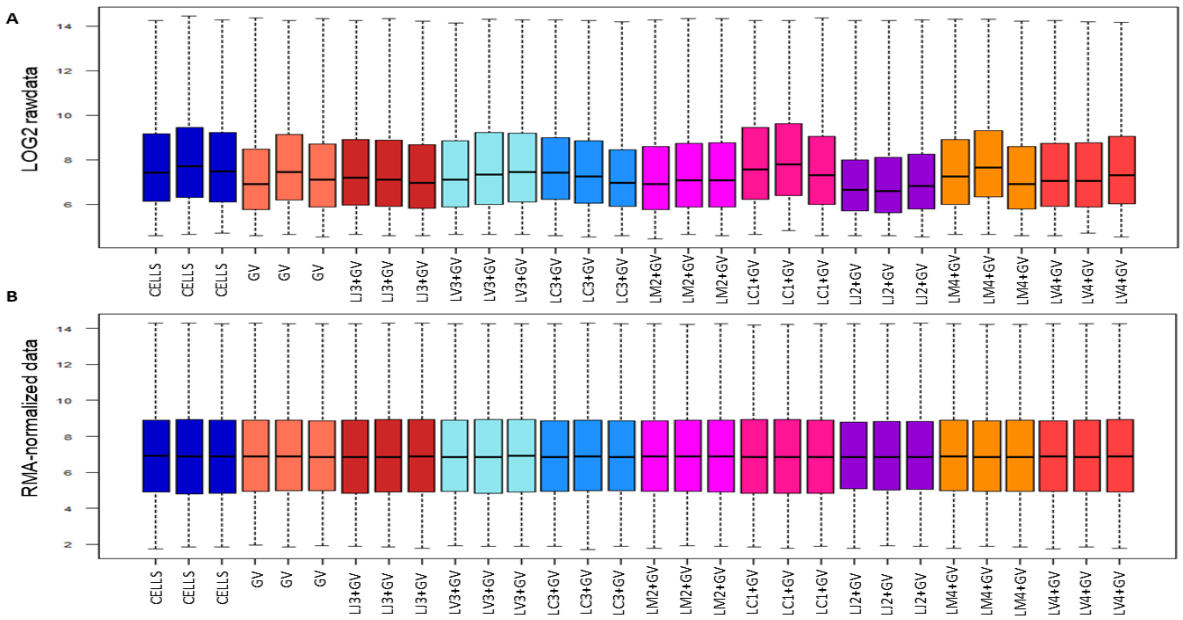

Figure 26 RMA normalization of Affymetrix raw data. A) Boxplots showing log_2-transformed raw data. **B)** Boxplots showing RMA normalization of raw data. VK2 cells were seeded into 24 well plates (0.5x10^6 cells/well) and grown to confluence. Monolayers were stimulated with each *Lactobacillus* isolate (4.18 X 10^{6}CFU/well) and incubated for 6 hours at 37°C, 5% CO_2. Thereafter, *G. vaginalis* (4.18x10^7 CFU/well) was then added to the *Lactobacillus*-VK2 cell cultures and incubated for an additional 6 hrs at 37°C, 5% CO_2. VK2 cells only and *G. vaginalis* only stimulated VK2 cells were included as controls. Triplicate independent assays were performed. VK2 cells were harvested following the stimulation assay and stored in RLT lysis buffer at -80°C. RNA was extracted using the Qiagen RNeasy mini kit and gene expression analysis was then performed using microarray Affymetrix GeneChip whole transcript array platform. The R Studio Bioconductor oligo package was used to normalize raw data using Robust MultiChip Average (RMA) normalization. **GV:** *G. vaginalis*, **LJ3:** *L. jensenii* 3, **LV3:** *L. vaginalis* 3, **LC3:** *L. crispatus* 3, **LM2:** *L. mucosae* 2, **LC1:** *L. crispatus* 1, **LJ2:** *L. jensenii* 2, **LM4:** *L. mucosae* 4. **LV4:** *L. vaginalis* 4.

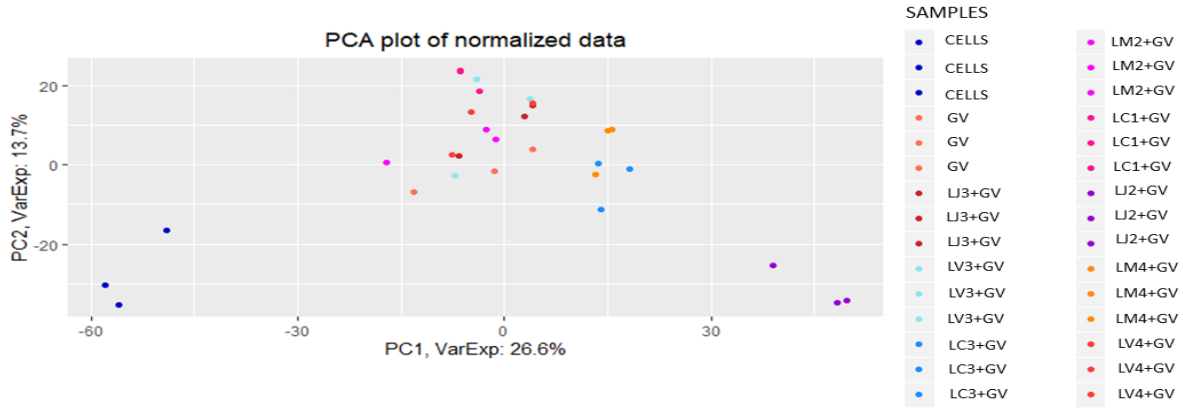

Figure 27 PCA clustering of samples based on total gene expression. VK2 cells were seeded into 24 well plates (0.5x10^6 cells/well) and grown to confluence. Monolayers were stimulated with each *Lactobacillus* isolate (4.18 X 10^{6}CFU/well) isolate and incubated for 6 hours at 37°C, 5% CO_2. Thereafter, *G. vaginalis* (4.18x10^7 CFU/well) was then added to the *Lactobacillus*-VK2 cell cultures and incubated for an additional 6 hrs at 37°C, 5% CO_2. VK2 cells only and *G. vaginalis* only stimulated VK2 cells were included as controls. Triplicate independent assays were performed. VK2 cells were harvested following the stimulation assay and stored in RLT lysis buffer at -80°C. RNA was extracted and gene expression analysis was then performed using microarray Affymetrix GeneChip whole transcript array platform. The R studio Bioconductor oligo package was used to normalize raw data using Robust MultiChip Average (RMA) normalization. Principal component analysis (PCA) was performed to evaluate clustering of the samples based on 27189 genes expressed. The PCA plot was generated using the R Studio ggplot2 package. **GV:** *G. vaginalis*, **LJ3:** *L. jensenii* 3, **LV3:** *L. vaginalis* 3, **LC3:** *L. crispatus* 3, **LM2:** *L. mucosae* 2, **LC1:** *L. crispatus* 1, **LJ2:** *L. jensenii* 2, **LM4:** *L. mucosae* 4. **LV4:** *L. vaginalis* 4, **PCA**: principal component analysis, **PC**: principal component.

3.10 Differential gene expression and signalling pathways in *G. vaginalis* stimulated VK2 cells compared to unstimulated VK2 cells

G. vaginalis ($4.28x10^7$CFU/well) was cultured with VK2 cells in 1ml of media and gene expression was assessed using the Affymetrix Microarray Platform. The R Studio Bioconductor limma package was used to determine differentially expressed genes between *G. vaginalis* stimulated VK2 cells compared to unstimulated VK2 cells. DAVID Bioinformatics Resources v6.8 was used to assess upregulated signaling pathways.

A total of 4421 genes were significantly differentially expressed by *G. vaginalis* stimulated VK2 cells compared to unstimulated cells (adj. p≤0.05), with 142 logFC≥1.5 upregulated (**Appendix XVI**) and 26 genes logFC≤-1.5 downregulated **(Table 3, Figure 28)**. Upregulated genes mapped to 28 KEGG signaling pathways **(Figure 29)**. The cytokine-cytokine interaction signaling pathway was the most significantly upregulated (adj. $p=3.60x10^{-6}$, **Figure 30**), with mediators including chemokines (CCL5, CXCL1, CXCL8, CXCL3, CXCL10, CXCL11), proinflammatory cytokines (IL-6, IL23A, IL1A, ILB), adaptive immune cytokines and receptors (IL2RG, TSLP), VEGI (dendritic cell maturation factor), TNF receptors (GITRL, 41BB) and INHBB (member of TGF-beta family) mapping to this pathway **(Figure 30)**. The TNF signaling pathway was also significantly upregulated (adj. p=0.0018, **Figure 29**) and included the mediators cIAP1/2 (member of the inhibitor of apotosis proteins), chemokines (CCL2, CCL5, CCL20, CXCL12, IL1B, IL6), Tnfaip3 (TNF induced protein), Icam1 (cell surface glycoprotein) and Ptgs2 (prostaglandin synthase, **Figure 31)**. The NF-κB signaling pathway was significantly upregulated (adj. p=0.0037, **Figure 29)**, with mediators including proinflammatory cytokines and chemokines (IL1B, IL8), receptor associated adaptor protein (EDARADD), members of the inhibitor of apotosis family proteins (cIAP1/2, BIRC2), RELB (NF-κB subunit), apotosis regulating proteins (Bcl.2, BCL2A), Tnfaip3 (also known as A20) and SLC (membrane transport protein) mapping to this pathway **(Figure 32)**. The NOD-like receptor signaling pathway was significantly upregulated (adj. p=0.0284, **Figure 29**), the mediators cIAP, Tnfaip3, proinflammatory cytokines and chemokines (proIL1β, IL-1β, IL18, IL10, IL8, CXCL) and defensins (host defense peptide) mapped to this pathway **(Figure 33)**. TLR signaling and MAPK signaling pathways were significantly upregulated ($p=1.19x10^{-4}$ and p=0.0172, respectively), however these were not upheld after adjusting or multiple comparisons (adj. p=0.1370 and adj. p=1, **Figure 29**). The mediators TLR2 (pattern recognition receptor), IRF7 (transcription factor), proinfammatory cytokines (IL1B, IL6, IL8, RANTES, IP10) and chemokine (ITAC) mapped to the TLR signaling pathway **(Figure 34)**, while the mediators GF (transcription factor), RTK (cell surface receptor), RasGRP (Ras activator), protein kinases (LZK, MKP), proinflammatory mediators (IL1, NF-κB) mapped to

the MAPK signaling pathway **(Figure 35)**. Key genes common to these pathways were CCL5, cIAP, IL-6, A20, CXCL10, CXCL18 and IL1B, which were significantly upregulated in *G. vaginalis* stimulated VK2 cells compared to unstimulated VK2 cells (adj. $p=3.2123x10^{-7}$, adj. $p=7.2093x10^{-8}$, adj. p=0.0008, adj. $p=1.0007x10^{-6}$, adj. $p= 1.1514x10^{-7}$, adj. $p= 1.0139x10^{-7}$, adj. $p= 1.1452x10^{-6}$, **Figure 36**).

A total of 27 genes were downregulated in *G. vaginalis*-stimulated VK2 cells compared to unstimulated VK2 cells (logFC≤-1.5, **Table 3, Figure 37**). PKA, Sestrins and PGC-1α mediators mapped to the KEGG longevity pathway **(Figure 38)**.

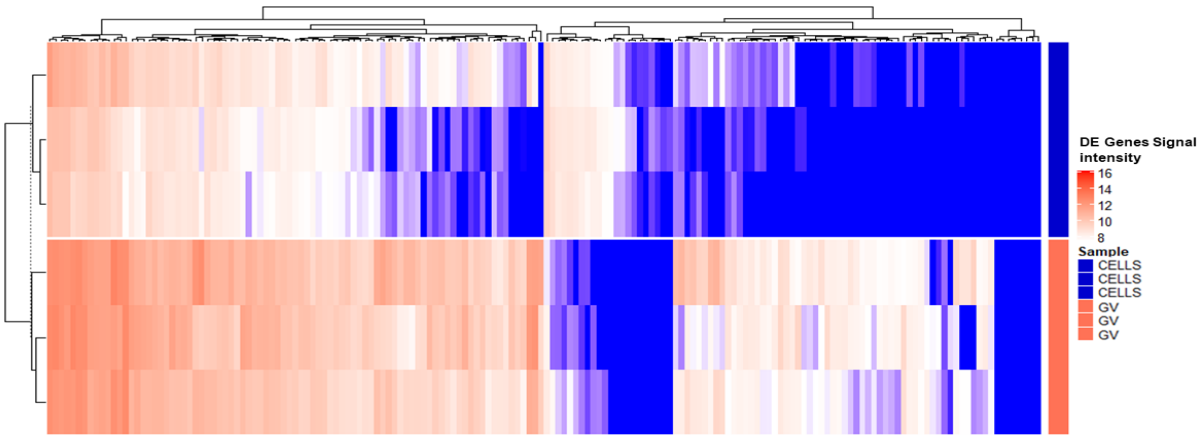

Figure 28 Heatmap showing upregulated and downregulated genes in VK2 cells stimulated with *G. vaginalis* compared to unstimulated cells. Unsupervised hierarchical clustering of groups based on differentially upregulated and downregulated genes in *G. vaginalis* stimulated VK2 cells compared to unstimulated VK2 cells. VK2 cells were seeded into 24 well plates ($0.5x10^6$ cells/well) and grown to confluence. *G. vaginalis* ($4.18x10^7$CFU/well) was added to the VK2 cell cultures and incubated for 6 hrs at 37°C, 5% CO_2, in triplicate independent assays. VK2 cells only controls were included in triplicate independent assays. VK2 cells were then harvested and RNA was extracted. Gene expression analysis was then performed using the microarray Affymetrix GeneChip whole transcript array platform. Affymetrix data were normalized using Robust Multichip Average (RMA) normalization. Differential gene expression analysis was performed using the R Bioconductor limma package. Genes were considered differentially expressed if adj. p≤0.05 and upregulated or downregulated if log fold change (FC) ≥ 1.5 or ≤ -1.5, respectively. The dendogram above the heatmap indicates the degree of relatedness between the genes expressed. The horizontal "branches" have arbitrary lengths and the lengths of the vertical "branches" indicate the degrees of similarity between the gene expression profiles. The left-hand side dendogram demonstrates relationships between the gene expression profiles of *G. vaginalis* stimulated and unstimulated VK2 cells. Shorter or longer horizontal branch lengths between the isolates for this dendogram, indicate higher or lower degrees of similarity between the gene expression profiles of samples, respectively. **DE**: differentially expressed genes. Blue, through white, to red indicates low to high gene expression.

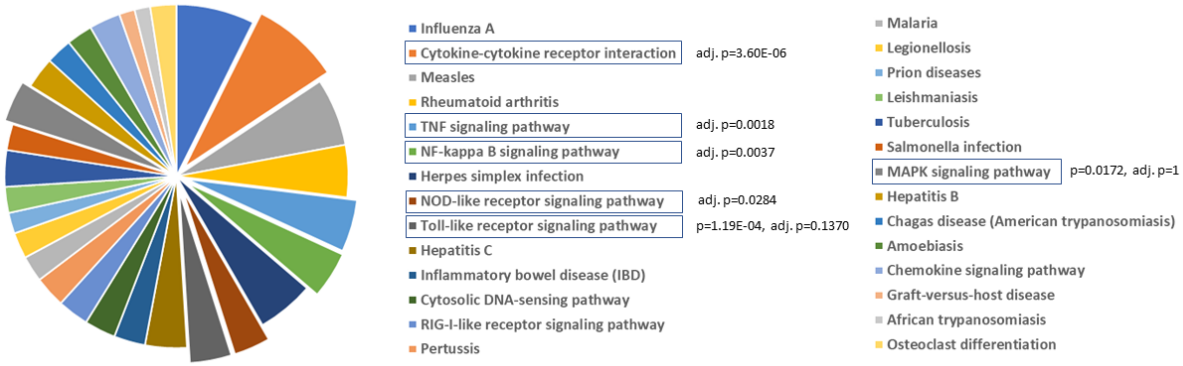

Figure 29 Upregulated genes mapped to pro-inflammatory signalling pathways in *G. vaginalis* stimulated VK2 cells compared to unstimulated VK2 cells. The pie chart shows the proportion of differentially expressed genes upregulated in G. *vaginalis* stimulated VK2 cells compared to unstimulated VK2 cells for each signaling pathway, key proinflammatory signaling pathways are boxed. VK2 cells were seeded into 24 well plates ($0.5x10^6$ cells/well) and grown to confluence. *G. vaginalis* ($4.18x10^7$CFU/well) was added to the VK2 cell cultures and incubated for 6 hrs at 37°C, 5% CO_2, in triplicate independent assays. VK2 cells only controls were included in triplicate independent assays. VK2 cells were then harvested and RNA was extracted. Gene expression analysis was then performed using microarray Affymetrix GeneChip whole transcript array platform. Affymetrix data were normalized using Robust Multichip Average (RMA) normalization. Differential gene expression analysis was performed using R Bioconductor limma package. Genes were considered differentially expressed if adj. p≤0.05 and upregulated or downregulated if log fold change (FC) ≥ 1.5 or ≤ -1.5, respectively. Genes were annotated using the Clariom S Human annotation file. Upregulated gene Entrez identity numbers were used in DAVID Bioinformatics Resources v6.8 to obtain biological pathways upregulated. **TNF**: Tumor Necrosis Factor, **NF-Kappa-B**: Nuclear factor kappa-light-chain-enhancer of activated B cells, **NOD-like**: Nucleotide-binding oligomerization domain-like, **MAPK**: Mitogen-activated protein kinase.

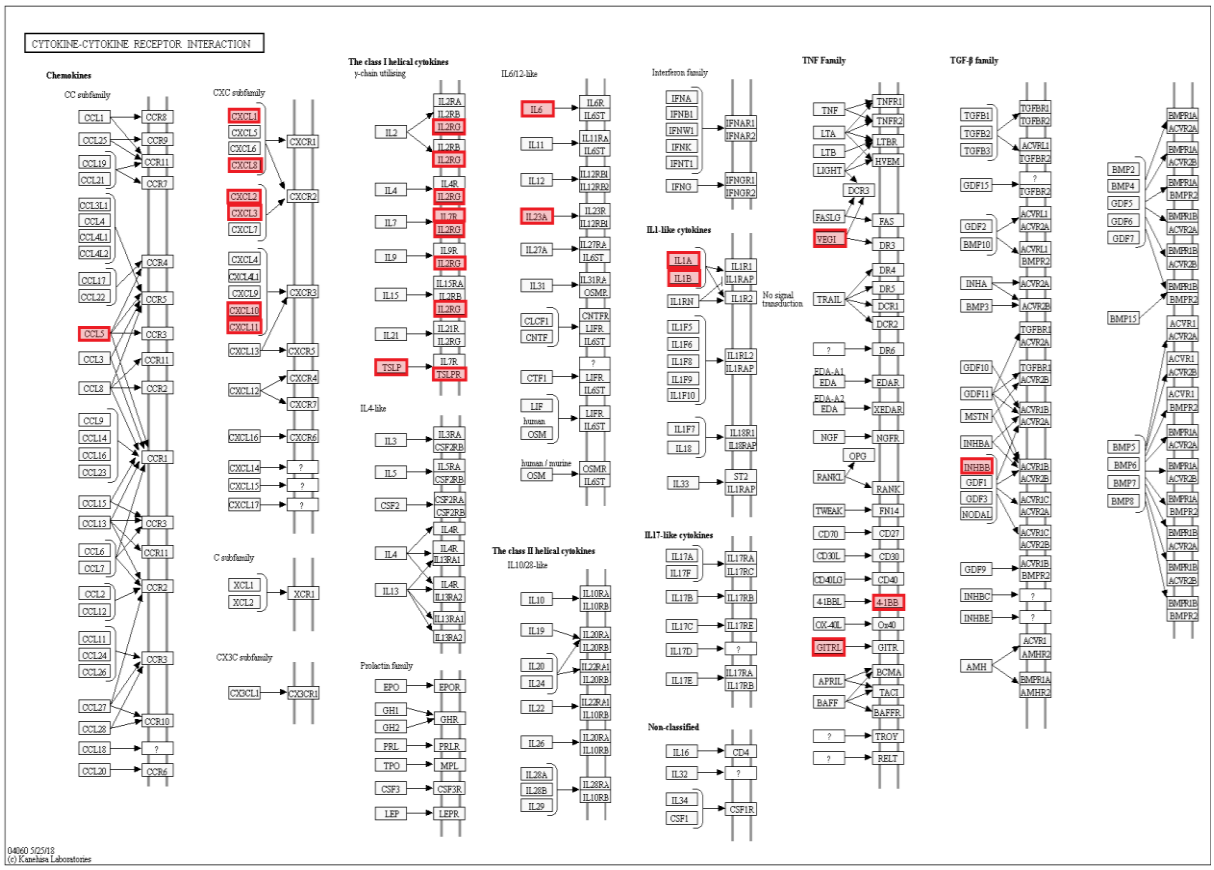

Figure 30 Upregulated genes in the cytokine-cytokine receptor signaling pathway in *G. vaginalis* stimulated VK2 cells compared to unstimulated VK2 cells. KEGG cytokine-cytokine signaling pathway adapted from DAVID Bioinformatics resources, upregulated in VK2 cells cultured with *G. vaginalis* ($4.18x10^7$CFU/well) compared to VK2 cell culture only, red boxes indicate mediators upregulated in *G. vaginalis* stimulated VK2 cells compared to VK2 cell culture only. VK2 cells were seeded into 24 well plates ($0.5x10^6$ cells/well) and grown to confluence. *G. vaginalis* ($4.18x10^7$CFU/well) was added to the VK2 cell cultures and incubated for 6 hrs at 37°C, 5% CO_2, in triplicate independent assays. VK2 cells only controls were included in triplicate independent assays. VK2 cells were then harvested and RNA was extracted. Gene expression analysis was then performed using microarray Affymetrix GeneChip whole transcript array platform. Affymetrix data were normalized using Robust Multichip Average (RMA) normalization. Differential gene expression analysis was performed using R Bioconductor limma package. Genes were considered differentially expressed if adj. p≤0.05 and upregulated or downregulated if log fold change (FC) ≥ 1.5 or ≤ -1.5, respectively. Genes were annotated using the Clariom S Human annotation file. Upregulated gene Entrez identity numbers were used in DAVID Bioinformatics resources v6.8 to obtain biological pathways upregulated. **CCL5**: chemokine c-c motif ligand 5, **CXCL2,-3,-8,-10,-11**: chemokine c-x-c motif ligand 2,-3,-8,-10,-11, **IL2RG**: Interleukin 2 receptor gamma, **IL7R**: IL-7 receptor, **TSLP**: thymic stromal lymphopoietin, **TSLPR:** thymic stromal lymphopoietin receptor, **IL-6**: Interleukin 6, **IL-1A**: Interleukin 1 alpha, **IL-23A**: Interleukin 23 alpha, **IL-1B**: interleukin 1 beta, **VEGI**: vascular epithelial growth inhibitor, **4IBB**: 4-IBB/CD137/tumor necrosis factor superfamily receptor 9, **GITRL**: glucocorticoid-induced TNFR-related protein/TNSF18-tumor necrosis factor superfamily member 18, **INHBB**: inhibin beta B.

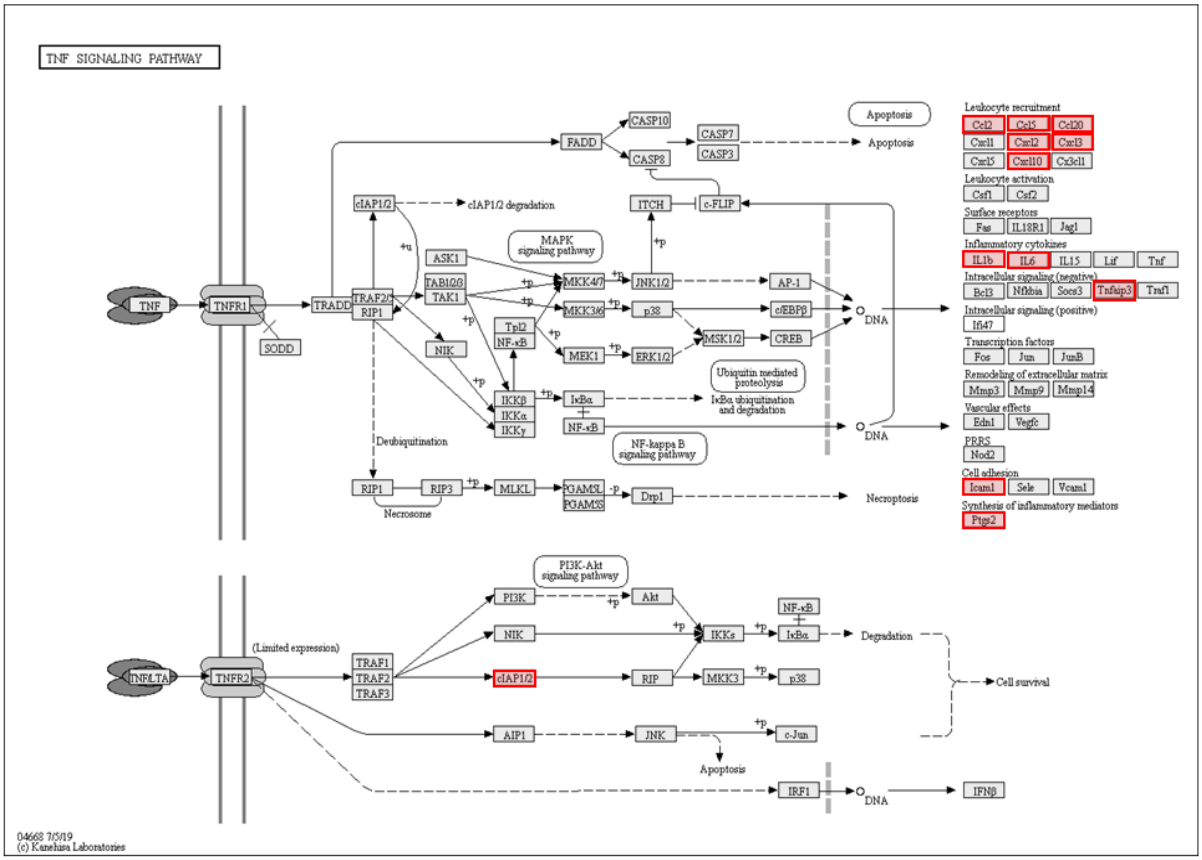

Figure 31 Upregulated genes in the tumor necrosis factor (TNF) signaling pathway in *G. vaginalis* stimulated VK2 cells compared to unstimulated VK2 cells. KEGG TNF signaling pathway adapted from DAVID Bioinformatics resources, upregulated in VK2 cells cultured with *G. vaginalis* ($4.18x10^7$CFU/well) compared to VK2 cell culture only, red boxes indicate mediators upregulated in *G. vaginalis* stimulated VK2 cells compared to VK2 cell culture only. VK2 cells were seeded into 24 well plates ($0.5x10^6$ cells/well) and grown to confluence. *G. vaginalis* ($4.18x10^7$CFU/well) was then added to the VK2 cell cultures and incubated for 6 hrs at 37°C, 5% CO_2, in triplicate independent assays. VK2 cells only were included in triplicate independent assays. VK2 cells were then harvested and RNA was extracted. Gene expression analysis was then performed using microarray Affymetrix GeneChip whole transcript array platform. Affymetrix data were normalized using Robust Multichip Average (RMA) normalization. Differential gene expression analysis was performed using R Bioconductor limma package. Genes were considered differentially expressed if, adj. p≤0.05 and upregulated or downregulated if log fold change (FC) ≥ 1.5 or ≤ -1.5, respectively. Genes were annotated using the Clariom S Human annotation file. Upregulated gene Entrez identity numbers were used in DAVID Bioinformatics resources v6.8 to obtain biological pathways upregulated. **TNF**: tumor necrosis factor, **CCL5**: chemokine c-c motif ligand 5, **CXCL10,-12,-13**: chemokine c-x-c motif ligand 10,-12,-13, **IL-6**: Interleukin 6, **IL-1B**: interleukin 1 beta, **Cc12,-15,-120**: chemokine c-c motif ligand 12,-15,-120, **Tnfaip3**: TNF alpha induced protein 3, **Icam1**: Intercellular adhesion molecule 1, **Ptgs2**: Prostaglandin-endoperoxide synthase 2.

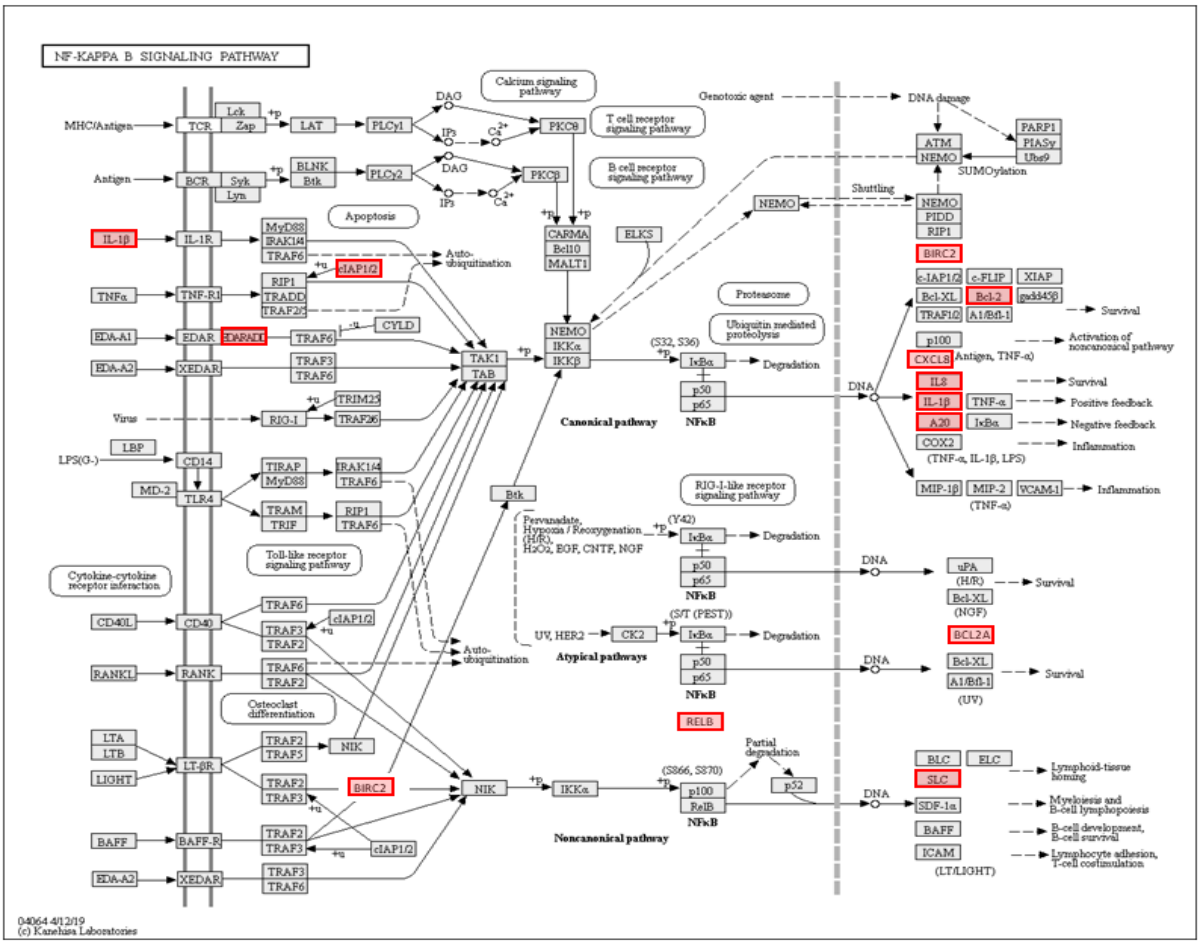

Figure 32 Upregulated genes in the NFκB signaling signaling pathway in *G. vaginalis* stimulated VK2 cells compared to unstimulated VK2 cells. KEGG NFκB signaling pathway adapted from DAVID Bioinformatics resources, upregulated in VK2 cells cultured with *G. vaginalis* ($4.18x10^7$CFU/well) compared to VK2 cell culture only, red boxes indicate mediators upregulated in *G. vaginalis* stimulated VK2 cells compared to VK2 cell culture only. VK2 cells were seeded into 24 well plates ($0.5x10^6$ cells/well) and grown to confluence. *G. vaginalis* ($4.18x10^7$CFU/well) was added to the VK2 cell cultures and incubated for 6 hrs at 37°C, 5% CO_2, in triplicate independent assays. VK2 cells only controls were included in triplicate independent assays. VK2 cells were then harvested and RNA was extracted. Gene expression analysis was then performed using microarray Affymetrix GeneChip whole transcript array platform. Affymetrix data were normalized using Robust Multichip Average (RMA) normalization. Differential gene expression analysis was performed using R Bioconductor limma package. Genes were considered differentially expressed if, adj. p≤0.05 and upregulated or downregulated if log fold change (FC) ≥ 1.5 or ≤ -1.5, respectively. Genes were annotated using the Clariom S Human annotation file. Upregulated gene Entrez identity numbers were used in DAVID Bioinformatics resources v6.8 to obtain biological pathways upregulated. **IL-1β**: Interleukin 1 beta, **cIAP1/2**: cellular inhibitor apoptosis protein 1 or 2, **EDARADD**: Ectodysplasin-A receptor-associated adapter protein, **BIRC2**: baculoviral IAP repeat-containing protein 2, **RELB**: transcription factor RelB, NFκB subunit, **Bcl.2**: B cell lymphoma 2, **CXCL8**: chemokine c-x-c motif ligand 8, **IL-8**: interleukin 8, **A20**: tumor necrosis factor, alpha-induced protein 3, **BCL2A**: B cell lymphoma 2 A, **SLC**: human solute carrier.

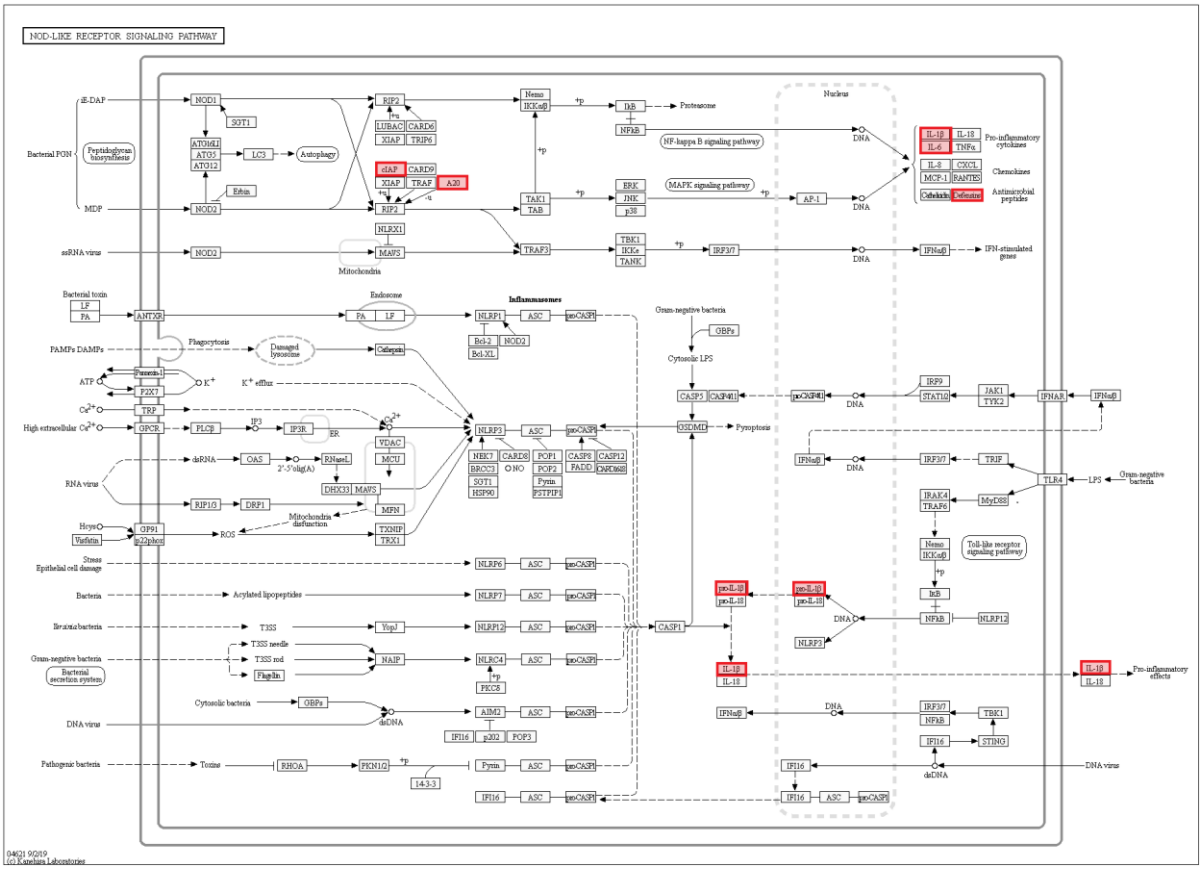

Figure 33 Upregulated genes in the nuclear oligomerization domain (NOD)-like receptor signalling pathway in *G. vaginalis* stimulated VK2 cells compared to unstimulated VK2 cells. KEGG NOD-like receptor signaling pathway adapted from DAVID Bioinformatics resources, upregulated in VK2 cells cultured with *G. vaginalis* compared to VK2 cell culture only, red boxes indicate mediators upregulated in *G. vaginalis* stimulated VK2 cells compared to VK2 cell culture only. VK2 cells were seeded into 24 well plates ($0.5x10^6$ cells/well) and grown to confluence. *G. vaginalis* ($4.18x10^7$CFU/well) was added to the VK2 cell cultures and incubated for 6 hrs at 37°C, 5% CO_2, in triplicate independent assays. VK2 cells only controls were included in triplicate independent assays. VK2 cells were then harvested and RNA was extracted. Gene expression analysis was then performed using microarray Affymetrix GeneChip whole transcript array platform. Affymetrix data were normalized using Robust Multichip Average (RMA) normalization. Differential gene expression analysis was performed using R Bioconductor limma package. Genes were considered differentially expressed if, adj. p≤0.05 and upregulated or downregulated if log fold change (FC) ≥ 1.5 or ≤ -1.5, respectively. Genes were annotated using the Clariom S Human annotation file. Upregulated gene Entrez identity numbers were used in DAVID Bioinformatics resources v6.8 to obtain biological pathways upregulated. **cIAP**: cellular inhibitor of apoptosis protein, **A20**: tumor necrosis factor, alpha-induced protein 3, **proIL1.β**: pro-interleukin 1 beta, **IL-6**: interleukin 6, **CXCL**: chemokine c-x-c motif ligand, **IL-8**: interleukin 8.

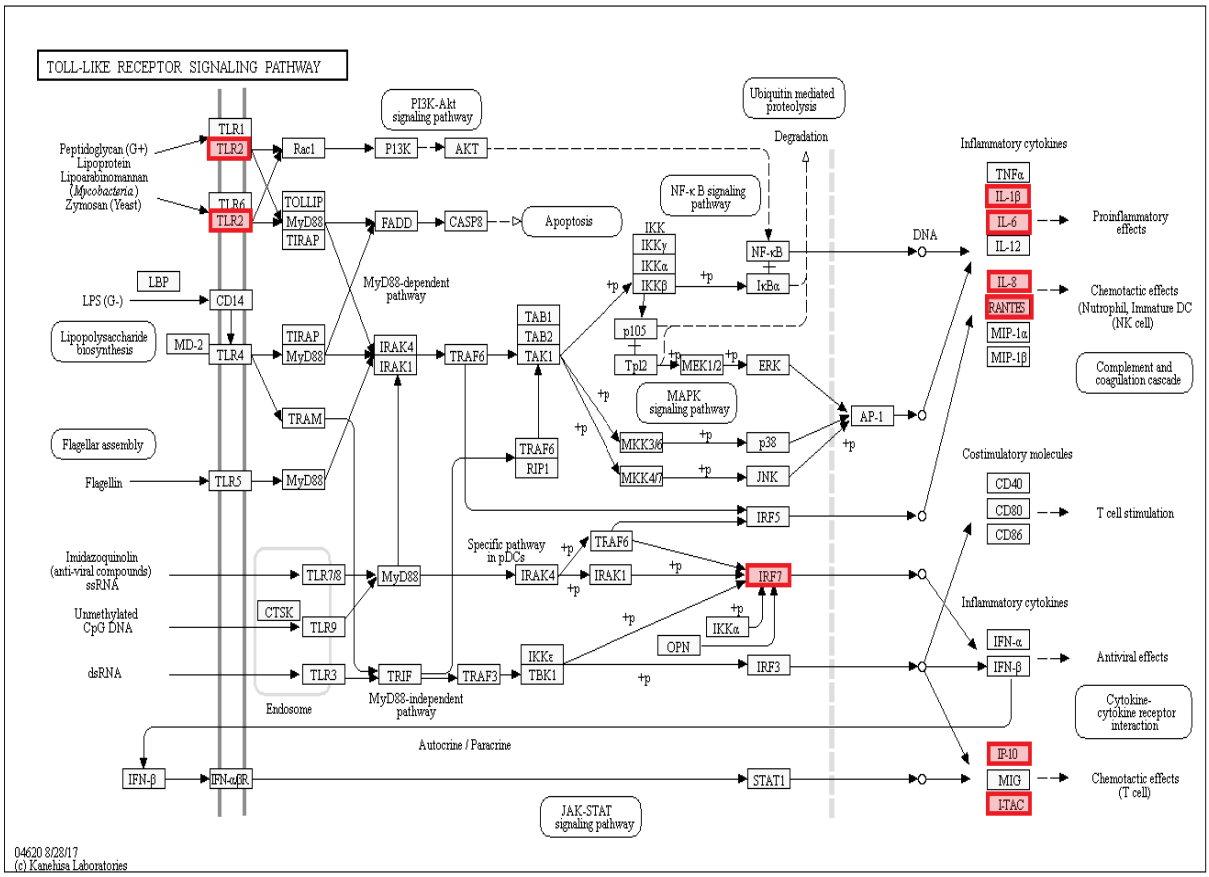

Figure 34 Upregulated genes in the toll-like receptor signalling pathway in *G. vaginalis* stimulated VK2 cells compared to unstimulated VK2 cells. KEGG toll-like receptor signaling pathway adapted from DAVID Bioinformatics resources, upregulated in VK2 cells cultured with *G. vaginalis* compared to VK2 cell culture only, red boxes indicate mediators upregulated in *G. vaginalis* stimulated VK2 cells compared to VK2 cell culture only. VK2 cells were seeded into 24 well plates ($0.5x10^6$ cells/well) and grown to confluence. *G. vaginalis* ($4.18x10^7$CFU/well) was added to the VK2 cell cultures and incubated for 6 hrs at 37°C, 5% CO_2, in triplicate independent assays. VK2 cells only controls were included in triplicate independent assays. VK2 cells were then harvested and RNA was extracted. Gene expression analysis was then performed using microarray Affymetrix GeneChip whole transcript array platform. Affymetrix data were normalized using Robust Multichip Average (RMA) normalization. Differential gene expression analysis was performed using R Bioconductor limma package. Genes were considered differentially expressed if, adj. p≤0.05 and upregulated or downregulated if log fold change (FC) ≥ 1.5 or ≤ -1.5, respectively. Genes were annotated using the Clariom S Human annotation file. Upregulated gene Entrez identity numbers were used in DAVID Bioinformatics resources v6.8 to obtain biological pathways upregulated. **TLR2**: toll-like receptor 2, **IL-6**: Interleukin 6, **IL-1B**: interleukin 1 beta, **IRF7**: interferon regulatory factor 7, **IL-8**: interleukin 8, **RANTES**: regulated on activation, normal T cell expressed and secreted/chemokine c-c motif ligand 5 (CCL5) , **IP-10**: interferon gamma induced protein 10/chemokine c-x-c motif ligand 10 (CXCL10), **I-TAC**: interferon inducible T cell alpha chemoattractant.

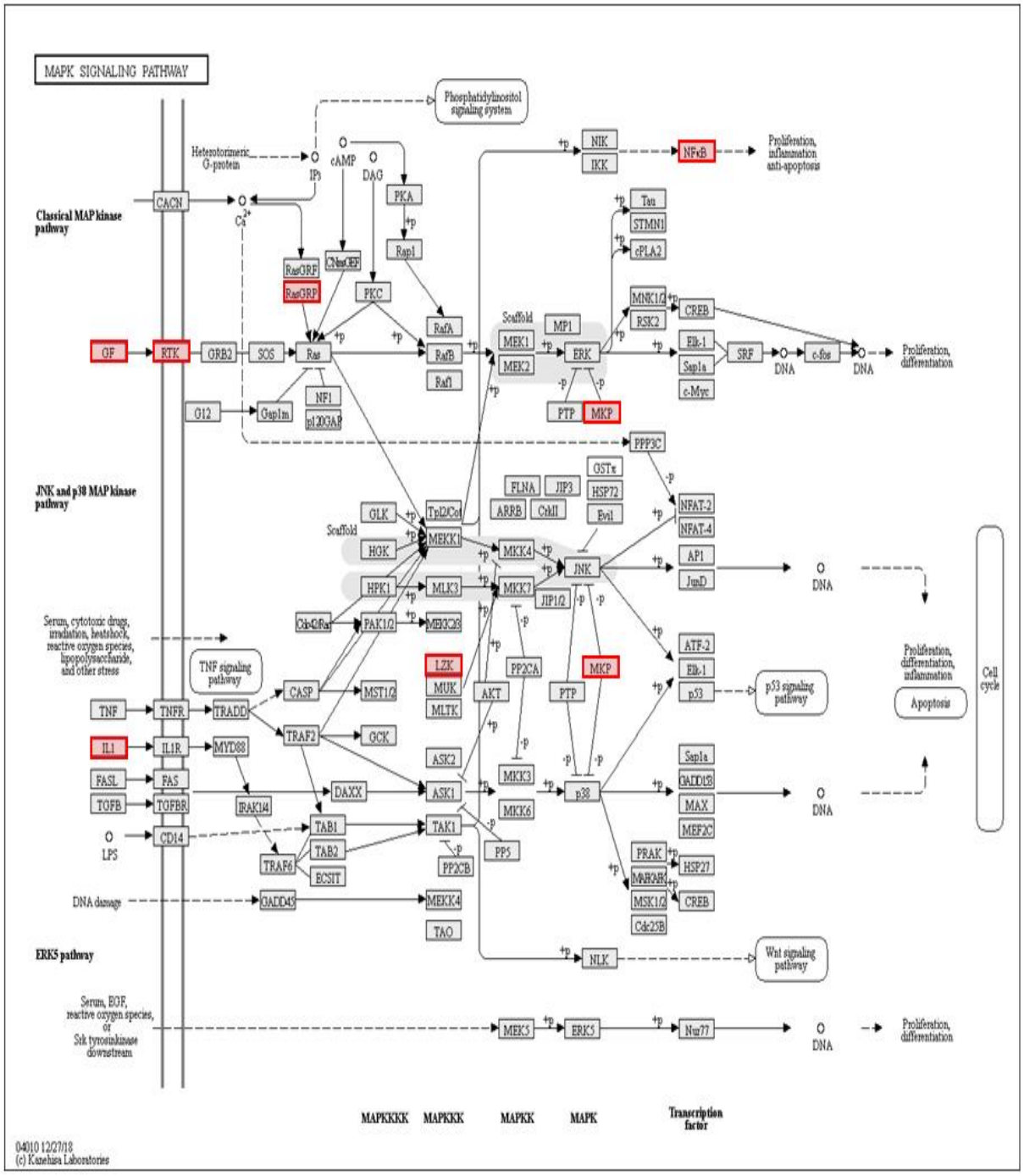

Figure 35 Upregulated genes in the mitogen activated protein kinase (MAPK) signalling pathway in *G. vaginalis* stimulated VK2 cells compared to unstimulated VK2 cells. KEGG MAPK signaling pathway adapted from DAVID Bioinformatics resources, upregulated in VK2 cells cultured with *G. vaginalis* compared to VK2 cell culture only, red boxes indicate mediators upregulated in *G. vaginalis* stimulated VK2 cells compared to VK2 cell culture only. VK2 cells were seeded into 24 well plates ($0.5x10^6$ cells/well) and grown to confluence. *G. vaginalis* ($4.18x10^7$CFU/well) was added to the VK2 cell cultures and incubated for 6 hrs at 37°C, 5% CO_2, in triplicate independent assays. VK2 cells only controls were included in triplicate independent assays. VK2 cells were then harvested and RNA was extracted. Gene expression analysis was then performed using microarray Affymetrix GeneChip whole transcript array platform. Affymetrix data were normalized using Robust Multichip Average (RMA) normalization. Differential gene expression analysis was performed using R Bioconductor limma package. Genes were considered differentially expressed if, adj. p≤0.05 and upregulated or downregulated if log fold change (FC) ≥ 1.5 or ≤ -1.5, respectively. Genes were annotated using the Clariom S Human annotation file. Upregulated gene Entrez identity numbers were used in DAVID Bioinformatics resources v6.8 to obtain biological pathways upregulated. **GF**: growth factor, **RTK**: receptor tyrosine kinase, **IL-1**: interleukin 1, **RasGRP**: RAS guanyl-releasing protein, **LZK**: leucine zipper-bearing kinase/mitogen activated protein kinase kinase kinase 13, **MKP**: mitogen activated protein kinase, **NFκB**: Nuclear factor kappa-light-chain-enhancer of activated B cells.

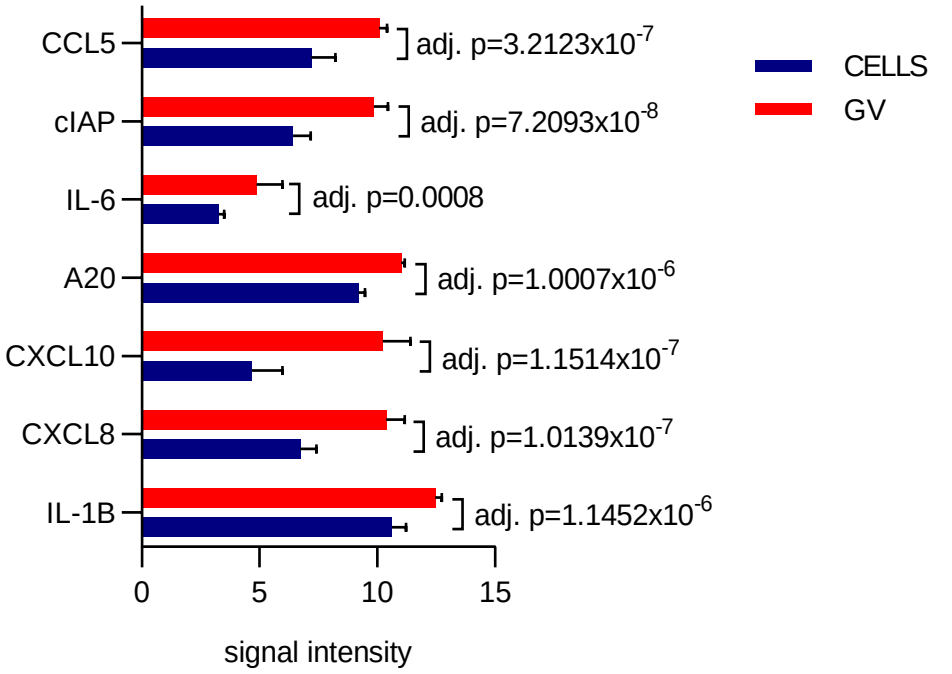

Figure 36 Key upregulated genes common to pro-inflammatory signaling pathways in *G. vaginalis* stimulated VK2 cells. Normalized signal intensity data for genes upregulated in *G. vaginalis* stimulated cells compared to unstimulated VK2 cells. Bars show mean signal intensities of genes and error bars indicate standard deviation of the mean. VK2 cells were seeded into 24 well plates ($0.5x10^6$ cells/well) and grown to confluence. *G. vaginalis* ($4.18x10^7$CFU/well) was added to the VK2 cell cultures and incubated for 6 hrs at 37°C, 5% CO_2, in triplicate independent assays. VK2 cells only were included as controls in triplicate independent assays. VK2 cells were then harvested and RNA was extracted. Gene expression analysis was then performed using microarray Affymetrix GeneChip whole transcript array platform. Affymetrix data were normalized using Robust Multichip Average (RMA) normalization. Differential gene expression analysis was performed using the R Bioconductor limma package. Genes were considered differentially expressed if adj. p≤0.05 and upregulated or downregulated if log fold change (FC) ≥ 1.5 or ≤ -1.5, respectively. Genes were annotated using the Clariom S Human annotation file. **CCL5:** chemokine c-c motif ligand 5, **cIAP:** cellular inhibitor of apoptosis protein, **IL-6**: interleukin 6, **A20**: tumor necrosis factor, alpha-induced protein 3, **A20**: tumor necrosis factor, alpha-induced protein 3, **CXCL10**: chemokine c-x-c motif ligand 10, **CXCL8**: chemokine c-x-c motif ligand 8, **IL-1B**: interleukin 1 beta.

Table 3 Downregulated genes in *G. vaginalis* stimulated VK2 cells compared to unstimulated VK2 cells.

Entrez gene ID	Gene symbol	DAVID bioinformatics gene name
261729	STEAP2	STEAP2 metalloreductase
4004	LMO1	LIM domain only 1
84455	EFCAB7	EF-hand calcium binding domain 7
9481	SLC25A27	solute carrier family 25 member 27
80312	TET1	tet methylcytosine dioxygenase 1
54677	CROT	carnitine O-octanoyltransferase
84125	LRRIQ1	leucine rich repeats and IQ motif containing 1
63920	ZBED8	zinc finger BED-type containing 8
57002	YAE1D1	Yae1 domain containing 1
90075	ZNF30	zinc finger protein 30
2825	GPR1	G protein-coupled receptor 1
158399	ZNF483	zinc finger protein 483
85016	C11orf70	chromosome 11 open reading frame 70
143686	SESN3	sestrin 3
5567	PRKACB	protein kinase cAMP-activated catalytic subunit beta
79634	SCRN3	secernin 3
6783	SULT1E1	sulfotransferase family 1E member 1
29904	EEF2K	eukaryotic elongation factor 2 kinase
1831	TSC22D3	TSC22 domain family member 3
120227	CYP2R1	cytochrome P450 family 2 subfamily R member 1
285440	CYP4V2	cytochrome P450 family 4 subfamily V member 2
55900	ZNF302	zinc finger protein 302
145957	NRG4	neuregulin 4
10891	PPARGC1A	PPARG coactivator 1 alpha
64172	OSGEPL1	O-sialoglycoprotein endopeptidase like 1
64288	ZSCAN31	zinc finger and SCAN domain containing 31
134728	IRAK1BP1	interleukin 1 receptor associated kinase 1 binding protein 1

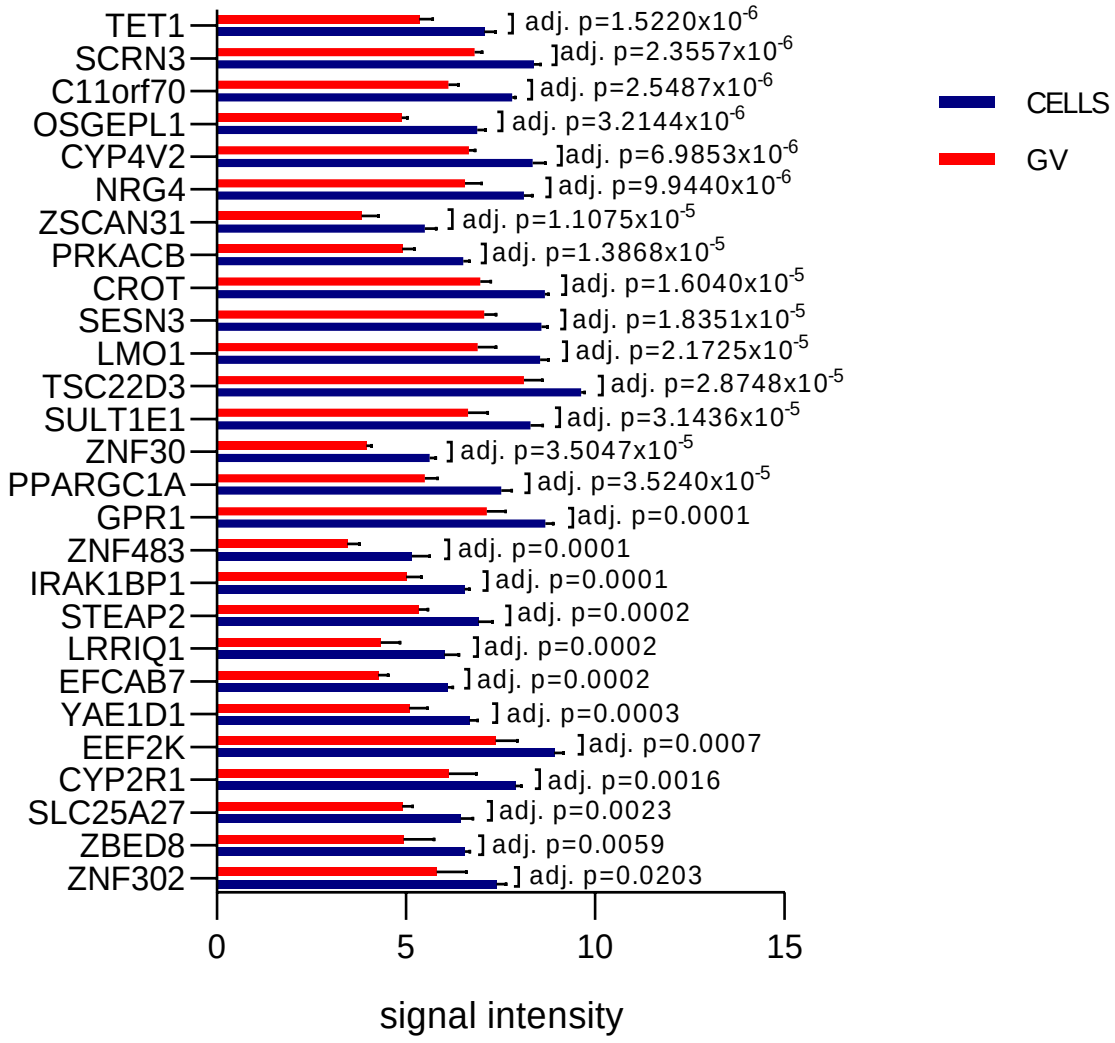

Figure 37 Downregulated genes in *G. vaginalis* stimulated VK2 cells compared to unstimulated VK2 cells. Normalized signal intensity data for genes downregulated in *G. vaginalis* stimulated cells compared to unstimulated VK2 cells. Bars show mean signal intensities of genes and error bars indicate standard deviation of the mean. VK2 cells were seeded into 24 well plates ($0.5x10^6$ cells/well) and grown to confluence. *G. vaginalis* ($4.18x10^7$CFU/well) was added to the VK2 cell cultures and incubated for 6 hrs at 37°C, 5% CO_2, in triplicate independent assays. VK2 cells only were included as controls in triplicate independent assays. VK2 cells were then harvested and RNA was extracted. Gene expression analysis was then performed using microarray Affymetrix GeneChip whole transcript array platform. Affymetrix data were normalized using Robust Multichip Average (RMA) normalization. Differential gene expression analysis was performed using the R Bioconductor limma package. Genes were considered differentially expressed if adj. p≤0.05 and upregulated or downregulated if log fold change (FC) ≥ 1.5 or ≤ -1.5, respectively.

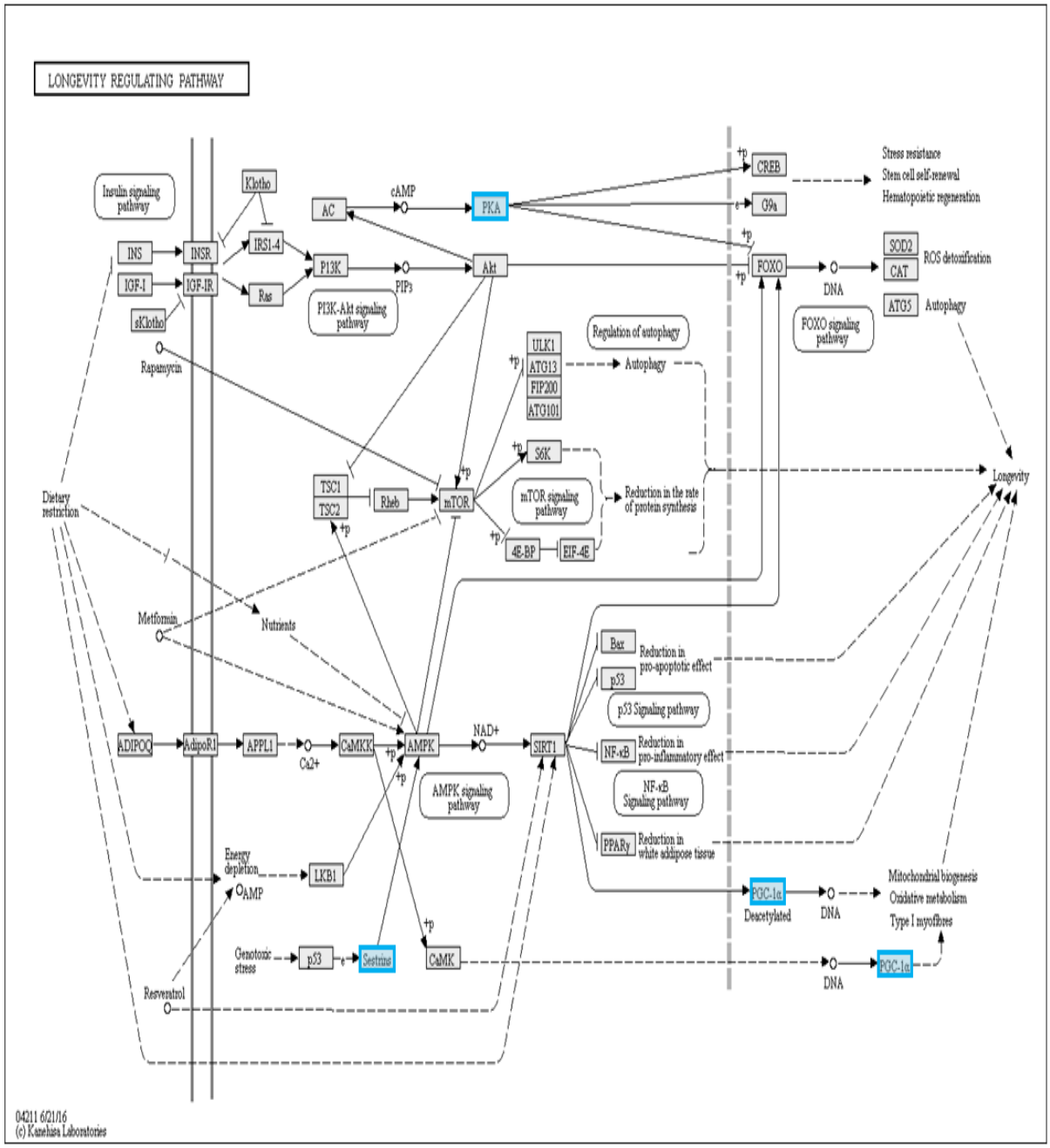

Figure 38 Genes downregulated in the longevity regulating signaling pathway in *G. vaginalis* stimulated VK2 cells compared to unstimulated VK2 cells. KEGG longevity signaling pathway adapted from WebGestalt, downregulated in VK2 cells cultured with *G. vaginalis* compared to VK2 cell culture only, blue boxes indicate mediators upregulated in *G. vaginalis* stimulated VK2 cells compared to VK2 cell culture only. VK2 cells were seeded into 24 well plates ($0.5x10^6$ cells/well) and grown to confluence. *G. vaginalis* ($4.18x10^7$CFU/well) was added to the VK2 cell cultures and incubated for 6 hrs at 37°C, 5% CO_2, in triplicate independent assays. VK2 cells only were included as controls in triplicate independent assays. VK2 cells were then harvested and RNA was extracted. Gene expression analysis was then performed using microarray Affymetrix GeneChip whole transcript array platform. Affymetrix data were normalized by Robust Multichip Average (RMA) normalization. Differential gene expression analysis was performed using R Bioconductor limma package. Genes were considered differentially expressed if, adj. p≤0.05 and upregulated or downregulated if log fold change (FC) ≥ 1.5 or ≤ -1.5, respectively. Upregulated gene Entrez identity numbers were used in WebGestalt to obtain biological pathways upregulated. **PKA**: protein kinase A, **PGC-1α**: peroxisome proliferator-activated receptor gamma coactivator 1-alpha.

3.11 Effect of *Lactobacillus* species on gene transcription and signalling pathways of VK2 cells stimulated by *G. vaginalis*

Affymetrix microarray was used to assess gene expression by VK2 cells cultured with *Lactobacillus* ($4.18x10^6$CFU/well) and *G. vaginalis* ($4.18x10^7$CFU/well) in combination in 1ml of media, in triplicate independent assays. The R studio Bioconductor limma package was used to assess differential gene expression in VK2 cells pre-incubated with *Lactobacillus* isolates and then *G. vaginalis* compared to VK2 cells stimulated only with *G. vaginalis*.

Heatmaps show the mean normalized signal intensities for genes upregulated and downregulated in VK2 cells cultured with lactobacilli and *G. vaginalis* in combination **(Figure 39).** For the *Lactobacillus* isolates that did not suppress inflammatory cytokine responses to *G. vaginalis*, the majority of the differentially expressed genes were upregulated compared to *G. vaginalis* only cultures. A total of 12/21 (57%), 7/12 (58%), 12/20 (60%), 17/26 (65%), and 92/146 (65%) were upregulated for LJ3, LV3, LC3, LC1 and LJ2, respectively **(Figures 39A-D and 40)**. In contrast, the majority of differentially expressed genes were downregulated for isolates that did suppress inflammatory cytokine responses to *G. vaginalis*, with 13/13 (100%), 35/64 (56%) and 10/13 (77%) genes downregulated for LM2, LM4 and LV4, respectively **(Figure 39E-F and 41)**.

Several unique genes were detected as upregulated or downregulated in VK2 cells co-cultured with certain *Lactobacillus* species (LM2, LM4, LJ3, LC1 and LJ2) and *G. vaginalis* in combination, compared to co-culture with *G. vaginalis* only. In contrast, no exclusively differentially expressed genes were detected in VK2 cells co-cultured with LV3, LC3 and LV4. **Figures 42 and 43** show genes that were differentially expressed only in cells pre-incubated with one specific *Lactobacillus* species, but not in cells pre-incubated with any of the other *Lactobacillus* species compared to co-culture with *G. vaginalis* only. A total of 2/2 (100%), 9/24 (37.5%), 2/11 (18%), 0/4 (0%) and 36/110 (32%) of the genes that were exclusively differentially expressed, were downregulated for LM2, LM4, LC1, LJ3 and LJ2 respectively **(Figures 42 and 43)**.

A separate limma analysis was performed which compared gene expression in VK2 cells co-cultured with *G. vaginalis* compared to co-culture with lactobacilli (normalized microarray data grouped for all 8 *Lactobacillus* isolates) and *G. vaginalis* in combination. Several genes, including DDX58, CXCL11, IFIT3, IFIT2, IL7R, APOL2, TNFSF18, were downregulated in VK2 cells co-cultured with lactobacilli and *G. vaginalis* in combination compared to co-culture with *G. vaginalis* only (**Figure 44**). In contrast, CYP1A1 was upregulated in VK2 cells co-cultured

with lactobacilli and *G. vaginalis* in combination compared to co-culture with *G. vaginalis* only (**Figure 44**).

With the exception of TNFSF18, the expression of these genes were largely unchanged between *Lactobacillus* isolates that reduced (LM2, LM4 and LV4) or did not reduce (LJ3, LV3, LC3, LC1 and LJ2) inflammatory cytokine production in response to *G. vaginalis* **(Figure 45)**. TNFS18 tended to be reduced in VK2 cells co-cultured with non-cytokine-suppressive lactobacilli compared to cytokine-suppressive lactobacilli, in combination with *G. vaginalis*, however not significantly (p=0.0643, **Figure 45**).

Of the downregulated genes in VK2 cells co-cultured with lactobacilli and *G. vaginalis* in combination compared to co-culture with *G. vaginalis* only, CXCL11, IL7R and TNFSF18 (also known as GITRL as shown in the cytokine-cytokine interaction pathway) mapped to the cytokine-cytokine receptor signaling pathway **(Figure 46)**.

An additional limma analysis was performed to detect differentially expressed genes in VK2 cells co-cultured with non-cytokine-suppressive lactobacilli and cytokine-suppressive lactobacilli (average normalized microarray data grouped for non-cytokine-suppressive and cytokine-suppressive isolates grouped separately) prior to incubation with *G. vaginalis*, compared to co-culture with *G. vaginalis* only. Downregulated genes in VK2 cells co-cultured with non-cytokine-suppressive lactobacilli or cytokine-suppressive lactobacilli and *G. vaginalis* in combination were similar **(Figure 47A and B)**, however, downregulation of SAMD9L, DDX58 and IFIT1 were detected only for cytokine-suppressive lactobacilli **(Figure 47B)**. While no upregulated genes were detected in VK2 cells co-cultured with cytokine-suppressive lactobacilli and *G. vaginalis* in combination, upregulation of CRCT1, CYP1A1, CYP1B1, TM4SF19, TMEM2 and RNASE7 was detected for non-cytokine-suppressive lactobacilli **(Figure 47C)**.

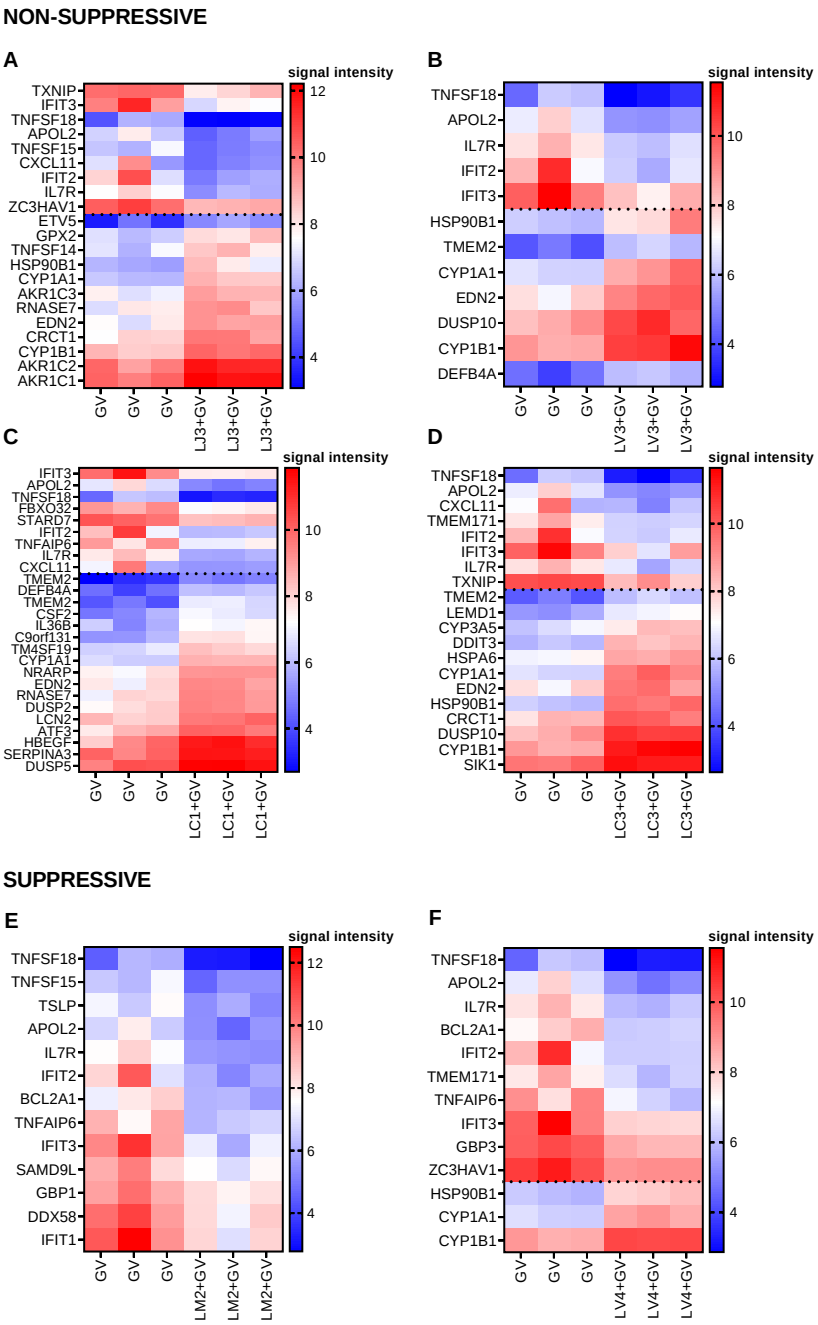

Figure 39 Heatmaps of downregulated and upregulated genes in VK2 cells co-cultured with *Lactobacillus* isolates and *G. vaginalis* in combination compared to co-culture with *G. vaginalis* only. Heatmaps show normalized signal intensities of biological replicates (n=3). Downregulated and upregulated genes are displayed above and beneath the black dotted line, respectively. VK2 cells were seeded into 24 well plates ($0.5x10^6$ cells/well) and grown to confluence. Monolayers were stimulated with *Lactobacillus* isolates ($4.18x10^6$CFU/well) and incubated for 6 hrs at 37°C, 5% CO_2, in triplicate independent assays. *G. vaginalis* ($4.18x10^7$CFU/well) was then added to the *Lactobacillus*-VK2 cell cultures and incubated for an additional 6 hrs at 37°C, 5% CO_2, in triplicate independent assays. VK2 cells were then harvested and RNA was extracted. Gene expression analysis was then performed using microarray Affymetrix GeneChip whole transcript array platform. Affymetrix data were normalized using Robust Multichip Average (RMA) normalization. Differential gene expression analysis was performed using R Bioconductor limma package. Genes were considered differentially expressed if adj. p≤0.05 and upregulated or downregulated if log fold change (FC) ≥ 1.5 or ≤ -1.5, respectively. Genes were annotated using the Clariom S Human annotation file. Heatmaps were generated using Graphpad Prism v8.0. Blue, through white to red indicates low to high gene expression, respectively. Gene symbols are displayed on the right-hand side. **GV:** *G. vaginalis*, **LJ3:** *L. jensenii* 3, **LV3:** *L. vaginalis* 3, **LC3:** *L. crispatus* 3, **LM2:** *L. mucosae* 2, **LC1:** *L. crispatus* 1, **LV4:** *L. vaginalis* 4.

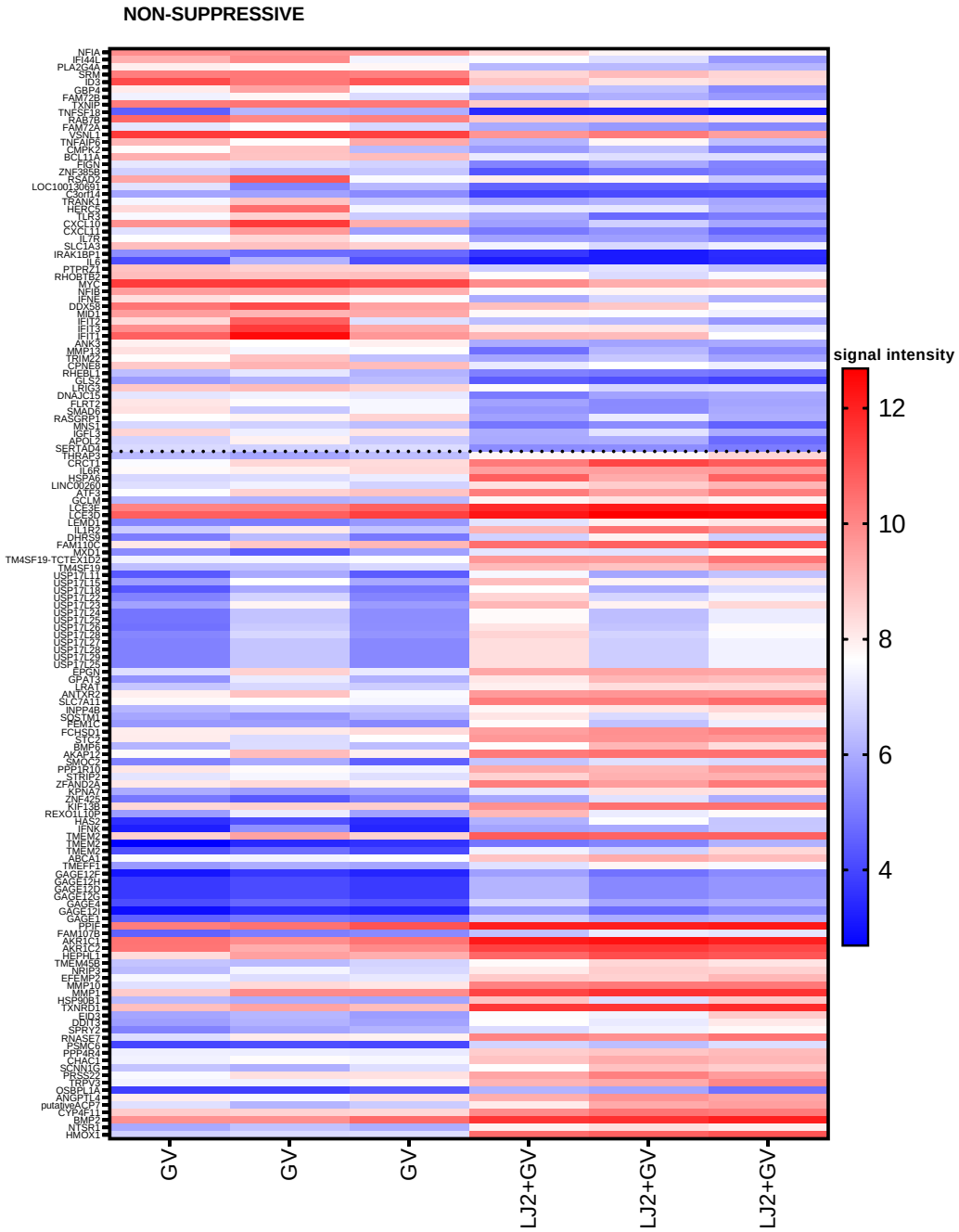

Figure 40 Heatmap of downregulated and upregulated genes in VK2 cells co-cultured with *L. jensenii* 2 and *G. vaginalis* in combination compared to co-culture with *G. vaginalis* only. Heatmaps show normalized signal intensities of biological replicates (n=3). Downregulated and upregulated genes are displayed above and beneath the black dotted line, respectively. VK2 cells were seeded into 24 well plates ($0.5x10^6$ cells/well) and grown to confluence. Monolayers were stimulated with *L. jensenii* 2 ($4.18x10^6$CFU/well) and incubated for 6 hrs at 37°C, 5% CO_2, in triplicate independent assays. *G. vaginalis* ($4.18x10^7$CFU/well) was then added to the *Lactobacillus*-VK2 cell cultures and incubated for an additional 6 hrs at 37°C, 5% CO_2, in triplicate independent assays. VK2 cells were then harvested and RNA was extracted. Gene expression analysis was then performed using microarray Affymetrix GeneChip whole transcript array platform. Affymetrix data were normalized using Robust Multichip Average (RMA) normalization. Differential gene expression analysis was performed using R Bioconductor limma package. Genes were considered differentially expressed if adj. p≤0.05 and upregulated or downregulated if log fold change (FC) ≥ 1.5 or ≤ -1.5, respectively. Genes were annotated using the Clariom S Human annotation file. Heatmap was generated using Graphpad Prism v8.0. Blue, through white to red indicates low to high gene expression, respectively. Gene symbols are displayed on the right-hand side. **GV:** *G. vaginalis*, **LJ2:** *L. jensenii* 2.

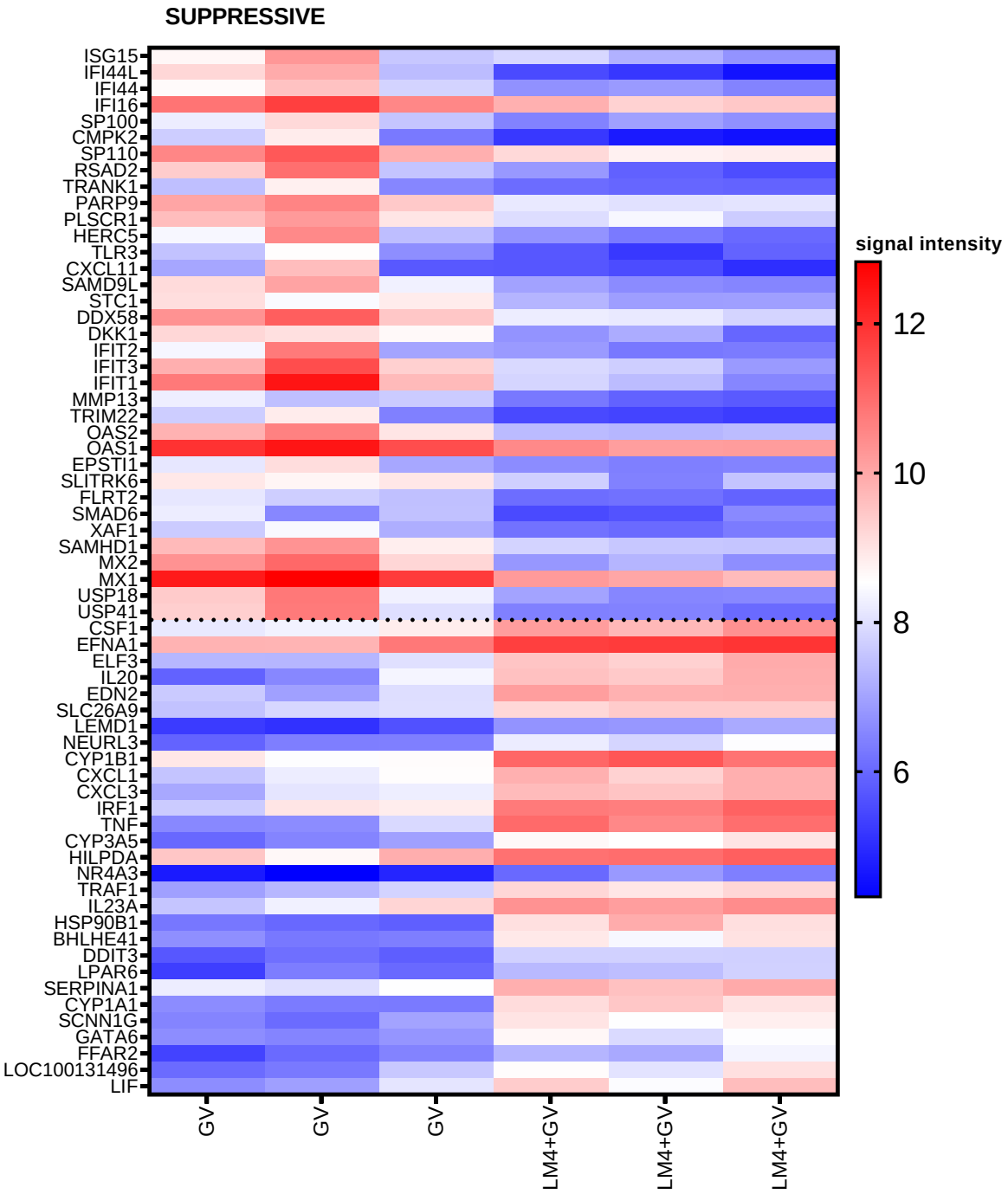

Figure 41 Heatmap of downregulated and upregulated genes in VK2 cells co-cultured with *L. mucosae* 4 and *G. vaginalis* in combination compared to co-culture with *G. vaginalis* only. Heatmaps show mean normalized signal intensities of biological replicates (n=3). Downregulated and upregulated genes are displayed above and beneath the black dotted line, respectively. VK2 cells were seeded into 24 well plates ($0.5x10^6$ cells/well) and grown to confluence. Monolayers were stimulated with *L. mucosae* 4 ($4.18x10^6$CFU/well) and incubated for 6 hrs at 37°C, 5% CO_2, in triplicate independent assays. *G. vaginalis* ($4.18x10^7$CFU/well) was then added to the *Lactobacillus*-VK2 cell cultures and incubated for an additional 6 hrs at 37°C, 5% CO_2, in triplicate independent assays. VK2 cells were then harvested and RNA was extracted. Gene expression analysis was then performed using microarray Affymetrix GeneChip whole transcript array platform. Affymetrix data were normalized using Robust Multichip Average (RMA) normalization. Differential gene expression analysis was performed using R Bioconductor limma package. Genes were considered differentially expressed if adj. p≤0.05 and upregulated or downregulated if log fold change (FC) ≥ 1.5 or ≤ -1.5, respectively. Genes were annotated using the Clariom S Human annotation file. Heatmap was generated using Graphpad Prism v8.0. Blue, through white to red indicates low to high gene expression, respectively. Gene symbols are displayed on the right-hand side. **GV:** *G. vaginalis*, **LM4:** *L. mucosae* 4.

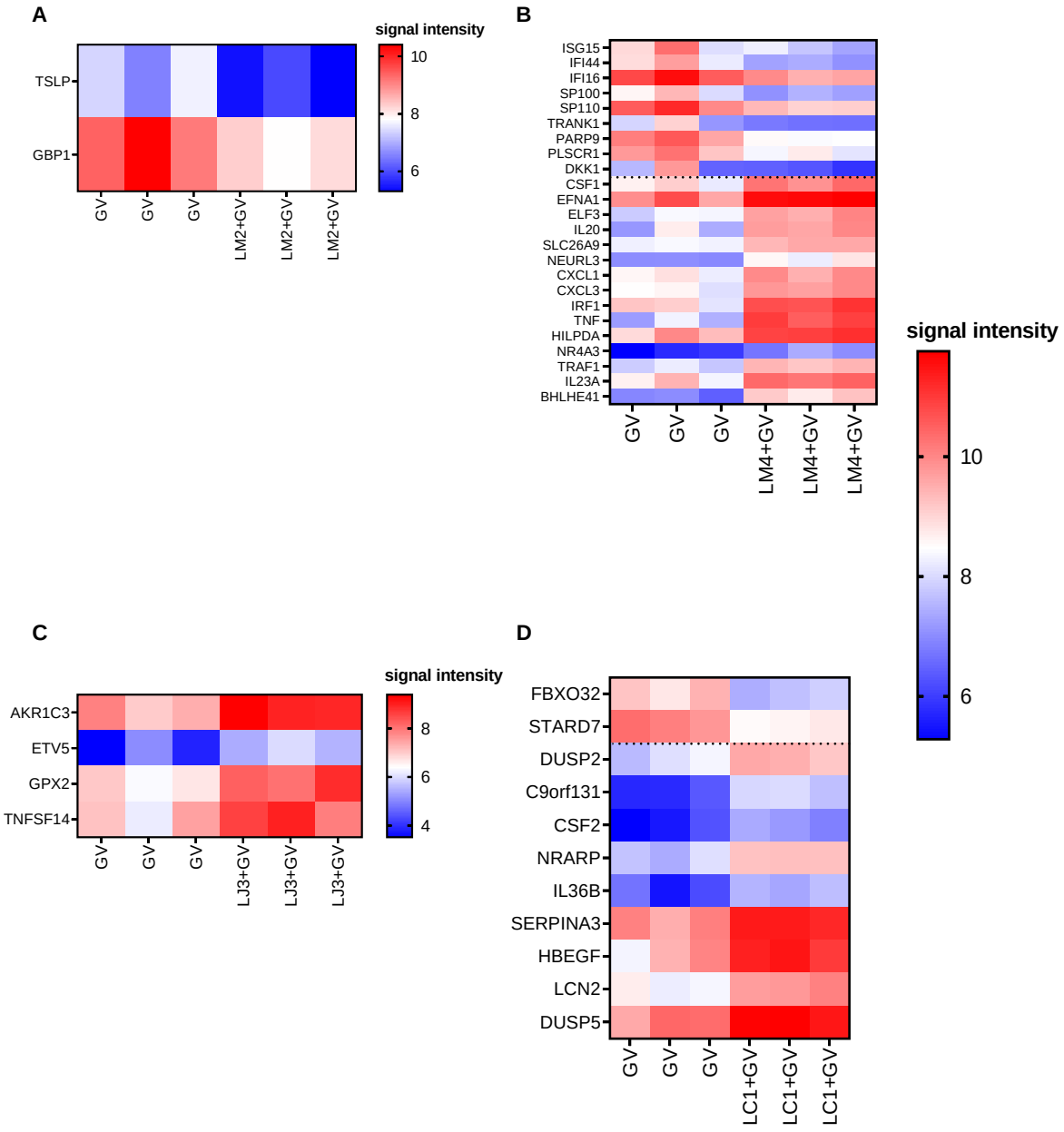

Figure 42 Genes exclusively downregulated and upregulated in VK2 cells co-cultured with certain *Lactobacillus* species and *G. vaginalis* in combination compared to *G. vaginalis*-only cultures. Heatmaps show normalized signal intensities for genes **(A)** downregulated and **(B)** upregulated in VK2 cells co-cultured with *L. mucosae* 2 and *L. mucosae* 4, **C-D)** downregulated and upregulated in VK2 cells co-cultured with *L. jensenii* 3 and *L. crispatus* 1, in combination with *G. vaginalis*. Heatmaps show the normalized signal intensities of biological replicates. Downregulated and upregulated genes are displayed above and beneath the black dotted lines in B) and D). VK2 cells were seeded into 24 well plates ($0.5x10^6$ cells/well) and grown to confluence. Monolayers were stimulated with *Lactobacillus* isolates ($4.18x10^6$CFU/well) and incubated for 6 hrs at 37°C, 5% CO_2, in triplicate independent assays. *G. vaginalis* ($4.18x10^7$CFU/well) was then added to the *Lactobacillus*-VK2 cell cultures and incubated for an additional 6 hrs at 37°C, 5% CO_2, in triplicate independent assays. VK2 cells were then harvested and RNA was extracted. Gene expression analysis was then performed using microarray Affymetrix GeneChip whole transcript array platform. Affymetrix data were normalized by Robust Multichip Average (RMA) normalization. Differential gene expression analysis was performed using R Bioconductor limma package. Genes were considered differentially expressed if adj. p≤0.05 and upregulated or downregulated if log fold change (FC) ≥ 1.5 or ≤ -1.5, respectively. Genes were annotated using the Clariom S HumanHT annotation file. Heatmaps were generated using Graphpad Prism v8.0. Blue, through white to red indicates low to high gene expression, respectively. Gene symbols are displayed on the right-hand side. **GV**: *G. vaginalis*, **LM4:** *L. mucosae* 4; **LM2:** *L. mucosae* 2, **LJ3**: *L. jensenii* 3, **LC1**: *L. crispatus* 1.

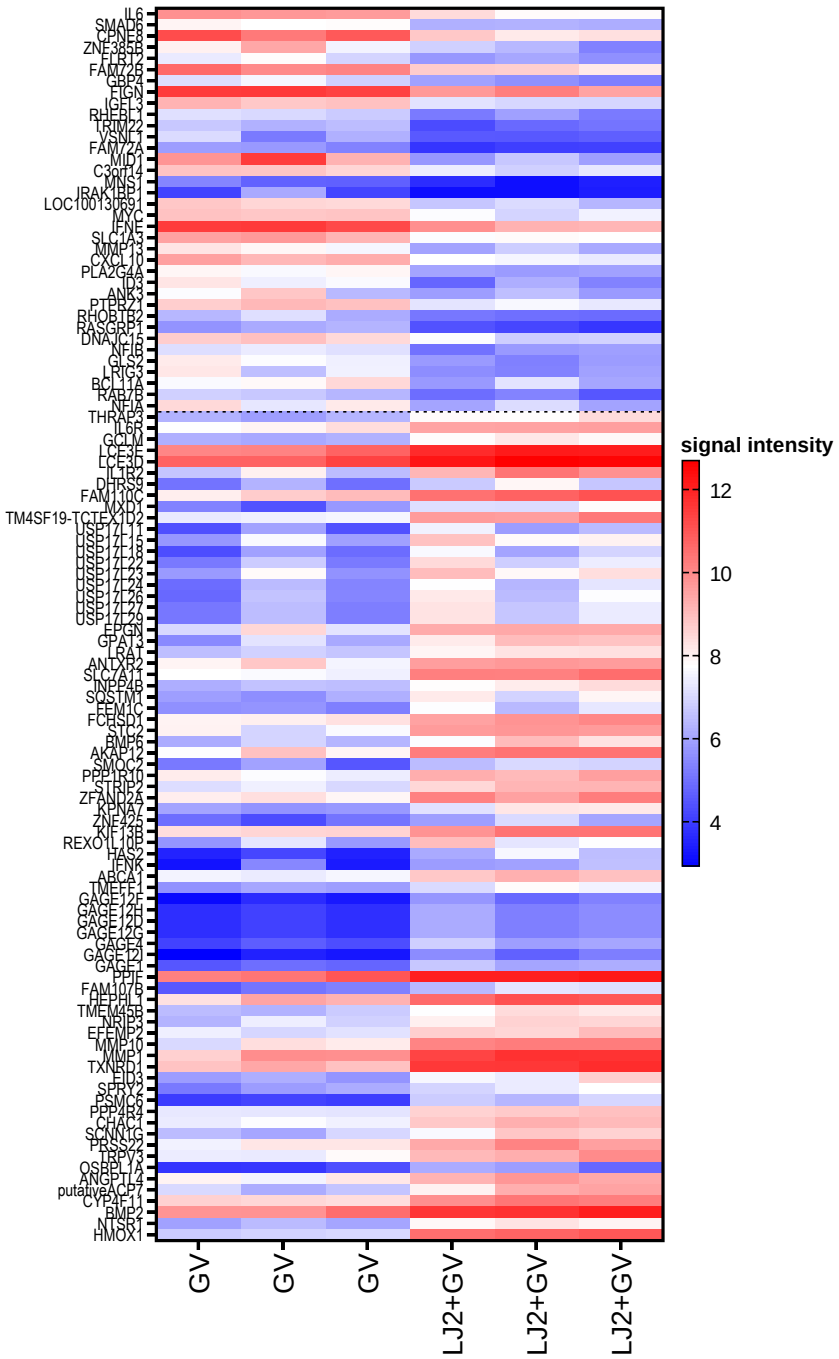

Figure 43 Genes exclusively downregulated and upregulated in VK2 cells co-cultured with *L. jensenii* 2 and *G. vaginalis* in combination compared to *G. vaginalis*-only cultures. Heatmap shows normalized signal intensities for genes downregulated and upregulated in VK2 cells co-cultured with *L. jensenii* 2 and in combination with *G. vaginalis*. Heatmap shows the normalized signal intensities of biological replicates (n=3). Downregulated and upregulated genes are displayed above and beneath the black dotted line. VK2 cells were seeded into 24 well plates ($0.5x10^6$ cells/well) and grown to confluence. Monolayers were stimulated with *L. jensenii* 2 ($4.18x10^6$CFU/well) and incubated for 6 hrs at 37°C, 5% CO_2, in triplicate independent assays. *G. vaginalis* ($4.18x10^7$CFU/well) was then added to the *Lactobacillus*-VK2 cell cultures and incubated for an additional 6 hrs at 37°C, 5% CO_2, in triplicate independent assays. VK2 cells were then harvested and RNA was extracted. Gene expression analysis was then performed using microarray Affymetrix GeneChip whole transcript array platform. Affymetrix data were normalized by Robust Multichip Average (RMA) normalization. Differential gene expression analysis was performed using R Bioconductor limma package. Genes were considered differentially expressed if adj. p≤0.05 and upregulated or downregulated if log fold change (FC) ≥ 1.5 or ≤ -1.5, respectively. Genes were annotated using the Clariom S HumanHT annotation file. Heatmap was generated using Graphpad Prism v8.0. Blue, through white to red indicates low to high gene expression, respectively. Gene symbols are displayed on the right-hand side. **GV**: *G. vaginalis*; **LJ2**: *L. jensenii* 2.

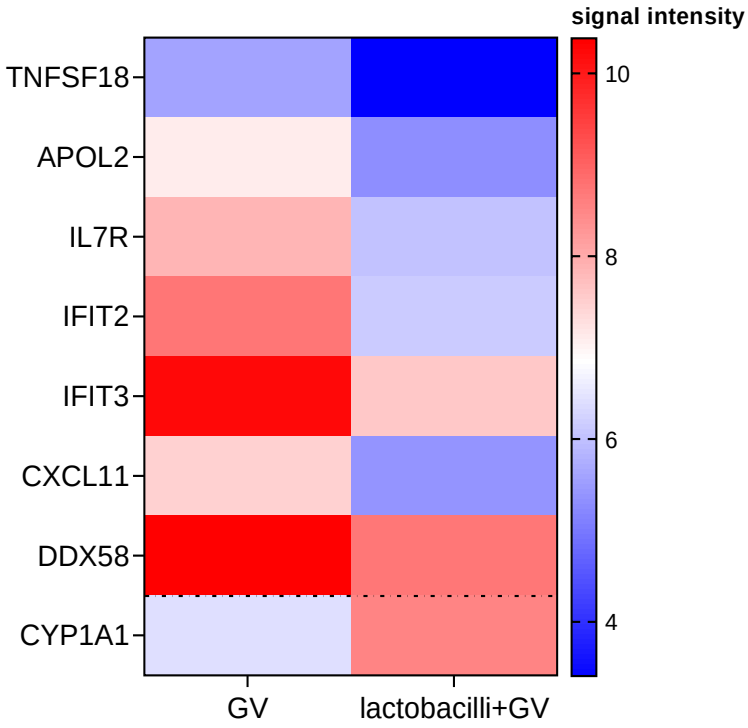

Figure 44 Genes commonly upregulated and downregulated in VK2 cells co-cultured with *Lactobacillus* isolates and *G. vaginalis* in combination (n=8) compared to *G. vaginalis* only cultures (n=3). Heatmap shows genes downregulated and upregulated in VK2 cells co-cultured with lactobacilli and *G. vaginalis* in combination compared to co-culture with *G. vaginalis* only. Downregulated and upregulated genes are displayed above and beneath the black dotted line. VK2 cells were seeded into 24 well plates ($0.5x10^6$ cells/well) and grown to confluence. Monolayers were stimulated with *Lactobacillus* isolates ($4.18x10^6$CFU/well) and incubated for 6 hrs at 37°C, 5% CO_2, in triplicate independent assays. *G. vaginalis* ($4.18x10^7$CFU/well) was then added to the *Lactobacillus*-VK2 cell cultures and incubated for an additional 6 hrs at 37°C, 5% CO_2, in triplicate independent assays. VK2 cells were then harvested and RNA was extracted. Gene expression analysis was then performed using microarray Affymetrix GeneChip whole transcript array platform. Affymetrix data were normalized using Robust Multichip Average (RMA) normalization. Differential gene expression analysis was performed using R Bioconductor limma package. Genes were considered differentially expressed if adj. p≤0.05 and upregulated or downregulated if log fold change (FC) ≥ 1.5 or ≤ -1.5, respectively. Genes were annotated using the Clariom S Human annotation file. Heatmap was generated using Graphpad Prism v8.0. Blue, through white to red indicates low to high gene expression, respectively. Gene symbols are displayed on the right-hand side. **GV**: *G. vaginalis*.

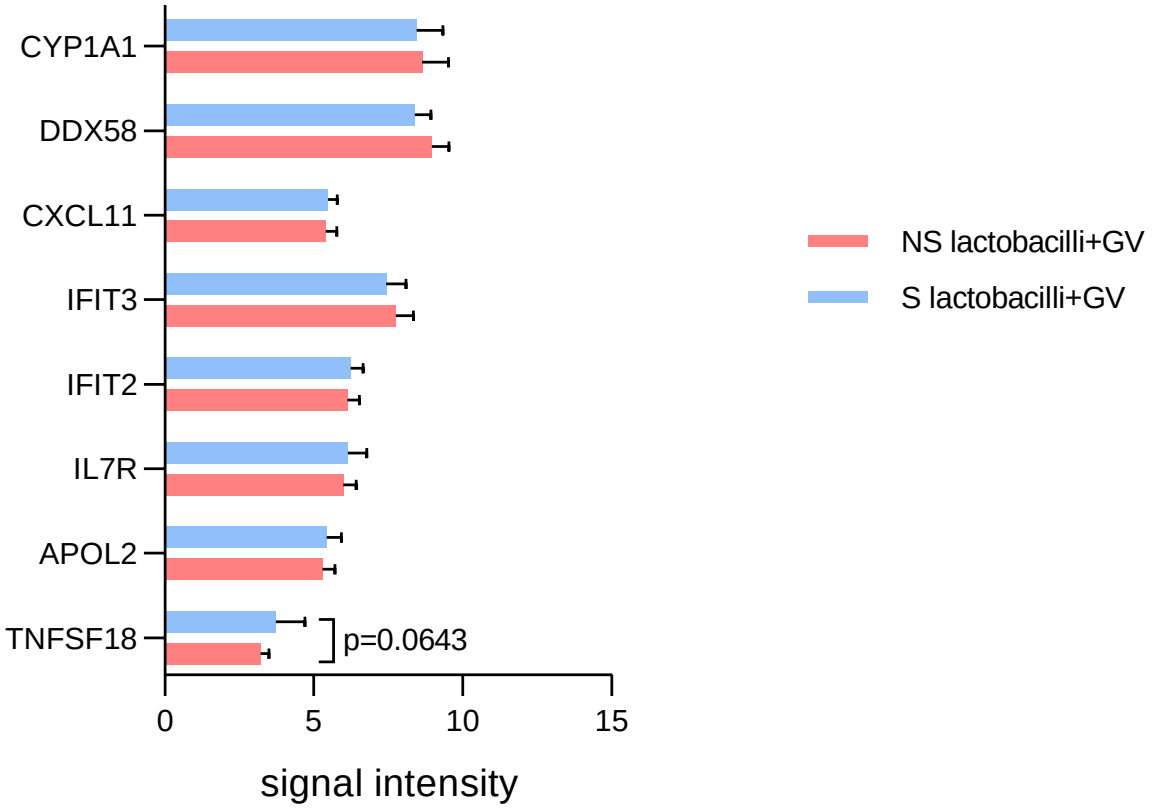

Figure 45 Genes commonly differentially expressed in VK2 cells co-cultured with *Lactobacillus* isolates and *G. vaginalis* in combination, stratified according to whether the lactobacilli suppressed (n=3) or did not suppress (n=5) inflammatory cytokine production in response to *G. vaginalis*. Bar graph shows gene upregulated and downregulated in non-suppressive and suppressive lactobacilli. Error bars indicate the standard deviation of the mean. VK2 cells were seeded into 24 well plates ($0.5x10^6$ cells/well) and grown to confluence. Monolayers were stimulated with *Lactobacillus* isolates ($4.18x10^6$CFU/well) and incubated for 6 hrs at 37°C, 5% CO_2, in triplicate independent assays. *G. vaginalis* ($4.18x10^7$CFU/well) was then added to the *Lactobacillus*-VK2 cell cultures and incubated for an additional 6 hrs at 37°C, 5% CO_2, in triplicate independent assays. VK2 cells were then harvested and RNA was extracted. Gene expression analysis was then performed using microarray Affymetrix GeneChip whole transcript array platform. Affymetrix data RMA normalized. Differential gene expression analysis was performed using R Bioconductor limma package. Genes were considered differentially expressed if $p \leq 0.05$ and upregulated or downregulated if log fold change (FC) ≥ 1.5 or ≤ -1.5, respectively. Genes were annotated using the Clariom S Human annotation file. Student's t test was used to statistically test the differences of gene expression between VK2 cells cultured with non-suppressive compared to *Lactobacillus* species and *G. vaginalis* in combination, $p \leq 0.05$ was considered significant. **CYP1A1**: cytochrome P450, family 1, subfamily A, polypeptide 1, **DDX58**: DExD/H-Box Helicase 58, **CXCL11**: chemokine c-x-c motif ligand 11, **IFIT**: interferon-induced protein with tetratricopeptide repeats, **IL7R**: interleukin 7 receptor, **APOL2**: apolipoprotein L2, **TNFSF18**: tumor necrosis factor ligand superfamily member 18.

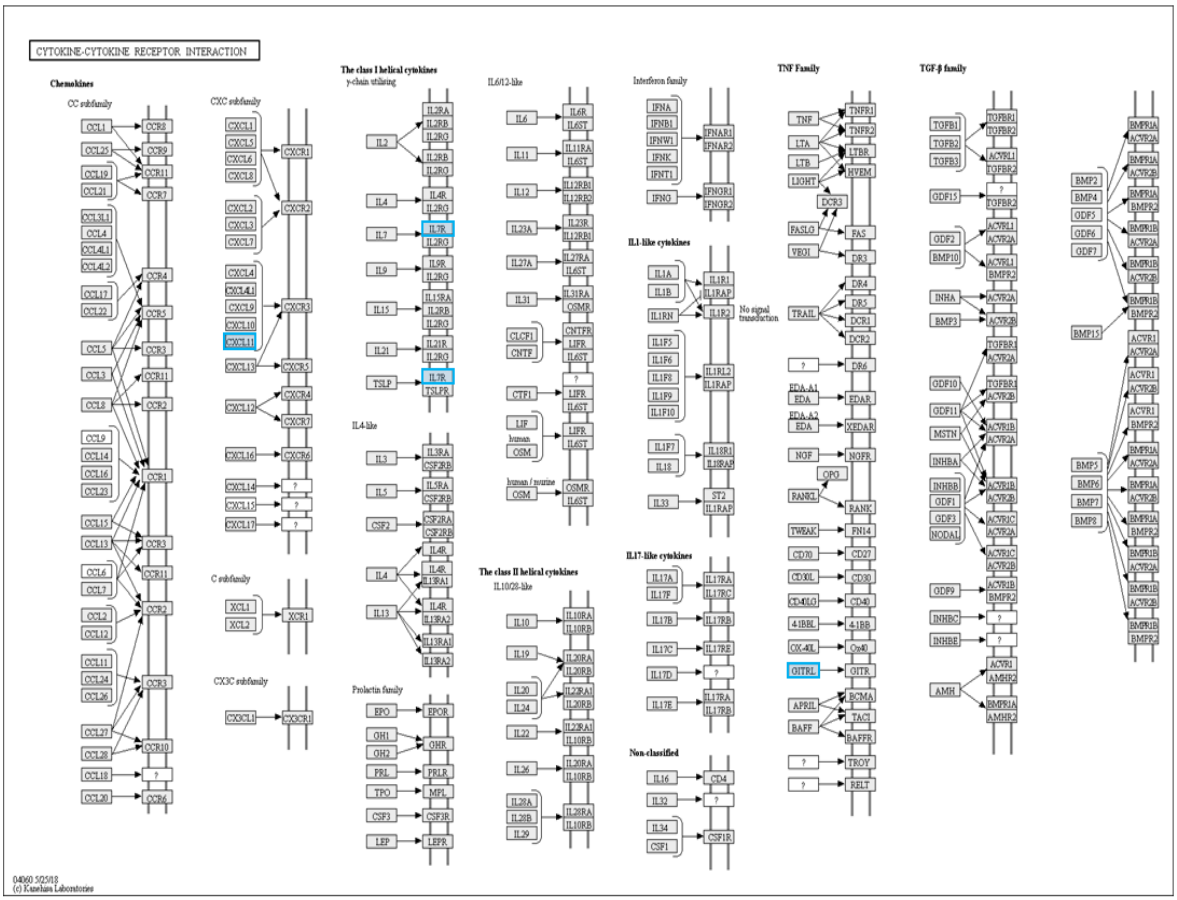

Figure 46 Downregulated genes in the cytokine-cytokine signalling pathway in VK2 cells co-cultured with *Lactobacillus* species and *G. vaginalis* in combination compared to co-culture with *G. vaginalis* only. KEGG cytokine-cytokine receptor interaction signalling pathway adapted from DAVID Bioinformatics is shown. Blue boxes indicate mediators downregulated in VK2 cells co-cultured with *Lactobacillus* isolates and *G. vaginalis* in combination, compared to *G. vaginalis* stimulated VK2 cells. VK2 cells were seeded into 24 well plates ($1x10^5$ cells/well) and grown to confluence. Monolayers were stimulated with *Lactobacillus* isolates ($4.18x10^6$CFU/well) and incubated for 6 hrs at 37°C, 5% CO_2, in triplicate independent assays. *G. vaginalis* ($4.18x10^7$CFU/well) was then added to the *Lactobacillus*-VK2 cell cultures and incubated for an additional 6 hrs at 37°C, 5% CO_2, in triplicate independent assays. VK2 cells were then harvested and RNA was extracted. Gene expression analysis was performed using the microarray Affymetrix GeneChIP whole transcript array platform. Affymetrix data were normalized using Robust Multichip (RMA) normalization. Differential gene expression analysis was performed using R Bioconductor limma package. Genes were considered differentially expressed if adj. p≤0.05 and upregulated or downregulated if log fold change (FC) ≥ 1.5 or ≤ -1.5, respectively. Genes were annotated using the Clariom S Human annotation file. Upregulated gene Entrez identity numbers were inputted to DAVID NIH to obtain biological pathways downregulated. **CXCL11**: chemokine c-x-c motif ligand 11, **IL7R**: interleukin 7 receptor, **GITRL**: glucocorticoid-induced TNF receptor ligand.

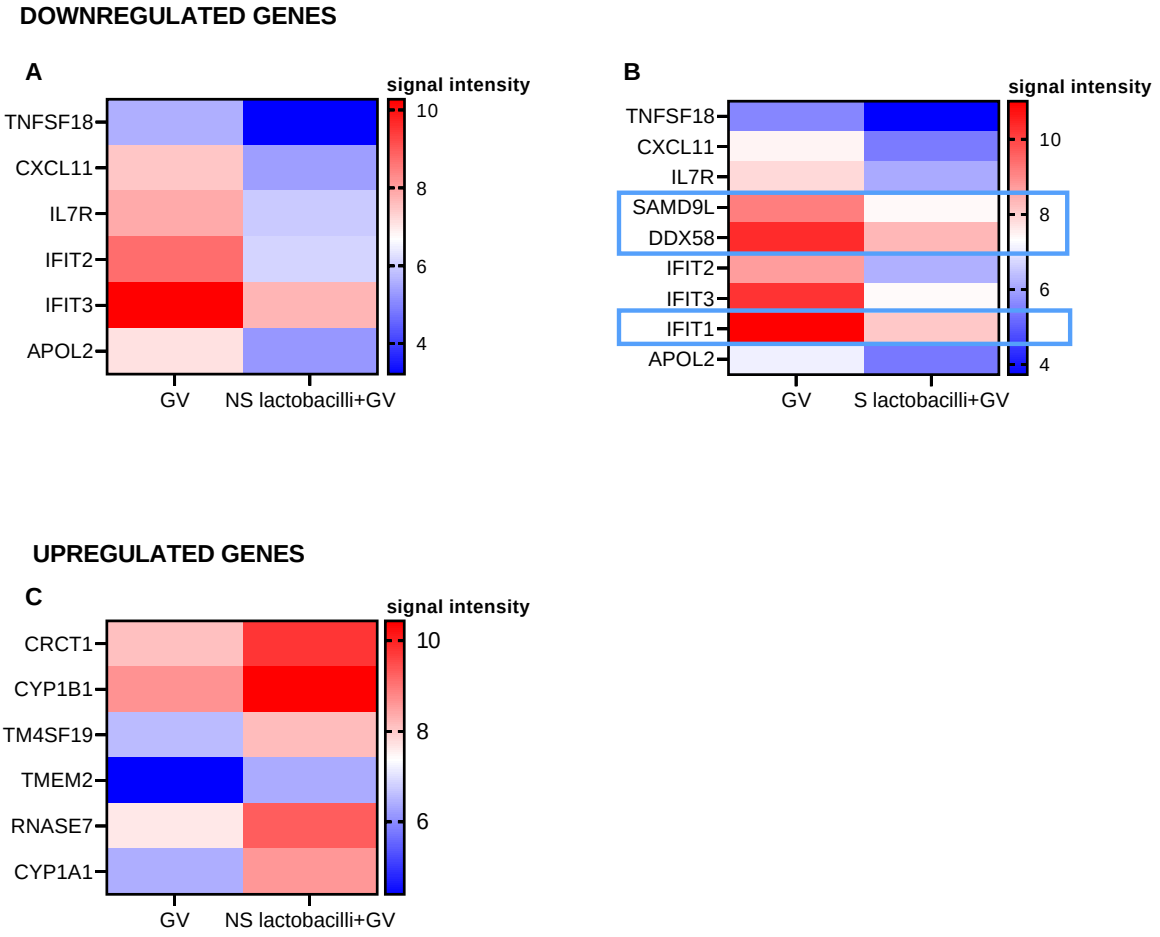

Figure 47 Genes downregulated and upregulated in VK2 cells co-cultured with suppressive and non-suppressive *Lactobacillus* isolates and *G. vaginalis* in combination compared to *G. vaginalis*-only cultures. Heatmaps show normalized signal intensities for genes **(A-B)** downregulated in VK2 cells co-cultured with cytokine non-suppressive (NS) and suppressive (S) lactobacilli and *G. vaginalis* in combination compared to co-culture with *G. vaginalis* only, **C)** upregulated in Vk2 cells co-cultured with cytokine non-suppressive (NS) lactobacilli and *G. vaginalis* in combination compared to co-culture with *G. vaginalis* only. Heatmaps show the mean normalized signal intensities, blue boxes indicate downregulated genes specific to VK2 cells co-cultured with suppressive lactobacilli and *G. vaginalis* in combination. VK2 cells were seeded into 24 well plates ($0.5x10^6$ cells/well) and grown to confluence. Monolayers were stimulated with *Lactobacillus* isolates ($4.18x10^6$CFU/well) and incubated for 6 hrs at 37°C, 5% CO_2, in triplicate independent assays. *G. vaginalis* ($4.18x10^7$CFU/well) was then added to the *Lactobacillus*-VK2 cell cultures and incubated for an additional 6 hrs at 37°C, 5% CO_2, in triplicate independent assays. VK2 cells were then harvested and RNA was extracted. Gene expression analysis was then performed using microarray Affymetrix GeneChip whole transcript array platform. Affymetrix data were normalized using Robust Multichip Average (RMA) normalization. Differential gene expression analysis was performed using R Bioconductor limma package. Genes were considered differentially expressed if adj. p≤0.05 and upregulated or downregulated if log fold change (FC) ≥ 1.5 or ≤ -1.5, respectively. Genes were annotated using the Clariom S HumanHT annotation file. Heatmaps were generated using Graphpad Prism v8.0. Blue, through white to red indicates low to high gene expression, respectively. Gene symbols are displayed on the right-hand side.

Chapter 4: Discussion

The maintenance of a microbial and immune homeostatic environment in the FGT is of utmost importance for favourable reproductive outcomes and reduced HIV and STI susceptibility. Defence against pathogenic microbes is crucial, while tolerance to commensal bacteria and allogenic sperm is maintained (47). Furthermore, the vaginal microbiome state plays an imperative role in the immunological environment of the FGT (81). A non-optimal vaginal microbiome and the inflammation caused by BV-associated bacteria is associated with an increased HIV acquisition (82) and HIV viral replication *in vitro*, which suggests possible increased HIV transmission *in vivo* (124) . Studies have shown that the optimal vaginal microbiome state, dominated by *Lactobacillus* species is associated with reduced inflammation and subsequent HIV susceptibility risk (21,29,81,85,125), however the mechanisms underlying the immunomodulatory capacity of these commensal bacteria is unknown. In this study, the gene expression patterns of cervicovaginal mononuclear cells (CMCs) and matched peripheral blood mononuclear cells (PBMCs) obtained from HIV chronically infected South African women, were evaluated to compare the expression of genes involved in microbial pattern recognition and inflammatory pathways between the two compartments. Furthermore, eight vaginal *Lactobacillus* species were chosen based on their immunomodulatory capabilities previously assessed *in vitro* (98), to evaluate their potential effect on the expression of VK2 cell inflammatory genes in response to a key BV-associated bacteria, *G. vaginalis*. It was found that 136 genes were differentially over-expressed, and 69 genes under-expressed in CMCs compared to PBMCs. These significantly upregulated genes were mapped to proinflammatory signaling pathways, NF-κB, TNF, TLR and NOD-like receptor signalling. Key genes in these pathways were IL1β, TNF-R1 and IL8. Significantly downregulated genes in CMCs compared to PBMCs were mapped to ribosome, sphingolipid, T cell receptor and natural killer cell mediated cytotoxicity signaling. Key genes in these pathways were Fyn, CD3ζ and PI3K. It was found that *G. vaginalis* induced a potent proinflammatory cytokine response by VK2 cells. In contrast, 3/8 *Lactobacillus* isolates (LM2, LM4 and LV4) reduced the level of inflammatory cytokine production by VK2 cells in response to *G. vaginalis*. A total of 142 genes were upregulated and 27 genes downregulated in *G. vaginalis*-stimulated VK2 cells compared to unstimulated VK2 cells. Similar to the upregulated pathways observed in CMCs compared to PBMCs, genes that were upregulated in VK2 cells in response to *G. vaginalis* mapped to inflammatory signaling, cytokine-cytokine interaction, TNF, NF-κB , NOD-like, TLR and MAPK signaling pathways. Key genes in these pathways were CCL5, cIAP, A20, CXCL10 (IP-10 gene), CXCL8 (IL-8 gene) and IL1B. In contrast, among the 27 genes that were downregulated in *G. vaginalis*-stimulated VK2 cells, were those encoding several zinc finger proteins. Moreover, several of these downregulated genes were

mapped to the KEGG longevity pathway. Pretreatment with lactobacilli resulted in a significant downregulation of several proinflammatory genes compared to cells cultured with *G. vaginalis* only. On the other hand, CYP1A gene expression was upregulated in cells pretreated with lactobacilli and compared to cells stimulated with *G. vaginalis* only. When gene expression in response to pretreatment with lactobacilli that suppressed cytokine production in response to *G. vaginalis* (LM2, LM4 and LV4; termed "cytokine-suppressive") was compared to lactobacilli that did not suppress cytokine production (LJ3, LV3, LC3, LC1 and LJ2; termed "non-cytokine-suppressive"), it was found that the expression of several genes (SAMD9L, DDX58, IFIT1) was downregulated in VK2 cells co-cultured with cytokine-suppressive lactobacilli, while RNASE7 and TMEM2 were upregulated in VK2 cells co-cultured with non-cytokine-suppressive lactobacilli. Furthermore, several genes involved in epithelial barrier function (DKK1, ELF3) and preterm birth (AKR1C1-C3) were upregulated by incubation with specific *Lactobacillus* spp. prior to *G. vaginalis* stimulation compared to stimulation with *G. vaginalis* only.

4.1 Gene expression patterns of the FGT compared to peripheral blood of HIV infected women

Although gene expression patterns in cervical cytobrush samples from HIV negative Canadian women has previously been studied (101), no previous studies have evaluated gene expression in these samples from HIV infected or South African women. This is likely because the extraction of intact mRNA of sufficient quantity and quality for microarray analysis is extremely challenging – for the present study, 28 cytobrush samples from both HIV infected and uninfected women were processed to optimize methodology for mRNA extraction, with only five having mRNA of sufficient quality to proceed with microarray analysis, even though all PBMC samples had high quality mRNA (not shown). Gene expression patterns of CMCs and matched PBMCs of HIV negative women were previously shown to be highly unique (101). Similarly, this study found that CMCs and PBMCs of HIV infected women had distinct gene expression patterns. Pathway analysis of over-expressed genes in CMCs compared to PBMCs revealed the over-expression of genes mapped to several proinflammatory (NF-κB, TNF) and microbial pattern recognition (TLR, NOD) signaling pathways. Similarly, Horton *et al*. (2009) (101) found that TLR and cytokine-cytokine receptor interaction signaling pathways were over-expressed in CMCs compared to matched PBMCs of HIV-negative women. The FGT mucosal surface is exposed to many microbes and thus it is to be expected that proinflammatory signaling pathways may be over-expressed at this site compared to

peripheral blood. In addition, vaginal microbiome state and STI status increases inflammation in the FGT (83,126). A limitation of the present study is that BV/STI diagnosis was solely based on the presence of clinical signs or symptoms, and thus asymptomatic BV/STI cases in this study population may have gone undetected, and potentially contributed to the over-expression of inflammatory pathways at this site compared to PBMCs. However, PCA analysis based on gene expression revealed that CMC samples were more heterogenous than PBMC samples. This heterogeneity may be explained by factors not evaluated, including, asymptomatic BV/STIs, vaginal microbiome composition, recent sexual activity, and vaginal hygiene practices, which may affect the microenvironment of the FGT (83,127,128). Although all participants were on ART, 2/5 had detectable plasma viral load. However, due to the small sample size, the study was not sufficiently powered to compare gene expression changes between women who were and were not virally suppressed. Vaginal HIV viral load was not assessed in this study, and therefore a direct link between inflammation and HIV viral shedding could not be evaluated. However, previous studies have found that inflammation in the FGT is associated with increased vaginal HIV shedding (129). In this study, IL-8 and NF-κB inhibitor alpha (NFKBIA), which is activated by NF-κB (130), expression was increased in CMCs compared to PBMCs. NF-κB increases activation of the HIV LTR, subsequently increasing viral replication (91) and IL-8 increases HIV replication in macrophages and T lymphocytes *in vitro* (131). Thus, increased expression of genes involved in pro-inflammatory signaling in the FGT, as found in this study, may increase HIV shedding and subsequent transmission.

Furthermore, this study found that genes mapped to the T cell receptor signaling and natural killer cell-mediated cytotoxicity pathways were under-expressed in CMCs compared to PBMCs of HIV-infected women. In contrast, Horton *et al.* (2009) (101) found these pathways to be over-expressed in CMCs compared to matched PBMCs of HIV negative women, although direction comparison of the results of these studies is not ideal, as they were based on very different populations of women. Nonetheless, under expression of genes mapping to these pathways in HIV-infected women may reflect CD4 T cell depletion at the genital mucosal site. Rapid CD4 T cell depletion occurs early in HIV infection at the gastrointestinal (GI) mucosal site (132). Similarly, CD4 T cells have been found to be depleted in the FGT during HIV infection, with an accumulation of terminally differentiated cells (133,134). Furthermore, IFN-γ and IL-2 T cell responses to HIV were lower in the cervix compared to blood of HIV-infected women (134,135). Studies have shown that, although peripheral blood CD4 T cell populations were recovered following ART initiation, CD4 T cells in both the GI tract and FGT remain depleted (132,133). Furthermore, mucosal CD4 T cell depletion in the GI tract was found to occur at all stages of HIV infection (136). Therefore, despite chronic infection and

ART initiation of all the participants of this present study, depletion of CD4 T cells and T cell dysfunction at the genital mucosal site during HIV infection is plausible for this cohort. In contrast, an increase of circulating natural killer cells was found in acute HIV infection, which returned to pre-infection levels in chronic infection, however, chronic HIV infection causes a defect in natural killer group 2 D (NKG2D)-mediated NK killing (137). Therefore, under-expression of T cell receptor signaling and natural killer cell-mediated cytotoxicity pathways in CMCs may be an HIV infection specific phenomenon. This study found that the mediators FYN, CD3ζ, PI3K and ITK were under-expressed in CMCs compared to matched PBMCs. Fyn and CD3ζ are required for T cell antigen receptor signal transduction, as the CD3 zeta chain is the signaling component of the TCR (138) and Fyn phosphorylates immunoreceptor tyrosine activation motifs in the CD3 zeta chains (139). Similarly, PI3K (phosphoinositide-3 kinase) is involved in innate immunity via TLR signaling and subsequent cytokine production, which influences adaptive immune responses (140). ITK (tyrosine-protein kinase) plays a role in T cell proliferation and differentiation via intracellular signaling (141). Thus, lower expression of these mediators in CMCs compared to PBMCs, as found in this study, potentially reflects reduced T cell activation and receptor signaling. Interestingly, a previous study by Trimble *et al.* (2000) (142) identified circulating HIV specific CD8 T cells by tetramer staining and found that these cells were CD3ζ-negative. These mediators are also components of the natural killer cell-mediated cytotoxicity pathway (115). A reduction in Fyn, CD3ζ and CD48 results in a reduction of lymphocyte activation (143–146). In addition, perforin was under-expressed in CMCs compared to PBMCs. Perforin is a cytolytic enzyme released by natural killer cells and cytotoxic T lymphocytes (CTLs) also known as CD8 T cells, which cause the formation of pores on target cells (147). Lower levels of perforin expression in CMCs may be explained by reduced frequency and/or compromised function of natural killer cells and CTLs at the cervix compared to PBMCs, as suggested by the under expression of Fyn, CD3ζ and CD48.

The role of natural killer cells in the FGT is imperative for defence against intracellular pathogens and CD8+ T cells (CTLs) predominate over CD4+ T cells in the FGT (148). The reduction of these cells in HIV infected women may increase their risk for co-infection with other STIs, while a simultaneous increase in the expression of non-specific proinflammatory pathways may reduce epithelial barrier integrity, further increasing susceptibility to opportunistic infections. However, in this study, it is not clear whether genital mucosal CTL populations were reduced during chronic HIV infection or whether their functionality was altered, as mentioned above. However, the unique gene expression patterns in CMCs compared to PBMCs found in this study are likely to be at least partly due to differences in the cell populations between these two anatomical compartments. These differences have previously been reported by Horton et al. (2009) using flow cytometry analysis, which found

an increase in the majority of immune cell types in CMCs compared to PBMCs obtained from HIV-1 negative Canadian women(101). Similarly, in this present study, CIBERSORT analysis of the microarray data revealed that CMCs tended to include increased predicted innate immune cell populations compared to PBMCs, except for monocytes and resting mast cells which were increased in PBMCs. Furthermore, the CIBERSORT analysis also predicted a reduced abundance of naïve CD4+ T cells, CD8+ T cells and activated NK cells in CMCs, which suggests that the under-expression of mediators mapping to the T cell signaling and natural killer cell-mediated cytotoxicity pathways are likely due to a reduction in these cell populations in CMCs compared to PBMCs. While similar results were obtained by xCell analysis of the microarray data, a greater diversity of cell types were detected. Particularly, the predicted abundances of epithelial cells and keratinocytes were higher in CMCs compared to PBMCs. Epithelial cells and keratinocytes are important sentinels of immunity in the FGT (149,150), thus, the distinct gene expression patterns observed in CMCs may be attributed to the greater abundances of these cells at this site.

Interestingly, this study found that genes mapped to the sphingolipid pathway were under-expressed in CMCs compared to PBMCs. The sphingolipid pathway plays an important role in immune cell activation, trafficking and retention in inflamed tissues (151). Specifically, sphingosine-1-phosphate (S1P) activation of sphingosine-1-phosphate receptors (S1PR) 1-5 expressed on immune cells, promotes the migration of lymphocytes from secondary lymphoid tissues to blood and lymphatic circulation (151). This migration of immune cells is largely dependent on the S1P concentration gradient and S1PR expression (151). Denton et al. (2014) found that in mice, activated T cell retention in lymph nodes was due to downregulation of S1PR expression by these cells (152). Similar findings were observed in peripheral tissue in mice, Mackay et al. (2015) found that the downregulation of S1PR coincides with the retention of CD8+ T cells in skin (153). Hence, in this present study, the under-expression of receptors S1P1 and S1P5 found in CMCs compared to PBMCs may provide insight to the mechanism of retention of the immune cells detected at this mucosal site. Notably, as discussed above, CD4+ and CD8+ T cells and NK cells were reduced in CMCs compared to PBMCs, thus it is unclear whether decreases in cytotoxicity genes such as perforin are due to reduced abundance of cytotoxic cells or impaired functionality. An upregulation of S1P gradient and S1PRs promotes the trafficking of immune cells from the circulation to sites of injury (151). Therefore, the overrepresentation of S1PRs in PBMCs compared to CMCs would suggest that immune cells would effectively migrate to the cervix. Thus, the reduction in certain immune cell populations found in CMCs may indicate HIV-1 specific immune dysregulation, however, further research is needed to elucidate this phenomenon.

Furthermore, in this study, several long and short ribosomal subunits were under-expressed in CMCs compared to PBMCs. Similarly, Kleinman *et al.* (2014) (154) found a downregulation of genes involved in ribosome biogenesis in HIV-infected Jurkat cells *in vitro* and suggested that this regulation of host gene expression was mediated by the virus, linking HIV replication and the nucleolus.

Therefore, the over- and under-expression of genes mapped to the respective signaling pathways mentioned above in CMCs relative to PBMCs from HIV infected women may play a role in increased HIV viral replication and transmission.

4.2 Suppression of cytokine responses of VK2 cells to *G. vaginalis* by *Lactobacillus* species

Previous studies have associated BV with increased proinflammatory mediators in the FGT (33,83,84). This study found that *G. vaginalis* (ATCC 14018) induced a proinflammatory response in VK2 cells, shown by significant increases in the production of proinflammatory cytokines and chemokines IL-8, IL-6 and IL-1α, chemokines IP-10, MIP-1α, MIP-1β and MIP-3α, as well as anti-inflammatory IL-1RA. These findings are consistent with Chetwin *et al.* (2019) (29) and Manhanzva*et al.* (2020) (98) that found that the same *G. vaginalis* reference strain elicited proinflammatory cytokine responses from ectocervical (CaSki) and VK2 cells *in vitro*. Similarly, recent studies have found that *G. vaginalis* induces TNF-α, IL-1β, IL-6 and IL-8 production by HeLa cells *in vitro* (86) and IL-6 production *in vivo* in cervicovaginal fluid of mice (87). Consonantly, *in vivo*, Lennard *et al*. (2018) found that BV was associated with increased genital inflammation in a cohort of adolescent South African women (126). Furthermore, the study found that BV-associated bacterial taxa abundance, including *G. vaginalis* was increased in women with high genital inflammation (126). Interestingly, while BV is associated with upregulation of pro-inflammatory cytokines, several studies have shown that downregulation of chemokines may occur (13,83).Upregulation of chemokines by this *G. vaginalis* strain suggests that other species or strains may be involved in chemokine downregulation associated with BV, or alternatively that other human cells (such as immune cells) are involved. Gibbs et al. (2017) found that innate-like mucosal-associated invariant T (MAIT) cells were present in the upper and lower FGT and expressed IL-17/IL-22 following stimulation by *E.coli in vitro* (155). The authors concluded that this distinct cytokine profile of MAIT cells is important for immune homeostasis of the FGT in response to microbial induced inflammation (155). Similarly, studies have found that T regulatory (Treg) cells are important

immune response regulators, which protect the mucosal tissue against excessive inflammation in the FGT (156). Thus, immune cells in the FGT likely play a crucial role in modulating inflammatory responses induced by microbes at this site. Future studies including immune cells in this culture system would be useful.

Modulation of chemokine production induced by *G. vaginalis* is of great significance in the FGT and HIV susceptibility. The MIP chemokine protein family are chemoattractants for immune cells and are secreted by several cell types, including epithelial cells (157). An increase in these chemokines in the FGT may increase HIV acquisition risk as many of the recruited immune cells are HIV target cells, especially CD4+ T cells (81). A study by Liebenberg *et al.* (2017) (125) found that genital IP-10 and MIP-1β concentrations were significantly associated with HIV acquisition in a cohort of South African women. Therefore, inflammation in the FGT induced by BV-associated bacteria is of utmost importance in the HIV prevention field.

Imperative to HIV prevention strategies is the maintenance of an optimal vaginal microbiome, dominated by *Lactobacillus* species, and an improved understanding of the immunomodulatory capabilities of these commensal bacteria is needed. In this study, the co-culture of *Lactobacillus* isolates and *G. vaginalis* elicited differing inflammatory responses by VK2 cells, as indicated by varying inflammatory principal component scores. The cytokine-suppressive lactobacilli LM2, LM4 and LV4 reduced the proinflammatory response of VK2 cells elicited by *G. vaginalis* and displayed significantly lower inflammatory estimate scores compared to non-cytokine-suppressive lactobacilli LJ3, LV3, LC3, LC1 and LJ2. Notably, VK2 co-culture with certain *Lactobacillus* species and *G. vaginalis* in combination, induced a greater cytokine response than co-culture with *G. vaginalis* only. This suggests that VK2 co-culture with certain lactobacilli only are inflammatory, as previously reported by Manhanzva *et al*. (2020) (98). While the underlying mechanism remains to be determined, differences in inflammatory profiles may be influenced by the peptidoglycan cell wall and membrane structures of particular strains, as well as proteins present in the cell wall. Previous studies have found that the immunomodulatory properties of *Lactobacillus* peptidoglycan, a toll like receptor (TLR) and nucleotide binding and oligomerization domain protein (NOD) agonist, are highly strain dependent (158,159). The IL-6 response of VK2 cells elicited by *G. vaginalis* was significantly reduced by each of the cytokine-suppressive lactobacilli and the IL-8 response tended to be reduced. IL-6 is a strong proinflammatory cytokine which recruits immune cells to injury sites and has shown to affect the longevity of T cells via an anti-apoptotic effect, promoting chronic inflammation (160). IL-8 functions similarly and both of these cytokines recruit and activate immune cells, including neutrophils and HIV target cells (161,162). Although neutrophil extracellular traps have been found to inhibit HIV infection *in vitro* (163),

their release of reactive oxygen species and proteases also contribute to tissue damage (164), which decreases FGT epithelial barrier integrity and may increase HIV acquisition risk (96). In addition, these cytokines recruit dendritic cells which have shown to increase HIV acquisition by trans-infection to CD4+ T cells (165). Moreover, dendritic cells also produce chemokines which recruit CD4 T cells (166). Hence, the immunosuppressive ability of lactobacilli to dampen the IL-6 and IL-8 responses induced by BV-associated bacteria in the FGT may reduce HIV acquisition risk in women. The mechanisms underlying the immunomodulatory effect of lactobacilli are not fully understood. Hearps *et al.* (2017) (28) found that both D- and L-lactic acid supress proinflammatory cytokine responses of cells from the FGT *in vitro*, suggesting that these metabolites that are produced by lactobacilli may be involved in their anti-inflammatory effects. Consistent with Hearps *et al.* (2017) (28), the present study found that increased L-lactate production by lactobacilli in the VK2 cell culture system was associated with reduced MIP-1α, MIP-1β and IL-8 responses by VK2 cells.

It was found that greater suppression of inflammatory cytokine production was observed following a 24 hour incubation period (98) compared to the 12 hour incubation time of this study. This finding may indicate that the ability of *Lactobacillus* isolates to dampen inflammatory responses of VK2 cells *in vitro* may be influenced by incubation time. The effect of incubation time on the cytokine suppressive capability of lactobacilli *in vitro* may suggest that their growth and subsequent metabolite (e.g. lactic acid) production in the VK2 cell culture system influences their anti-inflammatory capabilities. Additionally, the anti-inflammatory effect of lactic acid was found to be due to the protonated lactic acid, rather than lactate (28). Protonation occurs at low pH (28) and therefore, at earlier incubation times, the pH may still be too high for protonation to occur. In support, culture pH recorded in the present study was higher than observed following 24 hours of incubation (98). Future time series experiments assessing the growth of lactobacilli, metabolite production and cytokine responses in the VK2 cell culture system may be useful to elucidate this research question.

4.3 Gene expression of VK2 cells altered by *G. vaginalis*

The increase in inflammatory cytokine and chemokine production by VK2 cells in response to *G. vaginalis* that was observed is consistent with the microarray analysis of these cells which found that the majority of differentially expressed genes were upregulated. Gene expression analysis of *G. vaginalis* stimulated VK2 cells revealed an upregulation of 142 genes, which

mapped to key proinflammatory signaling pathways, including cytokine-cytokine receptor interaction, TNF, NF-κB, TLR, NOD-like receptor and MAPK signaling pathways.

Expression of several C-C and C-X-C motif chemokine ligands, proinflammatory cytokines, including IL-1α, IL-1β and IL-6, and mediators of the cytokine-cytokine receptor and TNF signaling pathways were upregulated in *G. vaginalis*-stimulated VK2 cells. Similarly, TLR and NF-κB signaling upregulation in *G. vaginalis*-stimulated VK2 cells indicates the induction of an inflammatory state. TLR2 expression was upregulated in *G. vaginalis* stimulated VK2 cells compared to unstimulated VK2 cells. TLR2 detects bacterial lipoproteins and the bacterial cell wall component peptidoglycan of Gram-positive bacteria (167). Hence, upregulation of TLR2 in response to *G. vaginalis* is appropriate, due to its Gram-positive cell wall structure which contains peptidoglycan (PGN) (168,169). Although, *G. vaginalis* displays Gram-variable staining, LPS (produced by Gram negative bacteria) has not been detected in its cell wall structure *in vitro* (168,170). Moreover, an *in vivo* study by Aroutcheva *et al.* (2008) (171) found only trace amounts of LPS in vaginal washes obtained from women with BV predominantly colonized by *G. vaginalis*. Consistent with a previous study by Fazeli *et al.* (2005) (65) showing that TLR4 is not expressed on vaginal epithelial cells *in vivo*, TLR4 expression was not upregulated in *G. vaginalis* stimulated-VK2 cells, while low level TLR4 expression was detected in all cultures.Thus it is unclear if these cells express surface TLR4, furthermore, *G. vaginalis* does not produce its LPS ligand which would induce a TLR4 response. Nonetheless, research on *G. vaginalis*-TLR interactions is limited and further studies using TLR reporter cell lines may be useful for the identification of other TLRs that are activated by *G. vaginalis*. TLR activation triggers a cascade of intracellular signaling which activates NF-κB and subsequently induces the transcription of inflammatory cytokines, IL-1β, IL-6, IL-8 and RANTES (172). Consistent with this known inflammatory signaling pathway, this study found an increase in the expression of NF-κB, as well as the cytokines mentioned above, thus providing an improved understanding of *G. vaginalis*-induced inflammation in cells of the FGT.

Interestingly, this study found that *G. vaginalis* downregulated the expression of certain host factors. A downregulation of expression of several zinc finger proteins (ZNF), ZNF30, ZNF302, ZNF483 and ZSCAN31, was found in *G. vaginalis*-stimulated VK2 cells compared to unstimulated VK2 cells. ZNF proteins have various molecular functions, among these are transcriptional regulation and signal transduction, as they interact with DNA, RNA and various proteins (173). Relevant to this present study, Hong *et al.* (2015) (174) found that ZNFA20 attenuated LPS-induced production of prostaglandin E2, cyclooxygenase (COX)-2 and proinflammatory cytokines in human periodontal ligament cells *in vitro*. Others have found that ZNFA20 also inhibits NF-κB activation and apoptosis (175). In addition, ZNF658 was found to regulate the transcription of genes involved in zinc homeostasis (176). Zinc itself has anti-

inflammatory and anti-oxidant properties, functioning intracellularly to regulate signaling pathways of the immune system (177). Zinc has been found to negatively regulate inflammation by modulating TLR and NF-κB signaling (178). Thus, zinc homeostasis plays an important role in inflammatory responses, and a heightened inflammatory response is a clinical manifestation of zinc deficiency in humans (177). Furthermore, zinc deficiency is associated with increased inflammatory cytokines *in vitro* and *in vivo* (178). Studies have found an increase in IL-1β production by PBMCs obtained from zinc-deficient adults compared to zinc-sufficient PBMCs, after LPS stimulation of these cells (179). Thus, reduced expression of several zinc finger proteins in *G. vaginalis* stimulated VK2 cells, may have exacerbated the inflammatory response. In addition to the regulation of zinc homeostasis by some ZNF proteins, zinc deficiency may impact the expression and functions of ZNP proteins and zinc supplementation has been found to increase the expression of ZNFA20 (180). Hence, it is likely that ZNF proteins themselves have anti-inflammatory effects and the reduction of these ZNFs in *G. vaginalis*-stimulated cells may have exacerbated the proinflammatory response. Interestingly, ZNF protein mutations are implicated in skin diseases. Studies have found that downregulation of ZNF750 causes a reduced expression of genes involved in skin barrier formation (173). Therefore, a *G. vaginalis*-induced reduction of ZNF proteins in the FGT may be implicated in reduced barrier function at the FGT, and increased susceptibility to STI acquisition. In addition, genes mapped to the KEGG longevity regulating pathway were downregulated in *G. vaginalis*-stimulated VK2 cells compared to unstimulated VK2 cells. The longevity regulating pathway functions in cellular fitness and the attenuation of proinflammatory mediators to increase cellular survival (181–183). Hence, reduction in mediators mapping to this pathway may contribute to an excessive pro-inflammatory state, as well as reduced VK2 cellular fitness and survival. Although, VK2 cell viability in this study remained unchanged with *G. vaginalis* stimulation for a relatively short time (6 hours), this finding is potentially significant *in vivo* where exposure of vaginal epithelial cells to *G. vaginalis* is greater than the incubation time used in this *in vitro* model.

4.4 Effect of *Lactobacillus* species on VK2 cell gene expression induced by *G. vaginalis*

4.4.1 Downregulated genes in VK2 cells co-cultured with lactobacilli and G. vaginalis in combination

The mechanisms underlying the immunomodulatory effect of vaginal lactobacilli are unknown. This study found that the expression of several genes, CXCL11, IFIT3, IFIT2, IL7R, APOL2,

DDX58 and TNFSF18, were downregulated in VK2 cells co-cultured with *Lactobacillus* spp. and *G. vaginalis* in combination, compared to cells stimulated only with *G. vaginalis*.

The chemokine CXCL11 (otherwise known as interferon-inducible T-cell alpha chemoattractant or interferon-gamma-inducible protein 9) is a chemoattractant for T lymphocytes and macrophages (184,185). CXCL11 expression in the vaginal tract is not well studied, however, a previous *in vivo* study of chronic obstructive pulmonary disease found that suppression of CXCL11 gene expression caused a reduction in T lymphocyte recruitment to the lungs of rats (185). Thus, the ability of lactobacilli to supress CXCL11 expression in VK2 cells induced by *G. vaginalis,* as found in this present study, provides insight into the protective capacity of lactobacilli against excessive recruitment of T lymphocytes (HIV target cells) to the FGT, potentially reducing HIV acquisition risk.

IFIT2 and 3 (interferon-induced protein with tetratricopeptide repeats) are well known for their antiviral activity (186), and are involved in interferon gamma signaling in the immune system (187). In contrast their role in bacterial infection is less clear (188). In the context of chronic mastitis, IFIT3 was found to be induced *in vitro* in mammary epithelial cells stimulated by LPS and lipoteichoic acid (LTA), which forms part of the cell walls of Gram-negative and Gram-positive bacteria, respectively (189). Thus, downregulation of IFIT3 in lactobacilli pre-treated VK2 cells is potentially an indication of an overall reduced inflammatory state. In contrast, *in vitro* overexpression of IFIT2 in transfected raw264.7 macrophages was found to supress LPS-induced TNF-α, IL-6 and MIP-2 protein expression (188). Thus, the potential immunomodulatory effect of reduced IFIT2 in lactobacilli pre-treated VK2 cells found in this study is unclear.

In this study, expression of the IL-7 receptor (IL-7R) gene was downregulated in VK2 cells cultured with lactobacilli and *G. vaginalis* in combination, compared to *G. vaginalis* only stimulated VK2 cells. The IL-7/IL-7R pathway is important for lymphocyte development and T cell homeostasis (190). An increase in IL-7 and its receptor is linked to several inflammatory diseases such as allograft rejection, rheumatoid arthritis, psoriasis, multiple sclerosis and inflammatory bowel disease (191,192). Using an *in vivo* mouse model, Schreiber *et al.* (2019) (193) found that hyperexpression of IL-7 in transplanted islets caused a decrease in graft survival and increased CD4+ and CD8+ T cell infiltration. Furthermore, studies have shown that IL-7 overexpression and T cells highly expressing IL-7R results in colitis (191,194). Interestingly, the IL-7/IL-7R is implicated in HIV/SIV infection, as IL-7 expression is markedly increased in HIV infection, perhaps as the body's physiological attempt to restore T cell loss (195), alternatively as a result of increased aberrant inflammation in HIV infection (196) . Moniuszko *et al.* (2006) (195) found a direct correlation between the absolute CD4 T cell

populations and IL-7R expressing T cells in blood, secondary lymphoid organs and various other tissues, including the vagina of SIV-infected macaques. The finding of this present study that lactobacilli reduced IL-7R expression on VK2 cells, suggests that these commensal bacteria could exert a similar effect on lymphocytes in the FGT, reducing HIV CD4 T cell targets at this site. However, further research is needed to elucidate the effect of lactobacilli on other cell populations in the FGT, in addition to epithelial cells. IL-7R is commonly expressed by lymphocytes (197). However, the IL-7R consists of an alpha chain and a common gamma chain, of which the IL-7Rα is lymphoid-specific, while the γ chain may be expressed by cells of various haematopoietic lineages (197). Yamada *et al*. (1997) found that bacterial invasion of colonic epithelial cells induced IL-7R expression *in vitro* (198). Furthermore, its expression has been found in decidua specimens obtained from a cohort of pregnant women in China (199). Thus, future research to confirm IL-7R expression by vaginal epithelial cells would be useful to support the findings of this present study and elucidate the role of IL-7/IL-7R in immune modulation by lactobacilli in this this model system. The IL-7/IL-7R has further been implicated in recurrent pregnancy loss. Wu *et al.* (2016) (199) found that IL-7R antagonist treatment in an abortion prone mouse model, significantly reduced fetal resorption rates via the downregulation of Th17 and upregulation of regulatory T cell (Treg)-related factors. The study also found that IL-7 treatment of non-abortion prone mice, significantly increased fetal resorption rates by upregulation of Th17 and downregulation of Treg-related factors. A study by Willis *et al.* (2012) (191) found that IL-7R blockade suppressed innate and adaptive responses in colitis. The study found that in mice, colitis was reduced by an anti-IL7R antibody blockage of the IL-7R which resulted in reduced T cell proliferation and function. Furthermore, the innate immune response was also downregulated, with a reduction in the abundance of macrophages and dendritic cells and their activity. Hence, IL-7 and IL-7R play an important role in inflammation and are potential therapeutic targets to reduce inflammation. Furthermore, thymic stromal lymphopoietin (TSLP) and its receptor (TSLPR) were upregulated in *G. vaginalis*-stimulated VK2 cells compared to unstimulated VK2 cells. TSLP pays an important role in immune responses, and signals through a heterodimeric receptor complex composed of an IL-7R alpha chain and a TSLPR (200). Thus, the reduction in IL-7R expression by lactobacilli pre-treated VK2 cells may be an important mechanism utilized by lactobacilli to reduce inflammatory responses induced by *G. vaginalis.* Taken together with previous research discussed above, modulation of IL-7/IL-7R signaling by an optimal vaginal microbiome dominant in *Lactobacillus* spp. in the FGT may reduce HIV susceptibility and improve pregnancy outcomes.

Apolipoprotein L2 (APOL2) is a lipid-binding protein found intracellularly in the cytoplasm where it is involved in the movement of lipids and lipid binding to organelles and plays a role

in the pathways of cholesterol and sphingolipid transport to the plasma membrane (201,202). Inflammatory stimuli such as TNF-α and IFN-γ induce APOL2 expression in human dermal microvascular endothelial cells *in vitro* (203). *G. vaginalis* produces a cholesterol-dependant pore-forming toxin called vaginolysin, which utilizes cholesterol of the host cell plasma membrane (94). Reduction of cholesterol by statin was found to reduce the colonization and pathogenesis of *G. vaginalis* in the FGT of mice (95). This present study found that APOL2 expression was downregulated in VK2 cells co-cultured with lactobacilli and *G. vaginalis* in combination compared to co-culture with *G. vaginalis* only. This finding may suggest a potential protective mechanism by lactobacilli against the pathogenesis of *G. vaginalis*, as a reduction in APOL2 may cause reduced transport of cholesterol to the plasma membrane of the VK2 cells, thus reducing the pathogenic effects of vaginolysin.

TNFSF18 gene expression was downregulated in VK2 cells co-cultured with lactobacilli and *G. vaginalis* in combination compared to co-culture with *G. vaginalis* only. The TNFSF18 gene encodes the protein TNF ligand superfamily member 18, also known as glucocorticoid-induced TNF receptor ligand (GITRL), a cytokine shown to modulate T lymphocyte survival (204). Its receptor is TNFRSF18/GITR (204). The cytokine is involved in proinflammatory responses and supresses Treg functions (205). Mahesh *et al.* (2006) (206) found that expression of TNFSF18 stimulates the secretion of proinflammatory cytokines and chemokines by T cells *in vitro*. Similarly, Bae *et al.* (2008) (207) found that the stimulation with TNFSF18 induced proinflammatory cytokine expression in a macrophage cell line and primary macrophages *in vitro*. Furthermore, the study found nuclear translocation of the NF-κB p50 subunit in response to TNFSF18 and the authors concluded that in macrophages, TNFSF18-mediated inflammatory activation likely plays a role in the pathogenesis of inflammatory diseases (207). Therefore, a reduction in TNFSF18/GITRL is likely to suppress proinflammatory cytokine secretion by potentially reducing NF-κB translocation into the nucleus. Thus, downregulation of this gene may be an anti-inflammatory mechanism in lactobacilli pre-treated cells.

4.4.2 Upregulated genes in VK2 cells co-cultured with lactobacilli and G. vaginalis in combination

In contrast to the downregulated genes discussed above, CYP1A1 gene expression was upregulated in VK2 cells co-cultured with lactobacilli and *G. vaginalis* in combination compared to co-culture with *G. vaginalis* only.

CYP1A1 is a member of the cytochrome p450 (CYP) family 1 and are involved in detoxification of xenobiotics, cellular metabolism and homeostasis (208). Studies have shown that these

enzymes are commonly downregulated during inflammation and host response to infection (209). This is consistent with the findings of this study, whereby higher expression of CYP enzymes was accompanied by a lower expression of proinflammatory cytokines by VK2 cells co-cultured with lactobacilli and *G. vaginalis* in combination compared to co-culture with *G. vaginalis* only. This suggests that higher proinflammatory cytokine expression in *G. vaginalis* only cultures resulted in a relative downregulation of CYP enzymes compared to lactobacilli and *G. vaginalis* co-cultures. In contrast, a previous study found that the proinflammatory cytokine TNF-α increased CYP1B1 expression in epithelial cells *in vitro* (210), thus the effect of cytokine production on these enzymes is heterogenous. Notably, TNF-α production was not measured in this study because it was not detected by Manhanzva *et al.* (2020) in the same culture system (98). However, of interest to this study is the potential anti-inflammatory effects of CYP enzymes. Arachidonic acid is metabolized into pro- and anti-inflammatory eicosanoids (211), via 3 major pathways COX, lipoxygenase (LOX) and CYP (212). CYP metabolizes arachidonic acid into epoxyeicosatrienoic acids (EETs) which display anti-inflammatory effects (213) both *in vitro* and *in vivo* (214). Thus, a potential increase in CYP expression in host cells induced by lactobacilli and subsequently increased production of EETs, may drive an anti-inflammatory response in the presence of BV-associated bacteria. However, additional research is needed to determine the potential production of EETs in this culture system. Furthermore, an *in vitro* study by Zhang *et al.* (2018) (215), which used inflammatory epithelial cells obtained from bovine mammary glands with mastitis, found that CYP1A1 reduced *in vitro* LPS-induced TNF-α and IL-6 responses and NF-κB activation. Moreover, the ability of non-cytokine-suppressive lactobacilli to induce CYP expression in VK2 cells may explain the ability of these isolates to suppress IL-6 responses of VK2 cells, albeit to a lesser extent than cytokine-suppressive lactobacilli.

4.4.3 Genes downregulated in VK2 cells co-cultured with cytokine-suppressive lactobacilli and G. vaginalis in combination

Grouped limma analyses to detect genes downregulated in VK2 cells pre-treated with cytokine-suppressive lactobacilli (LM2, LM4, LV4) and non-cytokine-suppressive lactobacilli (LJ3, LV3, LC3, LC1, LV4) compared to stimulation with *G. vaginalis* only revealed similar differential gene expression between these groups. However, three genes (SAMDL, DDX58 and IFIT1) were downregulated in VK2 cells co-cultured with cytokine-suppressive lactobacilli and *G. vaginalis* in combination compared to co-culture with *G. vaginalis* only.

The sterile alpha motif domain-containing 9-like (SAMD9L) gene encodes a protein that is typically involved in cell growth, division and maturation (216). SAMD9L expression has been

shown to be induced by cytokines, particularly IFNs, in CD34+ hematopoietic stem and progenitor cells *in vitro* (217). Although, the relationship between SAMD9L and cytokine expression is unclear, it is possible that the lower expression of this gene in VK2 cells pre-treated with cytokine-suppressive lactobacilli compared to stimulation with *G. vaginalis* only was due to reduced proinflammatory cytokine production. Alternatively, the inverse may be true and downregulation of SAMD9L may have contributed to the dampened pro-inflammatory responses observed in these cultures. Wang *et al.* (2014) (218) found that SAMD9L knockdown in hepatocellular (SK hep-1) cells was accompanied by a significant elevation in the Wnt/β-catenin signaling pathway, which has been shown to inhibit NF-κB *in vitro* (219,220).

DDX58 is also known as RIG-I, a member of the RIG-I like receptor family a cytoplasmic PRR that is well known for the detection of viral dsRNA (221). A microarray study by MacPherson *et al.* (2014) (222) found that a multistrain probiotic including *Lactobacillus helveticus*, attenuated gene expression involved in the proinflammatory Th1 and innate immune system antiviral responses induced by dsRNA in intestinal epithelial cells *in vitro.* Of interest to this study, RIG-I receptors also recognize DAMPs, particularly immunocomplexes of small nuclear ribonuclearproteins (snRNPs) (223). As discussed in Chapter 1, DAMPs are released by damaged host cells and are detected by PRRs and induce inflammation (61). *G. vaginalis* has been shown to cause epithelial damage *in vivo* (87), which potentially results in the release of DAMPs by damaged cells. Hence, the downregulation of DDX58 in VK2 cells pre-treated with cytokine-suppressive lactobacilli could potentially reduce DAMP-induced inflammatory responses. However, additional research is needed to investigate potential DAMPs induced by *G. vaginalis* in this culture system. Alternatively, Schmolke *et al.* (2014) (224) found that RIG-I receptors detected the mRNA of intracellular *Salmonella enterica* in fibroblasts *in vitro*. As uptake of *G. vaginalis* by vaginal epithelial cells *in vitro* has previously been reported (225), *G. vaginalis* uptake by VK2 cells may have occurred and subsequent detection by RIG-I receptors may have been reduced due to RIG-I downregulation by VK2 cell pre-treatment with cytokine-suppressive lactobacilli. However, VK2 uptake of *G. vaginalis* and detection of its mRNA by RIG-I in this culture system needs further research for this conclusion.

Similarly, interferon induced protein with tetratricopeptide repeats 1 (IFIT1) is well known for anti-viral function (187). IFIT1 has been shown to be induced by LPS via TIR-domain-containing adaptor protein inducing interferon (TRIF)-dependent interferon regulatory factor (IRF) 3 activation in macrophages *in vitro* (226). The adaptor molecule TRIF is crucial for signal transduction from intracellular TLR3 and TLR4, however, TLR2 has been found to utilize TRIF as well (226). Interestingly, using a TRIF-deficient mouse model, Petnicki-Ocwieja *et al.* (2013) (226) found that synthetic lipopeptide Pam_3CSK_4 stimulation of bone marrow derived macrophages (BMDMs) obtained from these mice, produced significantly less IL-6 than

BMDMs isolated from wildtype mice. Furthermore, the study also found Pam_3CSK_4 stimulation of BMDMs isolated from TRIF-deficient mice displayed significantly less IFIT1 expression compared to wildtype mouse BMDMs (226). As discussed above, *G. vaginalis* may induce an immune response via the TLR2, as TLR2 expression was upregulated in *G. vaginalis* stimulated VK2 cells compared to unstimulated cells. Therefore, a downregulation of IFIT1 in VK2 cells pre-treated with cytokine-suppressive lactobacilli suggests an immunomodulatory mechanism downstream of the TLR2 signaling pathway.

4.4.4 Genes upregulated in VK2 cells co-cultured with non-cytokine suppressive lactobacilli and G. vaginalis in combination

In contrast, the grouped limma analysis detected several genes upregulated in VK2 cells co-cultured with non-cytokine-suppressive lactobacilli (LJ3, LV3, LC3, LC1, LV4) and *G. vaginalis* in combination compared to co-culture with *G. vaginalis* only. Among these genes were RNase7 and TMEM2.

Ribonuclease A family member 7 (RNase7) is a protein with antimicrobial and ribonuclease activity, its expression occurs in several epithelial tissues, and it is highly expressed in the skin, tonsils, pharynx and genitourinary tract (227). The antimicrobial and immunomodulatory properties of RNase7 have largely been studied in keratinocytes and in the human skin (228). RNase 7 is induced by pro-inflammatory cytokines and it has been suggested that a local inflammatory environment, such as in the case of psoriasis and atopic dermatitis, increases the expression of RNase7 on the skin (227–229). Therefore, the upregulation of RNase7 in VK2 cells co-cultured with non-cytokine suppressive lactobacilli may be a result of the increased inflammatory environment of these cultures. In addition, RNase7 expression by keratinocytes *in vitro* is induced in the presence of microorganisms and skin commensals have been shown to induce its expression as well, thereby strengthening cutaneous defence (227,228). Hence, the significantly increased induction of RNase7 expression in VK2 cells co-cultured with lactobacilli and *G. vaginalis* in combination compared to co-culture with *G. vaginalis* only may be an antimicrobial protective mechanism by these commensal bacteria against *G. vaginalis*. RNase7 expression is rapidly increased on the skin surface following experimental barrier disruption (229), although it is not yet known whether RNase7 is expressed as part of the inflammatory response to barrier disruption or plays an active role in wound healing and further research is needed to elucidate its role in epithelial barrier function in the FGT. RNase7 has also shown to have immunomodulatory effects. Interestingly, RNase7 is able to convert usually non-immunogenic self-DNA into a danger signal which elicits an immune response (228). A study by Kopfnagel *et al.* (2018) (230) found that RNase7 in

conjunction with human self-DNA induced a powerful IFN-α response by plasmacytoid dendritic cells *in vitro*. Furthermore, the IFN-α response was protective against herpes simplex virus 1 (HSV-1) in keratinocytes *in vitro* (230). As noted by Rademacher *et al.* (2019) (228), RNase7 may function as an alarmin, detecting skin barrier disruption by converting released self-DNA into a danger signal. This is an intriguing phenomenon in this present study, as higher RNase7 in lactobacilli-*G. vaginalis*-VK2 co-cultures may have potentially induced a proinflammatory response by converting DNA released from damaged VK2 cells, into danger signals. This may explain the increased inflammatory responses observed in the VK2 cells co-cultured with non-suppressive lactobacilli and *G. vaginalis* in combination compared to co-culture with *G. vaginalis* only, as RNase7 expression was significantly higher in the former cultures compared to the latter. However, as mentioned above, RNase7 expression is also induced by a proinflammatory environment, thus it is unclear whether the increased RNase7 expression promoted the proinflammatory state or whether RNase7 expression was induced by the proinflammatory environment. Nonetheless, although RNase7 may play a role in antimicrobial and barrier function, it's immunomodulatory effects in the context of the FGT based on the findings of this study are unclear and further research is needed to investigate this protein as a potential immunomodulator utilized by *Lactobacillus* species.

Type II Transmembrane protein (TMEM2) is a member of the interferon-induced transmembrane (IFITM) protein superfamily, which functions as a hyaluronidase at the cell surface, which degrades hyaluronic acid (231). Studies investigating the immunomodulatory effect of hyaluronidases have mostly been on the skin surface and in the colon. Interestingly, Dokoshi et al. (2018) (232) found that the skin of mice treated with hyaluronidase had significantly reduced IL-6 expression after infection with *Staphylococcus aureus* and a reduced inflammatory infiltrate in the colon following dextran dulfate sodium-induced colitis, compared to control mice. Furthermore, RNA sequencing revealed that hyaluronidase altered genes involved in inflammatory, cytokine and immune-response related signaling pathways (232). In contrast, Fronza *et al.* (2014) (233) found that hyaluronidase treated rats had increased IL-1α, TNF-α, IL-4 and IL-10 compared to untreated rats in wound healing experiments. Notably, non-cytokine-suppressive lactobacilli dampened the IL-6 response of VK2 cells to *G. vaginalis*, albeit to a less extent than cytokine-suppressive lactobacilli. Hence, the upregulation of TMEM2 in VK2 cells pre-treated with these lactobacilli may suggest a hyaluronidase-mediated mechanism utilized to reduce the IL-6 response. Furthermore, the upregulation of TMEM2 may also explain why certain cytokines, e.g. IL-1α and IL-1β, were not dampened by lactobacilli. In addition, there may be a link between TMEM2 expression and endoplasmic reticulum (ER) stress. In the ER, the unfolded protein response (UPR) pathway is induced in attempt to maintain ER homeostasis during cellular stress, however in severe

stress, UPR promotes proinflammatory cytokine production (234). Several studies have implicated UPR in host cell cytotoxicity and inflammatory responses to bacterial infection (234). TMEM2 was found to modulate ER stress *in vitro* via the MAPK signaling pathway, promoting cell survival independent of the UPR pathway (235). However, one key mediator of the UPR pathway, transcription activator 4 (ATF4) was significantly increased in VK2 cells co-cultured with non-cytokine-suppressive lactobacilli and *G. vaginalis* in combination compared to co-culture with *G. vaginalis* only. Interestingly, Zhang *et al.* (2013) (236) found that *in vitro* ATF4-knockdown in stimulated human monocytes reduced the IL-8 and IL-6 responses. Higher ATF4 expression in cells stimulated with non-cytokine-suppressive lactobacilli prior to *G. vaginalis* may explain why IL-6 responses were higher compared to cells pre-treated with cytokine-suppressive lactobacilli. Furthermore, the upregulation of TMEM2 in VK2 cells pre-treated with non-cytokine-suppressive lactobacilli, could suggest that the increased proinflammatory response observed in these cells may be linked to increased ER stress. However, additional research is needed to fully understand the role of TMEM2 in inflammatory responses and ER stress in VK2 cells.

4.4.5 Differential expression of genes involved in epithelial barrier function in VK2 cells co-cultured with Lactobacillus spp. *and G. vaginalis in combination*

Dickkopf Wnt signaling pathway inhibitor 1 (DKK1) was downregulated in VK2 cells co-cultured with cytokine-suppressive LM4 and *G. vaginalis* in combination, compared to co-culture with *G. vaginalis* only. DKK1 is a Wnt antagonist, inhibiting the Wnt signaling pathway (237). Wnt signaling is important to maintain epithelial homeostasis and the inhibition of this pathway has resulted in crypt loss and tissue degradation in the context of colitis (238). The Wnt signaling pathway may be "a driver of injury repair" as it is integrated with proinflammatory signaling pathways, such as the NF-κB pathway and was found to inhibit NF-κB in colonic epithelial cells (219,220). Therefore, LM4-induced downregulation of DKK1 in VK2 cells and potential subsequent uninhibited Wnt signaling may be beneficial for the maintenance of epithelial homeostasis and reduced tissue degradation in the FGT. In addition, inhibited Wnt signaling may also lead to greater NF-κB inhibition in this culture system, as discussed above. Taken together with the downregulation of SAMD9L (which may also inhibit the Wnt signalling pathway discussed above), in VK2 cells pre-treated with cytokine-suppressive lactobacilli discussed above, the potential upregulation of the Wnt signaling pathway may be a crucial immunomodulatory and epithelial barrier protection mechanism utilized by these vaginal lactobacilli. Future studies with specific focus on this pathway and its mediators would be useful.

E74 like ETS transcription factor 3 (ELF3) and solute carrier family 26, member 9 (SLC26A9) were upregulated in VK2 cells co-cultured with cytokine-suppressive LM4 and *G. vaginalis* in combination compared to co-culture with *G. vaginalis* only. Interestingly, slight increases in these genes were also observed following co-culture with cytokine-suppressive LM2 and LV4, however not significantly. ELF3 is mostly involved in cell differentiation, proliferation and cell transformation (239). ELF3 has been shown to activate claudin-7, an essential component of epithelial tight junctions (240). Claudin-7 is a "pore-sealing" protein that increases the tightness of the epithelial monolayer marked by increased transepithelial electrical resistance (240). Thus, increased expression of ELF3 may result in increased claudin-7 activation and a strengthened epithelial barrier. Thus, upregulation of ELF3 in VK2 cells co-cultured with the cytokine-suppressive lactobacilli LM4 and *G. vaginalis* in combination and to a lesser extent LM2 and LV4, potentially increases epithelial barrier integrity in the presence of *G. vaginalis,* which would otherwise disrupt the epithelial barrier.

Similarly, SLC26A9 potentially plays a role in the epithelial barrier function of the FGT through its importance in mucus function. SLC26A9 is a coupled Cl^--HCO_3^- anion exchanger that is expressed on epithelial cells and is vital for epithelial function (241). Anion channels play important roles in mucus function. Mucus composition is 79% water and 3% solids, which is mainly comprised of mucins which are secreted in a dehydrated form. Thus, anion channel activity is needed to provide chloride and bicarbonate ions which ensure the mucus gel layer undergoes correct salination, hydration and proper pH regulation (242). Vaginal mucus viscosity, composition and pH are important for defence against pathogens, as well as fertility (64,243). Hence, the LM4 *Lactobacillus* sp. may potentially promote a favourable mucus environment in the FGT, promoting optimal microbial defence and fertility. Future studies to assess the influence of SLC26A9 expression on vaginal mucus consistency and function *in vivo* would be useful.

4.4. 6 Genes involved in preterm birth upregulated in VK2 cells co-cultured with non-cytokine suppressive LJ3 and G. vaginalis in combination

Members of the aldo-keto reductase family 1 (AKR1, AKR1C1-AKR1C3) were upregulated in VK2 cells co-cultured with the non-cytokine-suppressive lactobacilli LJ3 and *G. vaginalis* compared to co-culture with *G. vaginalis* only. AKR1 enzymes play an important role in steroid hormone, prostaglandin and xenobiotic metabolism (244). Wang *et al.* (2007) (244) found that AKR1 expression *in vitro* was closely related to chronic inflammatory conditions and that IL-6 induced AKR1C1 and AKR1C2 expression. Thus, it is likely that the pro-inflammatory conditions observed in VK2 co-culture with LJ3 and *G. vaginalis* in combination, induced AKR1

gene expression. However, whether these enzymes contribute to the lack of cytokine suppressive ability of LJ3 is unknown. Interestingly, AKR1 enzymes metabolize progesterone, thus causing a decrease in progesterone levels (245,246). Progesterone is vital for the maintenance of pregnancy and a reduced level in the FGT is linked to preterm birth (246,247). However, increased progesterone in the luteal phase of the menstrual cycle is associated with leukocyte recruitment to the endometrium and an increase in cervical CCR5+ CD4+ T cell populations (248,249). Hence, colonization by *Lactobacillus* sp. that cause increased AKR1 expression in the FGT may result in decreased progesterone levels in the FGT that may increase the risk of preterm birth. However, this may be accompanied by reduced HIV target cell recruitment and hence reduced risk of HIV acquisition. Furthermore, AKR1 displays prostaglandin-F synthase activity (244). During labour, prostaglandins induce uterine contractions and cervical ripening, and prostaglandin synthase inhibitors prolong pregnancy by reducing uterine activity (250,251). Moreover, prostaglandins are important mediators in inflammation and nonsteroidal anti-inflammatories reduce inflammation by blocking prostaglandin synthesis (252). Hence, taken together with the knowledge that inflammation in the FGT is associated with preterm birth (17), the upregulation of AKR1 by certain lactobacilli may increase prostaglandin-induced uterine activity and preterm birth. Increased prostaglandin synthesis and inflammation may result in increased risk of HIV acquisition, although the combined impact of reduced progesterone (and hence HIV targets cells) together with increased inflammatory responses is unclear. Nonetheless, it appears that the non-cytokine suppressive LJ3 may not beneficial for favourable reproductive outcomes in the FGT.

4.5 Limitations

Although the findings of this study have provided an improved understanding of gene expression patterns in the FGT compared to peripheral blood of HIV infected women, the sample size for the CMC compared to PBMC analysis was small. In addition, the study did not include samples obtained from HIV negative women. Future studies which include a larger sample size and HIV negative women will be useful to improve the power of the study and to improve the current understanding of the effect of HIV infection on gene expression patterns in the FGT.

Although this study has provided novel insight into the immunomodulatory mechanisms of vaginal *Lactobacillus* spp. obtained from South African women, the *in vitro* model system used transformed vaginal epithelial cells and future research including primary cells would increase

the biological relevance of the findings. In addition, the *in vitro* model used is very simplified, as immune cells, which also contribute to inflammatory responses *in vivo*, were not included and the effects of single bacterial strains, as opposed to complex microbial communities, were evaluated. Moreover, inflammatory responses are highly strain specific, thus future research which includes additional *G. vaginalis* strains would be useful. The main purpose of this study was to understand how lactobacilli modulate inflammatory responses, rather than assess the efficacy of the *Lactobacillus* isolates as probiotic candidates, hence the *in vitro* model was more indicative of the change from an optimal to a non-optimal vaginal microbiome state. However, future studies including a modified *in vitro* method to add *G. vaginalis* to cell cultures prior to lactobacilli would be useful to elucidate these *Lactobacillus* spp. as candidates for BV adjunctive treatment. Notably, this study was cross-sectional, thus future research should include a time-course experiment to fully elucidate the bacterial growth, metabolite production and inflammatory responses in the cell culture system at varying time points. This study identified host key genes downregulated and upregulated by lactobacilli which should be validated using quantitative polymerase chain reaction assays.

To focus on a greater effect size in gene expression changes, a logFC less than or equal to -1.5 or greater than or equal to 1.5 was used to detect differentially downregulated or upregulated genes, respectively. However, logFC cutoffs of -1.2 or 1.2 would also be appropriate to detect differentially downregulated or upregulated genes. Future work will include both logFC cutoffs for comparison.

4.6 Conclusion

The findings of this study have improved our understanding of gene expression patterns in the FGT and the immunomodulatory mechanisms of South African vaginal *Lactobacillus* species. Immune cells isolated from the FGTs of HIV-infected women were found to be highly inflammatory compared to PBMCs, with a signature of reduced potential for adaptive immunity. It was found that the immunomodulatory properties of different *Lactobacillus* strains were highly divergent, with different strains inducing varying inflammatory mediators. This suggests that detailed characterisation of individual isolates is critical for selection of optimal biotherapeutics aimed at reducing HIV infection risk and improving reproductive health. It was however found that there were several genes that were commonly downregulated, as well as upregulated, in response to cytokine-suppressive and non-cytokine suppressive isolates. These are perhaps key genes that could be specifically targeted to reduce aberrant

inflammation. In the future it would be interesting to compare the expression of these genes in CMCs from women with *Lactobacillus*-dominant microbiota to those with BV. In addition to improving our understanding of the immunomodulatory properties of lactobacilli, this study further provides insight into the inflammatory mechanisms of *G. vaginalis*, which are largely unknown at present. These results could potentially be harnessed to improve prevention strategies for HIV and poor reproductive outcomes.

References

1. Vitali D, Wessels JM, Kaushic C. Role of sex hormones and the vaginal microbiome in susceptibility and mucosal immunity to HIV-1 in the female genital tract. AIDS Res Ther [Internet]. 2017 Sep 12;14:39. Available from: http://www.ncbi.nlm.nih.gov/pmc/articles/PMC5594427/

2. Eschenbach DA, Davick PR, Williams BL, Klebanoff SJ, Young-Smith K, Critchlow CM, et al. Prevalence of hydrogen peroxide-producing Lactobacillus species in normal women and women with bacterial vaginosis. J Clin Microbiol [Internet]. 1989 Feb;27(2):251–6. Available from: http://www.ncbi.nlm.nih.gov/pmc/articles/PMC267286/

3. Atassi F, Brassart D, Grob P, Graf F, Servin AL. Lactobacillus strains isolated from the vaginal microbiota of healthy women inhibit Prevotella bivia and Gardnerella vaginalis in coculture and cell culture. FEMS Immunol Med Microbiol [Internet]. 2006 Oct 24;48(3):424–32. Available from: https://doi.org/10.1111/j.1574-695X.2006.00162.x

4. Cadieux P, Burton J, E D, G R. Lactobacillus by-products inhibit the growth and virulence of uropathogenic Escherichia coli. J Physiol Pharmacol. 2009;60(6):13–28.

5. O'Hanlon DE, Moench TR, Cone RA. In vaginal fluid, bacteria associated with bacterial vaginosis can be suppressed with lactic acid but not hydrogen peroxide. BMC Infect Dis [Internet]. 2011 Jul 19;11:200. Available from: http://www.ncbi.nlm.nih.gov/pmc/articles/PMC3161885/

6. De Gregorio PR, Tomás MSJ, Terraf MCL, Nader-Macías MEF. In vitro and in vivo effects of beneficial vaginal lactobacilli on pathogens responsible for urogenital tract infections. J Med Microbiol [Internet]. 2014;63(5):685–96. Available from: http://jmm.microbiologyresearch.org/content/journal/jmm/10.1099/jmm.0.069401-0

7. Jang S-E, Jeong J-J, Choi S-Y, Kim H, Han MJ, Kim D-H. Lactobacillus rhamnosus HN001 and Lactobacillus acidophilus La-14 Attenuate Gardnerella vaginalis-Infected Bacterial Vaginosis in Mice. Nutrients [Internet]. 2017 Jun 23;9(6):531. Available from: http://www.ncbi.nlm.nih.gov/pmc/articles/PMC5490510/

8. Kaewsrichan J, Peeyananjarassri K, Kongprasertkit J. Selection and identification of anaerobic lactobacilli producing inhibitory compounds against vaginal pathogens. FEMS Immunol Med Microbiol [Internet]. 2006 Jul 11;48(1):75–83. Available from:

https://doi.org/10.1111/j.1574-695X.2006.00124.x

9. Ravel J, Gajer P, Abdo Z, Schneider GM, Koenig SSK, McCulle SL, et al. Vaginal microbiome of reproductive-age women. Proc Natl Acad Sci U S A [Internet]. 2011 Mar 15;108(Suppl 1):4680–7. Available from: http://www.ncbi.nlm.nih.gov/pmc/articles/PMC3063603/

10. Jespers V, Crucitti T, Menten J, Verhelst R, Mwaura M, Mandaliya K, et al. Prevalence and Correlates of Bacterial Vaginosis in Different Sub-Populations of Women in Sub-Saharan Africa: A Cross-Sectional Study. Fredricks DN, editor. PLoS One [Internet]. 2014 Oct 7;9(10):e109670. Available from: http://www.ncbi.nlm.nih.gov/pmc/articles/PMC4188821/

11. Atashili J, Poole C, Ndumbe PM, Adimora AA, Smith JS. Bacterial vaginosis and HIV acquisition: A meta-analysis of published studies. AIDS [Internet]. 2008 Jul 31;22(12):1493–501. Available from: http://www.ncbi.nlm.nih.gov/pmc/articles/PMC2788489/

12. Low N, Chersich MF, Schmidlin K, Egger M, Francis SC, H. H. M. van de Wijgert J, et al. Intravaginal Practices, Bacterial Vaginosis, and HIV Infection in Women: Individual Participant Data Meta-analysis. Mofenson L, editor. PLoS Med [Internet]. 2011 Feb 15;8(2):e1000416. Available from: http://www.ncbi.nlm.nih.gov/pmc/articles/PMC3039685/

13. Deese J, Masson L, Miller W, Cohen M, Morrison C, Wang M, et al. Injectable Progestin-Only Contraception is Associated With Increased Levels of Pro-Inflammatory Cytokines in the Female Genital Tract. Am J Reprod Immunol [Internet]. 2015 Jul 22;74(4):357–67. Available from: https://doi.org/10.1111/aji.12415

14. Klatt NR, Cheu R, Birse K, Zevin AS, Perner M, Noël-Romas L, et al. Vaginal bacteria modify HIV tenofovir microbicide efficacy in African women. Science (80-) [Internet]. 2017 Jun 2;356(6341):938 LP – 945. Available from: http://science.sciencemag.org/content/356/6341/938.abstract

15. McKinnon LR, Liebenberg LJ, Yende-Zuma N, Archary D, Ngcapu S, Sivro A, et al. Genital inflammation undermines the effectiveness of tenofovir gel in preventing HIV acquisition in women. Nat Med [Internet]. 2018 Feb 26;24:491. Available from: http://dx.doi.org/10.1038/nm.4506

16. Borges S, Silva J, Teixeira P. The role of lactobacilli and probiotics in maintaining

vaginal health. Arch Gynecol Obstet [Internet]. 2014;289(3):479–89. Available from: https://doi.org/10.1007/s00404-013-3064-9

17. Hamilton S, Oomomian Y, Stephen G, Shynlova O, Tower CL, Garrod A, et al. Macrophages Infiltrate the Human and Rat Decidua During Term and Preterm Labor: Evidence That Decidual Inflammation Precedes Labor1. Biol Reprod [Internet]. 2012 Feb 1;86(2):1-9,1-39,39. Available from: http://dx.doi.org/10.1095/biolreprod.111.095505

18. Herrera CA, Stoerker J, Carlquist J, Stoddard GJ, Jackson M, Esplin S, et al. Cell-free DNA, inflammation, and the initiation of spontaneous term labor. Am J Obstet Gynecol [Internet]. 2017;217(5):583.e1-583.e8. Available from: http://www.sciencedirect.com/science/article/pii/S0002937817306361

19. van de Wijgert JHHM, Borgdorff H, Verhelst R, Crucitti T, Francis S, Verstraelen H, et al. The Vaginal Microbiota: What Have We Learned after a Decade of Molecular Characterization? Fredricks DN, editor. PLoS One [Internet]. 2014 Aug 22;9(8):e105998. Available from: http://www.ncbi.nlm.nih.gov/pmc/articles/PMC4141851/

20. Masson L, Arnold KB, Little F, Mlisana K, Lewis DA, Mkhize N, et al. Inflammatory cytokine biomarkers to identify women with asymptomatic sexually transmitted infections and bacterial vaginosis who are at high risk of HIV infection. Sex Transm Infect [Internet]. 2016 May 1;92(3):186 LP – 193. Available from: http://sti.bmj.com/content/92/3/186.abstract

21. Gosmann C, Anahtar MN, Handley SA, Farcasanu M, Abu-Ali G, Bowman BA, et al. Lactobacillus-Deficient Cervicovaginal Bacterial Communities are Associated with Increased HIV Acquisition in Young South African Women. Immunity [Internet]. 2017 Jan 17;46(1):29–37. Available from: http://www.ncbi.nlm.nih.gov/pmc/articles/PMC5270628/

22. Shisana O, Rehle T, Simbayi LC, Zuma K, Jooste S, Zungu N, et al. South African national HIV prevalence, incidence and behaviour survey, 2012 [Internet]. Cape Town: HSRC Press; 2014. Available from: http://hdl.handle.net/20.500.11910/2490

23. Chawanpaiboon S, Vogel JP, Moller A-B, Lumbiganon P, Petzold M, Hogan D, et al. Global, regional, and national estimates of levels of preterm birth in 2014: a systematic review and modelling analysis. Lancet Glob Heal. 2019 Jan;7(1):e37–46.

24. Luu TM, Rehman Mian MO, Nuyt AM. Long-Term Impact of Preterm Birth: Neurodevelopmental and Physical Health Outcomes. Clin Perinatol. 2017 Jun;44(2):305–14.

25. Anyalechi GE, Hong J, Kreisel K, Torrone E, Boulet S, Gorwitz R, et al. Self-Reported Infertility and Associated Pelvic Inflammatory Disease Among Women of Reproductive Age-National Health and Nutrition Examination Survey, United States, 2013-2016. Sex Transm Dis. 2019 Jul;46(7):446–51.

26. Haggerty CL, Totten PA, Tang G, Astete SG, Ferris MJ, Norori J, et al. Identification of novel microbes associated with pelvic inflammatory disease and infertility. Sex Transm Infect. 2016 Sep;92(6):441–6.

27. Abramov V, Khlebnikov V, Kosarev I, Bairamova G, Vasilenko R, Suzina N, et al. Probiotic Properties of Lactobacillus crispatus 2,029: Homeostatic Interaction with Cervicovaginal Epithelial Cells and Antagonistic Activity to Genitourinary Pathogens. Probiotics Antimicrob Proteins [Internet]. 2014;6(3):165–76. Available from: https://doi.org/10.1007/s12602-014-9164-4

28. Hearps AC, Tyssen D, Srbinovski D, Bayigga L, Diaz DJD, Aldunate M, et al. Vaginal lactic acid elicits an anti-inflammatory response from human cervicovaginal epithelial cells and inhibits production of pro-inflammatory mediators associated with HIV acquisition. Mucosal Immunol [Internet]. 2017 Apr 12;10:1480. Available from: http://dx.doi.org/10.1038/mi.2017.27

29. Chetwin E, Manhanzva M, Abrahams A, Froissart R, Gamieldien H, Jaspan H, et al. Antimicrobial and inflammatory properties of South African clinical Lactobacillus isolates and vaginal probiotics. Sci Rep. 2019 Dec 1;9.

30. Coudeyras S, Jugie G, Vermerie M, Forestier C. Adhesion of Human Probiotic Lactobacillus rhamnosus to Cervical and Vaginal Cells and Interaction with Vaginosis-Associated Pathogens. Infect Dis Obstet Gynecol [Internet]. 2008 Jan 27;2008:549640. Available from: http://www.ncbi.nlm.nih.gov/pmc/articles/PMC2631649/

31. Pendharkar S, Magopane T, Larsson P-G, Bruyn G de, Gray GE, Hammarström L, et al. Identification and characterisation of vaginal lactobacilli from South African women. BMC Infect Dis [Internet]. 2013 Jan 26;13:43. Available from: http://www.ncbi.nlm.nih.gov/pmc/articles/PMC3600991/

32. Jespers V, Kyongo J, Joseph S, Hardy L, Cools P, Crucitti T, et al. A longitudinal analysis of the vaginal microbiota and vaginal immune mediators in women from sub-Saharan Africa. Sci Rep [Internet]. 2017 Sep 20;7:11974. Available from: http://www.ncbi.nlm.nih.gov/pmc/articles/PMC5607244/

33. Campisciano G, Zanotta N, Licastro D, De Seta F, Comar M. In vivo microbiome and associated immune markers: New insights into the pathogenesis of vaginal dysbiosis. Sci Rep [Internet]. 2018 Feb 2;8:2307. Available from: http://www.ncbi.nlm.nih.gov/pmc/articles/PMC5797242/

34. Verstraelen H, Verhelst R, Claeys G, De Backer E, Temmerman M, Vaneechoutte M. Longitudinal analysis of the vaginal microflora in pregnancy suggests that L. crispatus promotes the stability of the normal vaginal microflora and that L. gasseri and/or L. iners are more conducive to the occurrence of abnormal vaginal microflora. BMC Microbiol [Internet]. 2009 Jun 2;9:116. Available from: http://www.ncbi.nlm.nih.gov/pmc/articles/PMC2698831/

35. van Houdt R, Ma B, Bruisten SM, Ravel AGCLSJ, Vries HJC de. Lactobacillus iners-dominated vaginal microbiota is associated with increased susceptibility to Chlamydia trachomatis infection in Dutch women: a case–control study. Sex Transm Infect [Internet]. 2018;94(2):117–23. Available from: http://dx.doi.org.ezproxy.uct.ac.za/10.1136/sextrans-2017-053133

36. Hütt P, Lapp E, Štšepetova J, Smidt I, Taelma H, Borovkova N, et al. Characterisation of probiotic properties in human vaginal lactobacilli strains. Microb Ecol Health Dis [Internet]. 2016 Aug 12;27:10.3402/mehd.v27.30484. Available from: http://www.ncbi.nlm.nih.gov/pmc/articles/PMC4985617/

37. Nugent RP, Krohn MA, Hillier SL. Reliability of diagnosing bacterial vaginosis is improved by a standardized method of gram stain interpretation. J Clin Microbiol [Internet]. 1991 Feb;29(2):297–301. Available from: http://www.ncbi.nlm.nih.gov/pmc/articles/PMC269757/

38. Muzny CA, Schwebke JR. Pathogenesis of Bacterial Vaginosis: Discussion of Current Hypotheses. J Infect Dis [Internet]. 2016 Aug 15;214(Suppl 1):S1–5. Available from: http://www.ncbi.nlm.nih.gov/pmc/articles/PMC4957507/

39. Sheiness D, Dix K, Watanabe S, Hillier SL. High levels of Gardnerella vaginalis detected with an oligonucleotide probe combined with elevated pH as a diagnostic indicator of bacterial vaginosis. J Clin Microbiol [Internet]. 1992 Mar;30(3):642–8.

Available from: http://www.ncbi.nlm.nih.gov/pmc/articles/PMC265125/

40. Pino A, Giunta G, Randazzo CL, Caruso S, Caggia C, Cianci A. Bacterial biota of women with bacterial vaginosis treated with lactoferrin: an open prospective randomized trial. Microb Ecol Health Dis [Internet]. 2017 Jan 1;28(1):1357417. Available from: http://www.ncbi.nlm.nih.gov/pmc/articles/PMC5614382/

41. Hickey RJ, Forney LJ. Gardnerella vaginalis does not always cause Bacterial Vaginosis. J Infect Dis [Internet]. 2014 Nov 15;210(10):1682–3. Available from: http://www.ncbi.nlm.nih.gov/pmc/articles/PMC4334793/

42. Machado D, Castro J, Martinez-de-Oliveira J, Nogueira-Silva C, Cerca N. Prevalence of bacterial vaginosis in Portuguese pregnant women and vaginal colonization by Gardnerella vaginalis. Mastrolia SA, editor. PeerJ [Internet]. 2017 Jun 21;5:e3750. Available from: http://www.ncbi.nlm.nih.gov/pmc/articles/PMC5580382/

43. Janulaitiene M, Paliulyte V, Grinceviciene S, Zakareviciene J, Vladisauskiene A, Marcinkute A, et al. Prevalence and distribution of Gardnerella vaginalis subgroups in women with and without bacterial vaginosis. BMC Infect Dis [Internet]. 2017 Jun 5;17:394. Available from: http://www.ncbi.nlm.nih.gov/pmc/articles/PMC5460423/

44. Machado A, Jefferson KK, Cerca N. Interactions between Lactobacillus crispatus and Bacterial Vaginosis (BV)-Associated Bacterial Species in Initial Attachment and Biofilm Formation. Int J Mol Sci [Internet]. 2013 Jun 5;14(6):12004–12. Available from: http://www.ncbi.nlm.nih.gov/pmc/articles/PMC3709769/

45. Machado D, Castro J, Palmeira-de-Oliveira A, Martinez-de-Oliveira J, Cerca N. Bacterial Vaginosis Biofilms: Challenges to Current Therapies and Emerging Solutions. Front Microbiol [Internet]. 2015 Jan 20;6:1528. Available from: http://www.ncbi.nlm.nih.gov/pmc/articles/PMC4718981/

46. Castro J, Alves P, Sousa C, Cereija T, França Â, Jefferson KK, et al. Using an in-vitro biofilm model to assess the virulence potential of Bacterial Vaginosis or non-Bacterial Vaginosis Gardnerella vaginalis isolates. Sci Rep [Internet]. 2015 Jun 26;5:11640. Available from: http://www.ncbi.nlm.nih.gov/pmc/articles/PMC4481526/

47. Belkaid Y, Hand T. Role of the Microbiota in Immunity and inflammation. Cell [Internet]. 2014 Mar 27;157(1):121–41. Available from: http://www.ncbi.nlm.nih.gov/pmc/articles/PMC4056765/

48. Wagner RD, Johnson SJ. Probiotic lactobacillus and estrogen effects on vaginal

epithelial gene expression responses to Candida albicans. J Biomed Sci [Internet]. 2012 Jun 20;19(1):58. Available from: http://www.ncbi.nlm.nih.gov/pmc/articles/PMC3404894/

49. Hickey DK, Patel M V, Fahey J V, Wira CR. Innate and adaptive immunity at Mucosal Surfaces of the Female Reproductive Tract: Stratification and Integration of Immune Protection against the Transmission of Sexually Transmitted Infections. J Reprod Immunol [Internet]. 2011 Mar 26;88(2):185–94. Available from: http://www.ncbi.nlm.nih.gov/pmc/articles/PMC3094911/

50. Arango Duque G, Descoteaux A. Macrophage cytokines: involvement in immunity and infectious diseases. Front Immunol [Internet]. 2014 Oct 7;5:491. Available from: https://www.ncbi.nlm.nih.gov/pubmed/25339958

51. Dembic Z. Chapter 6 - Cytokines of the Immune System: Interleukins. In: Dembic ZBT-TC of the IS, editor. Amsterdam: Academic Press; 2015. p. 143–239. Available from: http://www.sciencedirect.com/science/article/pii/B9780124199989000067

52. Borthwick LA. The IL-1 cytokine family and its role in inflammation and fibrosis in the lung. Semin Immunopathol. 2016 Jul;38(4):517–34.

53. Mihara M, Hashizume M, Yoshida H, Suzuki M, Shiina M. IL-6/IL-6 receptor system and its role in physiological and pathological conditions. Clin Sci (Lond). 2012 Feb;122(4):143–59.

54. Mayadas TN, Cullere X, Lowell CA. The multifaceted functions of neutrophils. Annu Rev Pathol [Internet]. 2013/09/16. 2014;9:181–218. Available from: https://www.ncbi.nlm.nih.gov/pubmed/24050624

55. Bhavsar I, Miller CS, Al-Sabbagh M. Macrophage Inflammatory Protein-1 Alpha (MIP-1 alpha)/CCL3: As a Biomarker. In: Preedy VR, Patel VB, editors. General Methods in Biomarker Research and their Applications [Internet]. Dordrecht: Springer Netherlands; 2015. p. 223–49. Available from: https://doi.org/10.1007/978-94-007-7696-8_27

56. Fitzgerald KA, O'Neill LAJ, Gearing AJH, Callard RE. MIP-1β. In: Fitzgerald KA, O'Neill LAJ, Gearing AJH, Callard REBT-TCF and W (Second E, editors. Factsbook [Internet]. London: Academic Press; 2001. p. 389–91. Available from: http://www.sciencedirect.com/science/article/pii/B9780121551421500853

57. Schutyser E, Struyf S, Van Damme J. The CC chemokine CCL20 and its receptor

CCR6. Cytokine Growth Factor Rev. 2003 Oct;14(5):409–26.

58. Dufour JH, Dziejman M, Liu MT, Leung JH, Lane TE, Luster AD. IFN-gamma-inducible protein 10 (IP-10; CXCL10)-deficient mice reveal a role for IP-10 in effector T cell generation and trafficking. J Immunol. 2002 Apr;168(7):3195–204.

59. Lee SK, Kim CJ, Kim D-J, Kang J. Immune Cells in the Female Reproductive Tract. Immune Netw [Internet]. 2015 Feb 17;15(1):16–26. Available from: http://www.ncbi.nlm.nih.gov/pmc/articles/PMC4338264/

60. Janssens S, Beyaert R. Role of Toll-Like Receptors in Pathogen Recognition. Clin Microbiol Rev [Internet]. 2003 Oct;16(4):637–46. Available from: http://www.ncbi.nlm.nih.gov/pmc/articles/PMC207104/

61. Tang D, Kang R, Coyne CB, Zeh HJ, Lotze MT. PAMPs and DAMPs: Signal 0s that Spur Autophagy and Immunity. Immunol Rev [Internet]. 2012 Sep;249(1):158–75. Available from: http://www.ncbi.nlm.nih.gov/pmc/articles/PMC3662247/

62. Broz P, Monack DM. Newly described pattern recognition receptors team up against intracellular pathogens. Nat Rev Immunol [Internet]. 2013 Jul 12;13:551. Available from: http://dx.doi.org/10.1038/nri3479

63. Mogensen TH. Pathogen Recognition and Inflammatory Signaling in Innate Immune Defenses. Clin Microbiol Rev [Internet]. 2009 Apr;22(2):240–73. Available from: http://www.ncbi.nlm.nih.gov/pmc/articles/PMC2668232/

64. Amjadi F, Salehi E, Mehdizadeh M, Aflatoonian R. Role of the innate immunity in female reproductive tract. Adv Biomed Res [Internet]. 2014 Jan 9;3:1. Available from: http://www.ncbi.nlm.nih.gov/pmc/articles/PMC3928842/

65. Fazeli A, Bruce C, Anumba DO. Characterization of Toll-like receptors in the female reproductive tract in humans. Hum Reprod [Internet]. 2005 May 1;20(5):1372–8. Available from: http://dx.doi.org/10.1093/humrep/deh775

66. Fichorova RN, Cronin AO, Lien E, Anderson DJ, Ingalls RR. Response to Neisseria gonorrhoeae by Cervicovaginal Epithelial Cells Occurs in the Absence of Toll-Like Receptor 4-Mediated Signaling. J Immunol [Internet]. 2002 Mar 1;168(5):2424 LP – 2432. Available from: http://www.jimmunol.org/content/168/5/2424.abstract

67. Zariffard MR, Novak RM, Lurain N, Sha BE, Graham P, Spear GT. Induction of Tumor

Necrosis Factor–α Secretion and Toll-Like Receptor 2 and 4 mRNA Expression by Genital Mucosal Fluids from Women with Bacterial Vaginosis. J Infect Dis [Internet]. 2005 Jun 1;191(11):1913–21. Available from: http://dx.doi.org/10.1086/429922

68. Hirbod T, Kaldensjö T, Broliden K. In Situ Distribution of HIV-Binding CCR5 and C-Type Lectin Receptors in the Human Endocervical Mucosa. Jin X, editor. PLoS One [Internet]. 2011 Sep 30;6(9):e25551. Available from: http://www.ncbi.nlm.nih.gov/pmc/articles/PMC3184149/

69. Hoving JC, Wilson GJ, Brown GD. Signalling C-Type lectin receptors, microbial recognition and immunity. Cell Microbiol [Internet]. 2014 Feb 10;16(2):185–94. Available from: http://www.ncbi.nlm.nih.gov/pmc/articles/PMC4016756/

70. Konaté A, Yavo W, Kassi FK, Djohan V, Angora EK, Barro-Kiki PC, et al. Aetiologies and contributing factors of vulvovaginal candidiasis in Abidjan (Cote d'Ivoire). J Mycol Med [Internet]. 2014;24(2):93–9. Available from: http://www.sciencedirect.com/science/article/pii/S115652331300200X

71. Babula O, Lazdane G, Kroica J, Ledger WJ, Witkin SS. Relation between Recurrent Vulvovaginal Candidiasis, Vaginal Concentrations of Mannose-Binding Lectin, and a Mannose-Binding Lectin Gene Polymorphism in Latvian Women. Clin Infect Dis [Internet]. 2003 Sep 1;37(5):733–7. Available from: http://dx.doi.org/10.1086/377234

72. Giraldo PC, Babula O, Gonçalves AKS, Linhares IM, Amaral RL, Ledger WJ, et al. Mannose-Binding Lectin Gene Polymorphism, Vulvovaginal Candidiasis, and Bacterial Vaginosis. Obstet Gynecol [Internet]. 2007;109(5). Available from: https://journals.lww.com/greenjournal/Fulltext/2007/05000/Mannose_Binding_Lectin_Gene_Polymorphism,.19.aspx

73. Matsumiya T, Stafforini DM. Function and regulation of retinoic acid-inducible gene-I. Crit Rev Immunol. 2010;30(6):489–513.

74. Sathe A, Reddy KVR. TLR9 and RIG-I Signaling in Human Endocervical Epithelial Cells Modulates Inflammatory Responses of Macrophages and Dendritic Cells In Vitro . Kumar A, editor. PLoS One [Internet]. 2014 Jan 7;9(1):e83882. Available from: http://www.ncbi.nlm.nih.gov/pmc/articles/PMC3883652/

75. Franchi L, Warner N, Viani K, Nuñez G. Function of Nod-like Receptors in Microbial Recognition and Host Defense. Immunol Rev [Internet]. 2009 Jan;227(1):106–28. Available from: http://www.ncbi.nlm.nih.gov/pmc/articles/PMC2679989/

76. Newton K, Dixit VM. Signaling in Innate Immunity and Inflammation. Cold Spring Harb Perspect Biol [Internet]. 2012 Mar;4(3):a006049. Available from: http://www.ncbi.nlm.nih.gov/pmc/articles/PMC3282411/

77. Karin M. How NF-κB is activated: the role of the IκB kinase (IKK) complex. Oncogene [Internet]. 1999 Nov 22;18:6867. Available from: http://dx.doi.org/10.1038/sj.onc.1203219

78. Hommes DW, Peppelenbosch MP, van Deventer SJH. Mitogen activated protein (MAP) kinase signal transduction pathways and novel anti-inflammatory targets. Gut [Internet]. 2003 Jan 3;52(1):144–51. Available from: http://www.ncbi.nlm.nih.gov/pmc/articles/PMC1773518/

79. Ono K, Han J. The p38 signal transduction pathway Activation and function. Cell Signal [Internet]. 2000;12(1):1–13. Available from: http://www.sciencedirect.com/science/article/pii/S0898656899000716

80. Kim Y-G, Ohta T, Takahashi T, Kushiro A, Nomoto K, Yokokura T, et al. Probiotic Lactobacillus casei activates innate immunity via NF-kappaB and p38 MAP kinase signaling pathways. Microbes Infect. 2006 Apr;8(4):994–1005.

81. Anahtar MN, Byrne EH, Doherty KE, Bowman BA, Yamamoto HS, Soumillon M, et al. Cervicovaginal bacteria are a major modulator of host inflammatory responses in the female genital tract. Immunity [Internet]. 2015 May 19;42(5):965–76. Available from: http://www.ncbi.nlm.nih.gov/pmc/articles/PMC4461369/

82. Masson L, Passmore J-AS, Liebenberg LJ, Werner L, Baxter C, Arnold KB, et al. Genital Inflammation and the Risk of HIV Acquisition in Women. Clin Infect Dis An Off Publ Infect Dis Soc Am [Internet]. 2015 Jul 15;61(2):260–9. Available from: http://www.ncbi.nlm.nih.gov/pmc/articles/PMC4565995/

83. Masson L, Mlisana K, Little F, Werner L, Mkhize NN, Ronacher K, et al. Defining genital tract cytokine signatures of sexually transmitted infections and bacterial vaginosis in women at high risk of HIV infection: a cross-sectional study. Sex Transm Infect [Internet]. 2014 Dec 1;90(8):580 LP – 587. Available from: http://sti.bmj.com/content/90/8/580.abstract

84. Kyongo JK, Crucitti T, Menten J, Hardy L, Cools P, Michiels J, et al. Cross-Sectional Analysis of Selected Genital Tract Immunological Markers and Molecular Vaginal Microbiota in Sub-Saharan African Women, with Relevance to HIV Risk and

Prevention. Hodinka RL, editor. Clin Vaccine Immunol [Internet]. 2015 May 28;22(5):526–38. Available from: http://www.ncbi.nlm.nih.gov/pmc/articles/PMC4412937/

85. Arnold KB, Burgener A, Birse K, Romas L, Dunphy LJ, Shahabi K, et al. Increased levels of inflammatory cytokines in the female reproductive tract are associated with altered expression of proteases, mucosal barrier proteins, and an influx of HIV-susceptible target cells. Mucosal Immunol [Internet]. 2015 Jun 24;9:194. Available from: http://dx.doi.org/10.1038/mi.2015.51

86. Santos CMA, Pires MC V, Leão TL, Silva AKS, Miranda LS, Martins FS, et al. Anti-inflammatory effect of two Lactobacillus strains during infection with Gardnerella vaginalis and Candida albicans in a HeLa cell culture model. Microbiology [Internet]. 2018;164(3):349–58. Available from: http://mic.microbiologyresearch.org/content/journal/micro/10.1099/mic.0.000608

87. Sierra L-J, Brown AG, Barilá GO, Anton L, Barnum CE, Shetye SS, et al. Colonization of the cervicovaginal space with Gardnerella vaginalis leads to local inflammation and cervical remodeling in pregnant mice. Fredricks DN, editor. PLoS One [Internet]. 2018 Jan 18;13(1):e0191524. Available from: http://www.ncbi.nlm.nih.gov/pmc/articles/PMC5773211/

88. Zhu X, Wang M, Mavi P, Rayapudi M, Pandey AK, Kaul A, et al. Interleukin-15 expression is increased in human eosinophilic esophagitis and mediates pathogenesis in mice. Gastroenterology [Internet]. 2010 Jul 8;139(1):182-93.e7. Available from: http://www.ncbi.nlm.nih.gov/pmc/articles/PMC4116278/

89. Rückert R, Brandt K, Ernst M, Marienfeld K, Csernok E, Metzler C, et al. Interleukin-15 stimulates macrophages to activate CD4(+) T cells: a role in the pathogenesis of rheumatoid arthritis? Immunology [Internet]. 2009 Jan 12;126(1):63–73. Available from: http://www.ncbi.nlm.nih.gov/pmc/articles/PMC2632696/

90. Selhorst P, Combrinck C, Ndabambi N, Ismail SD, Abrahams M-R, Lacerda M, et al. Replication Capacity of Viruses from Acute Infection Drives HIV-1 Disease Progression. Kirchhoff F, editor. J Virol [Internet]. 2017 Apr 15;91(8):e01806-16. Available from: http://www.ncbi.nlm.nih.gov/pmc/articles/PMC5375681/

91. Hiscott J, Kwon H, Génin P. Hostile takeovers: viral appropriation of the NF-kB pathway. J Clin Invest [Internet]. 2001 Jan 15;107(2):143–51. Available from: http://www.ncbi.nlm.nih.gov/pmc/articles/PMC199181/

92. Mitchell C, Hitti J, Paul K, Agnew K, Cohn SE, Luque AE, et al. Cervicovaginal Shedding of HIV Type 1 Is Related to Genital Tract Inflammation Independent of Changes in Vaginal Microbiota. AIDS Res Hum Retroviruses [Internet]. 2011 Jan;27(1):35–9. Available from: http://www.ncbi.nlm.nih.gov/pmc/articles/PMC3034096/

93. Mitchell C, Balkus JE, Fredricks D, Liu C, McKernan-Mullin J, Frenkel LM, et al. Interaction Between Lactobacilli, Bacterial Vaginosis-Associated Bacteria, and HIV Type 1 RNA and DNA Genital Shedding in U.S. and Kenyan Women. AIDS Res Hum Retroviruses [Internet]. 2013 Jan;29(1):13–9. Available from: http://www.ncbi.nlm.nih.gov/pmc/articles/PMC3537306/

94. Gelber SE, Aguilar JL, Lewis KLT, Ratner AJ. Functional and Phylogenetic Characterization of Vaginolysin, the Human-Specific Cytolysin from Gardnerella vaginalis . J Bacteriol [Internet]. 2008 Jun 4;190(11):3896–903. Available from: http://www.ncbi.nlm.nih.gov/pmc/articles/PMC2395025/

95. Abdelmaksoud AA, Girerd PH, Garcia EM, Brooks JP, Leftwich LM, Sheth NU, et al. Association between statin use, the vaginal microbiome, and Gardnerella vaginalis vaginolysin-mediated cytotoxicity. Fredricks DN, editor. PLoS One [Internet]. 2017 Aug 28;12(8):e0183765. Available from: http://www.ncbi.nlm.nih.gov/pmc/articles/PMC5573284/

96. Shen R, Richter HE, Smith PD. Interactions between HIV-1 and Mucosal Cells in the Female Reproductive Tract. Am J Reprod Immunol [Internet]. 2014 Jun 1;71(6):608–17. Available from: http://www.ncbi.nlm.nih.gov/pmc/articles/PMC4073589/

97. Rizzo A, Fiorentino M, Buommino E, Donnarumma G, Losacco A, Bevilacqua N. Lactobacillus crispatus mediates anti-inflammatory cytokine interleukin-10 induction in response to Chlamydia trachomatis infection in vitro. Int J Med Microbiol [Internet]. 2015;305(8):815–27. Available from: http://www.sciencedirect.com/science/article/pii/S1438422115000594

98. Manhanzva MT, Abrahams AG, Gamieldien H, Froissart R, Jaspan H, Jaumdally SZ, et al. Inflammatory and antimicrobial properties differ between vaginal Lactobacillus isolates from South African women with non-optimal versus optimal microbiota. Sci Rep. 2020 Apr;10(1):6196.

99. Finamore A, Roselli M, Imbinto A, Seeboth J, Oswald IP, Mengheri E. Lactobacillus amylovorus Inhibits the TLR4 Inflammatory Signaling Triggered by Enterotoxigenic

Escherichia coli via Modulation of the Negative Regulators and Involvement of TLR2 in Intestinal Caco-2 Cells and Pig Explants. Heimesaat MM, editor. PLoS One [Internet]. 2014 Apr 14;9(4):e94891. Available from: http://www.ncbi.nlm.nih.gov/pmc/articles/PMC3986366/

100. TOBITA K, WATANABE I, SAITO M. Specific vaginal lactobacilli suppress the inflammation induced by lipopolysaccharide stimulation through downregulation of toll-like receptor 4 expression in human embryonic intestinal epithelial cells. Biosci Microbiota, Food Heal [Internet]. 2017 Nov 3;36(1):39–44. Available from: http://www.ncbi.nlm.nih.gov/pmc/articles/PMC5301056/

101. Horton RE, Kaefer N, Songok E, Guijon FB, Kettaf N, Boucher G, et al. A Comparative Analysis of Gene Expression Patterns and Cell Phenotypes between Cervical and Peripheral Blood Mononuclear Cells. Unutmaz D, editor. PLoS One [Internet]. 2009 Dec 14;4(12):e8293. Available from: http://www.ncbi.nlm.nih.gov/pmc/articles/PMC2790076/

102. Zalenskaya IA, Joseph T, Bavarva J, Yousefieh N, Jackson SS, Fashemi T, et al. Gene Expression Profiling of Human Vaginal Cells In Vitro Discriminates Compounds with Pro-Inflammatory and Mucosa-Altering Properties: Novel Biomarkers for Preclinical Testing of HIV Microbicide Candidates. Garcia-Lerma JG, editor. PLoS One [Internet]. 2015 Jun 8;10(6):e0128557. Available from: http://www.ncbi.nlm.nih.gov/pmc/articles/PMC4459878/

103. Lee JM, Hwang K-T, Jun WJ, Park C-S, Lee M-Y. Antiinflammatory effect of lactic acid bacteria: inhibition of cyclooxygenase-2 by suppressing nuclear factor-kappaB in Raw264.7 macrophage cells. J Microbiol Biotechnol. 2008 Oct;18(10):1683–8.

104. Joo H-M, Hyun Y-J, Myoung K-S, Ahn Y-T, Lee J-H, Huh C-S, et al. Lactobacillus johnsonii HY7042 ameliorates Gardnerella vaginalis-induced vaginosis by killing Gardnerella vaginalis and inhibiting NF-κB activation. Int Immunopharmacol [Internet]. 2011;11(11):1758–65. Available from: http://www.sciencedirect.com/science/article/pii/S1567576911002736

105. Tachedjian G, Aldunate M, Bradshaw CS, Cone RA. The role of lactic acid production by probiotic Lactobacillus species in vaginal health. Res Microbiol [Internet]. 2017;168(9):782–92. Available from: http://www.sciencedirect.com/science/article/pii/S0923250817300839

106. Peter K, Rehli M, Singer K, Renner-Sattler K, Kreutz M. Lactic acid delays the

inflammatory response of human monocytes. Biochem Biophys Res Commun [Internet]. 2015;457(3):412–8. Available from: http://www.sciencedirect.com/science/article/pii/S0006291X1500011X

107. Sun K-Y, Xu D-H, Xie C, Plummer S, Tang J, Yang XF, et al. Lactobacillus paracasei modulates LPS-induced inflammatory cytokine release by monocyte-macrophages via the up-regulation of negative regulators of NF-kappaB signaling in a TLR2-dependent manner. Cytokine [Internet]. 2017;92:1–11. Available from: http://www.sciencedirect.com/science/article/pii/S1043466617300030

108. Karlsson M, Scherbak N, Reid G, Jass J. Lactobacillus rhamnosus GR-1 enhances NF-kappaB activation in Escherichia coli-stimulated urinary bladder cells through TLR4. BMC Microbiol [Internet]. 2012 Jan 22;12:15. Available from: http://www.ncbi.nlm.nih.gov/pmc/articles/PMC3305351/

109. Govindarajan R, Duraiyan J, Kaliyappan K, Palanisamy M. Microarray and its applications. J Pharm Bioallied Sci [Internet]. 2012 Aug 1;4(Suppl 2):S310–2. Available from: http://www.ncbi.nlm.nih.gov/pmc/articles/PMC3467903/

110. Barnabas SL, Dabee S, Passmore J-AS, Jaspan HB, Lewis DA, Jaumdally SZ, et al. Converging epidemics of sexually transmitted infections and bacterial vaginosis in southern African female adolescents at risk of HIV. Int J STD AIDS. 2018 May;29(6):531–9.

111. Ahmed A, Earl J, Retchless A, Hillier SL, Rabe LK, Cherpes TL, et al. Comparative Genomic Analyses of 17 Clinical Isolates of Gardnerella vaginalis Provide Evidence of Multiple Genetically Isolated Clades Consistent with Su. J Bacteriol [Internet]. 2012 Aug 1;194(15):3922 LP – 3937. Available from: http://jb.asm.org/content/194/15/3922.abstract

112. Rose WA, McGowin CL, Spagnuolo RA, Eaves-Pyles TD, Popov VL, Pyles RB. Commensal Bacteria Modulate Innate Immune Responses of Vaginal Epithelial Cell Multilayer Cultures. Bereswill S, editor. PLoS One [Internet]. 2012 Mar 7;7(3):e32728. Available from: http://www.ncbi.nlm.nih.gov/pmc/articles/PMC3296736/

113. Pan Du, Gang Feng, Warren A. Kibbe SL. Using lumi, a package processing Illumina Microarray [Internet]. 2010 [cited 2018 Aug 6]. Available from: https://www.bioconductor.org/packages//2.7/bioc/vignettes/lumi/inst/doc/lumi.pdf

114. Illumina. Illumina humanHT-12 v3 annotation file [Internet]. [cited 2018 Aug 20]. Available from: https://emea.support.illumina.com/downloads/humanht-12_v3_product_files.html

115. DAVID. DAVID Bioinformatics [Internet]. Available from: https://david.ncifcrf.gov/

116. Huang DW, Sherman BT, Lempicki RA. Bioinformatics enrichment tools: paths toward the comprehensive functional analysis of large gene lists. Nucleic Acids Res. 2009 Jan;37(1):1–13.

117. Huang DW, Sherman BT, Lempicki RA. Systematic and integrative analysis of large gene lists using DAVID bioinformatics resources. Nat Protoc. 2009;4(1):44–57.

118. Newman AM, Liu CL, Green MR, Gentles AJ, Feng W, Xu Y, et al. Robust enumeration of cell subsets from tissue expression profiles. Nat Methods. 2015 May;12(5):453–7.

119. Aran D, Hu Z, Butte AJ. xCell: digitally portraying the tissue cellular heterogeneity landscape. Genome Biol [Internet]. 2017;18(1):220. Available from: https://doi.org/10.1186/s13059-017-1349-1

120. Columb, M.O. & Sagadai S. Multiple comparisons. Trends Anaesth Crit care. 2006;

121. Klaus B, Reisenauer S. An end to end workflow for differential gene expression using Affymetrix microarrays [version 2; peer review: 2 approved]. F1000Research [Internet]. 2018;5(1384). Available from: http://openr.es/cwn

122. Affymetrix. Clariom S Human annotation file [Internet]. [cited 2019 Nov 15]. Available from: http://www.affymetrix.com/support/technical/byproduct.affx?product=clariom_s_hmr

123. WebGestalt. WebGestalt [Internet]. Available from: http://www.webgestalt.org/

124. Narimatsu R, Wolday D, Patterson BK. IL-8 Increases Transmission of HIV Type 1 in Cervical Explant Tissue. AIDS Res Hum Retroviruses [Internet]. 2005 Mar 1;21(3):228–33. Available from: https://doi.org/10.1089/aid.2005.21.228

125. Liebenberg LJP, Masson L, Arnold KB, Mckinnon LR, Werner L, Proctor E, et al. Genital—Systemic Chemokine Gradients and the Risk of HIV Acquisition in Women. JAIDS J Acquir Immune Defic Syndr [Internet]. 2017;74(3). Available from: https://journals.lww.com/jaids/Fulltext/2017/03010/Genital_Systemic_Chemokine_Gradients_and_the_Risk.13.aspx

126. Lennard K, Dabee S, Barnabas SL, Havyarimana E, Blakney A, Jaumdally SZ, et al. Microbial Composition Predicts Genital Tract Inflammation and Persistent Bacterial Vaginosis in South African Adolescent Females. Infect Immun. 2018 Jan;86(1).

127. Doncel GF, Anderson S, Zalenskaya I. Role of semen in modulating the female genital tract microenvironment--implications for HIV transmission. Am J Reprod Immunol. 2014 Jun;71(6):564–74.

128. Aslan E, Bechelaghem N. To “douche” or not to “douche”: hygiene habits may have detrimental effects on vaginal microbiota. J Obstet Gynaecol J Inst Obstet Gynaecol. 2018 Jul;38(5):678–81.

129. Mitchell C, Balkus JE, McKernan-Mullin J, Cohn SE, Luque AE, Mwachari C, et al. Associations between genital tract infections, genital tract inflammation, and cervical cytobrush HIV-1 DNA in US versus Kenyan women. J Acquir Immune Defic Syndr. 2013 Feb;62(2):143–8.

130. Paciolla M, Boni R, Fusco F, Pescatore A, Poeta L, Ursini M V, et al. Nuclear factor-kappa-B-inhibitor alpha (NFKBIA) is a developmental marker of NF-kappaB/p65 activation during in vitro oocyte maturation and early embryogenesis. Hum Reprod. 2011 May;26(5):1191–201.

131. Lane BR, Lore K, Bock PJ, Andersson J, Coffey MJ, Strieter RM, et al. Interleukin-8 stimulates human immunodeficiency virus type 1 replication and is a potential new target for antiretroviral therapy. J Virol. 2001 Sep;75(17):8195–202.

132. Mehandru S, Poles MA, Tenner-Racz K, Horowitz A, Hurley A, Hogan C, et al. Primary HIV-1 infection is associated with preferential depletion of CD4+ T lymphocytes from effector sites in the gastrointestinal tract. J Exp Med. 2004 Sep;200(6):761–70.

133. Nkwanyana NN, Gumbi PP, Roberts L, Denny L, Hanekom W, Soares A, et al. Impact of human immunodeficiency virus 1 infection and inflammation on the composition and yield of cervical mononuclear cells in the female genital tract. Immunology. 2009 Sep;128(1 Suppl):e746-57.

134. Gumbi PP, Jaumdally SZ, Salkinder AL, Burgers WA, Mkhize NN, Hanekom W, et al. CD4 T Cell Depletion at the Cervix during HIV Infection Is Associated with Accumulation of Terminally Differentiated T Cells. J Virol [Internet]. 2011 Dec 15;85(24):13333 LP – 13341. Available from:

http://jvi.asm.org/content/85/24/13333.abstract

135. Gumbi PP, Nkwanyana NN, Bere A, Burgers WA, Gray CM, Williamson A-L, et al. Impact of mucosal inflammation on cervical human immunodeficiency virus (HIV-1)-specific CD8 T-cell responses in the female genital tract during chronic HIV infection. J Virol. 2008 Sep;82(17):8529–36.

136. Brenchley JM, Schacker TW, Ruff LE, Price DA, Taylor JH, Beilman GJ, et al. CD4+ T cell depletion during all stages of HIV disease occurs predominantly in the gastrointestinal tract. J Exp Med. 2004 Sep;200(6):749–59.

137. Mikulak J, Oriolo F, Zaghi E, Di Vito C, Mavilio D. Natural killer cells in HIV-1 infection and therapy. Vol. 31, AIDS (London, England). 2017. p. 2317–30.

138. Johansson B, Palmer E, Bolliger L. The Extracellular Domain of the ζ-Chain Is Essential for TCR Function. J Immunol [Internet]. 1999 Jan 15;162(2):878 LP – 885. Available from: http://www.jimmunol.org/content/162/2/878.abstract

139. Palacios EH, Weiss A. Function of the Src-family kinases, Lck and Fyn, in T-cell development and activation. Oncogene. 2004 Oct;23(48):7990–8000.

140. Hazeki K, Nigorikawa K, Hazeki O. Role of phosphoinositide 3-kinase in innate immunity. Biol Pharm Bull. 2007 Sep;30(9):1617–23.

141. Zhong Y, Johnson AJ, Byrd JC, Dubovsky JA. Targeting Interleukin-2-Inducible T-cell Kinase (ITK) in T-Cell Related Diseases. Postdoc J a J Postdr Res Postdr Aff [Internet]. 2014 Jun;2(6):1–11. Available from: https://www.ncbi.nlm.nih.gov/pubmed/27917390

142. Trimble LA, Shankar P, Patterson M, Daily JP, Lieberman J. Human immunodeficiency virus-specific circulating CD8 T lymphocytes have down-modulated CD3zeta and CD28, key signaling molecules for T-cell activation. J Virol [Internet]. 2000 Aug;74(16):7320–30. Available from: https://www.ncbi.nlm.nih.gov/pubmed/10906185

143. González-Cabrero J, Wise CJ, Latchman Y, Freeman GJ, Sharpe AH, Reiser H. CD48-deficient mice have a pronounced defect in CD4(+) T cell activation. Proc Natl Acad Sci U S A [Internet]. 1999 Feb 2;96(3):1019–23. Available from: https://www.ncbi.nlm.nih.gov/pubmed/9927686

144. Lovatt M, Filby A, Parravicini V, Werlen G, Palmer E, Zamoyska R. Lck Regulates the

Threshold of Activation in Primary T Cells, While both Lck and Fyn Contribute to the Magnitude of the Extracellular Signal-Related Kinase Response. Mol Cell Biol [Internet]. 2006 Nov 15;26(22):8655 LP – 8665. Available from: http://mcb.asm.org/content/26/22/8655.abstract

145. Chaimowitz NS, Falanga YT, Ryan JJ, Conrad DH. Fyn Kinase Is Required for Optimal Humoral Responses. PLoS One [Internet]. 2013 Apr 8;8(4):e60640. Available from: https://doi.org/10.1371/journal.pone.0060640

146. Appleby L, Nausch N, Bourke C, Mutapi F, Midzi N, Mduluza T, et al. Down regulation of the TCR complex CD3 ζ-chain on CD3+ T cells: a potential mechanism for helminth mediated immune modulation [Internet]. Vol. 6, Frontiers in Immunology . 2015. p. 51. Available from: https://www.frontiersin.org/article/10.3389/fimmu.2015.00051

147. Osińska I, Popko K, Demkow U. Perforin: an important player in immune response. Cent J Immunol [Internet]. 2014/04/17. 2014;39(1):109–15. Available from: https://www.ncbi.nlm.nih.gov/pubmed/26155110

148. Reis Machado J, da Silva MV, Cavellani CL, dos Reis MA, Monteiro MLG dos R, Teixeira V de PA, et al. Mucosal immunity in the female genital tract, HIV/AIDS. Biomed Res Int [Internet]. 2014/09/15. 2014;2014:350195. Available from: https://www.ncbi.nlm.nih.gov/pubmed/25313360

149. Wira CR, Grant-Tschudy KS, Crane-Godreau MA. Epithelial cells in the female reproductive tract: a central role as sentinels of immune protection. Am J Reprod Immunol. 2005 Feb;53(2):65–76.

150. Stanley MA. Epithelial cell responses to infection with human papillomavirus. Clin Microbiol Rev. 2012 Apr;25(2):215–22.

151. Aoki M, Aoki H, Ramanathan R, Hait NC, Takabe K. Sphingosine-1-Phosphate Signaling in Immune Cells and Inflammation: Roles and Therapeutic Potential. Mediators Inflamm. 2016;2016:8606878.

152. Denton AE, Roberts EW, Linterman MA, Fearon DT. Fibroblastic reticular cells of the lymph node are required for retention of resting but not activated CD8+ T cells. Proc Natl Acad Sci U S A. 2014 Aug;111(33):12139–44.

153. Mackay LK, Braun A, Macleod BL, Collins N, Tebartz C, Bedoui S, et al. Cutting edge: CD69 interference with sphingosine-1-phosphate receptor function regulates peripheral T cell retention. J Immunol. 2015 Mar;194(5):2059–63.

154. Kleinman CL, Doria M, Orecchini E, Giuliani E, Galardi S, De Jay N, et al. HIV-1 infection causes a down-regulation of genes involved in ribosome biogenesis. PLoS One. 2014;9(12):e113908.

155. Gibbs A, Leeansyah E, Introini A, Paquin-Proulx D, Hasselrot K, Andersson E, et al. MAIT cells reside in the female genital mucosa and are biased towards IL-17 and IL-22 production in response to bacterial stimulation. Mucosal Immunol. 2017 Jan;10(1):35–45.

156. Jiang J, Kelly KA. Phenotype and function of regulatory T cells in the genital tract. Curr Trends Immunol. 2011;12:89–94.

157. Driscoll KE. Macrophage inflammatory proteins: biology and role in pulmonary inflammation. Exp Lung Res. 1994;20(6):473–90.

158. Macho Fernandez E, Valenti V, Rockel C, Hermann C, Pot B, Boneca IG, et al. Anti-inflammatory capacity of selected lactobacilli in experimental colitis is driven by NOD2-mediated recognition of a specific peptidoglycan-derived muropeptide. Gut. 2011 Aug;60(8):1050–9.

159. Chapot-Chartier M-P, Kulakauskas S. Cell wall structure and function in lactic acid bacteria. Microb Cell Fact. 2014 Aug;13 Suppl 1:S9.

160. Gabay C. Interleukin-6 and chronic inflammation. Arthritis Res Ther. 2006;8 Suppl 2:S3.

161. Barnes TC, Anderson ME, Moots RJ. The many faces of interleukin-6: the role of IL-6 in inflammation, vasculopathy, and fibrosis in systemic sclerosis. Int J Rheumatol. 2011;2011:721608.

162. Allen TC, Kurdowska A. Interleukin 8 and acute lung injury. Arch Pathol Lab Med. 2014 Feb;138(2):266–9.

163. Saitoh T, Komano J, Saitoh Y, Misawa T, Takahama M, Kozaki T, et al. Neutrophil extracellular traps mediate a host defense response to human immunodeficiency virus-1. Cell Host Microbe. 2012 Jul;12(1):109–16.

164. Hensley-McBain T, Klatt NR. The Dual Role of Neutrophils in HIV Infection. Curr HIV/AIDS Rep [Internet]. 2018 Feb;15(1):1–10. Available from: https://www.ncbi.nlm.nih.gov/pubmed/29516266

165. Blanchet F, Moris A, Mitchell JP, Piguet V. A look at HIV journey: from dendritic cells

to infection spread in CD4(+) T cells. Curr Opin HIV AIDS. 2011 Sep;6(5):391–7.

166. Li Q, Estes JD, Schlievert PM, Duan L, Brosnahan AJ, Southern PJ, et al. Glycerol monolaurate prevents mucosal SIV transmission. Nature [Internet]. 2009/03/04. 2009 Apr 23;458(7241):1034–8. Available from: https://www.ncbi.nlm.nih.gov/pubmed/19262509

167. Hashimoto M, Tawaratsumida K, Kariya H, Aoyama K, Tamura T, Suda Y. Lipoprotein is a predominant Toll-like receptor 2 ligand in Staphylococcus aureus cell wall components. Int Immunol [Internet]. 2005 Dec 22;18(2):355–62. Available from: https://doi.org/10.1093/intimm/dxh374

168. Sadhu K, Domingue PA, Chow AW, Nelligan J, Cheng N, Costerton JW. Gardnerella vaginalis has a gram-positive cell-wall ultrastructure and lacks classical cell-wall lipopolysaccharide. J Med Microbiol. 1989 Jul;29(3):229–35.

169. Catlin BW. Gardnerella vaginalis: characteristics, clinical considerations, and controversies. Clin Microbiol Rev. 1992 Jul;5(3):213–37.

170. Marín E, Haesaert A, Padilla L, Adán J, Hernáez ML, Monteoliva L, et al. Unraveling Gardnerella vaginalis Surface Proteins Using Cell Shaving Proteomics [Internet]. Vol. 9, Frontiers in Microbiology . 2018. p. 975. Available from: https://www.frontiersin.org/article/10.3389/fmicb.2018.00975

171. Aroutcheva A, Ling Z, Faro S. Prevotella bivia as a source of lipopolysaccharide in the vagina. Anaerobe [Internet]. 2008/09/20. 2008 Nov;14(5):256–60. Available from: https://www.ncbi.nlm.nih.gov/pubmed/18849004

172. Kawasaki T, Kawai T. Toll-Like Receptor Signaling Pathways [Internet]. Vol. 5, Frontiers in Immunology . 2014. p. 461. Available from: https://www.frontiersin.org/article/10.3389/fimmu.2014.00461

173. Cassandri M, Smirnov A, Novelli F, Pitolli C, Agostini M, Malewicz M, et al. Zinc-finger proteins in health and disease. Cell Death Discov [Internet]. 2017;3(1):17071. Available from: https://doi.org/10.1038/cddiscovery.2017.71

174. Hong J-Y, Bae W-J, Yi J-K, Kim G-T, Kim E-C. Anti-inflammatory and anti-osteoclastogenic effects of zinc finger protein A20 overexpression in human periodontal ligament cells. J Periodontal Res. 2015 Nov 9;51.

175. Evans PC, Ovaa H, Hamon M, Kilshaw PJ, Hamm S, Bauer S, et al. Zinc-finger

protein A20, a regulator of inflammation and cell survival, has de-ubiquitinating activity. Biochem J. 2004 Mar;378(Pt 3):727–34.

176. Ogo OA, Tyson J, Cockell SJ, Howard A, Valentine RA, Ford D. The zinc finger protein ZNF658 regulates the transcription of genes involved in zinc homeostasis and affects ribosome biogenesis through the zinc transcriptional regulatory element. Mol Cell Biol [Internet]. 2015/01/12. 2015 Mar;35(6):977–87. Available from: https://www.ncbi.nlm.nih.gov/pubmed/25582195

177. Wessels I, Maywald M, Rink L. Zinc as a Gatekeeper of Immune Function. Nutrients. 2017 Nov;9(12).

178. Gammoh NZ, Rink L. Zinc in Infection and Inflammation. Nutrients. 2017 Jun;9(6).

179. Foster M, Samman S. Zinc and Regulation of Inflammatory Cytokines: Implications for Cardiometabolic Disease. Vol. 4, Nutrients . 2012.

180. Hongxia L, Yuxiao T, Zhilei S, Yan S, Yicui Q, Jiamin S, et al. Zinc inhibited LPS-induced inflammatory responses by upregulating A20 expression in microglia BV2 cells. J Affect Disord. 2019 Apr;249:136–42.

181. Kanehisa M, Goto S. KEGG: kyoto encyclopedia of genes and genomes. Nucleic Acids Res. 2000 Jan;28(1):27–30.

182. Kanehisa M. Toward understanding the origin and evolution of cellular organisms. Protein Sci. 2019 Nov;28(11):1947–51.

183. Kanehisa M, Sato Y, Furumichi M, Morishima K, Tanabe M. New approach for understanding genome variations in KEGG. Nucleic Acids Res. 2019 Jan;47(D1):D590–5.

184. Hirota Y, Osuga Y, Koga K, Yoshino O, Hirata T, Morimoto C, et al. The expression and possible roles of chemokine CXCL11 and its receptor CXCR3 in the human endometrium. J Immunol. 2006 Dec;177(12):8813–21.

185. Li Q, Sun J, Cao Y, Liu B, Li L, Mohammadtursun N, et al. Bu-Shen-Fang-Chuan formula attenuates T-lymphocytes recruitment in the lung of rats with COPD through suppressing CXCL9/CXCL10/CXCL11-CXCR3 axis. Biomed Pharmacother. 2019 Dec;123:109735.

186. Diamond MS, Farzan M. The broad-spectrum antiviral functions of IFIT and IFITM proteins. Nat Rev Immunol [Internet]. 2012/12/14. 2013 Jan;13(1):46–57. Available

from: https://www.ncbi.nlm.nih.gov/pubmed/23237964

187. Fensterl V, Sen GC. Interferon-Induced Ifit Proteins: Their Role in Viral Pathogenesis. Goff SP, editor. J Virol [Internet]. 2015 Mar 1;89(5):2462 LP – 2468. Available from: http://jvi.asm.org/content/89/5/2462.abstract

188. Berchtold S, Manncke B, Klenk J, Geisel J, Autenrieth IB, Bohn E. Forced IFIT-2 expression represses LPS induced TNF-alpha expression at posttranscriptional levels. BMC Immunol. 2008 Dec;9:75.

189. Bulgari O, Dong X, Roca AL, Caroli AM, Loor JJ. Innate immune responses induced by lipopolysaccharide and lipoteichoic acid in primary goat mammary epithelial cells. J Anim Sci Biotechnol. 2017;8:29.

190. Gao J, Zhao L, Wan YY, Zhu B. Mechanism of Action of IL-7 and Its Potential Applications and Limitations in Cancer Immunotherapy. Int J Mol Sci. 2015 May;16(5):10267–80.

191. Willis CR, Seamons A, Maxwell J, Treuting PM, Nelson L, Chen G, et al. Interleukin-7 receptor blockade suppresses adaptive and innate inflammatory responses in experimental colitis. J Inflamm [Internet]. 2012;9(1):39. Available from: https://doi.org/10.1186/1476-9255-9-39

192. Wang Y, Dai H, Liu Z, Cheng X, Tellides G, Dai Z. Neutralizing IL-7 promotes long-term allograft survival induced by CD40/CD40L costimulatory blockade. Am J Transplant. 2006 Dec;6(12):2851–60.

193. Schreiber M, Weigelt M, Karasinsky A, Anastassiadis K, Schallenberg S, Petzold C, et al. Inducible IL-7 Hyperexpression Influences Lymphocyte Homeostasis and Function and Increases Allograft Rejection. Front Immunol [Internet]. 2019;10:742. Available from: https://www.frontiersin.org/article/10.3389/fimmu.2019.00742

194. Belarif L, Danger R, Kermarrec L, Nerriere-Daguin V, Pengam S, Durand T, et al. IL-7 receptor influences anti-TNF responsiveness and T cell gut homing in inflammatory bowel disease. J Clin Invest. 2019 Apr;129(5):1910–25.

195. Moniuszko M, Edghill-Smith Y, Venzon D, Stevceva L, Nacsa J, Tryniszewska E, et al. Decreased number of CD4+ and CD8+ T cells that express the interleukin-7 receptor in blood and tissues of SIV-infected macaques. Virology. 2006 Dec;356(1–2):188–97.

196. Zicari S, Sessa L, Cotugno N, Ruggiero A, Morrocchi E, Concato C, et al. Immune Activation, Inflammation, and Non-AIDS Co-Morbidities in HIV-Infected Patients under Long-Term ART. Viruses [Internet]. 2019 Feb 27;11(3):200. Available from: https://www.ncbi.nlm.nih.gov/pubmed/30818749

197. Reth M, Nielsen P. Chapter Four - Signaling Circuits in Early B-Cell Development. In: Alt FW, editor. Academic Press; 2014. p. 129–75. (Advances in Immunology; vol. 122). Available from: http://www.sciencedirect.com/science/article/pii/B9780128002674000043

198. Yamada K, Shimaoka M, Nagayama K, Hiroi T, Kiyono H, Honda T. Bacterial invasion induces interleukin-7 receptor expression in colonic epithelial cell line, T84. Eur J Immunol. 1997 Dec;27(12):3456–60.

199. Wu L, Li J, Xu HL, Xu B, Tong XH, Kwak-Kim J, et al. IL-7/IL-7R signaling pathway might play a role in recurrent pregnancy losses by increasing inflammatory Th17 cells and decreasing Treg cells. Am J Reprod Immunol. 2016 Dec;76(6):454–64.

200. Zhong J, Sharma J, Raju R, Palapetta SM, Prasad TSK, Huang T-C, et al. TSLP signaling pathway map: a platform for analysis of TSLP-mediated signaling. Database (Oxford) [Internet]. 2014 Feb 25;2014:bau007–bau007. Available from: https://www.ncbi.nlm.nih.gov/pubmed/24573880

201. RefSeq. APOL2 apolipoprotein L2 [Homo sapiens (human)] [Internet]. 2008 [cited 2019 Dec 10]. Available from: https://www.ncbi.nlm.nih.gov/gene/23780

202. O'Leary NA, Wright MW, Brister JR, Ciufo S, Haddad D, McVeigh R, et al. Reference sequence (RefSeq) database at NCBI: current status, taxonomic expansion, and functional annotation. Nucleic Acids Res. 2016 Jan;44(D1):D733-45.

203. Khalil A, Poelvoorde P, Fayyad-Kazan M, Rousseau A, Nuyens V, Uzureau S, et al. Apoliporotein L3 interferes with endothelial tube formation via regulation of ERK1/2, FAK and Akt signaling pathway. Atherosclerosis [Internet]. 2018 Dec 1;279:73–87. Available from: https://doi.org/10.1016/j.atherosclerosis.2018.10.023

204. Gurney AL, Marsters SA, Huang RM, Pitti RM, Mark DT, Baldwin DT, et al. Identification of a new member of the tumor necrosis factor family and its receptor, a human ortholog of mouse GITR. Curr Biol. 1999 Feb;9(4):215–8.

205. You S, Poulton L, Cobbold S, Liu C-P, Rosenzweig M, Ringler D, et al. Key role of the GITR/GITRLigand pathway in the development of murine autoimmune diabetes: a

potential therapeutic target. PLoS One. 2009 Nov;4(11):e7848.

206. Mahesh SP, Li Z, Liu B, Fariss RN, Nussenblatt RB. Expression of GITR ligand abrogates immunosuppressive function of ocular tissue and differentially modulates inflammatory cytokines and chemokines. Eur J Immunol. 2006 Aug;36(8):2128–38.

207. Bae EM, Kim W-J, Suk K, Kang Y-M, Park J-E, Kim WY, et al. Reverse signaling initiated from GITRL induces NF-kappaB activation through ERK in the inflammatory activation of macrophages. Mol Immunol. 2008 Jan;45(2):523–33.

208. Manikandan P, Nagini S. Cytochrome P450 Structure, Function and Clinical Significance: A Review. Curr Drug Targets. 2018;19(1):38–54.

209. Morgan ET. Regulation of cytochrome p450 by inflammatory mediators: why and how? Drug Metab Dispos. 2001 Mar;29(3):207–12.

210. Šmerdová L, Svobodová J, Kabátková M, Kohoutek J, Blažek D, Machala M, et al. Upregulation of CYP1B1 expression by inflammatory cytokines is mediated by the p38 MAP kinase signal transduction pathway. Carcinogenesis [Internet]. 2014 Sep 18;35(11):2534–43. Available from: https://doi.org/10.1093/carcin/bgu190

211. Christmas P. Role of Cytochrome P450s in Inflammation. Adv Pharmacol. 2015;74:163–92.

212. Fer M, Dreano Y, Lucas D, Corcos L, Salaun J-P, Berthou F, et al. Metabolism of eicosapentaenoic and docosahexaenoic acids by recombinant human cytochromes P450. Arch Biochem Biophys. 2008 Mar;471(2):116–25.

213. Schuck RN, Zha W, Edin ML, Gruzdev A, Vendrov KC, Miller TM, et al. The Cytochrome P450 Epoxygenase Pathway Regulates the Hepatic Inflammatory Response in Fatty Liver Disease. PLoS One [Internet]. 2014 Oct 13;9(10):e110162. Available from: https://doi.org/10.1371/journal.pone.0110162

214. Thomson SJ, Askari A, Bishop-Bailey D. Anti-inflammatory effects of epoxyeicosatrienoic acids. Int J Vasc Med [Internet]. 2012/07/16. 2012;2012:605101. Available from: https://www.ncbi.nlm.nih.gov/pubmed/22848834

215. Zhang W-Y, Wang H, Qi S, Wang X, Li X, Zhou K, et al. CYP1A1 Relieves Lipopolysaccharide-Induced Inflammatory Responses in Bovine Mammary Epithelial Cells. Mediators Inflamm. 2018;2018:4093285.

216. Chen D-H, Below JE, Shimamura A, Keel SB, Matsushita M, Wolff J, et al. Ataxia-

Pancytopenia Syndrome Is Caused by Missense Mutations in SAMD9L. Am J Hum Genet. 2016 Jun;98(6):1146–58.

217. Tesi B, Davidsson J, Voss M, Rahikkala E, Holmes TD, Chiang SCC, et al. Gain-of-function SAMD9L mutations cause a syndrome of cytopenia, immunodeficiency, MDS, and neurological symptoms. Blood. 2017 Apr;129(16):2266–79.

218. Wang Q, Zhai Y-Y, Dai J-H, Li K-Y, Deng Q, Han Z-G. SAMD9L Inactivation Promotes Cell Proliferation via Facilitating G1-S Transition in Hepatitis B Virus-associated Hepatocellular Carcinoma. Int J Biol Sci [Internet]. 2014;10(8):807–16. Available from: http://www.ijbs.com/v10p0807.htm

219. Deng J, Miller SA, Wang H-Y, Xia W, Wen Y, Zhou BP, et al. beta-catenin interacts with and inhibits NF-kappa B in human colon and breast cancer. Cancer Cell. 2002 Oct;2(4):323–34.

220. Liu X, Lu R, Wu S, Zhang Y-G, Xia Y, Sartor RB, et al. Wnt2 inhibits enteric bacterial-induced inflammation in intestinal epithelial cells. Inflamm Bowel Dis. 2012 Mar;18(3):418–29.

221. Jang M-A, Kim EK, Now H, Nguyen NTH, Kim W-J, Yoo J-Y, et al. Mutations in DDX58, which encodes RIG-I, cause atypical Singleton-Merten syndrome. Am J Hum Genet. 2015 Feb;96(2):266–74.

222. Macpherson C, Audy J, Mathieu O, Tompkins TA. Multistrain probiotic modulation of intestinal epithelial cells' immune response to a double-stranded RNA ligand, poly(i·c). Appl Environ Microbiol. 2014 Mar;80(5):1692–700.

223. Jounai N, Kobiyama K, Takeshita F, Ishii K. Recognition of damage-associated molecular patterns related to nucleic acids during inflammation and vaccination [Internet]. Vol. 2, Frontiers in Cellular and Infection Microbiology . 2013. p. 168. Available from: https://www.frontiersin.org/article/10.3389/fcimb.2012.00168

224. Schmolke M, Patel JR, de Castro E, Sánchez-Aparicio MT, Uccellini MB, Miller JC, et al. RIG-I Detects mRNA of Intracellular Salmonella enterica Serovar Typhimurium during Bacterial Infection. Lipkin WI, editor. MBio [Internet]. 2014 May 1;5(2):e01006-14. Available from: http://mbio.asm.org/content/5/2/e01006-14.abstract

225. Marrs CN, Knobel SM, Zhu WQ, Sweet SD, Chaudhry AR, Alcendor DJ. Evidence for

Gardnerella vaginalis uptake and internalization by squamous vaginal epithelial cells: implications for the pathogenesis of bacterial vaginosis. Microbes Infect. 2012 Jun;14(6):500–8.

226. Petnicki-Ocwieja T, Chung E, Acosta DI, Ramos LT, Shin OS, Ghosh S, et al. TRIF mediates Toll-like receptor 2-dependent inflammatory responses to Borrelia burgdorferi. Infect Immun. 2013 Feb;81(2):402–10.

227. Rademacher F, Simanski M, Harder J. RNase 7 in Cutaneous Defense. Int J Mol Sci [Internet]. 2016 Apr 14;17(4):560. Available from: https://www.ncbi.nlm.nih.gov/pubmed/27089327

228. Rademacher F, Dreyer S, Kopfnagel V, Glaser R, Werfel T, Harder J. The Antimicrobial and Immunomodulatory Function of RNase 7 in Skin. Front Immunol. 2019;10:2553.

229. Harder J, Dressel S, Wittersheim M, Cordes J, Meyer-Hoffert U, Mrowietz U, et al. Enhanced expression and secretion of antimicrobial peptides in atopic dermatitis and after superficial skin injury. J Invest Dermatol. 2010 May;130(5):1355–64.

230. Kopfnagel V, Wagenknecht S, Harder J, Hofmann K, Kleine M, Buch A, et al. RNase 7 Strongly Promotes TLR9-Mediated DNA Sensing by Human Plasmacytoid Dendritic Cells. J Invest Dermatol. 2018 Apr;138(4):872–81.

231. Yamaguchi Y, Yamamoto H, Tobisawa Y, Irie F. TMEM2: A missing link in hyaluronan catabolism identified? Matrix Biol. 2019 May;78–79:139–46.

232. Dokoshi T, Zhang L, Nakatsuji T, Adase CA, Sanford JA, Paladini RD, et al. Hyaluronidase inhibits reactive adipogenesis and inflammation of colon and skin. JCI Insight [Internet]. 2018 Nov 2;3(21). Available from: https://doi.org/10.1172/jci.insight.123072

233. Fronza M, Caetano GF, Leite MN, Bitencourt CS, Paula-Silva FWG, Andrade TAM, et al. Hyaluronidase modulates inflammatory response and accelerates the cutaneous wound healing. PLoS One. 2014;9(11):e112297.

234. Tentaku A, Shimohata T, Hatayama S, Kido J, Nguyen AQ, Kanda Y, et al. Host cellular unfolded protein response signaling regulates Campylobacter jejuni invasion. PLoS One. 2018;13(10):e0205865.

235. Schinzel RT, Higuchi-Sanabria R, Shalem O, Moehle EA, Webster BM, Joe L, et al.

The Hyaluronidase, TMEM2, Promotes ER Homeostasis and Longevity Independent of the UPRER. Cell [Internet]. 2019;179(6):1306-1318.e18. Available from: http://www.sciencedirect.com/science/article/pii/S0092867419311687

236. Zhang C, Bai N, Chang A, Zhang Z, Yin J, Shen W, et al. ATF4 is directly recruited by TLR4 signaling and positively regulates TLR4-trigged cytokine production in human monocytes. Cell Mol Immunol [Internet]. 2012/12/17. 2013 Jan;10(1):84–94. Available from: https://www.ncbi.nlm.nih.gov/pubmed/23241898

237. Niehrs C. Function and biological roles of the Dickkopf family of Wnt modulators. Oncogene. 2006 Dec;25(57):7469–81.

238. Moparthi L, Koch S. Wnt signaling in intestinal inflammation. Differentiation [Internet]. 2019;108:24–32. Available from: http://www.sciencedirect.com/science/article/pii/S0301468118301336

239. Trojanowska M. Ets factors and regulation of the extracellular matrix. Oncogene. 2000 Dec;19(55):6464–71.

240. Khan N, Asif AR. Transcriptional regulators of claudins in epithelial tight junctions. Mediators Inflamm [Internet]. 2015/04/08. 2015;2015:219843. Available from: https://www.ncbi.nlm.nih.gov/pubmed/25948882

241. Dorwart MR, Shcheynikov N, Wang Y, Stippec S, Muallem S. SLC26A9 is a Cl− channel regulated by the WNK kinases. J Physiol [Internet]. 2007 Oct 1;584(1):333–45. Available from: https://doi.org/10.1113/jphysiol.2007.135855

242. Sala-Rabanal M, Yurtsever Z, Berry KN, Brett TJ. Novel Roles for Chloride Channels, Exchangers, and Regulators in Chronic Inflammatory Airway Diseases. Mediators Inflamm. 2015;2015:497387.

243. Nakano FY, Leão R de BF, Esteves SC. Insights into the role of cervical mucus and vaginal pH in unexplained infertility . Vol. 2, MedicalExpress . scielo ; 2015.

244. Wang H-W, Lin C-P, Chiu J-H, Chow K-C, Kuo K-T, Lin C-S, et al. Reversal of inflammation-associated dihydrodiol dehydrogenases (AKR1C1 and AKR1C2) overexpression and drug resistance in nonsmall cell lung cancer cells by wogonin and chrysin. Int J cancer. 2007 May;120(9):2019–27.

245. Rižner TL, Penning TM. Role of aldo-keto reductase family 1 (AKR1) enzymes in human steroid metabolism. Steroids. 2014 Jan;79:49–63.

246. Zeng C, Zhu D, You J, Dong X, Yang B, Zhu H, et al. Liquiritin, as a Natural Inhibitor of AKR1C1, Could Interfere With the Progesterone Metabolism. Front Physiol. 2019;10:833.

247. Norwitz ER, Caughey AB. Progesterone supplementation and the prevention of preterm birth. Rev Obstet Gynecol [Internet]. 2011;4(2):60–72. Available from: https://www.ncbi.nlm.nih.gov/pubmed/22102929

248. Wira CR, Rodriguez-Garcia M, Patel M V. The role of sex hormones in immune protection of the female reproductive tract. Nat Rev Immunol. 2015 Apr;15(4):217–30.

249. Byrne EH, Anahtar MN, Cohen KE, Moodley A, Padavattan N, Ismail N, et al. Association between injectable progestin-only contraceptives and HIV acquisition and HIV target cell frequency in the female genital tract in South African women: a prospective cohort study. Lancet Infect Dis. 2016 Apr;16(4):441–8.

250. Patel FA, Challis JR. Prostaglandins and uterine activity. Front Horm Res. 2001;27:31–56.

251. Jeyabalan A, Caritis SN. Pharmacologic inhibition of preterm labor. Clin Obstet Gynecol. 2002 Mar;45(1):99–113.

252. Allaj V, Guo C, Nie D. Non-steroid anti-inflammatory drugs, prostaglandins, and cancer. Cell Biosci. 2013 Feb;3(1):8.

Appendices

Appendix I: Bacterial culture media preparation

Mann Rogosa, Sharp (MRS) broth (1L):

Added 51g of MRS powder, 50mg Cystein and 1ml Tween 80 to 500ml of pre-warmed reverse osmosis (RO)-water and mixed well. Once all reagents were dissolved, volume was made up to 1L with 500ml of RO-water. The broth was then autoclaved at 121°C for 30 minutes. Broth was stored at 4°C.

Brain, Heart Infusion (BHI) broth (1L):

Added 37g of BHI powder, 10g yeast extract, 1g soluble starch to 500ml of pre-warmed RO-water and mixed well. Once all reagents were dissolved, volume was made up to 1L with 500ml of RO-water. The broth was then autoclaved at 121°C for 30 minutes. Broth was stored at 4°C.

Appendix II: Luminex standard curves

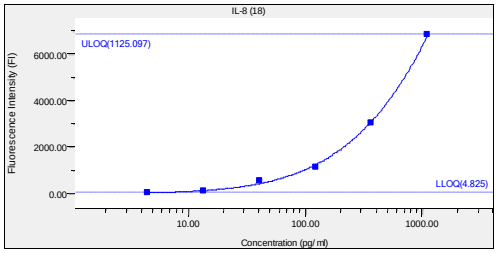

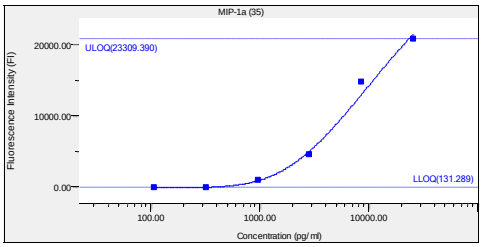

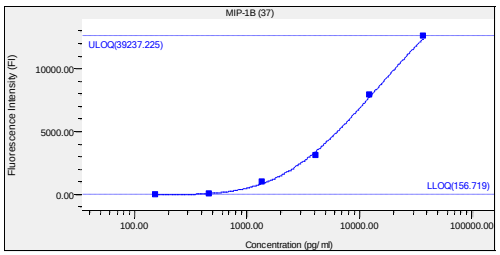

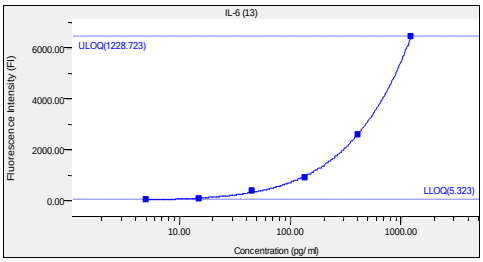

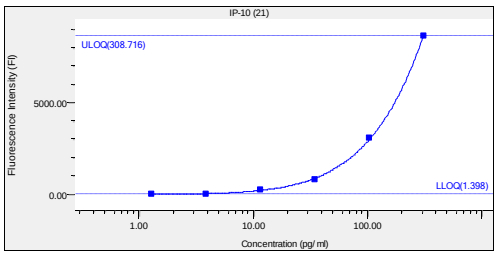

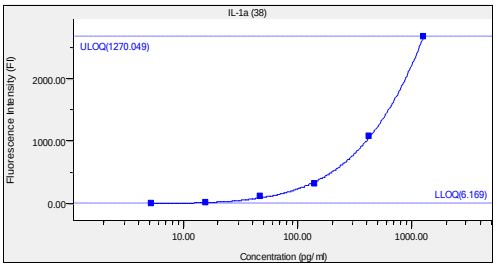

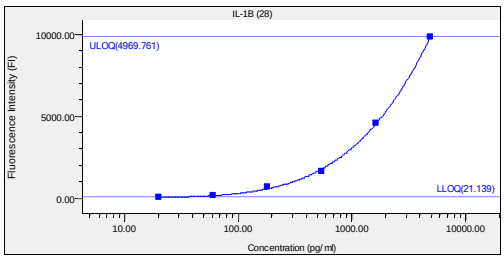

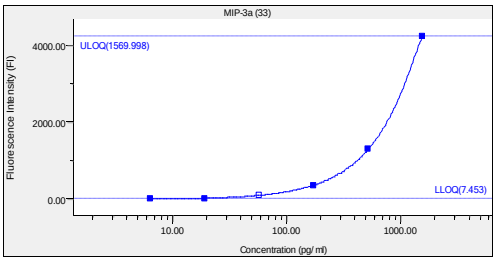

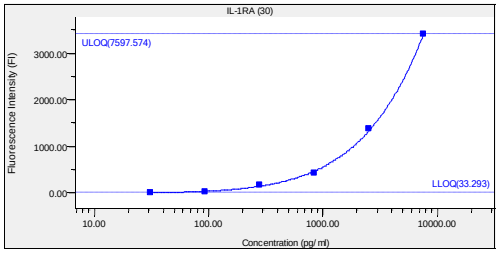

Figure 48 Luminex standard curves for IL-8, MIP-1α, MIP-1β, IL-6, IP-10, IL-1α, IL-1β, IL-1RA**.** VK2 cells were seeded into 24 well plates ($0.5x10^6$ cells/well) and grown to confluence. Monolayers were stimulated with *Lactobacillus* isolates ($4.18x10^6$ CFU/well) and incubated for 6 hrs at 37°C, 5% CO_2. *G. vaginalis* ($4.18x10^7$ CFU/well) was then added to the *Lactobacillus*-VK2 cell cultures and incubated for an additional 6 hrs at 37°C, 5% CO_2. Triplicate independent assays were performed. VK2 cells only and *G. vaginalis* only stimulated VK2 cells were included as controls, in duplicate for each independent assay. Cell culture supernatants were collected, and cytokine production assessed by Luminex assay. IL-8: interleukin-8, **MIP-1α**: macrophage inflammatory protein 1 alpha, **MIP-1β**: macrophage inflammatory protein 1 beta, **IL-6**: interleukin-6, **IP-10**: interferon gamma induced protein 10, **IL-1α**: interleukin 1 alpha, **IL-1β**: interleukin 1 beta, **MIP-3α**: macrophage inflammatory protein 3 alpha, **IL-1RA**: interleukin 1 receptor antagonist.

Appendix III: D- and L- lactate standard curves

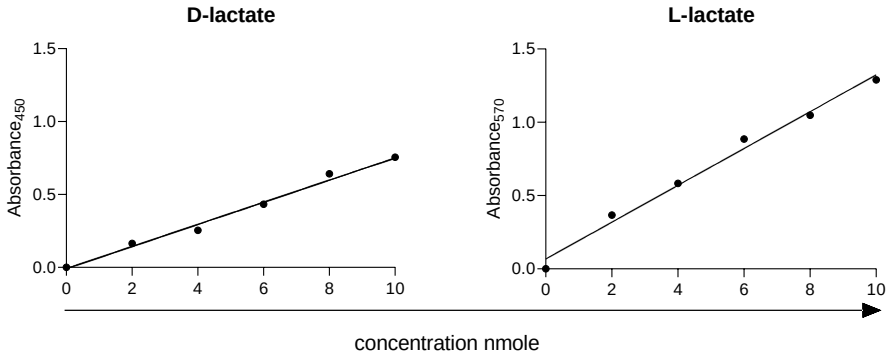

Figure 49: **D- and L- lactate standard curves.** D- and L- standards were prepared as per the kit protocol, generating 0, 2, 4, 6, 8 and 10nmole standards, in duplicate.

Appendix IV: Equations to calculate D- and L- lactate sample concentrations

D-lactate

Sa = Amount of D-Lactate in unknown sample (nmole) from standard curve

Sv = Sample volume (µl) added into the wells

C = Concentration of D-Lactate in sample

D-Lactate molecular weight (MW): 90.08 g/mole

Sample Calculation

Concentration of D-Lactate in sample:

Sa/Sv = C nmole/µl

C nmole/µl x D-lactate MW= C ng/µl

L-lactate

Sa = Amount of lactate acid in unknown sample (nmole) from standard curve

Sv = Sample volume (µl) added into the wells.

C = Concentration of lactate acid in sample

Lactate molecular weight (MW): 89.07 g/mole

Sample Calculation

Amount of Lactate (Sa) = 5.07 nmole

Sample volume (Sv) = 50 µl

Concentration of lactate in sample:

Sa/Sv = C nmole/µl

C nmole/ µl x L-lactate MW= C ng/ µl

Appendix V: Affymetrix GeneChip Whole Transcript (WT) Expression array assay protocol

Control RNA preparation

Control RNA (1mg/ml total RNA from HeLa cells) was used for the positive control reaction to verify that all reagents worked as expected. A total of 2µl of the control RNA was added to 78µl of nuclease-free water to obtain 80µl of 25ng/µl control RNA.

Poly-A RNA control preparation

Poly-A RNA controls were used to provide exogenous positive controls in order to monitor the entire target preparations. Serial dilutions of 1:20, 1:50, 1:10 of the poly-A RNA control was performed. A total of 2µl of the 4^{th} dilution was added to total RNA.

First-Strand cDNA synthesis

Total RNA samples were first normalized to 100ng, which was used as input into the first-strand cDNA synthesis reaction. The first-strand master mix was prepared for all the RNA samples, which contained 1µl of the first-strand enzyme added to 4µl of the first-strand buffer required for each sample. The master mix was vortexed and centrifuged briefly to mix and then collect the mixture at the bottom of the tube. On ice, 5µl of each RNA sample and 5µl

first-strand master mix was added to wells on a 96 well plate, for a final reaction volume of 10µl/well and vortexed gently. The plate was incubated for 1hr at 25°C, then for 1hr at 42°C, then for 2min at 4°C in a thermal cycler. Thereafter, the plate was centrifuged briefly to collect the first-strand cDNA at the bottom of the wells and placed on ice for 2 min to cool the plate.

Second-Strand cDNA synthesis

The second-strand master mix was prepared for all first-strand cDNA samples, which contained 2µl of second-strand enzyme added to 18µl of second-strand buffer required for each sample. The master mix was vortexed and centrifuged briefly to mix and collect the mixture at the bottom of the tube. On ice, 20µl of the second-strand master mix and 10µl of the first-strand cDNA sample was added to wells on a 96 well plate for a final volume of 30µl/well for each sample and vortexed gently. The plate was incubated for 1hr at 16°C, then for 10min at 65°C, then for 2min at 4°C in a thermal cycler. Thereafter, the plate was briefly centrifuged to collect the second-strand cDNA at the bottom of the wells and placed on ice.

cRNA synthesis by in vitro Transcription (IVT)

The IVT master mix was prepared for all second-strand cDNA samples, which contained 6µl of IVT enzyme added to 24µl IVT buffer required for each sample. The master mix was vortexed and centrifuged briefly to mix and collect the mixture at the bottom of the tube. At room temperature, 30µl of the IVT master mix and 30µl of second-strand cDNA was added to wells on a 96 well plate for a final volume of 60µl/well for each sample. The plate was incubated for 16hrs at 40°C, then at 4°C in a thermal cycler. Thereafter, the plate was centrifuged briefly to collect cRNA at the bottom of the well and placed on ice.

cRNA Purification

A total of 100µl of purification beads were added to 60µl of cRNA sample and transferred to a U-bottom 96 well plate and mixed thoroughly by pipetting up and down 10 times. The plate was incubated for 10 min at room temperature to allow the cRNA in the sample to bind to the purification beads. Thereafter, the plate was placed on a magnetic stand for 5min to capture the purification beads. The plate was kept on the magnetic stand and the supernatants were aspirated and discarded. Thereafter, the purification beads were washed 3 times with 200µl of 80% ethanol wash solution and left to dry for 5 min. The plate was then removed from the magnetic stand and 27µl of preheated (65°C) nuclease-free water was added to each sample,

incubated for 1 min to elute the cRNA. Eluted cRNA was mixed well by pipetting up and down 10 times. Thereafter, the plate was placed on a magnetic stand for 5 min to capture the purification beads and the supernatant containing the eluted cRNA was transferred to a 96 well plate and placed on ice.

Assessment of cRNA yield and size distribution

The cRNA concentration for each sample was determined by UV absorbance at 260nm using a NanoDrop Spectrophotometer. An agilent 2100 Bioanalyzer was used to assess the cRNA size distribution.

2nd-cycle single-stranded cDNA synthesis

All cRNA samples were normalized to 625ng/µl. On ice, 24µl of normalized cRNA sample and 4µl of 2nd-cycle primers were added to wells on a 96 well plate and vortexed. The plate was incubated for 5 min at 70°C, then for 5 min at 25°C, then for 2 min at 4°C in a thermal cycler. Thereafter, the plate was briefly centrifuged to collect the cRNA/primers mix at the bottom of the well and placed on ice. The 2nd-cycle ss-cDNA master mix was prepared for all cRNA/primers samples, which contained 4µl of 2nd-cylce ss-cDNA enzyme added to 8µl 2nd-cylce ss-cDNA buffer required for each sample. On ice, 12µl of 2nd-cycle ss-cDNA master mix and 28µl cRNA/primers sample was added to wells on a 96 well plate for a final volume of 40µl. The plate was incubated for 10 min at 25°C, then for 90 min at 42°C, then for 10 min at 70°C and for 2 min at 4°C in a thermal cycler. Thereafter, the plate was briefly centrifuged to collect the 2nd-cycle ss-cDNA at the bottom of the wells and placed on ice.

RNA hydrolysis using RNase H

On ice, 4µl of RNase H was added to each 2nd-cycle ss-cDNA sample and incubated for 45 min at 37°C, then for 5 min at 95°C, then for 2 min at 4°C in a thermal cycler. Thereafter, the plate was briefly centrifuged to collect the hydrolysed 2nd-cycle ss-cDNA sample at the bottom of the wells. On ice, 11µl of nuclease-free water was added to hydrolysed 2nd-cycle ss-cDNA samples, vortexed and centrifuged briefly and the plate was placed on ice.

Purification of 2nd-cycle ss-cDNA

The 2nd-cycle ss-cDNA samples were purified using purification beads as described above for cRNA.

Assessment of cDNA yield and size distribution

2nd-cycle ss-cDNA yield and size distribution was assessed as described above for cRNA.

Fragmentation and labelling of ss-cDNA

The ss-cDNA samples were first normalised to 176ng/µl. On ice, the fragmentation master mix was then prepared for all the samples, containing 1µl apurinic/apryrimidinic endonuclease 1(APE1), 1µl uracil-DNA glycosylase (UDG) and 4.8µl cDNA fragmentation buffer and 10µl nuclease-free water, required for each sample. On ice, 16.8µl of the fragmentation master mix was added to 31.2µl of each ss-cDNA sample and incubated for 1hr at 37°C, then for 2 min at 93°C and then for 2 min at 4°C in a thermal cycler. The plate was briefly centrifuged to collect the fragmented ss-cDNA at the bottom of the wells and placed on ice. The labelling master mix was then prepared for all fragmented ss-cDNA samples, containing 2µl terminal deoxynucleotidyl transferase (TdT), 1µl DNA labelling reagent and 12µl TdT buffer required for each sample. On ice, 15µl of the labelling master mix and 45µl of the fragmented sscDNA sample was added to wells on a 96 well plate. The plate was incubated for 1hr at 37°C, then for 10 min at 70°C and then for 2 min at 4°C in a thermal cycler. The plate was then placed on ice before proceeding to array hybridization.

Whole Transcript array Hybridization

All reagents were thawed at room temperature. The hybridization oven was preheated at 45°C and the rotation set to 60rpm. The hybridization controls were preheated for 5 min at 65°C in a thermal cycler. The hybridization master mix was prepared for all fragmented and biotin-labelled ss-cDNA samples, 1.7µl control oligo, 5µl hybridization controls (bioB, bioC, cre), 50µl hybridization mix, 7µl dimethylsulfoxide (DMSO) and 9.3µl nuclease-free water. A total of 73µl of hybridization master mix was added to 27µl of each fragmented and biotin-labelled ss-cDNA sample in a 96 well plate. The plate was then incubated for 5 min at 95°C, then for 5 min at 45°C in a thermal cycler. Thereafter, the plate was centrifuged briefly to collect the contents at the bottom of the wells. A total of 80µl of sample was loaded onto a Genechip cartridge

array, 1 sample/cartridge and placed into hybridization oven trays, loaded into the hybridization oven and incubated with rotation at 60rpm for 16hr at 45°C.

Wash and staining of Arrays

The arrays were removed from the hybridization oven and the samples removed. The arrays were then filled with wash buffer A. A total of 3 vials containing 600µl stain cocktail 1, 600µl stain cocktail 2 and 800µl stain cocktail 3, respectively, were placed into sample holders on fluidics stations. The arrays were then washed according to the fluidics protocol FS450_0007. Thereafter, the arrays were scanned by the GeneChip™ scanner 3000 7G (Thermofisher, USA).

Appendix VI: Illumina data analysis R script

```
#import illumina data into R
my_data <- read.table(file.choose(),header=T,sep="\t")

#load the library:
library(lumi)

#Read beadstudio output file and create lumiBatch object:
my_data <- lumiR('microarray data 2010.txt')
#summary of data:
my_data
#summary of quality control information:
summary(my_data, 'QC')

#preprocessing and quality control:
lumi.N <- lumiExpresso(my_data)
#Plot the density:
density(my_data)
#Plot of cumulative Distribution Function (CDF):
```

```
plotCDF(my_data, reverse=TRUE)
#plot pairwise sample correlation
#plot the pair plot:
pairs(my_data)
#pairwise scatter plot with smoothing:
pairs(my_data, smoothScatter=T)
#Pairwise MA plot:
MAplot(my_data)
#with smoothing:
MAplot(my_data, smoothScatter=TRUE)
# estimate the coefficient of variance and plot the density plot of it
cv <- estimateLumiCV(my_data, ifPlot = TRUE)

#Plot sample relation with hierarchial clustering:
plotSampleRelation(example.lumi, method='cluster')
# plot the sample relations with MDS:
plotSampleRelation(example.lumi, col=c(..))

#perform quantile between microarray normalization
lumi.T<- lumiT(my_data)
lumi.N <- lumiN(lumi.T)

#qualtity control estimation after normalization:
lumi.N.Q <- lumiQ(lumi.N)
#Summary of the quality control:
summary(lumi.N.Q, 'QC')
#Plot the density:
density(lumi.N.Q)
#Plot boxplot:
boxplot(lumi.N.Q)
```

```
#Pairwise plot:
pairs(lumi.N.Q)
MAplot(lumi.N.Q)
#Plot samplesRlation using hierachical clustering:
plotSampleRelation(lumi.N.Q, method='cluster')
#plot sample relation using MDS:
plotSampleRelation(lumi.N.Q, method='mds', col=c(…)
#DEG list generation
#Identify differentially expressed genes
library(limma)
dataMatrix <- exprs(lumi.N.Q)
presentCount <- detectionCall(my_data)
selDataMatrix <- dataMatrix[presentCount > 0,]
probeList <- rownames(selDataMatrix)

## Specify the sample type
Treatment <- factor(rep(c('CMC', 'PBMC'),5))
###  compare 'cmc' and 'pbmc'
design <- model.matrix(~Treatment)
fit <- lmFit(selDataMatrix, design)
fit <- eBayes(fit)
####Save to CSV
Toplist<-(topTable(fit, coef = c(1-2), adjust='fdr', number=10000)) ###or
write.csv (Toplist, file="Toplistadj.csv")
```

Appendix VII: R script for Cytokine PCA and heatmap generation

```
#Load library for mixOmics package
library(mixOmics)

#Import cytokine data
```

```
my_data<-  read.table(file = "clipboard", sep = "\t", header=TRUE) #to copy from excel

X<-my_data[,2:ncol(my_data)] #x variables from column 2

Y<-my_data$Samples #identify y variable


#PCA

pca.res <- pca(X, ncomp = 5, scale = TRUE)

plot(pca.res) #plot variance per PC

print(pca.res) #shows eigenvalues

mycols <- c("blue3", "coral1","firebrick3","cadetblue2","dodgerblue", "magenta", "deeppink", "darkviolet", "darkorange", "brown1") #to change plot colours

plotIndiv(pca.res, group = my_data$samples, ind.names = FALSE, ellipse = TRUE, legend = TRUE, col=mycols, title = 'PCA')

plotIndiv(pca.res, group = my_data$samples, ind.names = FALSE, ellipse = TRUE, legend = TRUE, col=mycols, title = 'PCA', style='3d')

head(selectVar(pca.res, comp = 1)) #show loadings for PC1

head(selectVar(pca.res, comp = 2)) #show loadings for PC2

pca.res$rotation #see loadings for all PCs

#heatmap

my_data<-  read.table(file = "clipboard", sep = "\t", header=TRUE) #to copy from excel

rnames <- my_data[,1] #where the name for each row is

mat_data <- data.matrix(my_data[,2:ncol(my_data)]) #labeling numerical data as matrix

rownames(mat_data) <- my_data[,1] #assigns the row names to the matrix

col<- colorRampPalette(c("blue", "white", "red"))(256)

heatmap(scale(as.matrix(mat_data)), scale = "none", col =  col, RowSideColors = c(rep("dodgerblue", 142), rep("darkmagenta", 142), rep("coral1", 142), rep("darkorange")))
```

Appendix VIII: Affymetrix microarray data analysis R script

```
#set working directory

#load oligo package

library(oligo)

#Importing cel files:
```

```
celpath = "C:/Users/27812/Desktop/Masters 2019/Results/Affymetrix/1213AFM/1213AFM"

celFiles <- list.celfiles(full.names=TRUE)

rawdata <- read.celfiles(celFiles)

#Quality control of raw data:

exp_raw <- log2(Biobase::exprs(rawdata)) #log2 transform data


#PCA to view clustering and potential outliers:

PCA_raw <- prcomp(t(exp_raw), scale = FALSE)

percentVar <- round(100*PCA_raw$sdev^2/sum(PCA_raw$sdev^2))

sd_ratio <- sqrt(percentVar[2] / percentVar[1])

dataGG <- data.frame(PC1 = PCA_raw$x[,1], PC2 = PCA_raw$x[, 2], SAMPLES =
sampleNames(rawdata))

ggplot(dataGG, aes(PC1, PC2)) + geom_point(aes(colour = SAMPLES)) +  ggtitle("PCA plot of the log-
transformed raw expression data") +   xlab(paste0("PC1, VarExp: ", percentVar[1], "%")) +
ylab(paste0("PC2, VarExp: ", percentVar[2], "%")) +   theme(plot.title = element_text(hjust = 0.5))+
coord_fixed(ratio = sd_ratio) +   scale_shape_manual(values = c(4,15)) +  scale_color_manual(values
= c(…)

#boxplot of probe intensities (1 box/individual array):

oligo::boxplot(rawdata, target = "core", main = "Boxplot of log2-intensitites for the raw data", las =
2, cex.axis = 0.7, col = cols1)

cols1 <- colours(c(…))


#ArrayQuality Metrics:

arrayQualityMetrics(expressionset = rawdata, outdir = tempdir(), force = TRUE, do.logtransform =
TRUE)


#Applying full Robust Multichip Average (RMA) normalization:

affy_eset_norm <- oligo::rma(rawdata)

write.exprs(affy_eset_norm, file="affy_array.txt") #extract normalized data


#PCA plot of normalized data

exp_affy <- Biobase::exprs(affy_eset_norm)

PCA <- prcomp(t(exp_affy), scale = FALSE)
```

```
percentVar <- round(100*PCA$sdev^2/sum(PCA$sdev^2),1)

sd_ratio <- sqrt(percentVar[2] / percentVar[1])

dataGG <- data.frame(PC1 = PCA$x[,1], PC2 = PCA$x[,2], SAMPLES = sampleNames(rawdata))

ggplot(dataGG, aes(PC1, PC2)) + stat_ellipse() + geom_point(aes(colour = SAMPLES)) +  ggtitle("PCA plot of normalized data") +   xlab(paste0("PC1, VarExp: ", percentVar[1], "%")) +   ylab(paste0("PC2, VarExp: ", percentVar[2], "%")) +   theme(plot.title = element_text(hjust = 0.5))+   coord_fixed(ratio = sd_ratio) +   scale_shape_manual(values = c(4,15)) +  scale_color_manual(values = c(…)

PCA$rorotation #loadings for PCs

#Boxplot of normalized data

oligo::boxplot(affy_eset_norm, target = "core", main = "Boxplot of normalized data", las = 2, cex.axis = 0.7, col = cols1)


#DEG list generation

library(limma)


#Import array.txt file

df<-  read.table(file = "clipboard", sep = "\t", header=TRUE, row.names = 1) #COPY DATA

##data matrix

dataMatrix<-data.matrix(df)


#Detect differentially expressed genes

#Design model and applying it to data columns

design <- model.matrix(~ 0+factor(c(1,1,1,2,2,2,3,3,3,4,4,4,5,5,5,6,6,6,7,7,7,8,8,8,9,9,9,10,10,10)))

colnames(design) <- c("group1", "group2", "group3", "group4", "group5", "group6", "group7", "group8", "group9", "group10")

fit <- lmFit(affy_eset_norm, design)

contrast.matrix <- makeContrasts(groupB-groupA,levels=design)

fit2 <- contrasts.fit(fit, contrast.matrix)

fit2 <- eBayes(fit2)

Toplist <-  topTable(fit2, coef=1, adjust="fdr")

#Extract DEG list

write.csv(Toplist, file="Toplistadj.csv")
```

Appendix IX: RNA yield and quality for Illumina microarray data

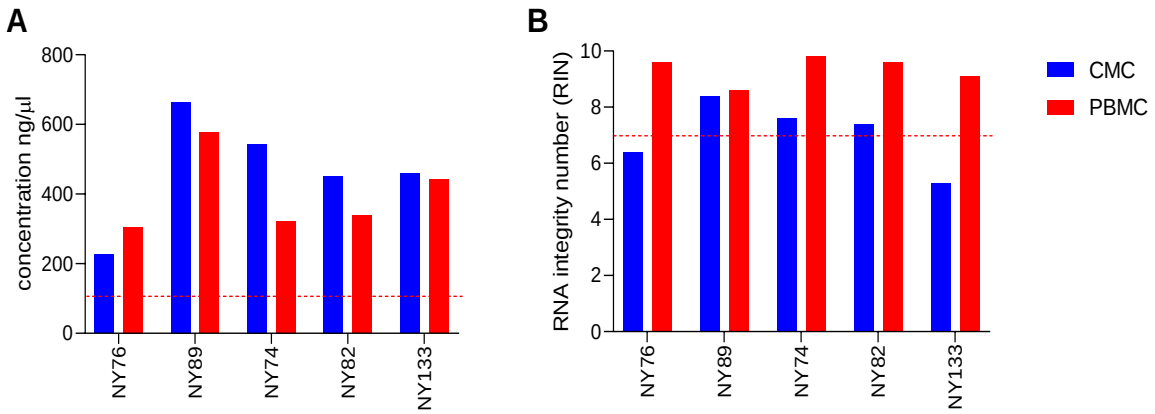

Figure 50 RNA yield and quality for Illumina microarray data. Bar graphs showing **A)** RNA yield and **B)** RNA integrity numbers (RINs) for 5 cervical mononuclear cells (CMC) and matched peripheral blood mononuclear cells (PBMC) samples. Each bar represents a separate RNA sample extracted from CMC and matched PBMC for each participant denoted by the y axis. Red dotted lines indicate the recommended 100ng RNA input for microarray and 7.0 RIN lower limit for "good" RNA integrity. RNA was extracted from matched CMCs and PBMCs isolated from cervical cytobrush and blood samples obtained from chronically HIV-infected women. RNA quality and quantity were assessed using an Agilent 2100 Bioanalyzer and NanoDrop 8000 spectrometer.

Appendix X: Illumina microarray data post-normalization pre-processing

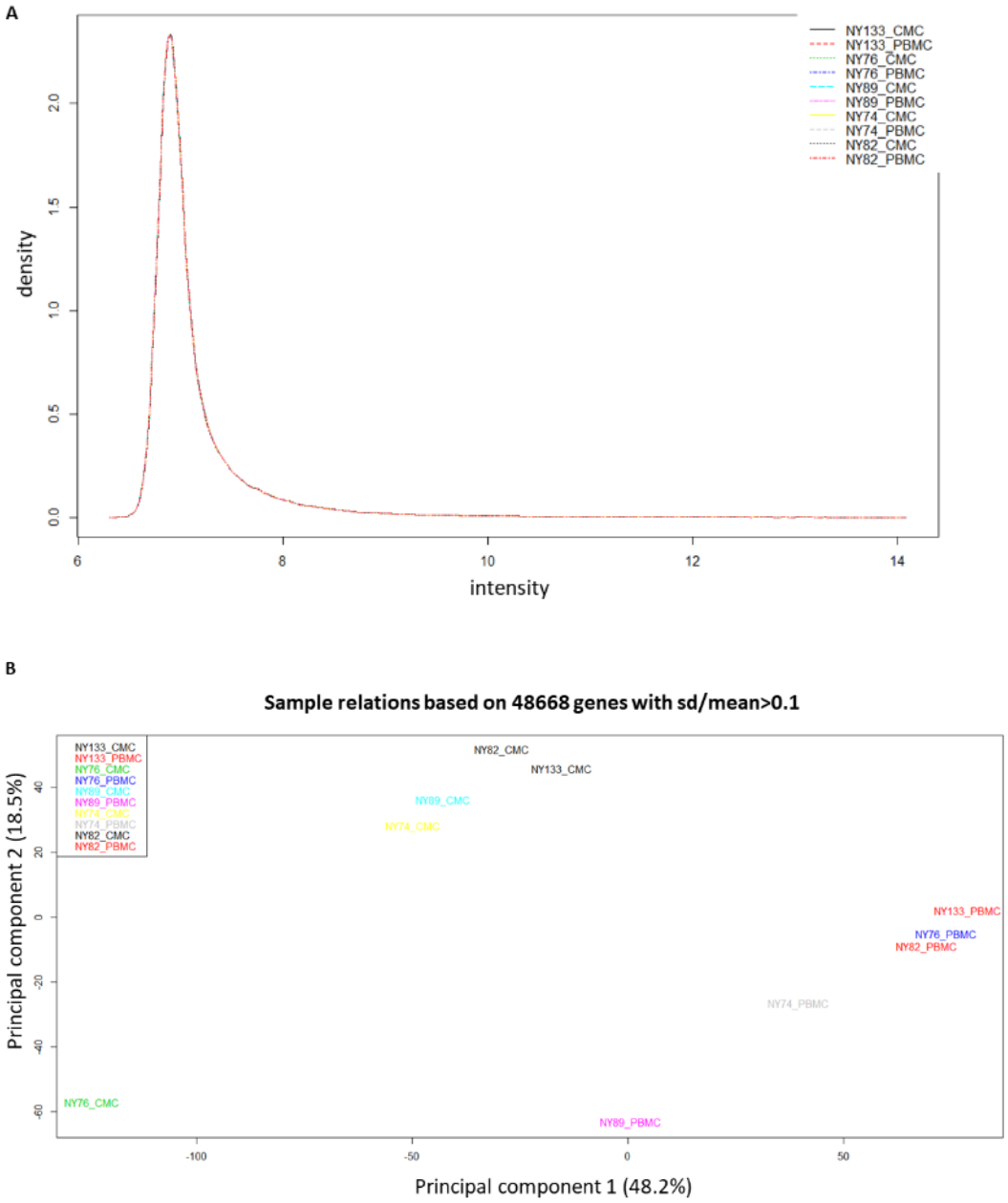

Figure 51 Illumina data post-normalization quality control figures. A) Density of normalized expression values for arrays of 5 cervical mononuclear cells (CMC) and matched peripheral blood mononuclear cells (PBMC) samples and indicates the signal intensity distribution for all samples. **B)** Multidimensional scaling (MDS) plot of 5 CMC and matched PBMC sample relationships based on normalized expression of 48664 genes. RNA was extracted from matched CMCs and PBMCs isolated from cervical cytobrush and blood samples obtained from chronically HIV-infected women. RNA quality and quantity were assessed using an Agilent 2100 Bioanalyzer and NanoDrop 8000 spectrometer. Gene expression analysis of RNA samples was evaluated using Illumina Human HT-12 V3 Gene Expression Beadchip. Quantile normalization was performed on raw data and quality control figures were generated using the lumi R package.

Appendix XI: Upregulated and downregulated genes in CMCs compared to PBMCs

Table 4: Upregulated and downregulated genes in CMCs compared to PBMCs of chronically HIV-infected women

Entrez Gene ID	Gene Symbol	Gene name
Upregulated genes		
133	ADM	adrenomedullin
220	ALDH1A3	aldehyde dehydrogenase 1 family member A3
301	ANXA1	annexin A1
302	ANXA2	annexin A2
390	RND3	Rho family GTPase 3
445	ASS1	argininosuccinate synthase 1
481	ATP1B1	ATPase Na+/K+ transporting subunit beta 1
595	CCND1	cyclin D1
629	CFB	complement factor B
718	C3	complement C3
1087	CEACAM7	carcinoembryonic antigen related cell adhesion molecule 7
1356	CP	ceruloplasmin
1476	CSTB	cystatin B
1514	CTSL1	cathepsin L
1893	ECM1	extracellular matrix protein 1
2012	EMP1	epithelial membrane protein 1
2139	EYA2	EYA transcriptional coactivator and phosphatase 2
2152	F3	coagulation factor III, tissue factor
2215	FCGR3B	Fc fragment of IgG receptor IIIb
2564	GABRE	gamma-aminobutyric acid type A receptor epsilon subunit
2568	GABRP	gamma-aminobutyric acid type A receptor pi subunit
3099	HK2	hexokinase 2
3303	HSPA1A	heat shock protein family A (Hsp70) member 1A
3304	HSPA1B	heat shock protein family A (Hsp70) member 1B
3310	HSPA6	heat shock protein family A (Hsp70) member 6
3553	IL1B	interleukin 1 beta
3557	IL1RN	interleukin 1 receptor antagonist
3576	IL8	C-X-C motif chemokine ligand 8
3853	KRT6A	keratin 6A
3854	KRT6B	keratin 6B
3880	KRT19	keratin 19
3914	LAMB3	laminin subunit beta 3
3934	LCN2	lipocalin 2
4070	TACSTD2	tumor-associated calcium signal transducer 2
4071	TM4SF1	transmembrane 4 L six family member 1
4072	TACSTD1	tumor-associated calcium signal transducer 1
4082	MARCKS	myristoylated alanine rich protein kinase C substrate
4118	MAL	mal, T-cell differentiation protein like

4487	MSX1	msh homeobox 1
4582	MUC1	mucin 1, cell surface associated
4585	MUC4	mucin 4, cell surface associated
4680	CEACAM6	carcinoembryonic antigen related cell adhesion molecule 6
4792	NFKBIA	NFKB inhibitor alpha
5055	SERPINB2	serpin family B member 2
5209	PFKFB3	6-phosphofructo-2-kinase/fructose-2,6-biphosphatase 3
5266	PI3	peptidase inhibitor 3
5284	PIGR	polymeric immunoglobulin receptor
5507	PPP1R3C	protein phosphatase 1 regulatory subunit 3C
5743	PTGS2	prostaglandin-endoperoxide synthase 2
5768	QSOX1	quiescin sulfhydryl oxidase 1
6278	S100A7	S100 calcium binding protein A7
6279	S100A8	S100 calcium binding protein A8
6280	S100A9	S100 calcium binding protein A9
6284	S100A13	S100 calcium binding protein A13
6286	S100P	S100 calcium binding protein P
6288	SAA1	serum amyloid A1
6289	SAA2	serum amyloid A2
6303	SAT1	spermidine/spermine N1-acetyltransferase 1
6372	CXCL6	C-X-C motif chemokine ligand 6
6446	SGK	serum/glucocorticoid regulated kinase 1
6590	SLPI	secretory leukocyte peptidase inhibitor
6648	SOD2	superoxide dismutase 2, mitochondrial
6696	SPP1	secreted phosphoprotein 1
6700	SPRR2A	small proline rich protein 2A
6703	SPRR2D	small proline rich protein 2D
6704	SPRR2E	small proline rich protein 2E
6705	SPRR2F	small proline rich protein 2F
6707	SPRR3	small proline rich protein 3
7033	TFF3	trefoil factor 3
7082	TJP1	tight junction protein 1
7132	TNFRSF1A	TNF receptor superfamily member 1A
7851	MALL	mal, T-cell differentiation protein like
8842	PROM1	prominin 1
8857	FCGBP	Fc fragment of IgG binding protein
8870	IER3	immediate early response 3
9123	SLC16A3	solute carrier family 16 member 3
9245	GCNT3	glucosaminyl (N-acetyl) transferase 3, mucin type
9528	TMEM59	transmembrane protein 59
9982	FGFBP1	fibroblast growth factor binding protein 1
10079	ATP9A	ATPase phospholipid transporting 9A
10135	NAMPT	nicotinamide phosphoribosyltransferase
10170	DHRS9	dehydrogenase/reductase 9

10205	MPZL2	myelin protein zero like 2
10221	TRIB1	tribbles pseudokinase 1
10276	NET1	neuroepithelial cell transforming 1
10409	BASP1	brain abundant membrane attached signal protein 1
10562	OLFM4	olfactomedin 4
10653	SPINT2	serine peptidase inhibitor, Kunitz type 2
11005	SPINK5	serine peptidase inhibitor, Kazal type 5
23589	CARHSP1	calcium regulated heat stable protein 1
25878	MXRA5	matrix remodeling associated 5
26298	EHF	ETS homologous factor
26353	HSPB8	heat shock protein family B (small) member 8
29949	IL19	interleukin 19
30001	ERO1A	endoplasmic reticulum oxidoreductase 1 alpha
49860	CRNN	cornulin
50848	F11R	F11 receptor
54544	CRCT1	cysteine rich C-terminal 1
54869	EPS8L1	EPS8 like 1
57162	PELI1	pellino E3 ubiquitin protein ligase 1
57447	NDRG2	NDRG family member 2
58489	FAM108C1	abhydrolase domain containing 17C
60675	PROK2	prokineticin 2
65009	NDRG4	NDRG family member 4
65249	ZSWIM4	zinc finger SWIM-type containing 4
79689	STEAP4	STEAP4 metalloreductase
83959	SLC4A11	solute carrier family 4 member 11
84419	C15orf48	chromosome 15 open reading frame 48
84518	CNFN	cornifelin
84659	RNASE7	ribonuclease A family member 7
132724	TMPRSS11 B	transmembrane protease, serine 11B
144568	A2ML1	alpha-2-macroglobulin like 1
150696	PROM2	prominin 2
196374	KRT78	keratin 78
646786	LOC646786	PREDICTED: similar to Afadin (AF-6 protein)
649768	LOC649768	PREDICTED: mucin MUC5B
653108	CXADRP1	coxsackie virus and adenovirus receptor pseudogene 1
653381	SORD2P	sorbitol dehydrogenase 2, pseudogene
727897	MUC5B	mucin 5B, oligomeric mucus/gel-forming
Downregulated genes		
678	ZFP36L2	ZFP36 ring finger protein like 2
894	CCND2	cyclin D2
919	CD247	CD247 molecule
994	CDC25B	cell division cycle 25B
1043	CD52	CD52 molecule

1901	EDG1	endothelial differentiation, sphingolipid G-protein-coupled receptor, 1
2113	ETS1	ETS proto-oncogene 1, transcription factor
2219	FCN1	ficolin 1
2534	FYN	FYN proto-oncogene, Src family tyrosine kinase
2999	GZMH	granzyme H
3021	H3F3B	H3 histone family member 3B
3040	HBA2	hemoglobin subunit alpha 2
3043	HBB	hemoglobin subunit beta
3148	HMGB2	high mobility group box 2
3702	ITK	IL2 inducible T-cell kinase
3945	LDHB	lactate dehydrogenase B
4050	LTB	lymphotoxin beta
5295	PIK3R1	phosphoinositide-3-kinase regulatory subunit 1
5551	PRF1	perforin 1
6139	RPL17	ribosomal protein L17
6143	RPL19	ribosomal protein L19
6144	RPL21	ribosomal protein L21
6156	RPL30	ribosomal protein L30
6188	RPS3	ribosomal protein S3
6189	RPS3A	ribosomal protein S3A
6194	RPS6	ribosomal protein S6
6206	RPS12	ribosomal protein S12
6208	RPS14	ribosomal protein S14
6209	RPS15	ribosomal protein S15
6210	RPS15A	ribosomal protein S15a
6218	RPS17	ribosomal protein S17
6232	RPS27	ribosomal protein S27
6233	RPS27A	ribosomal protein S27a
6235	RPS29	ribosomal protein S29
6352	CCL5	C-C motif chemokine ligand 5
8367	HIST1H4E	histone cluster 1 H4 family member e
8473	OGT	O-linked N-acetylglucosamine (GlcNAc) transferase
8905	AP1S2	adaptor related protein complex 1 sigma 2 subunit
9452	ITM2A	integral membrane protein 2A
9806	SPOCK2	SPARC/osteonectin, cwcv and kazal like domains proteoglycan 2
10235	RASGRP2	RAS guanyl releasing protein 2
10578	GNLY	granulysin
25777	UNC84B	Sad1 and UNC84 domain containing 2
51176	LEF1	lymphoid enhancer binding factor 1
53637	S1PR5	sphingosine-1-phosphate receptor 5
54504	CPVL	carboxypeptidase, vitellogenic like
54855	FAM46C	family with sequence similarity 46 member C
83888	FGFBP2	fibroblast growth factor binding protein 2
128346	C1orf162	chromosome 1 open reading frame 162

149628	PYHIN1	pyrin and HIN domain family member 1
286530	P2RY8	purinergic receptor P2Y8
400963	LOC400963	ribosomal protein S2 pseudogene 17
401019	LOC401019	ribosomal protein S15 pseudogene 4
402057	LOC402057	ribosomal protein S17 pseudogene 16
439949	LOC439949	PRKCQ antisense RNA 1
647361	LOC647361	PREDICTED:similar to 40S ribosomal protein S29
649821	LOC649821	PREDICTED: similar to 60S ribosomal protein L14 (CAG-ISL 7), transcript variant 1

Appendix XII: Immune cell populations in CMCs and PBMCs

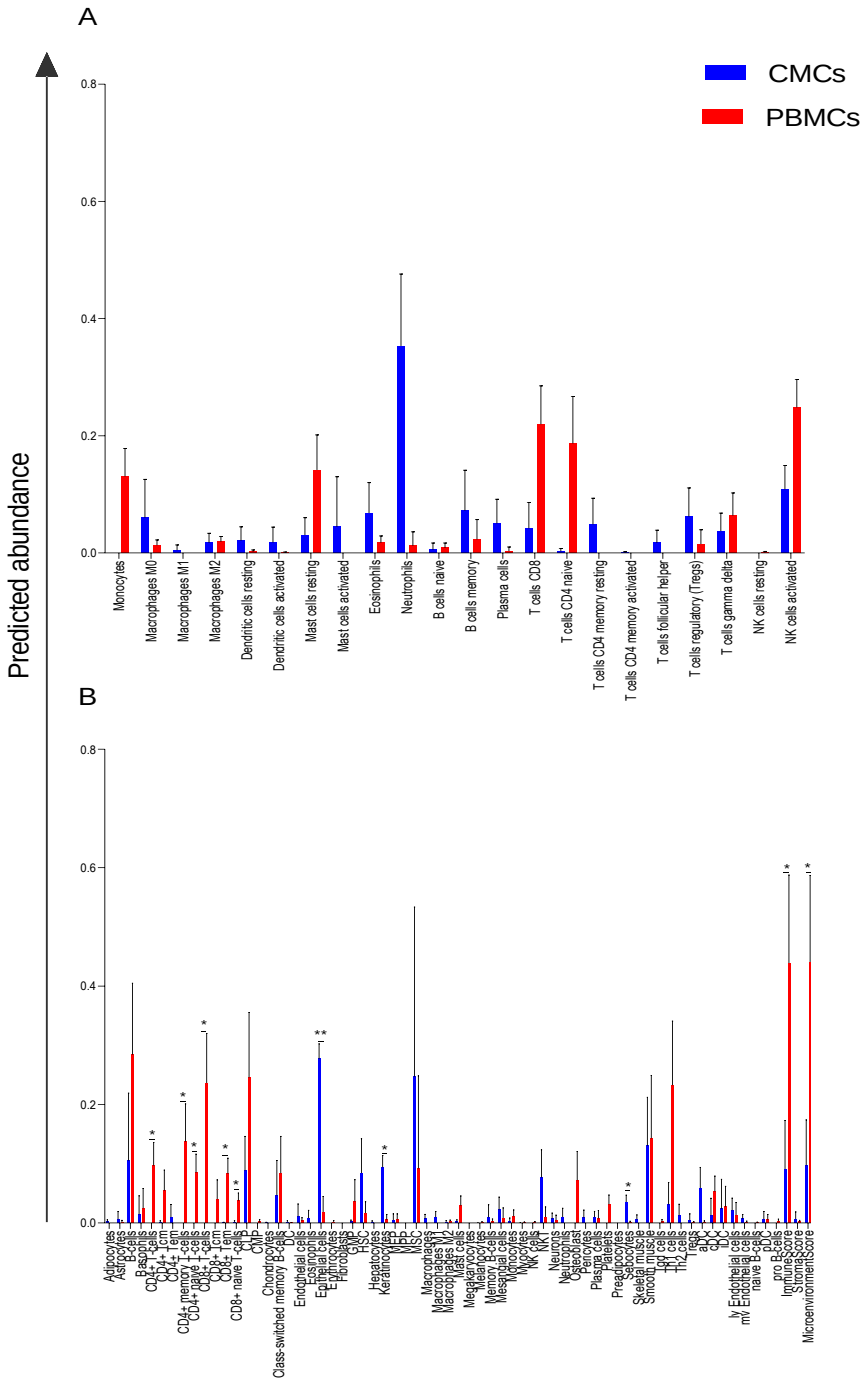

Figure 52 Immune cell populations in CMC and PBMC samples. Bar graph shows absolute abundances of immune cells in CMC and PBMC samples. Microarray data were used for **A)** CIBERSORT and **B)** xCell analyses to detect cell populations in each sample type. A paired t test was used to statistically test the differences in predicted cell populations in CMCs compared to PBMCs, p-value < 0.05 was considered significant. A false discovery rate step down procedure was used to adjust for multiple comparisons, adj. p-value < 0.05 was considered significant. **CMC**: cervical mononuclear cells, **PBMC**: peripheral blood mononuclear cells.

Appendix XIII: Electropherograms of RNA extracted from VK2 cells stored in RNALater and RLT Buffer

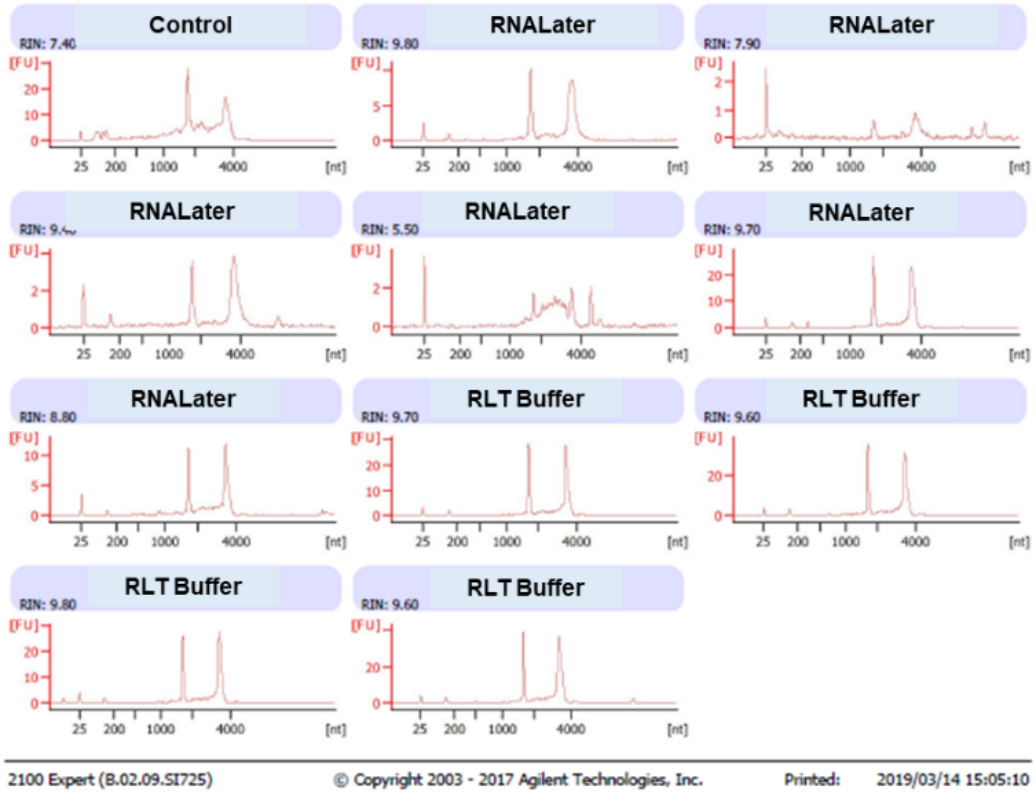

Figure 53 Electropherograms of total RNA extracted from VK2 cells stored in RNALater and RLT buffer. VK2 cells were cultured in 24mm transwell inserts with 0.4µm pores, at 37°C, 5% CO_2 for 7 days, with media changed every 2-3 days. The cells were harvested and stored in either RNALater or RLT lysis buffer, at -80°C. RNA was extracted using the Qiagen RNeasy Mini kit. RNA integrity was assessed using an Agilent 2100 Bioanalyzer. **RIN**: RNA integrity number.

Appendix XIV: Culture pH of VK2 cells co-cultured with *Lactobacillus* spp. and *G. vaginalis* in combination in 24 well cell plates

Table 5: Culture pH of VK2 cell bacterial stimulation in 24 well plates

Sample	Culture pH
CELLS	8
CELLS	8
CELLS	8
CELLS	8
CELLS	8
CELLS	8
GV	8
GV	8
GV	8
GV	8
GV	8
LJ3+GV	8
LJ3+GV	7
LJ3+GV	8
LV3+GV	9
LV3+GV	7
LV3+GV	8
LC3+GV	7
LC3+GV	8
LC3+GV	7
LM2+GV	8
LM2+GV	8
LM2+GV	8
LC1+GV	8
LC1+GV	8
LC1+GV	8
LJ2+GV	7
LJ2+GV	7
LJ2+GV	7
LM4+GV	8
LM4+GV	7
LM4+GV	7
LV4+GV	7
LV4+GV	8
LV4+GV	7

Appendix XV: Electropherograms of RNA extracted from unstimulated and stimulated VK2 cells

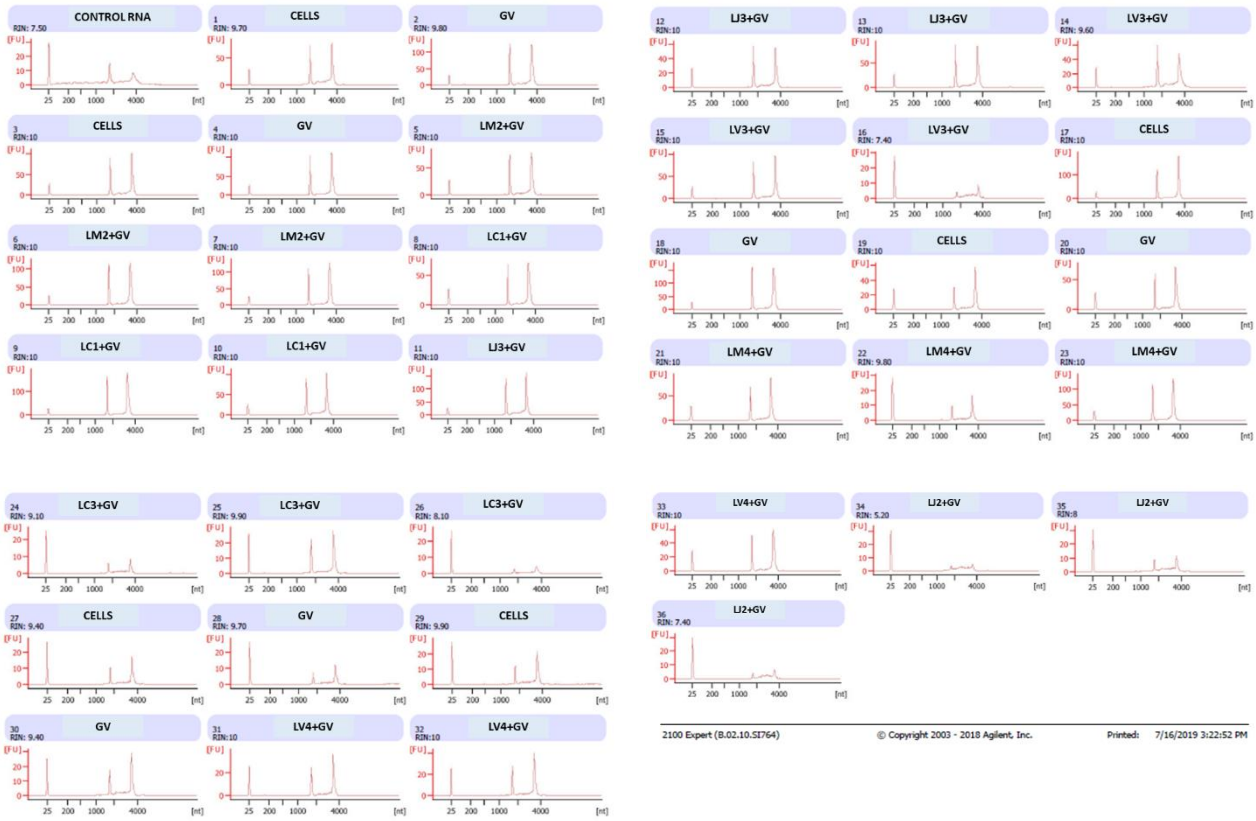

Figure 54 Electropherograms of RNA extracted from stimulated VK2 cells and unstimulated cells. VK2 cells were seeded into 24 well plates ($0.5x10^6$ cells/well) and grown to confluence. Monolayers were stimulated with each *Lactobacillus* isolate ($4.18x10^6$CFU/well) in 500µl media and incubated for 6 hours at 37°C, 5% CO_2. Thereafter, *G. vaginalis* ($4.18x10^7$ CFU/well) in 500µl was added to the *Lactobacillus*-VK2 cell cultures and incubated for an additional 6 hrs at 37°C, 5% CO_2. Triplicate independent assays were performed. VK2 cells only and *G. vaginalis* only stimulated VK2 cells were included as controls, in duplicate for each independent assay. VK2 cells were harvested following the stimulation assay and stored in RLT lysis buffer at -80°C. RNA was extracted using the Qiagen RNeasy mini kit and RNA integrity assessed using an Agilent 2100 Bioanalyzer. **RIN**: RNA integrity number.

Appendix XVI: Upregulated genes in *G. vaginalis*-stimulated VK2 cells compared to unstimulated cells

Table 6: Upregulated genes in *G. vaginalis*-stimulated VK2 cells compared to unstimulated cells

Entrez gene ID	Gene symbol	DAVID Bioinformatics resources gene name
4312	MMP1	matrix metallopeptidase 1
3624	INHBA	inhibin beta A subunit
629	CFB	complement factor B
3569	IL6	interleukin 6
3659	IRF1	interferon regulatory factor 1
83666	PARP9	poly(ADP-ribose) polymerase family member 9
8995	TNFSF18	tumor necrosis factor superfamily member 18
634	CEACAM1	carcinoembryonic antigen related cell adhesion molecule 1
55966	AJAP1	adherens junctions associated protein 1
50486	G0S2	G0/G1 switch 2
3552	IL1A	interleukin 1 alpha
1594	CYP27B1	cytochrome P450 family 27 subfamily B member 1
6515	SLC2A3	solute carrier family 2 member 3
3553	IL1B	interleukin 1 beta
330	BIRC3	baculoviral IAP repeat containing 3
3433	IFIT2	interferon induced protein with tetratricopeptide repeats 2
80149	ZC3H12A	zinc finger CCCH-type containing 12A
2919	CXCL1	C-X-C motif chemokine ligand 1
10318	TNIP1	TNFAIP3 interacting protein 1
6352	CCL5	C-C motif chemokine ligand 5
3431	SP110	SP110 nuclear body protein
54739	XAF1	XIAP associated factor 1
9966	TNFSF15	tumor necrosis factor superfamily member 15
2247	FGF2	fibroblast growth factor 2
162394	SLFN5	schlafen family member 5
205860	TRIML2	tripartite motif family like 2
54498	SMOX	spermine oxidase
9582	APOBEC3B	apolipoprotein B mRNA editing enzyme catalytic subunit 3B
64135	IFIH1	interferon induced with helicase C domain 1
22822	PHLDA1	pleckstrin homology like domain family A member 1
200315	APOBEC3A	apolipoprotein B mRNA editing enzyme catalytic subunit 3A
7128	TNFAIP3	TNF alpha induced protein 3
6737	TRIM21	tripartite motif containing 21
8843	HCAR3	hydroxycarboxylic acid receptor 3
5791	PTPRE	protein tyrosine phosphatase, receptor type E
219285	SAMD9L	sterile alpha motif domain containing 9 like
3665	IRF7	interferon regulatory factor 7
12	SERPINA3	serpin family A member 3

81848	SPRY4	sprouty RTK signaling antagonist 4
3656	IRAK2	interleukin 1 receptor associated kinase 2
101730217	SPECC1L-ADORA2A	SPECC1L-ADORA2A readthrough (NMD candidate)
3434	IFIT1	interferon induced protein with tetratricopeptide repeats 1
55332	DRAM1	DNA damage regulated autophagy modulator 1
5971	RELB	RELB proto-oncogene, NF-kB subunit
10221	TRIB1	tribbles pseudokinase 1
79689	STEAP4	STEAP4 metalloreductase
4973	OLR1	oxidized low density lipoprotein receptor 1
5744	PTHLH	parathyroid hormone like hormone
3627	CXCL10	C-X-C motif chemokine ligand 10
4599	MX1	MX dynamin like GTPase 1
5743	PTGS2	prostaglandin-endoperoxide synthase 2
51561	IL23A	interleukin 23 subunit alpha
129607	CMPK2	cytidine/uridine monophosphate kinase 2
4688	NCF2	neutrophil cytosolic factor 2
3669	ISG20	interferon stimulated exonuclease gene 20
85480	TSLP	thymic stromal lymphopoietin
2113	ETS1	ETS proto-oncogene 1, transcription factor
5270	SERPINE2	serpin family E member 2
2635	GBP3	guanylate binding protein 3
8482	SEMA7A	semaphorin 7A (John Milton Hagen blood group)
7127	TNFAIP2	TNF alpha induced protein 2
27071	DAPP1	dual adaptor of phosphotyrosine and 3-phosphoinositides 1
3604	TNFRSF9	TNF receptor superfamily member 9
6648	SOD2	superoxide dismutase 2, mitochondrial
5329	PLAUR	plasminogen activator, urokinase receptor
10561	IFI44	interferon induced protein 44
51191	HERC5	HECT and RLD domain containing E3 ubiquitin protein ligase 5
51458	RHCG	Rh family C glycoprotein
6364	CCL20	C-C motif chemokine ligand 20
374	AREG	amphiregulin
91543	RSAD2	radical S-adenosyl methionine domain containing 2
7097	TLR2	toll like receptor 2
5055	SERPINB2	serpin family B member 2
115019	SLC26A9	solute carrier family 26 member 9
4953	ODC1	ornithine decarboxylase 1
3576	CXCL8	C-X-C motif chemokine ligand 8
5265	SERPINA1	serpin family A member 1
3038	HAS3	hyaluronan synthase 3
85441	HELZ2	helicase with zinc finger 2
51312	SLC25A37	solute carrier family 25 member 37
25841	ABTB2	ankyrin repeat and BTB domain containing 2
115361	GBP4	guanylate binding protein 4

7378	UPP1	uridine phosphorylase 1
23586	DDX58	DExD/H-box helicase 58
597	BCL2A1	BCL2 related protein A1
24145	PANX1	pannexin 1
341208	HEPHL1	hephaestin like 1
84419	C15orf48	chromosome 15 open reading frame 48
11274	USP18	ubiquitin specific peptidase 18
10964	IFI44L	interferon induced protein 44 like
6288	SAA1	serum amyloid A1
9636	ISG15	ISG15 ubiquitin-like modifier
2069	EREG	epiregulin
27074	LAMP3	lysosomal associated membrane protein 3
56937	PMEPA1	prostate transmembrane protein, androgen induced 1
338442	HCAR2	hydroxycarboxylic acid receptor 2
4600	MX2	MX dynamin like GTPase 2
10346	TRIM22	tripartite motif containing 22
7130	TNFAIP6	TNF alpha induced protein 6
6373	CXCL11	C-X-C motif chemokine ligand 11
2633	GBP1	guanylate binding protein 1
6289	SAA2	serum amyloid A2
134285	TMEM171	transmembrane protein 171
1969	EPHA2	EPH receptor A2
7039	TGFA	transforming growth factor alpha
3437	IFIT3	interferon induced protein with tetratricopeptide repeats 3
3561	IL2RG	interleukin 2 receptor subunit gamma
6523	SLC5A1	solute carrier family 5 member 1
26525	IL36RN	interleukin 36 receptor antagonist
8061	FOSL1	FOS like 1, AP-1 transcription factor subunit
113277	TMEM106A	transmembrane protein 106A
220	ALDH1A3	aldehyde dehydrogenase 1 family member A3
3383	ICAM1	intercellular adhesion molecule 1
9175	MAP3K13	mitogen-activated protein kinase kinase kinase 13
4938	OAS1	2'-5'-oligoadenylate synthetase 1
9674	KIAA0040	KIAA0040
1847	DUSP5	dual specificity phosphatase 5
57458	TMCC3	transmembrane and coiled-coil domain family 3
114770	PGLYRP2	peptidoglycan recognition protein 2
6705	SPRR2F	small proline rich protein 2F
5017	OVOL1	ovo like transcriptional repressor 1
1839	HBEGF	heparin binding EGF like growth factor
4322	MMP13	matrix metallopeptidase 13
1848	DUSP6	dual specificity phosphatase 6
4319	MMP10	matrix metallopeptidase 10
8638	OASL	2'-5'-oligoadenylate synthetase like
3575	IL7R	interleukin 7 receptor
2643	GCH1	GTP cyclohydrolase 1

4939	OAS2	2'-5'-oligoadenylate synthetase 2
11254	SLC6A14	solute carrier family 6 member 14
91351	DDX60L	DEAD-box helicase 60-like
8676	STX11	syntaxin 11
30844	EHD4	EH domain containing 4
10125	RASGRP1	RAS guanyl releasing protein 1
4940	OAS3	2'-5'-oligoadenylate synthetase 3
56300	IL36G	interleukin 36, gamma
639	PRDM1	PR/SET domain 1
85463	ZC3H12C	zinc finger CCCH-type containing 12C
10468	FST	follistatin

Appendix XVII: GAPDH expression in unstimulated and stimulated VK2 cells

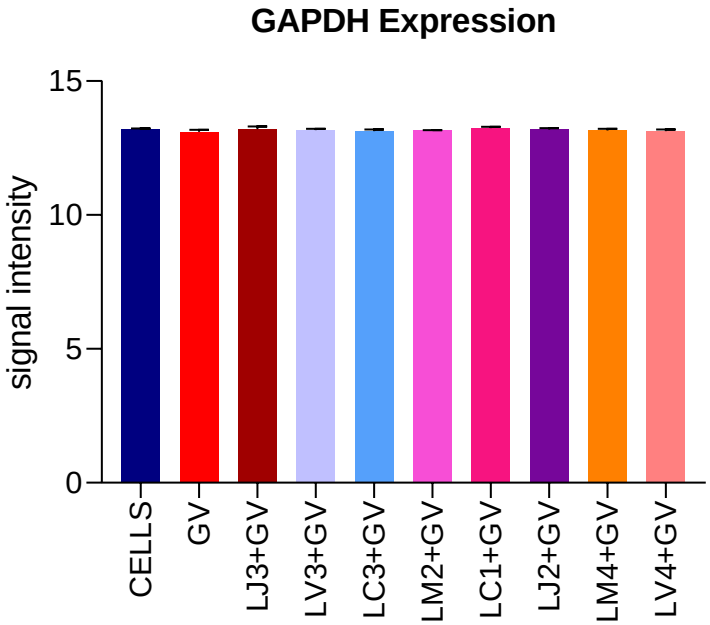

Figure 55 Housekeeping gene Glyceraldehyde-3-phosphate dehydrogenase (GAPDH) expression in unstimulated and stimulated VK2 cells. VK2 cells were seeded into 24 well plates ($0.5x10^6$ cells/well) and grown to confluence. Monolayers were stimulated with each *Lactobacillus* isolate ($4.18 X 10^6$CFU/well) in 500µl media and incubated for 6 hours at 37°C, 5% CO_2. Thereafter, *G. vaginalis* ($4.18x10^7$ CFU/well) in 500µl was then added to the *Lactobacillus*-VK2 cell cultures and incubated for an additional 6 hrs at 37°C, 5% CO_2. Triplicate independent assays were performed. VK2 cells only and *G. vaginalis* only stimulated VK2 cells were included as controls, in duplicate for each independent assay. VK2 cells were harvested following the stimulation assay and stored in RLT lysis buffer at -80°C. RNA was extracted using the Qiagen RNeasy mini kit and RNA integrity assessed using an Agilent 2100 Bioanalyzer. RNA was extracted using the Qiagen RNeasy mini kit and gene expression analysis was then performed using microarray Affymetrix GeneChip whole transcript array platform. The R Studio Bioconductor Oligo package was used to normalize raw data using Robust MultiChip Average (RMA) normalization. Genes were annotated using the Clariom S Human annotation file. **GV:** *G. vaginalis*, **LJ3:** *L. jensenii* 3, **LV3:** *L. vaginalis* 3, **LC3:** *L. crispatus* 3, **LM2:** *L. mucosae* 2, **LC1:** *L. crispatus* 1, **LJ2:** *L. jensenii* 2, **LM4:** *L. mucosae* 4. **LV4:** *L. vaginalis* 4.